Systematics of the South American Native Ungulates and the Neogene Evolution of Mammals from Northern South America

---

Dissertation

zur

Erlangung der naturwissenschaftlichen Doktorwürde
(Dr. sc. nat.)

vorgelegt der

Mathematisch-naturwissenschaftlichen Fakultät

der

Universität Zürich

von

Juan David Carrillo Sánchez

aus

Kolumbien

Promotionskommission

Prof. Dr. Marcelo R. Sánchez-Villagra
(Leitung der Dissertation und Vorsitz)
Dr. Robert J. Asher
PD. Dr. Torsten Scheyer
Dr. Guillaume Billet (Gutachter)

Zürich, 2017

Table of contents

South America was isolated from other continents during most of the Cenozoic and it was home of an endemic mammalian fauna. Among the most characteristic faunal elements are the South American native ungulates (SANUs), a group of ungulate-grade mammals that were widespread and highly diverse in the continent. Despite of significant advances, the phylogenetic interrelationships of SANUs are not fully resolved, and remain a major challenge in palaeomammalogy. The evolutionary history of SANUs and other endemic mammals is recorded mostly in higher latitudes; however, most of the mammal diversity today is found in lower latitudes, and there is a need to increase the record of Neotropical fossils in order to better understand the evolution of diversity gradients in mammals. The aim of this dissertation is to study exceptional new fossils that serve to address the phylogenetic relationships of one of the main SANU clades (Notoungulata) with other placentals, and review the systematics and diversity of Neogene mammals based on the documentation of new fossil assemblages from northern South America.

Chapter one presents the description of the oldest notoungulate skeleton with associated dental and postcranial remains: *Thomashuxleya externa* (Isotemnidae, Notoungulata) from the middle Eocene of Patagonia, Argentina. The exceptionally complete specimen is the basis of an estimate of body size of approximately 235 kg; the fossil is integrated in an examination of the phylogenetic hypotheses for the relationships of Notoungulata with other placentals. An analysis combining morphological and molecular data favours a limited number of hypothetical trees, but it cannot definitely arbitrate between affinities of *Thomashuxleya* with Afrotheria or Laurasiatheria. When constrained as monophyletic with the Pleistocene notoungulate *Toxodon* (known for collagen sequences), *Thomashuxleya* is reconstructed on the stem to Euungulata (Perissodactyla + Artiodactyla) or as sister to Perissodactyla.

The isolation of South America finished with the formation of the Isthmus of Panama, which established a land connection with North America and facilitated the faunal exchange between the two continents, a biotic event known as the Great American Biotic Interchange (GABI). Chapter two presents a biogeographic analysis of the mammalian faunas in South America from the Miocene to the Pliocene, and a revision of the temporal and geographic distribution of mammals during the GABI. It shows that the tropical and temperate faunas can be clearly differentiated since at least the middle Miocene, and documents a strong sampling bias in the fossil record towards higher latitudes and younger localities, which represents a challenge to paleontological studies of the GABI.

Chapter three and four represent contributions towards filling this temporal and geographic gap in the Neotropical fossil record based on the description of new material from the Cocinetas (northern Colombia) and Falcón (northwestern Venezuela) basins. Chapter three describes new

remains of giant rodents (Neoepiblemidae, Caviomorpha) from the Urumaco Formation (late Miocene), in the Falcón basin. It documents the presence of at least two taxa of neoepiblemids in the assemblage, *Phoberomys* and *Neoepiblema*. Furthermore, the dental variation observed suggests that several of the *Phoberomys* species previously described represent different ontogenetic stages of only few taxa.

Chapter four describes Neogene SANU material from the Cocinetas and Falcón basins, and it provides a phylogenetic analysis for Astrapotheriidae and Toxodontidae. In the Cocinetas basin, the middle Miocene fauna of the Castilletes Formation includes *Hilarcotherium* sp. nov. (Astrapotheriidae), cf. *Huilatherium* (Leontiniidae), and *Neodolodus* cf. *colombianus* (Proterotheriidae). The late Pliocene fauna of the Ware Formation includes Toxodontinae indet. and the oldest record of Camelidae indet. (Artiodactyla) in South America. In the Falcón basin, the Pliocene faunas of the Codore and San Gregorio Formations include Toxodontidae gen. et sp. nov. and Protherotheriidae indet. These new data add evidence to the tropical provinciality documented for Astrapotheria, Leontiniidae during the middle Miocene. The Pliocene faunas from the Ware and San Gregorio formations are characterized by the predominance of native South American taxa, despite their proximity to the Isthmus of Panama. Only one North American ungulate herbivore immigrant is present (Camelidae indet.). The Pliocene faunas also document an important landscape change in the region and suggest that ecological processes and biotic interactions could have affected the diversity dynamics and biogeographic patterns of SANUs during the GABI.

Key words

Mammalia, Notoungulata, Litopterna, Astrapotheria, Caviomorpha, Neotropics, Patagonia, Argentina, Colombia, Venezuela, Phylogeny, Biogeography, Eocene, Miocene, Pliocene, Great American Biotic Interchange

Der südamerikanische Kontinent war für einen Grossteil des Känozoikums von den anderen Kontinenten isoliert und bildete die Heimat einer endemischen Säugetierfauna. Zu den charakteristischen Elementen dieser Fauna gehörten die südamerikanisch-einheimischen Huftiere (SANUs): eine Gruppe von huftierartigen Säugetieren, die auf dem Kontinent weit verbreitet und sehr divers waren. Trotz signifikanter wissenschaftlicher Fortschritte sind die phylogenetischen Beziehungen der SANUs noch nicht vollständig geklärt und stellen weiterhin eine grosse Herausforderung der Paleosäugetierkunde dar. Die Evolutionsgeschichte der SANUs und anderer endemischer Säugetiere wird meist in den höheren Breitengraden aufgezeichnet. Da allerdings der Grossteil der heutigen Säugetierdiversität in den niedrigeren Breitengerade zu finden ist, ist es notwendig die Aufzeichnung von neotropischen Fossilien zu erhöhen, um die Evolution von Diversitätsgradienten in Säugetieren besser zu verstehen. Das Ziel dieser Dissertation ist die Studie von aussergewöhnlichen neuen Fossilien, die dazu dienen die phylogenetischen Beziehungen zwischen einer der Hauptkladen der SANUs (Notungulaten) und anderen Plazentatieren zu adressieren. Des Weiteren wird die Systematik und die Diversität neogener Säugetiere basierend auf der Dokumentation von neuen Fossilsammlungen aus dem Norden Südamerikas überprüft.

Das erste Kapitel präsentiert die Beschreibung des ältesten Skeletts eines Notungulaten mit assoziierten dentalen und postkranialen Überresten: *Thomashuxleya externa* (Isotemnidae, Notoungulata) aus dem mittleren Eozän aus Patagonien, Argentinien. Dieses aussergewöhnlich vollständige Exemplar dient als Grundlage für die geschätzte Körpermasse von etwa 235 kg. Des Weiteren ist das Fossil in die Untersuchung einer phylogenetischen Hypothese für die Verwandtschaftsbeziehungen zwischen Notungulaten und anderen Plazentatieren integriert. Eine Analyse, die morphologische und molekulare Daten kombiniert, begünstigt zwar eine begrenzte Anzahl an hypothetischen Stammbäumen, kann jedoch *Thomashuxleya* nicht eindeutig zu Afrotheria oder Laurasiatheria zuordnen. Wenn *Thomashuxleya* monophyletisch an den pleistozänen Notungulaten *Toxodon* (anhand von Kollagensequenzen) gebunden ist, wird es an den Stamm der Euungulaten (Perissodactyla & Artiodactyla) oder als Schwestergruppe zu den Perissodactyla plaziert.

Die Isolation des südamerikanischen Kontinents endete mit der Bildung(Formation?) des Isthmus von Panama, der eine Landbrücke mit dem nordamerikanischen Kontinent formte und dadurch den Austausch der Fauna beider Kontinente ermöglichte. Dieses biotische Ereignis ist bekannt als der grosse amerikanische Faunenaustausch (GABI). Das zweite Kapitel enthält die biogeographische Analyse der südamerikanischen Säugetierfaunen vom Miozän bis zum Pliozän und die Revision der zeitlichen und räumlichen Verteilung der Säugetiere während des GABIs. Es zeigt, dass die tropischen und gemässigten Faunen mindestens seit dem mittleren Miozän klar unterschieden werden können und dokumentiert eine starke Verzerrung des Fossilberichts in Richtung höherer Breitengrade und jüngerer Fundorte, was eine Herausforderung für paleontologische Studien des grossen amerikanischen Faunenaustauschs darstellt.

Das dritte und vierte Kapitel tragen dazu bei, die zeitliche und geographische Lücke im neotropischen Fossilbericht anhand der Beschreibung von neuem Material aus dem Cocinetas (Nordkolumbien) und dem Fálcon (Nordwestvenezuela) Becken zu schliessen. Das dritte Kapitel beschreibt neue Überreste von Riesennagern (Neoepiblemidae, Caviomorpha) aus der Urumaco Formation (spätes Miozän) im Falcon Becken. Es dokumentiert das Vorhandensein von mindestens zwei neoepiblemiden Taxa in der Formation, *Phoberomys* and *Neoepiblema.* Des Weiteren deutet die beobachtete Zahnvariation darauf hin, dass mehrere der zuvor beschriebenen *Phoberomys* Arten verschiedene ontogenetische Stadien einiger weniger Taxa darstellen.

Das vierte Kapitel beschreibt das neogene SANU Material aus dem Cocinetas und dem Fálcon Becken und liefert eine phylogenetische Analyse für Astrapotheriidae and Toxodontidae. Im Cocinetas Becken beinhaltet die Miozänfauna der Castilletes Formation *Hilarcotherium* sp. nov (Astrapotherijdae), cf. *Huilatherium* (Leontiniidae) und *Neodolodus* cf. *colombianus* (Proterotheriidae). Die späte Pliozänfauna der Ware Formation beinhaltet Toxodontinae indet. und die älteste Aufzeichnung eines Camelidae indet. (Artiodactyla) in Südamerika. Die Pliozänfauna der Codore und San Gregorio Formationen im Fálcon Becken beinhalten Toxodontidae gen. et sp. nov. and Protherotheriidae indet. Diese neuen Daten tragen zusätzliche Belege zur tropischen Provinzilatität bei, die für Astrapotheria, Leontiniidae während des mittleren Miozäns dokumentiert ist. Die Pliozänfaunen der Ware und der San Gregorio Formation werden trotz ihrer Nähe zum Isthmus von Panama durch die Dominanz einheimischer südamerikanischer Taxa charakterisiert. Lediglich ein nordamerikanischer, ungulater und pflanzenfressender Einwanderer ist vorhanden (Camelidae indet.). Die Pliozänfaunen belegen ausserdem wichtige Veränderungen der Landschaft in dieser Region und deuten darauf hin, dass ökologische Prozesse und biotische Interaktionen die Dynamik der Diversität sowie die biogeograpischen Muster von SANUs während des grossen amerikanischen Faunenaustausch beeinflusst haben könnten.

Schlüsselwörter

Mammalia, Notoungulata, Litopterna, Astrapotheria, Caviomorpha, Neotropen

Patagonien, Argentinien, Kolumbien, Venezuela, Phylogenese, Biogeographie, Eozän, Miozän, Pliozän, grosser amerikanischer Faunenaustausch

All the chapters of this dissertation are the result of collaborations and are presented as multi-authors publications. Below I detail the contribution of each author for each chapter.

Chapter 1: An exceptionally well-preserved skeleton of *Thomashuxleya externa* (Mammalia, Notoungulata), from the Eocene of Patagonia, Argentina. *Paleontologia Electronica* 20.2.34A: 1-33

Authors: Juan D. Carrillo and Robert J. Asher

Contributions: JDC and RJA designed the research, performed the analysis, and wrote the manuscript; JDC collected the data.

Chapter 2: Neotropical mammal diversity and the Great American Biotic Interchange: spatial and temporal variation in South America's fossil record. *Frontiers in Genetics* 5:451

Authors: Juan D. Carrillo, Analía Forasiepi, Carlos Jaramillo, and Marcelo R. Sánchez-Villagra.

Contributions: JDC, AF, CJ, and MRS-V designed the research; JDC, AF, and CJ collected the data; JDC and CJ performed the analysis; JDC wrote the manuscript; AF, CJ and MRS-V edited the manuscript.

Chapter 3: Giant rodents from the Neotropics: diversity and dental variation of late Miocene neoepiblemid remains from Urumaco, Venezuela. *Paläontologische Zeitschrift* 89(4):1057-1071.

Authors: Juan D. Carrillo, and Marcelo R. Sánchez-Villagra.

Contributions: JDC and MRS-V designed the research, and performed the analysis; JDC wrote the manuscript; MRS-V edited the manuscript; MRS-V funded and organized the field expeditions; JDC collected the data.

Chapter 4: The Neogene record of northern South American native ungulates. Formatted for *Smithsonian Contributions to Paleobiology*

Authors: Juan D. Carrillo, Eli Amson, Carlos Jaramillo, Rodolfo Sánchez, Luis Quiroz, Carlos Cuartas, and Marcelo R. Sánchez-Villagra.

Contributions: MRS-V and CJ funded and organized the field expeditions; RS contributed to the collection and preparation of the material; CJ, LQ and CC collected and analyzed stratigraphic data; JDC, CJ, and MRS-V designed the research; JDC and EA collected morphological data; JDC performed the analyses and wrote the manuscript; EA, CJ, and MRS-V edited the manuscript.

Introduction

South America was isolated from other continents from the early Eocene (ca. 50 Ma) when it separated from Antarctica (Pascual, 2006; Wilf et al. 2013), until the late Miocene-Pliocene (ca. 15-3 Ma) when the formation of the Isthmus of Panama established a land connection with North America (Montes et al. 2015; O'Dea et al. 2016). During this time, South America was home of an endemic mammalian fauna that evolved in isolation, with punctuated dispersal events into the continent from Africa (Simpson, 1980; Croft, 2012, 2016). The Cenozoic can be divided in a series of phases that represent the major events in the mammalian evolution in South America (Figure 1; Patterson and Pascual, 1972; Simpson, 1980; Croft, 2016).

Early South American phase: The South American native ungulates

The early South American phase of mammalian evolution (Figure 1) is characterized by the predominance of endemic taxa such as marsupials, xenarthrans and native ungulates (Croft, 2016). The latter is a group of ungulate-grade placentals that have been classified in 'Meridiungulata' (McKenna and Bell, 1997), most likely a paraphyletic group (Muizon and Cifelli, 2000). They are informally known as South American Native Ungulates ("SANUs"; Welker et al. 2015). SANUs include the clades Astrapotheria, Litopterna, Notoungulata, Pyrotheria, and Xenungulata. Despite substantial recent progress, their phylogenetic relationships are not fully unresolved (Figure 2). The cranial and dental anatomy support the inclusion of Pyrotheria within Notoungulata (Billet, 2010). Amino acid sequences of collagen chains and postcranial anatomy support a close relationship between Notoungulata and Litopterna (Horovitz, 2004; Buckley, 2015; Welker et al. 2015). Cranial and dental anatomy suggest a close relationship between Astrapotheria and Notoungulata (Billet, 2010), but this was not supported by a cladistics analysis of postcranial anatomy alone based on 70 taxa and 240 characters (Horovitz, 2004). The consideration of SANU groups relationships among them and to other clades of placentals can benefit from our understanding of the phylogeny of the latter.

Studies on placental phylogenies have

Figure 1. Geologic time scale of the Cenozoic illustrating the South American Land Mammal Ages (SALMAs), and the phases of mammal evolution and dispersal events (Croft, 2016). The South American Native Ungulates are one of the predominant groups during the Early South American phase, represented in the image by the middle Eocene notoungulate *Thomashuxleya externa* (Artwork by Stjepan Lukac). The Trans-Atlantic Dispersal Interval records the arrival of caviomorph rodents and platyrrhine monkeys. The Late South American phase records the diversification of caviomorph and platyrrhines, and the appearance of new native lineages; this is illustrated by the late Miocene fauna of the Urumaco Formation, in northwestern Venezuela (Artwork by Jorge González; Sánchez-Villagra et al. 2010). The Interamerican phase records the mixing of faunas from North and South America as result of the Great American Biotic Interchange; this is illustrated by the Pleistocene fauna in Falcón, northwestern Venezuela (Artwork by Jorge González; Sánchez-Villagra, 2012).

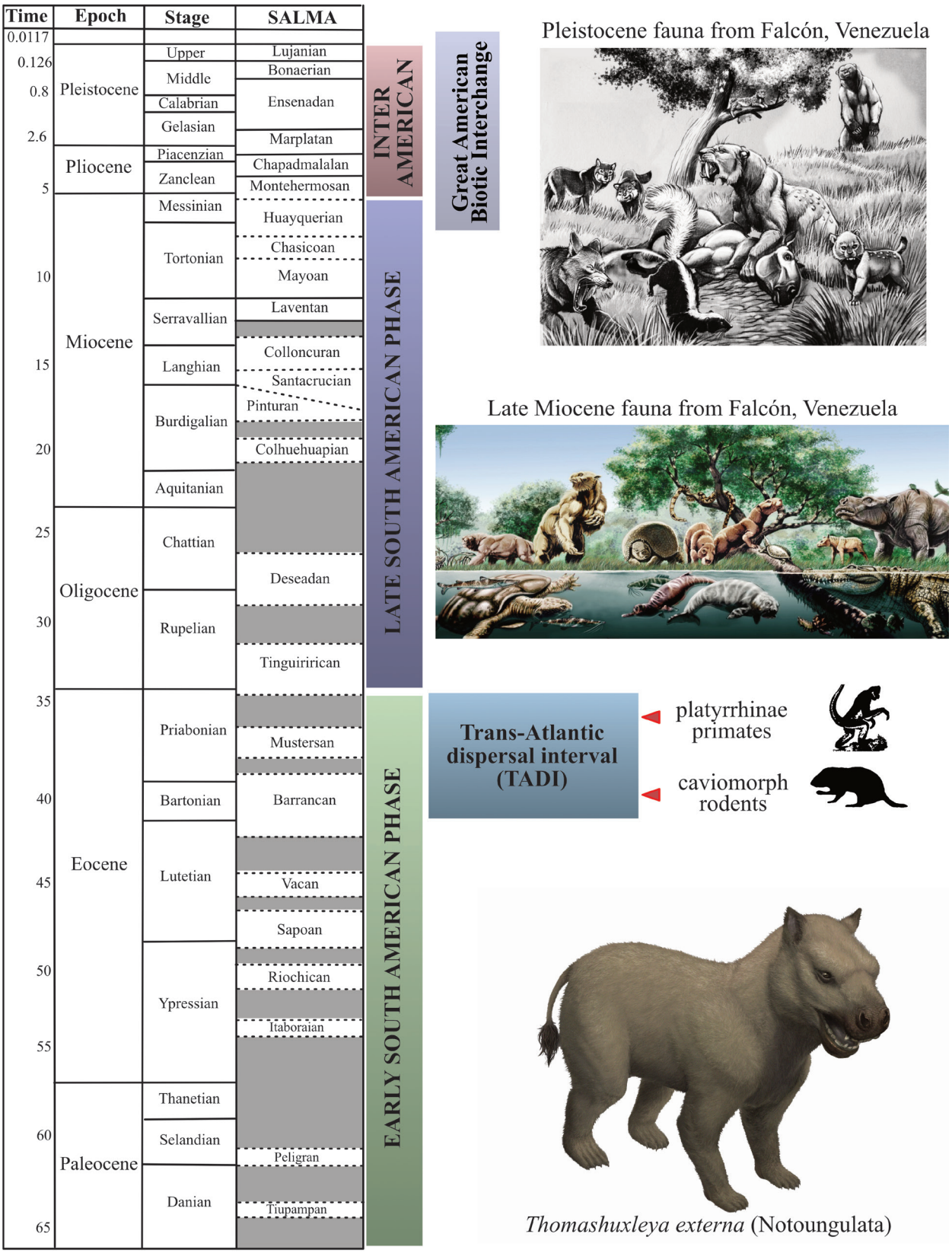

reached a high level of agreement in the recognition of four major clades: Afrotheria, Euarchontoglires, Laurasiatheria, and Xenarthra (Murphy et al. 2001; Tarver et al. 2016). This solid framework has not led to the resolution of the phylogenetic relationships of SANUs with other placentals. O'Leary et al. (2013) combined morphological data for

extinct and extant taxa, and molecular data for extant taxa, to study the relationships among placentals. O'Leary et al. (2013) placed the Paleogene taxa *Thomashuxleya* (Notoungulata) and *Carodnia* (Xenungulata) within Afrotheria, whereas *Protolipterna* and *Didolodus* (Litopterna) were recovered within Laurasiatheria. Welker et al. (2015; see also Buckley, 2015) presented the most significant break-through in this question enabling collagen sequences of Pleistocene representatives of Notoungulata (*Toxodon*) and Litopterna (*Macrauchenia*) to further inform their phylogenetic relationships. Welker et al. (2015) recovered Notoungulata and Litopterna as sister group of Perissodactyla, within Laurasiatheria. Further analysis combining different data sources are needed to support or reject the different phylogenetic hypothesis of SANUs.

Late South American phase: The fossil record of northern South America

The early South American phase finishes with the Trans-Atlantic Dispersal Interval, which refers to the arrival of caviomorph rodents and platyrrhine monkeys from Africa (Figure 1; Croft, 2016). Caviomorph rodents arrived to South America by the middle Eocene (ca. 41 Ma; Antoine et al. 2012; Voloch et al. 2013), and they rapidly diversified (Vucetich et al. 2015). The earliest record of platyrrhine primates is from the late Eocene (Figure 1; Bond et al. 2015); South American monkeys subsequently diversified and dispersed throughout South America and the Antilles (Kay, 2015).

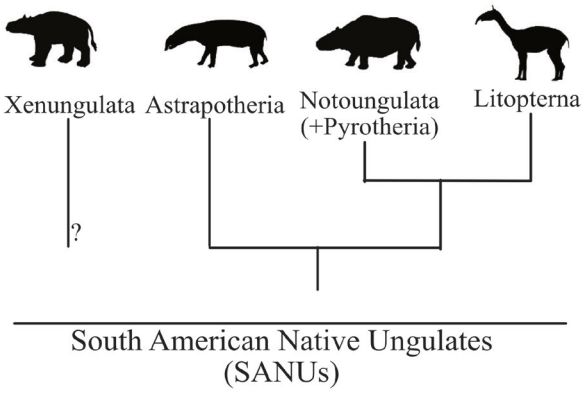

Figure 2. Hypothesis of phylogenetic relationships of South American Native Ungulates, following Welker et al. (2015), and Billet (2010).

The late South American phase covers the diversification of caviomorphs and platyrrhines, and extends until the beginning of the Great American Biotic Interchange (Figure 1; Croft, 2016). Despite the growing knowledge of the fossil faunas from the Neotropics (MacFadden, 2006), there are still major temporal and geographic gaps in the mammalian fossil record from the Oligocene to the Pliocene (Figure 3). Mammals attain their highest species diversity in low latitudes (Rolland et al. 2014), and more data from the Neotropics is needed to better understand the mammal evolution in South America.

One of the better known faunal assemblages from northern South America comes from deposits near Urumaco, in the Falcón basin (Figure 3; Sánchez-Villagra et al. 2010). The Urumaco sequence includes four geological formations with reports of fossil mammals: Socorro, Urumaco, Codore, and San Gregorio, which together span from the middle Miocene to the late Pliocene

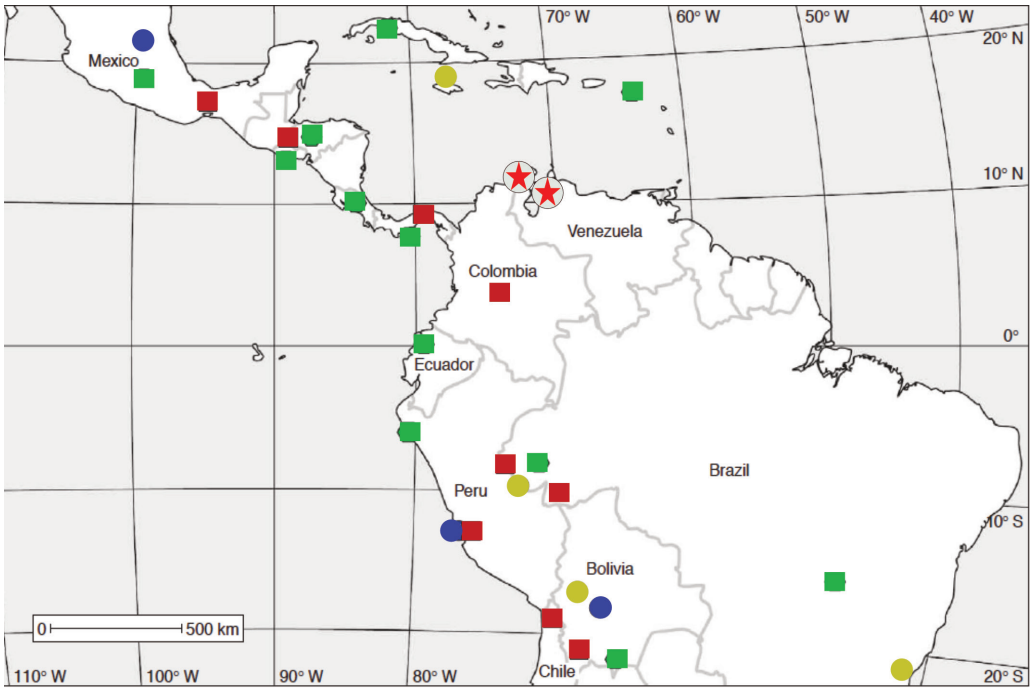

Figure 3. Representative fossil Neotropical localities (modified from MacFadden, 2006). Eocene and Oligocene localities are shown as yellow circles, Miocene localities are red squares, Pliocene localities are blue circles, and Pleistocene localities are green squares. The starts show the location of the Cocinetas basin (Miocene-Pliocene) in Colombia, and the Falcón basin (Miocene-Pliocene) in Venezuela.

(Quiroz and Jaramillo, 2010). To date, most of the mammal systematic work has been carried out in the Urumaco Formation (late Miocene), which is characterized by high diversity of xenarthrans (Straehl et al. 2012) and the presence of giant neoepiblemid caviomorphs (Horovitz et al. 2010). The Codore and San Gregorio formations remain less explored. More recently, another tropical fauna was described from the Cocinetas basin, in northern Colombia (Figure 3; Moreno et al. 2015). Mammal reports from the Cocinetas basin come from the Castilletes (middle Miocene) and Ware (late Pliocene) formations. Due to their geographic proximity and temporal overlap, the faunas from the Falcón and Cocinetas basins promise to provide important data to better understand the faunal evolution in northern South America during the late Neogene.

Interamerican phase: The Great American Biotic Interchange

The late South American phase finishes with the Great American Biotic Interchange (GABI; Figure 1), which refers to the faunal exchange between North and South America as a consequence of the formation of the Isthmus of Panama (Marshall et al. 1982; Webb, 2006; Woodburne, 2010). The timing of the closure of the Isthmus of Panama is a subject of an ongoing debate (e.g., Montes et al. 2015; O'Dea et al. 2016). The geologic collision between Central and South America took place in the early Miocene, with a subsequent shallowing of the Isthmus with presence of narrow and shallow marine passage by the middle Miocene. The final closure of the Isthmus occurred sometime

between ca.15 and ca.3 Ma (Figure 4; Coates et al. 2004; Montes et al. 2012; Coates and Stallard, 2013).

The GABI records some early migrations of mammal by the late Miocene, but most of the interchange took place after the Pliocene (Webb, 2006; Cione et al. 2015), and a series of migration pulses can be recognized in the fossil record (Woodburne, 2010). Most of the records that document the GABI come from higher latitudes (Webb, 1991), and environmental variables and biogeography needs to be integrated to better understand the GABI (Webb, 1991; Vrba, 1992; Woodburne, 2010). Therefore, more data from lower latitudes are needed to constrain the timing of the different migrations, and characterize the biogeography during the interchange.

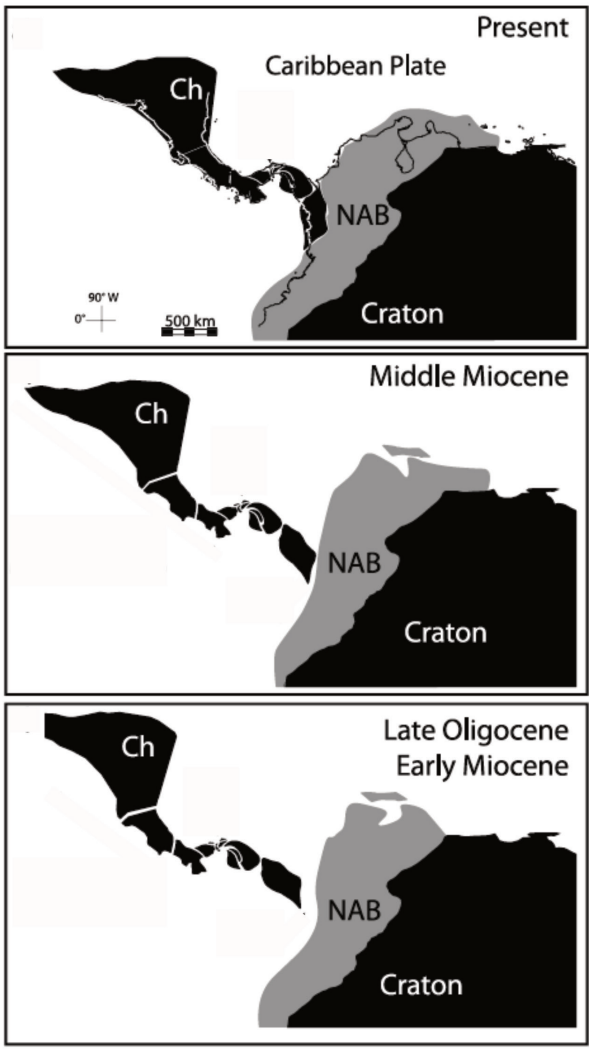

Figure 4. Reconstruction of the formation of the Isthmus of Panama (modified from Montes et al. 2012). Ch= Chortis block, NAB= northern Andean block.

Aims and overview

Despite recent advances, the phylogenetic relationship of SANUs are not fully resolved. The combination of morphological and molecular data in extant and extinct taxa can provide more precise and robust hypotheses for several extinct clades of mammals (e.g., Asher et al. 2005; Muizon et al. 2015; Pattinson et al. 2015). Regarding the interrelationships within the different clades of SANUs, new material from the Neotropics has the potential to provide data to inform their phylogenetic relationships and biogeography. Neotropical data should also reveal if the timing and outcome of the GABI is homogeneous in South America, or if the environmental changes and geography affected the GABI dynamics, as it has been suggested (Webb, 1991; Woodburne, 2010; Bacon et al. 2016).

This work aims to revise the systematics and biogeography of different groups of SANUs, with an emphasis in the Neotropics. We tested previous hypothesis and provide new ones regarding the phylogenetic relationship of Notoungulata. We also revised the interrelationships and biogeography of different clades within Astrapotheria, Litopterna, and Notoungulata, on the light of the new discoveries from the Cocinetas

and Falcón basins. Finally, we studied the Miocene and Pliocene faunas from northern South America, in the context of the GABI.

In chapter one, we described the oldest notoungulate skeleton with associated dental and postcranial remains: *Thomashuxleya externa* (Isotemnidae, Notoungulata) from the middle Eocene of Patagonia, Argentina. We provide a body size estimate, described its osteology and bone histology and studied its phylogenetic position. The material we studied belonged to a skeletally matured individual, and for it we estimated a weight of approximately 235 kg. A phylogenetic analysis of a combined DNA, collagen, and morphology matrix favour a limited number of hypothetical trees, but it cannot definitely arbitrate between affinities with Afrotheria or Laurasiatheria. When constrained as monophyletic with the Pleistocene notoungulate *Toxodon* (known for collagen sequences), *Thomashuxleya* is reconstructed on the stem to Euungulata (Perissodactyla + Artiodactyla) or as sister to Perissodactyla.

Chapter two presents a biogeographic analysis of the mammalian faunas in South America from the Miocene to the Pliocene, and a revision of the temporal and geographic distribution of mammals during the GABI. It shows that the tropical and temperate mammal faunas can be clearly differentiated since at least the middle Miocene, and documents a strong sampling bias in the fossil record towards higher latitudes and younger localities, which represents a challenge to paleontological studies of the GABI.

Chapter three and four are contributions towards filling this gap of knowledge in the Neotropical paleomammalogy. Chapter three presents a description of new remains of giant rodents (Neoepiblemidae, Caviomorpha) from the Urumaco Formation (late Miocene), in the Falcón basin. We documented the dental variation that indicates the presence of at least two taxa, namely *Phoberomys* and *Neoepiblema*. Furthermore, the dental variation suggests that several of the species previously described within *Phoberomys* represent different ontogenetic stages of only few taxa.

In chapter four, we studied the systematics, palaeogeography, and palaeoecology of Neogene SANUs from northern South America. We described new SANU material from the Cocinetas and Falcón basins, and we provided a phylogenetic analysis for Astrapotheriidae and Toxodontidae. In the Cocinetas basin, the middle Miocene fauna of the Castilletes Formation includes *Hilarcotherium* sp. nov. (Astrapotheriidae), cf. *Huilatherium* (Leontiniidae), and *Neodolodus* cf. *colombianus* (Proterotheriidae). The late Pliocene fauna of the Ware Formation includes Toxodontinae indet. and the putative oldest record of Camelidae indet. in South America. In the Falcón basin, the Pliocene faunas of the Codore and San Gregorio Formations include Toxodontidae gen. et sp. nov. and Protherotheriidae indet. These new data document a tropical provinciality during the middle Miocene for some SANU clades (e.g., Astrapotheria, Leontiniidae), in contrast with the widespread distribution of

other mammals present in the assemblage. The Pliocene faunas from the Ware and San Gregorio formations are characterized by the predominance of native taxa, despite its proximity to the Isthmus of Panama. Only one North American ungulate herbivore immigrant is present (Camelidae indet.). The Pliocene faunas also document an important landscape change in the region and suggest that ecological processes and biotic interactions could have affected the diversity dynamics and biogeographic patterns of SANUs during the Great American Biotic Interchange.

References

Antoine, P.-O., L. Marivaux, D. A. Croft, G. Billet, M. Ganerod, C. Jaramillo, T. Martin, M. J. Orliac, J. Tejada, A. J. Altamirano, F. Duranthon, G. Fanjat, S. Rousse, and R. S. Gismondi. 2012. Middle Eocene rodents from Peruvian Amazonia reveal the pattern and timing of caviomorph origins and biogeography. *Proceedings of the Royal Society B: Biological Sciences 279*:1319–1326.

Asher, R. J., R. J. Emry, and M. C. Mckenna. 2005. New material of *Centetodon* (Mammalia, Lipotyphla) and the importance of (missing) DNA sequences in systematic paleontology. *Journal of Vertebrate Paleontology* 25:911–923.

Bacon, C. D., P. Molnar, A. Antonelli, A. J. Crawford, C. Montes, and M. C. Vallejo-Pareja. 2016. Quaternary glaciation and the Great American Biotic Interchange. *Geology* 44:375–378.

Billet, G. 2010. New observations on the skull of *Pyrotherium* (Pyrotheria, Mammalia) and new phylogenetic hypotheses on South American ungulates. *Journal of Mammalian Evolution* 17:21–59.

Bond, M., M. F. Tejedor, K. E. Campbell, L. Chornogubsky, N. Novo, and F. Goin. 2015. Eocene primates of South America and the african origins of new world monkeys. *Nature* 520:538–541.

Buckley, M. 2015. Ancient collagen reveals evolutionary history of the endemic South American "ungulates." *Proceedings of Royal Society of Biology* 282:20142671.

Cione, A. L., G. M. Gasparini, E. Soibelzon, L. H. Soibelzon, and E. P. Tonni. 2015. The GABI in Southern South America; pp. 71–96 in *The Great American Biotic Interchange: A South American Perspective*. Springer Netherlands, Dordrecht.

Coates, A. G., and R. F. Stallard. 2013. How old is the isthmus of Panama? *Bulletin of Marine Science* 89:801–813.

Coates, A. G., L. S. Collins, M. P. Aubury, and W. A. Berggren. 2004. The geology of the Darien, Panama, and the late Miocene-Pliocene collision of the Panama arc with northwestern South America. *Bulletin of the Geological Society of Amer*ica 116:1327–1344.

Croft, D. A. 2012. Punctuated isolation. The making and mixing of South America's mammals; pp. 9–19 in B. D. Patterson and L. P. Costa (eds.), *Bones, clones and biomes. The history and geography of recent neotropical mammals*. University of Chicago Press, Chicago and London.

Croft, D. A. 2016. *Horned Armadillos and Rafting Monkeys. The Fascinating Fossil Mammals of South America*. Indiana University Press, Bloomington and Indianapolis.

Horovitz, I. 2004. Eutherian mammal systematics and the origins of South American ungulates as based on postcranial osteology. *Bulletin of Carnegie Museum of Natural History* 36:63–79.

Horovitz, I., M. R. Sánchez-Villagra, M. G. Vucetich, and O. A. Aguilera. 2010. Fossil rodents from the late Miocene Urumaco and middle Miocene Cumaca Formations, Venezuela; pp. 214–232 in M. R. Sánchez-Villagra, O. A. Aguilera, and A. A. Carlini (eds.), *Urumaco and venezuelan paleontology. The fossil record of the northern Neotropics*. Indiana University Press, Bloomington and Indianapolis.

Kay, R. F. 2015. Biogeography in deep time - What do phylogenetics, geology, and paleoclimate tell us about early platyrrhine evolution? *Molecular Phylogenetics and Evolution* 82:358–374.

MacFadden, B. J. 2006. Extinct mammalian biodiversity of the ancient New World tropics. *Trends in Ecology and Evolution* 21:157–165.

Marshall, L. G., S. D. Webb, J. J. Sepkoski, and D. M. Raup. 1982. Mammalian evolution and the Great American Interchange. *Science* 215:1351–1357.

McKenna, M. C., and S. K. Bell. 1997. *Classification of Mammals above the Species Level*. Columbia University Press, New York.

Montes, C., G. Bayona, A. Cardona, D. M. Buchs, C. A. Silva, S. Morón, N. Hoyos, D. A. Ramírez, C. A. Jaramillo, and V. Valencia. 2012. Arc-continent collision and orocline formation: Closing of the Central American seaway. *Journal of Geophysical Research: Solid Earth* 117:1–25.

Montes, C., A. Cardona, C. Jaramillo, A. Pardo, J. C. Silva, V. Valencia, C. Ayala, L. C. Pérez-Angel, L. Rodriguez-Parra, V. Ramirez, and H. Niño. 2015. Middle Miocene closure of the Central American Seaway. *Science* 348:226–229.

Moreno, F., A. J. W. Hendy, L. Quiroz, N. Hoyos, D. S. Jones, V. Zapata, S. Zapata, G. A. Ballen, E. Cadena, A. L. Cárdenas, J. D. Carrillo-Briceño, J. D. Carrillo, D. Delgado-Sierra, J. Escobar, J. I. Martínez, C. Martínez, C. Montes, J. Moreno, N. Pérez, R. Sánchez, C. Suárez, M. C. Vallejo-Pareja, and C. Jaramillo. 2015. Revised stratigraphy of Neogene strata in the Cocinetas Basin, La Guajira, Colombia. *Swiss Journal of Palaeontology* 134:5–43.

Muizon, C. de, R. L. Cifelli. 2000. The "condylarths" (archaic Ungulata, Mammalia) from the early Palaeocene of Tiupampa (Bolivia): implications on the origin of the South American ungulates. *Geodiversitas* 22(1):47-150

Muizon, C. de, G. Billet, C. Argot, S. Ladeveze, and F. Goussard. 2015. *Alcidedorbignya inopinata*, a basal pantodont (Placentalia , Mammalia) from the early Palaeocene of Bolivia: anatomy, phylogeny and palaeobiology. *Geodiversitas* 37:397–634.

Murphy, W. J., E. Eizirik, W. E. Johnson, Y. P. Zhang, O. A. Ryder, and S. J. O'Brien. 2001. Molecular phylogenetics and the origins of placental mammals. *Nature* 409:614–618.

O'Dea, A., H. A. Lessios, A. G. Coates, R. I. Eytan, S. A. Restrepo-Moreno, A. L. Cione, L. S. Collins, A. de Queiroz, D. W. Farris, R. D. Norris, R. F. Stallard, M. O. Woodburne, O. Aguilera, M.-P. Aubry, W. A. Berggren, A. F. Budd, M. A. Cozzuol, S. E. Coppard, H. Duque-Caro, S. Finnegan, G. M. Gasparini, E. L. Grossman, K. G. Johnson, L. D. Keigwin, N. Knowlton, E. G. Leigh, J. S. Leonard-Pingel, P. B. Marko, N. D. Pyenson, P. G. Rachello-Dolmen, E. Soibelzon, L. Soibelzon, J. A. Todd, G. J. Vermeij, and J. B. C. Jackson. 2016. Formation of the Isthmus of Panama. *Science Advances* 2:e1600883.

O'Leary, M. A., J. I. Bloch, J. J. Flynn, T. J. Gaudin, A. Giallombardo, N. P. Giannini, S. L. Goldberg, B. P. Kraatz, Z. Luo, J. Meng, X. Ni, M. J. Novacek, F. A. Perini, Z. S. Randall, G. W. Rougier, E. J. Sargis, M. T. Silcox, N. B. Simmons, M. Spaulding, P. M. Velazco, M. Weksler, J. R. Wible, and A. L. Cirranello. 2013. The placental mammal ancestor and the post-K-Pg radiaton of placentals. *Science* 339:662–667.

Pascual, R. 2006. Evolution and geography: The biogeographic history of South American land mammals. *Annual of the Missouri Botanical Garden* 93:209–230.

Patterson, B., and Pascual R. 1972. The fossil mammal fauna of South America; pp.247-309 in A. Keast, F. C. Erk, and B. Glass (eds.), *Evolution, mammals, and southern continents. State Univ. New York Press. Albany.*

Pattinson, D. J., R. S. Thompson, A. K. Piotrowski, and R. J. Asher. 2015. Phylogeny, paleontology, and primates: do incomplete fossils bias the tree of life? *Systematic Biology* 64:169–86.

Quiroz, L. I., and C. A. Jaramillo. 2010. Stratigraphy and sedimentary environments of Miocene shallow to marginal marine deposits in the Urumaco trough, Falcón basin, western Venezuela; pp. 153–172 in M. R. Sánchez-Villagra, O. A. Aguilera, and A. A. Carlini (eds.), *Urumaco and venezuelan paleontology. The fossil record of the northern Neotropics*. Indiana University Press, Bloomington and Indianapolis.

Rolland, J., F. L. Condamine, F. Jiguet, and H. Morlon. 2014. Faster speciation and reduced extinction in the Tropics contribute to the mammalian latitudinal diversity gradient. *PLoS Biology* 12:e1001775.

Sánchez-Villagra, M. R., O. A. Aguilera, and A. A. Carlini. 2010. *Urumaco and Venezuelan Paleontology. The Fossil Record of the Northern Neotropics*. Indiana University

Press, Bloomington and Indianapolis.

Sánchez-Villagra, M. R. 2012. *Venezuela Paleontológica. Evolución de la biodiversidad en el pasado geológico*. Universität Zurich, Zürich.

Simpson, G. G. 1980. *Splendid Isolation. The Curious History of South American Mammals*. Yale University Press, New Haven and London.

Straehl, F., M. Chassagne, and A. A. Carlini. 2012. La diversidad e historia evolutiva de las perezas, cachicamos y sus parientes; pp. 283–300 in M. R. Sánchez-Villagra (ed.), *Venezuela Paleontológica. Evolución de la biodiversidad en el pasado geológico*. Universität Zurich, Zürich.

Tarver, J. E., M. dos Reis, S. Mirarab, R. J. Moran, S. Parker, J. E. O'Reilly, B. L. King, M. J. O'Connell, R. J. Asher, T. Warnow, K. J. Peterson, P. C. J. Donoghue, and D. Pisani. 2016. The interrelationships of placental mammals and the limits of phylogenetic inference. *Genome Biology and Evolution* 8:330–344.

Voloch, C. M., J. F. Vilela, L. Loss-Oliveira, and C. G. Schrago. 2013. Phylogeny and chronology of the major lineages of New World hystricognath rodents: insights on the biogeography of the Eocene/Oligocene arrival of mammals in South America. *BMC Research Notes* 6:160.

Vrba, E. S. 1992. Mammals as a key to evolutionary theory. *Journal of Mammalogy* 73:1–28.

Vucetich, M. G., M. Arnal, C. M. Deschamps, M. E. Perez, and E. C. Vieytes. 2015. A brief history of caviomorph rodents as told by the fossil record; pp. 11–62 in A. I. Vassallo and D. Antenucci (eds.), *Biology of Caviomorph rodents: Diversity and evolution*. SAREM, Buenos Aires.

Webb, S. D. 1991. Ecogeography and the Great American Interchange. *Paleobiology* 17:266–280.

Webb, S. D. 2006. The Great American Biotic Interchange: Patterns and processes. *Annals of the Missouri Botanical Garden* 93:245–257.

Welker, F., M. J. Collins, J. A. Thomas, M. Wadsley, S. Brace, E. Cappellini, S. T. Turvey, M. Reguero, J. N. Gelfo, A. Kramarz, J. Burger, J. Thomas-Oates, D. A. Ashford, P. D. Ashton, K. Rowsell, D. M. Porter, B. Kessler, R. Fischer, C. Baessmann, S. Kaspar, J. V Olsen, P. Kiley, J. A. Elliott, C. D. Kelstrup, V. Mullin, M. Hofreiter, E. Willerslev, J.-J. Hublin, L. Orlando, I. Barnes, and R. D. E. MacPhee. 2015. Ancient proteins resolve the evolutionary history of Darwin's South American ungulates. *Nature* 522:81–84.

Wilf, P., N. R. Cúneo, I. H. Escapa, D. Pol, and M. O. Woodburne. 2013. Splendid and seldom isolated: The paleobiogeography of Patagonia. *Annual Review of Earth and Planetary Sciences* 41:561–603.

Woodburne, M. 2010. The Great American Biotic Interchange: Dispersals, tectonics, climate, sea level and holding pens. *Journal of Mammalian Evolution* 17:245–264.

CHAPTER 1

An exceptionally well-preserved skeleton of *Thomashuxleya externa* (Mammalia, Notoungulata) from the Eocene of Patagonia, Argentina

Thomashuxleya externa. Artwork: Stjepan Lukac

Juan D. Carrillo and Robert J. Asher. 2017. *Paleontologia Electronica*, 20.2.34.A:1-33

Palaeontologia Electronica
palaeo-electronica.org

An exceptionally well-preserved skeleton of *Thomashuxleya externa* (Mammalia, Notoungulata), from the Eocene of Patagonia, Argentina

Juan D. Carrillo and Robert J. Asher

ABSTRACT

We describe one of the oldest notoungulate skeletons with associated craniodental and postcranial elements: *Thomashuxleya externa* (Isotemnidae) from Cañadón Vaca in Patagonia, Argentina (Vacan subage of the Casamayoran SALMA, middle Eocene). We provide body mass estimates given by different elements of the skeleton, describe the bone histology, and study its phylogenetic position. We note differences in the scapulae, humerii, ulnae, and radii of the new specimen in comparison with other specimens previously referred to this taxon. We estimate a body mass of 84 ± 24.2 kg, showing that notoungulates had acquired a large body mass by the middle Eocene. Bone histology shows that the new specimen was skeletally mature. The new material supports the placement of *Thomashuxleya* as an early, divergent member of Toxodontia. Among placentals, our phylogenetic analysis of a combined DNA, collagen, and morphology matrix favor only a limited number of possible phylogenetic relationships, but cannot yet arbitrate between potential affinities with Afrotheria or Laurasiatheria. With no constraint, maximum parsimony supports *Thomashuxleya* and *Carodnia* with Afrotheria. With Notoungulata and Litopterna constrained as monophyletic (including *Macrauchenia* and *Toxodon* known for collagens), these clades are reconstructed on the stem to Euungulata (i.e., Perissodactyla and Artiodactyla). Unconstrained, Bayesian analysis weakly supports the possibility that *Thomashuxleya* is a stem xenarthran; with Notoungulata and Litopterna constrained as monophyletic, the two clades are recovered as sister to Perissodactyla. Anatomical data sampled thus far for *Thomashuxleya*, combined with collagen amino acids for Pleistocene meridiungulates, substantially limit the number of possible affinities for endemic South American species among mammals, although ambiguity still remains.

INTRODUCTION

South America was isolated during most of the Cenozoic and was home to a highly endemic fauna (Simpson, 1980; Pascual, 2006; Wilf et al., 2013). South American Native Ungulates, or "SANUs" (Welker et al., 2015), were classified in Meridiungulata by McKenna (1975). Meridungulates are a conspicuous faunal element of the South American Cenozoic, with an extensive fossil record that spans the early Paleocene (~ 64 Ma, Tiupampan South American Land Mammal age or SALMA; Gelfo et al., 2009; Woodburne et al., 2014a, 2014b) to late Pleistocene (~11-7 ka, Cione et al., 2003; ~ 11-13 ka, Barnosky and Lindsey, 2010). Notoungulata is the major clade within Meridiungulata and exhibits a high taxonomic diversity (> 140 genera and 13 families; Croft, 1999), large morphological disparity, wide range of body masses (Giannini and García-López, 2014), different degrees of hypsodonty, and diverse diets (MacFadden, 2005; Townsend and Croft, 2008; Cassini et al., 2011; Madden, 2015). The monophyly of Notoungulata is generally accepted, with Pyrotheria sometimes included (Patterson, 1977; Billet, 2010, 2011) or excluded (Roth, 1903; Cifelli, 1993; Simpson, 1978). Alignments of amino acid residues of alpha 1 and 2 collagen chains support a close relationship of Pleistocene members of Notoungulata (*Toxodon*) and Litopterna (*Macrauchenia*) with extant Perissodactyla (Welker et al., 2015). Another analysis of alpha 1 and 2 collagen amino acids also supported *Toxodon* and *Macrauchenia* with perissodactyls. However, this study (Buckley, 2015, figure 2) gave likelihood bootstrap support values below 50 for this clade, and (unlike Welker et al., 2015) the alignments from Buckley (2015) are not publicly accessible as of this writing.

Most of the earliest members of the notoungulate radiation in South America are known from dental and isolated postcranial remains (e.g., Horovitz, 2004; Bergqvist, et al., 2007; Shockey, and Flynn, 2007; Lorente et al., 2014; Lorente, 2015). Specimens with associated cranial and postcranial elements are extremely rare. The Isotemnidae (Notoungulata) has been interpreted as a basal group within Toxodontia (Simpson, 1936; Cifelli, 1993). More recent evidence suggests that Isotemnidae could be polyphyletic (Billet, 2011) and defined by plesiomorphic traits among Toxodontia (Simpson, 1967; Billet, 2011).

Remains of *Thomashuxleya* (Isotemnidae) are among the earliest known associated notoungulate skeletons (Simpson, 1936, 1967). However, the original descriptions of Simpson were idealized and based on a composite skeleton representing three different genera: *Thomashuxleya, Anisotemnus*, and *Pleurostylodon* (Simpson, 1967; Shockey and Flynn, 2007). This reduces the value of Simpson's skeletal reconstruction for palaeobiological inference in general and phylogenetic analysis in particular. *Thomashuxleya* is middle Eocene in age, and our material derives from the Vacan subage of the Casamayoran SALMA, older than the adjacent Barrancan subage (Cifelli, 1985; Gelfo et al., 2009; Kay et al., 1999; Woodburne et al., 2014a). *Thomashuxleya* has previously been referred to a relatively basal clade within Toxodontia (Billet, 2011), making it particularly relevant to understand the early radiation of notoungulate mammals.

At least 28 mammal taxa are recognized for the Cañadón Vaca local fauna (Cifelli, 1985, table 5; Shockey and Flynn, 2007). Among Isotemnidae (*sensu* McKenna and Bell, 1997), four species are present: *Pleurostylodon similis*, *Isotemnus primitivus*, *Thomashuxleya externa*, and *Anisotemnus distentus* (Cifelli, 1985; Shockey and Flynn, 2007).

In this contribution, we describe a specimen consisting of a single individual of *Thomashuxleya externa* with a well-preserved skull and jaws associated with postcrania from Cañadón Vaca, east of Colhué Huapí Lake in Chubut Province, Argentina (Figure 1) (Simpson, 1948; Cifelli, 1985). Parts of most elements of the skeleton are represented, including the skull, mandible, vertebrae, fore- and hind-limbs, shoulder, and pelvic girdles. Associated remains of other individuals found at the same locality include a partially articulated manus. This discovery provides an unusually complete anatomical basis to study the biology and phylogenetic position of an early member of toxodont notoungulates.

MATERIALS AND METHODS

Institutional Abbreviations

MPEF-PV: Museo Paleontológico Egidio Feruglio-Paleontolgía de Vertebrados, Trelew, Chubut, Argentina; AMNH: American Museum of Natural History, New York, USA; MNHN: Muséum national d'Histoire naturelle, Paris, France.

Anatomical Description

We follow Smith and Dodson (2003) for the dental orientation, where mesial and distal designate the tooth surface directions facing forward and away from the mandibular symphysis, respec-

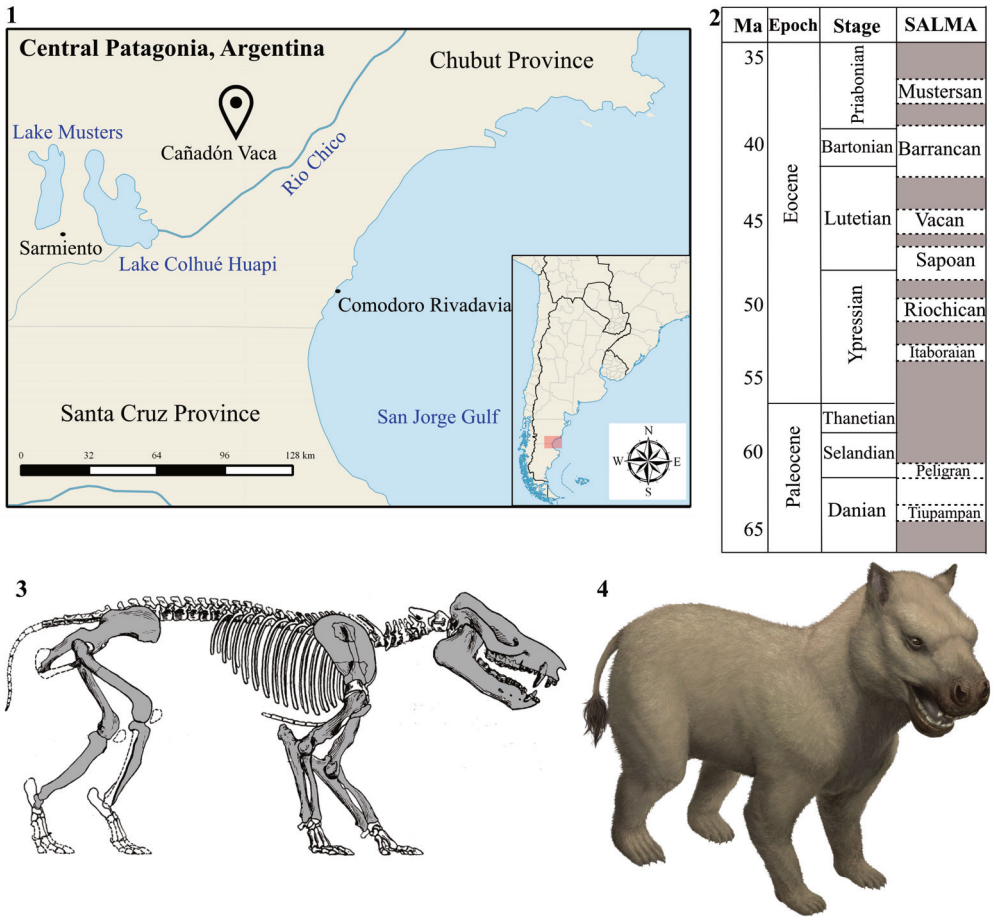

FIGURE 1. Geographical and stratigraphical occurrence of MPEF-PV 8166. **1** location of Cañadón Vaca, Chubut, Argentina; **2** Paleogene time table and South American Land Mammal Ages (SALMAs) after (Woodburne et al. 2014a,b); **3** skeletal restoration of *Thomashuxleya* modified from Simpson (1936); **4** artistic reconstruction of *Thomashuxleya externa* (by Stjepan Lukac).

tively. We follow Madden (1990) for the notoungulate dental terminology and Cerdeño et al. (2012) for the orientation of the postcranial bones.

The skull, mandible, and dentition of MPEF-PV 8166 were compared with different isotemnids as reviewed by Simpson (1967) and the original descriptions of Ameghino (1901). The postcranial elements of MPEF-PV 8166 were compared with AMNH 28905 referred to *T. externa* and originally described by Simpson (1936, 1967), and recently reviewed by Shockey and Flynn (2007). In addition, O'Leary et al. (2013) included much of the anatomy of published specimens in their phylogenetic study of living and fossil mammals. We made additional comparisons with other isotemnid specimens as described by Simpson (1936, 1967) and reviewed by Shockey and Flynn (2007), and also with other basal notoungulates (Bergqvist et al., 2007; Lorente et al., 2014; Lorente, 2015). Our associated remains of *Thomashuxleya* (primarily MPEF-PV 8166) provided the basis for revising and scoring new postcranial character states for *T. externa* using the morphological dataset of O'Leary et al. (2013). Our revised character states have been accessioned in MorphoBank (Project 2084).

Body Mass Estimation

We used the specimen to test the congruence between body mass estimations with regression equations from the crania and postcrania. We took standard linear measurements of the limb bones, skull, and dentition with calipers to the nearest 0.1 mm. When the right and left limb bones could be measured, we used the average. In order to generate body mass estimations for MPEF-PV 8166, we used craniodental regression equations selected from Janis (1990) and multivariate regression algorithms following Mendoza et al. (2006). Postcranial regression equations follow Scott (1990) for the

limb bones and Tsubamoto (2014) for the astragalus (see Appendix 1-2).

The regression equations were selected based on their high r^2 value (> 0.90), a percentage of predicted error (PE) below 40%, and presence of relevant anatomy in MPEF-PV 8166. Janis (1990) and Scott (1990) obtained regression equations using a dataset of extant ungulates and these have been used previously to estimate body mass for notoungulates (e.g., Cassini et al., 2012;Elissamburu, 2012). The dataset of Tsubamoto (2014) included several orders of living mammals.

To obtain body mass estimates we log-transformed (base 10) the body mass estimates from the regression equations from Janis (1990) and Scott (1990), and used a natural log transformation for Tsubamoto (2014). We compared the results from the different subsets of measurements, namely skull, teeth, long bones, and astragalus. We calculated the statistical descriptors and moments (minimum, maximum and mean values, median, mode, skewness, and kurtosis). We resampled with replacement (i.e., bootstrap) with 1000 replications and calculated 95% confidence intervals (CI) using R (R Core Team, 2016).

Bone Histology

We took a cortical slice of 1 cm from the midshaft of the right femur. The section was embedded in Araldite® 2020 prior to sawing and grinding. For the production of thin sections we followed protocols of Straehl et al. (2013). The section (PHZ 950) was observed in normal transmitted and cross-polarized light using a Leica DM 2500 M microscope equipped with a Leica DFC 420 C digital camera. In order to infer the bone microstructure, we also took a photograph of the complete section and transformed to a binary image with Affinity Designer® 1.5.4, where black represents the bone and white the cavities.

Phylogenetic Analysis

Relationships of *Thomashuxleya* within Notoungulata. To study the phylogenetic relationship of *Thomashuxleya* within Isotemnidae, and with other Paleogene notoungulates, we added the information of the new *Thomashuxleya* specimen (MPEF-PV 8166) to the character matrix of Deraco and García-López (2015). The matrix includes 68 taxa (59 of which are notoungulates) and 146 craniodental characters. We ordered 10 characters, following Deraco and García-López (2015); two others (37 and 119) ordered by them are binary. Searches used 500 replicates of random addition sequence, holding 10 trees per replication, using tree bisection reconnection (TBR) for branch swapping.

Relationships of *Thomashuxleya* within Placentalia. Postcranial characters were scored for the almost complete *Thomashuxleya externa* specimen (MPEF-PV 8166), using the morphological dataset of O'Leary et al. (2013; Morphobank project 773); cranial characters were the same as in O'Leary et al. (2013). The specimens used by O'Leary et al. (2013) to score the craniodental characters were referred to *T. externa* by Simpson (1967) and are not associated with postcranial remains. This resulted in 3660 craniodental and postcranial characters for 87 taxa, available in MorphoBank (Project 2084). We concatenated the morphological dataset with the amino acid alignment of Meredith et al. (2011; TreeBase number S11872), which comprises 11010 amino acids for 169 taxa, and the collagen alignment of Welker et al. (2015), with 2028 amino acids for 77 taxa. For the phylogenetic analysis, we combined the morphological and amino acid data using R (R Core Team, 2016), merging species of the same genus and where necessary coding data as absent for fossils (e.g., for most sequence data). To increase the analytical tractability of our dataset, we excluded non-mammals, living mammals with more than 50% missing data, non-placental fossils, and fossils with over 90% missing data (except meridiungulates) from our morphological dataset.

For the parsimony analysis, we applied parsimony as the optimality criterion in TNT (Goloboff et al., 2008a), PAUP 4.0a150 (Swofford, 2002), and PAUPrat (Sykes and Lewis, 2001) to a dataset consisting of 182 taxa and 16698 characters (13038 amino acids and 3660 morphological characters). All characters were unordered. We explored equal weights and extended implied weighting; the latter weights the two character sets (amino acids and morphology) using their average homoplasy (Goloboff et al., 2008b, Goloboff, 2014). In order to account for characters with many missing entries that would received artificially high implied weights, we used the command "xpiwe (*", which sets a concavity value (k) according to the number of missing entries (Goloboff, 2014). In addition to our unconstrained analyses, we also explored a number of backbone constraints. Following Tarver et al. (2016) we constrained monophyly of Atlantogenata (Xenarthra + Afrotheria) and Boreutheria (Laurasiatheria + Euarchontoglires) as shown in Tarver et al. (2016, figure 1). We also explored the impact of constraining 1) monophyly

of each meridiungulate clade in our sample (i.e., the two notoungulates and two litopterns) and 2) all six meridiungulates. We compared the resulting trees of the unconstrained and constrained analyses using a Wilcoxon rank sum test in PAUP* (Swofford, 2002). Parsimony searches included 500 replicates of random addition sequence, holding 10 trees per replication, using tree bisection reconnection (TBR) for branch swapping.

To make Bayesian searches tractable given our available computing resources, we further decreased the number of living taxa to those under 25% missing data (except meridiungulates), leaving 51 taxa. We obtained partitioning schemes and substitution models for the protein alignment with Partition Finder Protein v1.1.0 using the strict hierarchical clustering algorithm and the Bayesian Information Criterion for model selection (Lanfear et al., 2012). The best model partition scheme resulted in 20 partitions (out of 22 total coding genes) and assigned the JTT+G model for each amino acid partition and the MTMAM+G model for the collagen alpha 1 and 2. We used the standard discrete model implemented by MrBayes (Ronquist et al. 2011) for the morphological characters (Table 1). The dataset was analysed with MrBayes (Ronquist et al., 2012) and BEAGLE to utilize both GPU and CPU during searches. We used Tracer (Rambaut et al., 2014) for the visualisation and diagnostics of the MCMC output. We ran two analyses, one unconstrained and one constraining monophyly of the two notoungulates and two litopterns in our sample, as described above.

We used three runs of 3,000,000 generations with five chains (four heated and one cold) for the unconstrained analysis and two runs of 3.500,000 generations with four chains (three heated and one cold) for the constrained analysis. We sampled every 1000 generations, and use a temperature of 0.5.

RESULTS

Systematic Paleontology

NOTOUNGULATA Roth, 1903
ISOTEMNIDAE Ameghino, 1897
Thomashuxleya Ameghino, 1901

Type species. *Thomashuxleya rostrata* Ameghino, 1901, by original designation

Thomashuxleya externa (Ameghino, 1901)
Thomashuxleya artuata Ameghino, 1901;

TABLE 1. Best partition scheme for Bayesian analysis as obtained from Partition Finder (Lanfear et al., 2012).

Best model	Subset partitions	Subset sites
JTT+G	TTN	1-1479
JTT+G	CNR1	1480-1814
JTT+G	BCHE	1815-2146
JTT+G	EDG1	2147-2466
JTT+G	RAG1	2467-3066
JTT+G	RAG2	3067-3215
JTT+G	ATP7A	3216-3444
JTT+G	TYR1	3445-3587
JTT+G	Adora3	3588-3698
JTT+G	BDNF	3699-3885
JTT+G	ADRB2	3886-4153
JTT+G	PNOC	4154-4260
JTT+G	A2AB	4261-4543
JTT+G	BRCA1, BRCA2	4544-5574, 5575-7256
JTT+G	APOB, DMP1	7257-7710, 9718-10592
JTT+G	GHR	7711-8026
JTT+G	VWF	8027-8417
JTT+G	ENAM	8418-9717
JTT+G	IRBP	10593-11010
MTMAM+G	Collagen alpha 1 and 2	11011-13038
Standard discrete	Morphology	13039-16698

TABLE 2. Skeletal elements of isotemnid specimens from Cañadón Vaca.

	T. externa MPEF-PV 8166	*T. externa* MNHN CAS 844	*T. externa* MNHN CAS 64	*T. externa* AMNH 28698	*T. externa* AMNH 28447	*T. externa* AMNH 28905	*T. externa* AMNH 28563	*cf. T. externa* AMNH 142463	*A. distentus* AMNH 28906	*A.distentus* AMNH 28647	*P. similis* AMNH 28904	*P. similis* AMNH 28635	Isotemnidae indet. AMNH 28690
Skull	x	x		x							M1 only		
Mandible	x		x		x								
Scapula	x					x			x				
Humerus	x					x	x		x		x		
Ulna	x					x	x		x		x		
Radius	x						x		x	x	x		
Manus									x	x	x		
Pelvis	x					x							
Femur	x					x						x	x
Tibia	x										x	x	x
Pes	x							x	x		x		x

synonymized with *T. externa* by Simpson, 1967, p. 159

Stratigraphic provenance. MPEF-PV 8166 came from the Cañadón Vaca member of the Sarmiento Formation (Bellosi and Krause, 2014). An age of ~45 Ma has been proposed for the "Vacan" subage (Cifelli, 1985; Carlini et al., 2005; Woodburne et al., 2014). Bellosi and Krause (2014) estimated a range of 43.1-46.9 Ma for the Cañadón Vaca member.

***Thomashuxleya* systematics.** Ameghino (1901) first described *Thomashuxleya* based on material from the "couches a *Notostylops*" (now known to be part of the Casamayoran, middle Eocene) and originally assigned it to Homalodotheriidae ("Homalodontotheridae" in Ameghino, 1901). Ameghino designated *T. rostrata* as the type species (Ameghino, 1901, p. 177). In the same publication, Ameghino recognized three more species within the genus: *T. artuata*, *T. robusta*, and *T. externa* (Ameghino, 1901, p. 179).

Simpson (1967) considered *Thomashuxleya* to be part of Isotemnidae. Simpson (1967, p. 121) considered five Casamayoran Isotemnidae genera to be valid: *Pleurostylodon* (Ameghino, 1897), *Anisotemnus* (Ameghino, 1902), *Plexotemnus* (Ameghino, 1904a), *Isotemnus* (Ameghino, 1897), and *Thomashuxleya* (Ameghino, 1897). For *Thomashuxleya*, Simpson (1967) recognized two species: *T. externa* and *T. rostrata;* the latter is recorded in the local fauna south of Colhué Huapí Lake in Gran Barranca, (Barracan; Woodburne et al., 2014a). Other isotemnids present in the fauna of Colhué Huapí are *Pleurostylodon modicus* and *Isotemnus primitivus* (Cifelli, 1985).

Shockey and Flynn (2007) studied several of the postcranial elements referred to *Thomashuxleya* by Simpson (1936, 1967), and recognized that at least three genera were included in Simpson's (1936, 1967) skeletal reconstruction. Based on the material then available, they inferred a straight posture, plantigrade or semi-digitigrade locomotion, and lack of running among Vacan isotemnids. Of the known Isotemnidae specimens recovered from Cañadón Vaca, MEPF-PV 8166 is the only one with associated craniodental and postcranial elements (Table 2).

Description

Skull. MPEF-PV 8166 preserves most of the skull, including the cranium with maxillae, palatines, zygomatic arches, nasal, frontal, temporal and occipital, and the almost complete mandible. The skull of MPEF-PV 8166 measures 28 cm from the most posterior point of the sagittal crest to the most anterior point of the snout. Due to the preservation, the sutures are not visible. In lateral view, the rostrum is high (Figure 2.2). The zygomatic arch is wide and robust, more than in *Pleurostylodon* (Simpson, 1967). There is a well-defined sagittal crest (Figure 2.2), and the glenoid fossa is wide and concave (Figure 2.1), as in *Pleurostylodon* (Simpson, 1967). The occipital condyles are oval with a deep intercondylar notch. The paracondylar processes of the exoccipitals are long and narrow. The nuchal crest forms a semicircular outline in

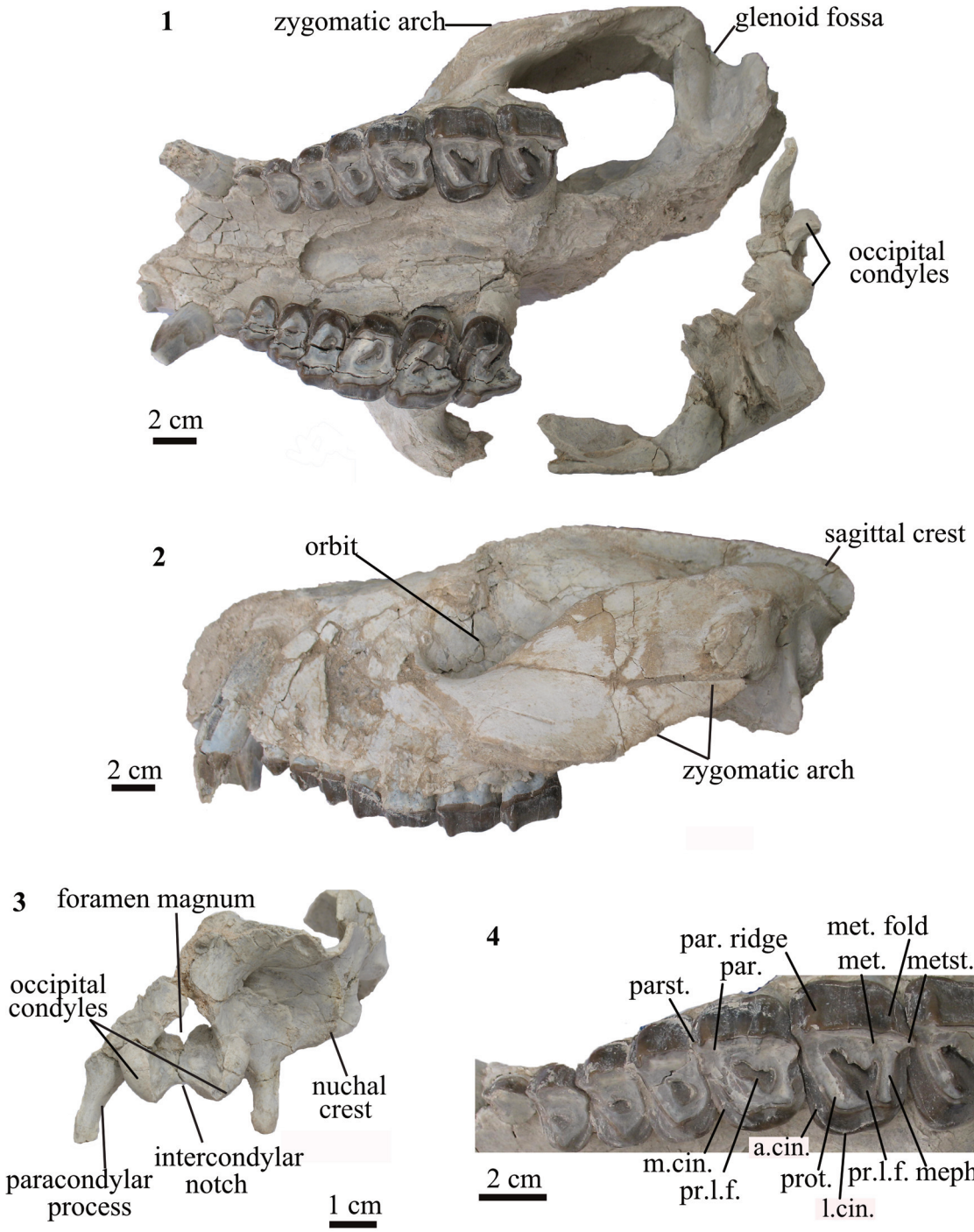

FIGURE 2. Skull of *T. externa* (MPEF-PV 8166). **1** ventral view; **2** lateral view; **3** occiput in caudal view; **4** detail of upper dentition in occlusal view. Abbreviations are prot=protocone (part of the protoloph), par=paracone (part of the ectoloph), parst=parastyle, met=metacone (part of the ectoloph), metst=metastyle, meph=metaloph, pr.l.f.=primary lingual fold, m.cin=mesial cingulum, l.cin=lingual cingulum.

posterior view and does not project below the level of the occipital condyles (Figure 2.3). The palate is triangular (Figure 2.2).

Upper dentition. The upper canines are clearly differentiated from the rest of the teeth. The mesiodistal length of each tooth steadily increases from P1 to M3 (Figure 2.1). The P1 is longer than wide, in contrast with *Anisotemnus distentus*, which has the opposite condition (Simpson, 1967). The P1 is oval in occlusal view and with a single mediolabial cusp (Figure 2.4). It has no mesial or distal stylar projections, in contrast to *Pleurostylodon* (Simpson, 1967). The P2-P4 are similar, increasing in labio-lingual width from P2 to P4 (Figure 2.4). They have a well-defined paracone ridge, and mesial to it there is a small parastyle, less prominent that in *Pleurolystodon* (Simpson, 1967). The metacone fold is absent (Figure 2.4). There is a mesial and distal cingulum, as in *Pleurolystodon* (Simpson, 1967).

The upper molars have a paracone ridge (Figure 2.4) which is less developed than in *Pleurostylodon* (Simpson, 1967). The metacone fold is observed as a very smooth ridge (Figure 2.4), less defined than in *Pleurostylodon* and *Isotemnus* (Simpson, 1967). There is a metastyle, which is more defined in M2 and M3 than in M1 (Figure 2.4). The upper molars have a primary lingual fold surrounded by the protoloph, ectoloph, and metaloph (Figure 2.4). As the teeth wear down, the primary lingual fold closes, forming a fossa (Simpson, 1967), as seen in M1 (Figure 2.4). There is a continuous labial, mesial, and lingual cingula, as in *Thomashuxleya* (Simpson, 1967). The mesial cingulum surrounds the protocone, reaching the lingual face of the teeth (Figure 2.4), in contrast to *Isotemnus*, which does not have lingual cingula (Simpson, 1967). The upper molars have no fossettes, which were “numerous and somewhat persistent with wear” in *Anisotemnus* according to Simpson (1967, p. 136). MPEF-PV 8166 is referred to *Thomashuxleya* based on the presence of a continuous lingual cingulum in the upper molars and dental dimensions (Simpson, 1967).

In addition of the differences with *Pleurostylodon* and *Isotemnus* mentioned above, MPEF-PV 8166 is about 60% larger than the specimens referred to *P. similis* and about 85% larger than *I. primitivus* (also recorded in Cañadón Vaca) based on the upper molar dimensions (Table 3; Simpson, 1967, table 45,49,54).

Mandible. The horizontal ramus is straight (Figure 3.2). The vertical ramus is wide and high (Figure 3.2). The masseteric fossa is large and oval (Figure 3.2). The condylar process is wide medio-laterally and narrow rostro-caudally (Figure 3.1). The coronoid process is narrow and high, extending more dorsally than the condylar process (Figure 3.2). The symphysis extends caudally to the level of p3/p4 (Figure 3.1), whereas in *Pleurostylodon* it extends to the level of p2 (Simpson, 1967). There are two mental foramina in the right horizontal ramus, one at the level of the mesial border of p2 and the other at the level of the mesial border of p3. In *Pleurostylodon*, the mental foramina are at the level of p3 and p4 (Simpson, 1967).

Lower dentition. The lower dentition has a small diastema of approximately 2 mm between p1 and p2. As in the upper teeth, the size increases from p1 to m3 (Figure 3.1). The p1 is triangular in lingual and labial views (Figure 3.2), and it has a median main cusp (Figure 3.3). The p2 has a large protoconid, with a crest projecting mesially, as in *Pleurostylodon* (Simpson, 1967). The metaconid projects lingually (Figure 3.3) and at its base shows a cingulid (Figure 3.2). The p3 and p4 are bicrescentic in occlusal view and show a high degree of wear. They have a well-defined labial fold (Figure 3.3) and a labial cingulid (Figure 3.2).

The lower molars have well-defined labial and lingual cingulids (Figure 3.2). The talonids are longer mesio-distally than the trigonids (Figure 3.3). The metaconid projects lingually and not distally as in *Pleurostylodon* (Simpson, 1967). The meta-entoconid fold is mesio-distally long and labio-lingually broad (Figure 3.3). The m3 has a long talonid, with the entoconid separated from the hypoconulid (Figure 3.3), as in *Pleurostylodon* (Simpson, 1967). Of the two species currently recognized for *Thomashuxleya*, we assign MPEF-PV 8166 to *T. externa* based on the well-defined labial and lingual cingulid (Ameghino, 1901) and its dental dimensions (Table 3; Simpson, 1967).

Scapula. The scapulae of MPEF-PV 8166 differ from AMNH 28905, previously referred to *T. externa* and *Anisotemnus distentus* (AMNH 28906). The comparison between the two *T. externa* specimens is difficult because MPEF-PV 8166 does not preserve the complete blade, and AMNH 28905 has been modified by post-recovery restoration. When comparing MPEF-PV 8166 with AMNH 28905 as coded by (O’Leary et al., 2013), we observed some differences: the coracoid process is pointing towards the axillary edge of the scapula and not perpendicular to the blade (Figure 4.1-2); the infraspinous fossa does not reach the rim of the glenoid fossa; and it is triangular rather than rectangular in lateral view (Figure 4.3).

TABLE 3. Dental measurements of *Thomashuxleya*; * =taken from Simpson (1967).

		p1		p2		p3		p4		m1		m2		m3	
		Length	Width	Length	Width	Length	Width	Length	Width	Length	Width	Length	Width	Length	Width
T. rostrata	MACN 10370*	13.7	11.8	17.5	12.7	18.1	14.8	20.9	16.6						
	MACN 10539*							19.9	17.8	26	19.8	26.4	19.5	37.2	16.9
	MACN 10546*							21.5	16.8						
	AMNH 28692*					19.5	16.5			26	16.4	28.5	18.8		
	AMNH 28764*							21.8	13.7						
	Mean	13.7	11.8	17.5	12.7	18.8	15.7	21.0	16.2	26	18.1	27.5	19.2	37.2	16.9
	SD	NA	NA	NA	NA	1.0	1.2	0.8	1.8	0.0	2.4	1.5	0.5	NA	NA
	n	1	1	1	1	2	2	4	4	2	2	2	2	1	1
T. externa	MACN 10540*					16.5	14.6	19	17.2	21		28		37	
	MACN 10537*							16.3	13	19.5	14	23	15.5		
	AMNH 28447*			14.2	11.1	16.2	11.6	18.1	13	22.0	15.6	27.5	16.5	31.6	15.8
	AMNH 28697*							17.3	14.2	23.2	15.9	25.5	17.2	36	16.6
	AMNH 28756*			14.7	10.9	15.7	12.8	16.4	14.2	21.8	16.3	25.6	17.8	32.3	16.3
	AMNH 28698*	11.0	10.0	15.1	12.6	16.7	13.6	16.5	14.6	24	16.1	26	17.8	37	17
	AMNH 28686*													34.5	17.0
	AMNH 28822*									20	16.4	23	18.0		
	Mean*	11	10	14.7	11.5	16.3	13.2	17.3	14.4	21.6	15.7	25.5	17.1	34.7	16.5
	SD*	NA	NA	0.5	0.9	0.4	1.3	1.1	1.5	1.6	0.9	2.0	1.0	2.4	0.5
	n*	1	1	3	3	4	4	6	6	7	6	7	7	6	5
	MPEF-PV 8166	12.8	8.3	15.4	10	16.5	10.1	16.4	13.3	20.1	15.6	22.5	15.3	32.3	15.7

		P1		P2		P3		P4		M1		M2		M3	
		Length	Width	Length	Width	Length	Width	Length	Width	Length	Width	Length	Width	Length	Width
T. rostrata	MACN 10370*	15.4	15.7	17.0	27.2	19.5	31.2	21	35						
	MACN 10542*									29.5	41.8	33.0	44.2	28.8	40.8
	Mean*	15.4	15.7	17	27.2	19.5	31.2	21	35	29.5	41.8	33	44.2	28.8	40.8
	SD*	NA	NA	NA	NA	NA	NA	NA	NA	NA	NA	NA	NA	NA	NA
	n*	1	1	1	1	1	1	1	1	1	1	1	1	1	1
T. externa	MACN 10543*									24	34	28.5	35.9		
	AMNH 28699*			17.5	22.1	16.8	26.4	18.5	32.1	23.8	35.8	26.7	42		39.5
	AMNH 28757*	13.8	11.5	15.2	22.1	18	26			25.7		27.2	39.2		
	AMNH 28698*	10	11			16		18	33.2	23.9	38.7	27.2	41	26	41
	MNHN CAS 844	10.84	13.86	17.79	22.93	18.94	26.80	19.13	31.25	21.40	32.75	22.71	35.98	26.55	35.46
	Mean*	11.5	12.1	16.8	22.4	17.4	26.4	18.5	32.2	23.8	35.3	26.5	38.8	26.3	38.7
	SD*	2.0	1.5	1.4	0.5	1.3	0.4	0.6	1.0	1.5	2.6	2.2	2.8	0.4	2.9
	n*	3	3	3	3	4	3	3	3	5	4	5	5	2	3
	MPEF-PV 8166	10.2	10.5	14.0	16.2	15.0	21.6	14.6	25.9	25.2	31.3	27.9	36.9	24.0	32.0

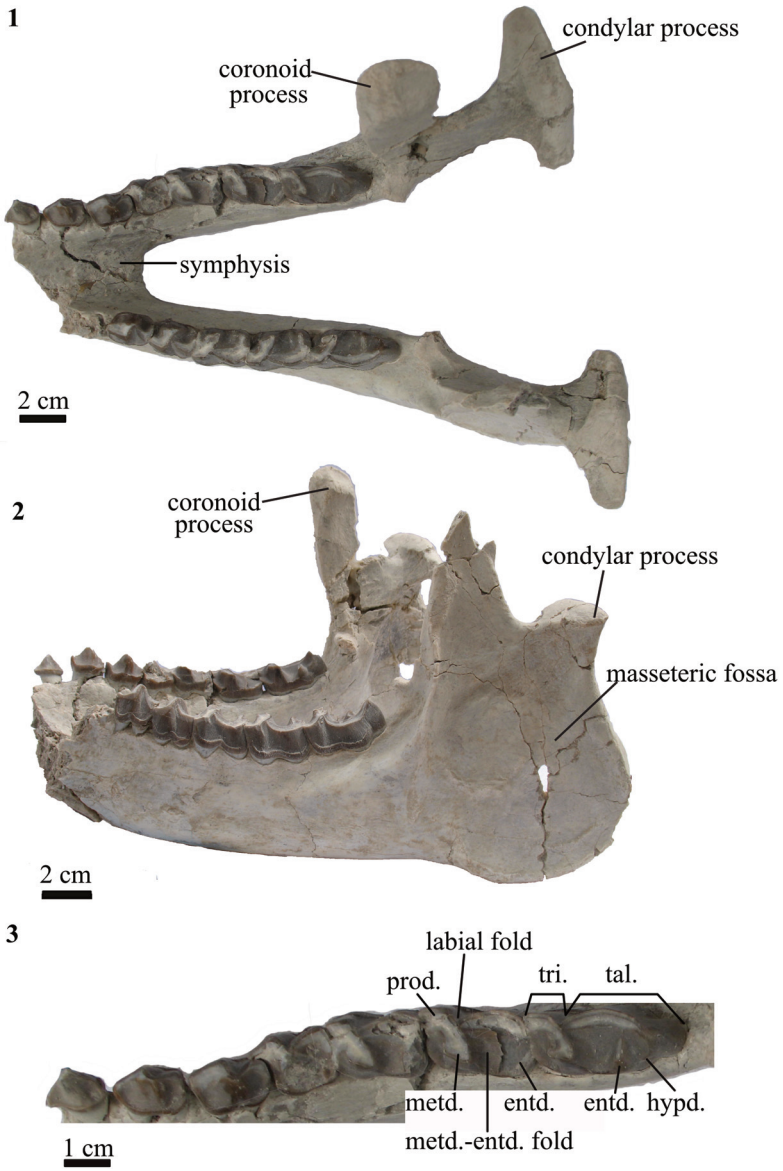

FIGURE 3. Mandible of *T. externa* (MPEF-PV 8166) in **1** dorsal and **2** lateral views; **3** lower dentition in occlusal view. Abbreviations are tri=trigonid, tal=talonid, prod=protoconid, metd=metaconid, entd=entoconid, hypd=hypoconulid.

In MPEF-PV 8166, the preserved portion of the supraspinous fossa is larger than the infraspinous fossa, as in *Anisotemnus* (Shockey and Flynn, 2007). The infraspinous fossa narrows proximally towards the glenoid fossa. A narrow portion of the fossa for the teres minor muscle is present. The spine is high, with a lateral projection equal to the medio-lateral width of the glenoid fossa, and narrower than that of *Anisotemmnus* in lateral view (Figure 4.2-3).

In MPEF-PV 8166 the acromion is not preserved. *Thomashuxleya* has a well-developed metacromion with quadrangular shape in lateral view; its presence is uncertain in *Anisotemnus* (Shockey and Flynn, 2007). The glenoid fossa is circular, as in *Anisotemnus*, and oriented perpendicular to the main axis of the scapula. In the right scapula of MPEF-PV 8166, the glenoid fossa is taphonomically compressed in the mediolateral plane, resulting in a more oval shape. There is a conspicuous supraglenoid tubercle (Figure 4.1). The coracoid process is well developed and narrower than *Anisotemnus*, although this could be due to diagenetic compression. The length of the coracoid process is smaller than the maximum diameter of the glenoid fossa. The neck is short and wide, similar to *Anisotemnus*.

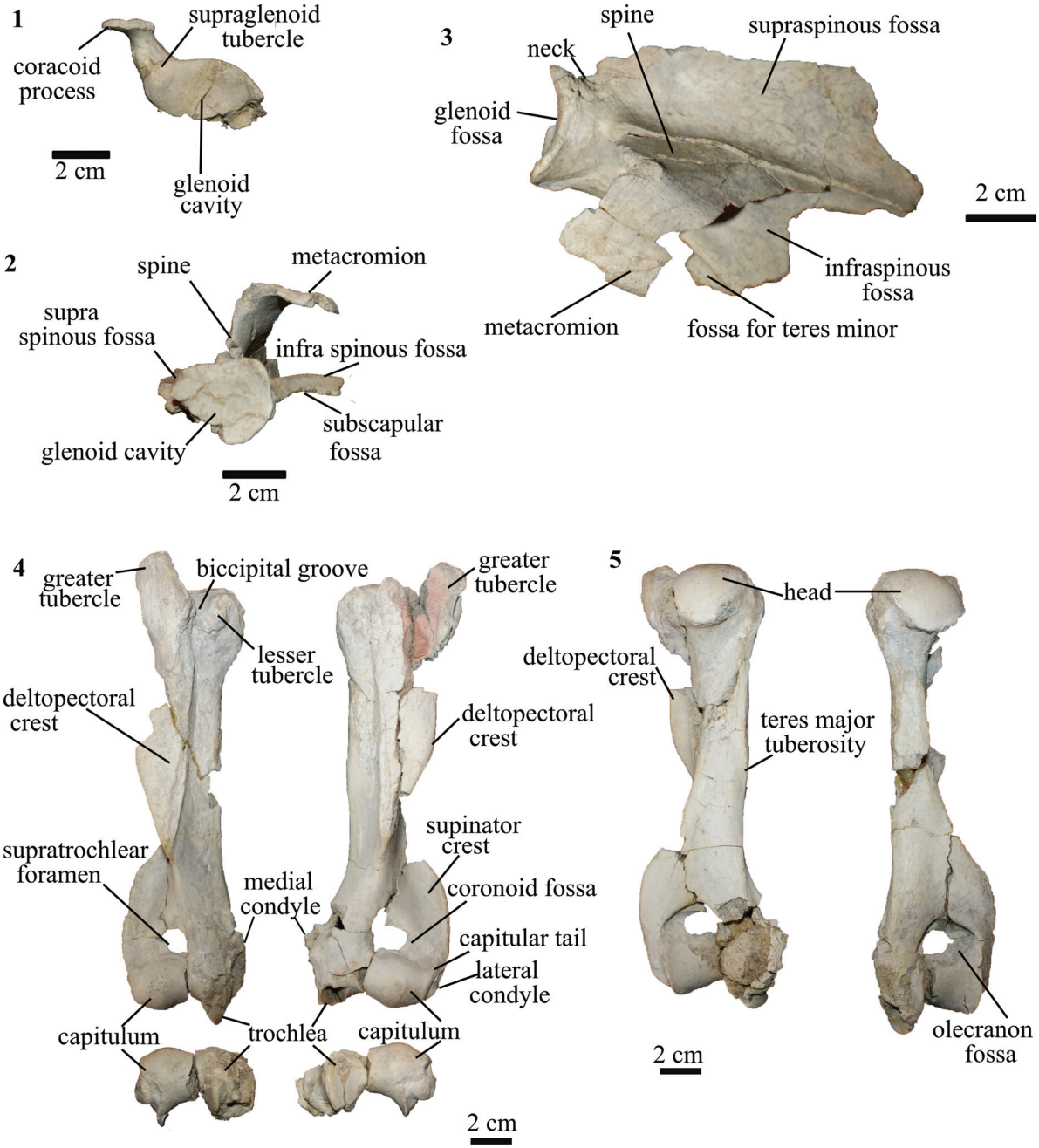

FIGURE 4. Scapulae and humeri of *T. externa* (MPEF-PV 8166). **1** right and **2** left scapulae in proximal view; **3** left scapula in dorsolateral view; right and left humeri in **4** right and left humeri in anterior (top) and distal (bottom) views; **5** right and left humeri in posterior view.

Humerus. In MPEF-PV 8166 both left and right humeri are almost complete (Figure 4.4-4.5). The greater tubercle is high, protruding proximally from the level of the head, as in AMNH 28905. The lesser tubercle is smaller than the greater tubercle and much less developed than in *Anisotemnus* (Shockey and Flynn, 2007). The bicipital groove is shallow as in *Anisotemnus* and other specimens of *Thomashuxleya*. The articular surface of the head is oriented posteriorly. The anterior margin of the shaft is convex and the posterior one is straight, and the midshaft is triangular in cross-section. The pectoral (medial) and the deltoid (lateral) crest unite to form a deltopectoral crest, which is large, tilts medially towards its distal end, and extends distal to the midshaft, as in *Anisotemnus* (Shockey

and Flynn, 2007). On the medial side of the shaft, there is a small Teres major tuberosity, less developed than that of *Anisotemnus*. The supinator crest is well developed and blade-like as in *Anisotemnus* and *Pleurostylodon*.

The capitulum is rounded, similar to *Anisotemnus*, and is oblique (i.e., directed proximomedially) relative to the proximodistal axis, as in other specimens of *Thomashuxleya*, and as opposed to the orthogonal orientation in *Anisotemnus* (Shockey and Flynn, 2007). The medial border of the trochlea is oriented distomedially. The capitulum is wider than the trochlea. The medial crest of the trochlea extends more distally than the capitulum, as in other isotemnids. There is a small, concave capitular tail. The olecranon fossa is shallow (i.e., its depth is less than the maximum diameter of the fossa). The supratrochlear foramen is smaller than the oleocraneon fossa. The presence of the supratrochlear foramen in MPEF-PV 8166 can be assessed with confidence because the borders are preserved. Its presence is uncertain in other *Thomashuxleya* specimens (O'Leary et al., 2013), and it is absent in *Pleurostylodon* and likely absent in *Anisotemnus* (Shockey and Flynn, 2007). The medial condyle is not well preserved, and is not possible to assess the presence of an entepicondylar foramen, which is otherwise present in other *Thomashuxleya* specimens, *Anisotemnus* and *Pleurostylodon*. The lateral condyle is located more distally than the medial condyle, and there is a distinct radial fossa.

Differences between the humeri of MPEF-PV 8166 and AMNH 28905 (O'Leary et al., 2013) are as follows: in MPEF-PV 8166 the bicipital groove is narrower; the lateral condyle (ectepicondyle) is lateral and not proximal to the capitulum; the coronoid fossa is perforated by the supratrocheal foramen; and the anterior border of the trochlea does not project beyond the plane of the anterior border of the shaft.

Ulna. The right and left ulnae are almost complete except for the most distal portion on the left and the incomplete styloid process on the right (Figure 5.1). The shaft is straight. When articulated, the ulna extends distally as long as the radius. Similar to *Anisotemnus* (AMNH 28906), the shaft does not taper distally and is strongly excavated in the lateral side. In *Pleurostylodon* (AMNH 28904), the lateral margin is less excavated. In lateral view, the shaft is straight along its whole length and not anteriorly concave as observed in other *Thomashuxleya* specimens (e.g., AMNH 28653; Shockey and Flynn, 2007).

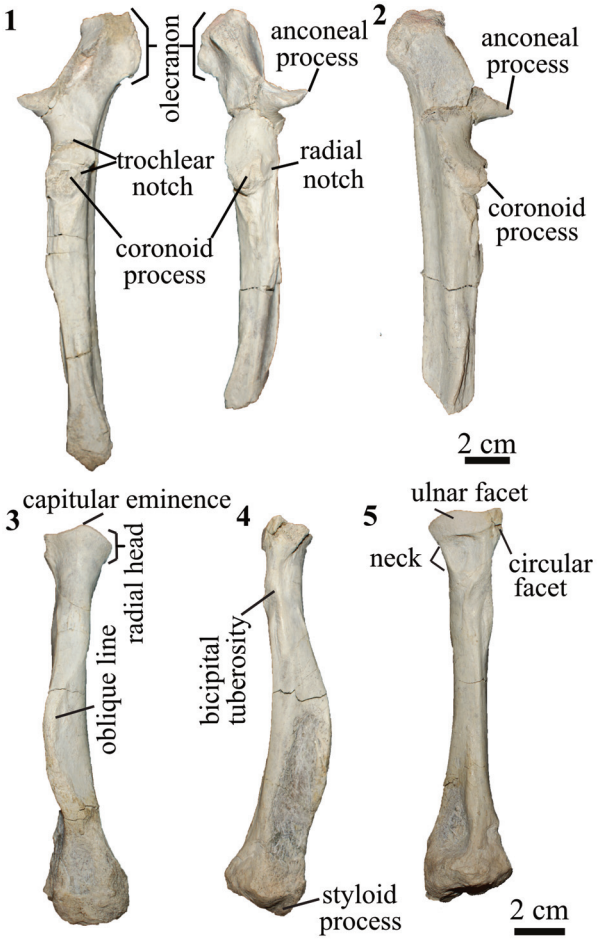

FIGURE 5. Forelimb of *T. externa* (MPEF-PV 8166). **1** right and left ulnae in frontal view; **2** left ulna in medial view; right radius in **3** frontal, **4** lateral, and **5** posterior views.

The olecranon process of the ulna is long (longer than the trochlear notch) and tilts medially as in *Anisotemnus* and as opposed to *Pleurostylodon*, where it is straight (Shockey and Flynn, 2007). In lateral view, the olecranon extends posterior to the level of the shaft, in contrast with *Anisotemnus* and *Pleurostylodon*, where it is more aligned with the shaft (Shockey and Flynn, 2007). The trochlear notch forms a crescent in lateral view and is wider than the midshaft. The coronoid process is as large as the radial notch, in contrast with the larger radial notch in *Anisotemnus* (Shockey and Flynn, 2007). The anconeal process extents laterally and anteriorly (more anterior than the coronoid process), and its width represents about 63% of that of the trochlear notch (Table 4).

The ulnae of MPEF-PV 8166 differ from AMNH 28905 (O'Leary et al., 2013) in the following characters: the absence of a ridge on the lateral

TABLE 4. Postcranial measurements of MPEF-PV 8166. * Translated from Spanish in Elissamburu (2012).

	Value (mm)		Acronym	
	Left	**Rigth**	**Scott (1990)**	**Elissamburu (2012)**
Scapula				
Height of the spine	31.0	31.4		
Humerus				
Humerus functional length*	193	204	H1	LFH
Humerus trochlear diameter*	52.0	43.3	H4	DtrH
Maximum length	211	210		
Maximum diameter of the head	44.0	40.5		
Maximum diameter of the mayor tuberosity		46.6		
Maximum diameter of the minor tuberosity		16.6		
Maximum widht of the trochlea	30			
Radius				
Maximum length	155	153		
Maximum mediolateral width of the medial shaft	14.1	14.0		
Maximum diameter of the head	32.0			
Minimum diameter of the head	20.3	20.4		
Maximum diameter of the neck	20.3	19.5		
Mediolateral width of the distal epiphysis		36.0		
Diameter perpendicular to the maximum width of the distal epiphysis		31.6		
Ulna				
Anteroposterior diameter of the diaphysis	28.3	28.1		
Olecraneum height	64.9	63.7		
Anteroposterior diameter of the oleocranon	32.6			
Proximo-distal length of the trochlear notch	35.9			
Trochlear notch width		32.6		
Width of anconeal process		20.5		
Femur				
Anteroposterior diameter of the shaft		25.5	F7	DAPF
Mediolateral diameter of the shaft		36.2	F6	DTF
Tibia				
Mediolateral diameter of proximal epiphysis		55.0	T2	DTpT
Anteroposterior diameter of proximal epiphysis		44.8		
Lateral condyle transverse width		28.0		
Lateral condyle anteroposterior width		25.0		
Astragalus				
Transverse width of tibial trochlea	27.7		Li 1	
Minimum width of the neck	14.8			
Width sustentacular facet	17.4			
Navicular				
"Dorsal-plantar" width		25.6		
Astragalar facet transverse width		24.0		
Astragalar facet dorsoventral depth		25.0		
Pelvis				
Maximum width of the ilium, above the acetabulum		42.3		

side of the olecranon, the medial inclination of the olecranon, and the absence of a tuberosity on the anterior surface distal to the trochlear notch.

Radius. The radius is approximately 70% the length of the ulna (Table 4). The anterior margin of the shaft is convex in lateral view (Figure 5.4) and widens distally, as in *Anisotemnus* and *Pleurostylodon*. The midshaft is oval in cross-section. The head is oval in proximal view. There is a conspicuous capitular eminence, more developed than in *Pleurostylodon*, but less than in *Anisotemnus* (Shockey and Flynn, 2007). The bicipital tuberosity is small and placed below an enlarged fossa (Figure 5.4). The ulnar facet is broad and convex (Figure 5.5). There is a circular facet lateral to the ulnar facet as in *Anisotemnus*. It articulates with the radial notch of the ulna, and it does not seem to be a facet for an elbow sesamoid, as observed in *Nesodon* (Scott, 1912) or *Adinotherium* (Croft et al., 2004). The styloid process is short and projects distally, and there is a conspicuous oblique line on the anterior margin (Figure 5.3-5.4). The distal epiphysis is wider than the shaft, and the main axis of the distal articular surface is posterolateral to anteromedial in distal view. In the left radius, the distal epiphysis was diagenetically compressed in the anteroposterior axis.

The radii of MPEF-PV 8166 differ from AMNH 28905 (O'Leary et al., 2013) in having a proximolateral radial facet, an oval rather than round midshaft cross-section, the presence of an anterior oblique line, and a wide distal epiphysis (but not more than twice as wide as the shaft).

Pelvis. Among isotemnids, the pelvis is only known for *Thomashuxleya* (Simpson, 1936, 1967). In MPEF-PV 8166 the pelvis preserves portions of the right ilium and ischium, but not the pubis (Figure 6.1-6.2). The anterior process of ilium is mediolaterally broad and elongated (Figure 6.1) as in AMNH 28905 (Simpson, 1936; O'Leary et al., 2013); in lateral view (Figure 6.2), the ilium is straight and thin. The acetabulum is circular and oriented posterolaterally. The ischium is in the same anterodorsal plane that the ilium, and projects dorsally from the acetabulum. The posterior part of the ischium is missing.

Femur. In both femora, the proximal and distal epiphyses are missing and only the shaft and isolated head are preserved (Figure 6.3). Limb suture closure sequence is highly variable in mammals, and several placentals show incomplete fusion of growth plates in adulthood (Geiger et al., 2014). Bone histology from femoral cross-section indicates the specimen was skeletally mature (see below). This suggests that *Thomashuxleya* had unfused femoral epiphyses into adulthood, as seen in some other mammals (Geiger et al., 2014). The head is spherical with a fovea capitis, enclosed in the articular surface. The trochanteric fossa is deep; the lesser trochanter is smaller than that of AMNH 28905 (O'Leary et al., 2013) and the third trochanter is conspicuous. In lateral view, the anterior border of the shaft is curved and the posterior border is concave.

Tibia. In *Thomashuxleya* (MPEF-PV 8166) the tibia and fibula are not fused. In proximal view, the mediolateral width of the proximal epiphysis is greater than the anteroposterior depth, the tibial tuberosity is robust and there are no signs for intercondylar eminences (Figure 6.4). The lateral condyle is circular there is a shallow fossa. The cross section at midshaft is crescent-like, with a lateral concavity. The postero-medial portion of the distal epiphysis of the tibia is not preserved. The distal articulation surface of the tibia with the fibula is small and visible in distal view (Figure 6.4). In other isotenmids, a partial tibia is only known for an indeterminate isotemnid (AMNH 28690) and *Pleurostylodon* (AMNH 28904) (Shockey and Flynn, 2007; Simpson, 1936, 1967).

Astragalus. The astragalus of MPEF-PV 8166 is the first isotemnid found in association with dental remains that corroborates its species-level identification. It is a left astragalus missing the posteriormost portion of the body (Figure 6.5-6). The astragalus of MPEF-PV 8166 is similar in the overall morphology of AMNH 142463, which, based on its size, was referred to cf. *Thomashuxleya externa* by Shockey and Flynn (2007) (Table 5).

In MPEF-PV 8166 the body is broad and short, as in AMNH 142463. It has a relative shorter neck in comparison with the elements referred to *Thomashuxleya rostrata*, *Pleurostylodon modicus*, and other isotemnid specimens (Ameghino, 1904b: figures 24, 28-30). The presence of an enlarged medial plantar tuberosity ("medial process" in Shockey and Flynn, 2007; "anterior medial plantar tuberosity" in Szalay, 1994) could not be confirmed as the structure is broken. The trochlear groove is shallow, and the lateral and medial borders of the trochlea are at the same height, in contrast to AMNH 142463 and AMNH 28690 (Isotemnidae indet.) where the lateral border is slightly higher than the medial (Shockey and Flynn, 2007). The trochlea is wider relative to the astragalar length in MPEF-PV 8166 than in AMNH 142463 and the plane of the articulation surface of the lateral facet is almost perpendicular to the trochlear width. The

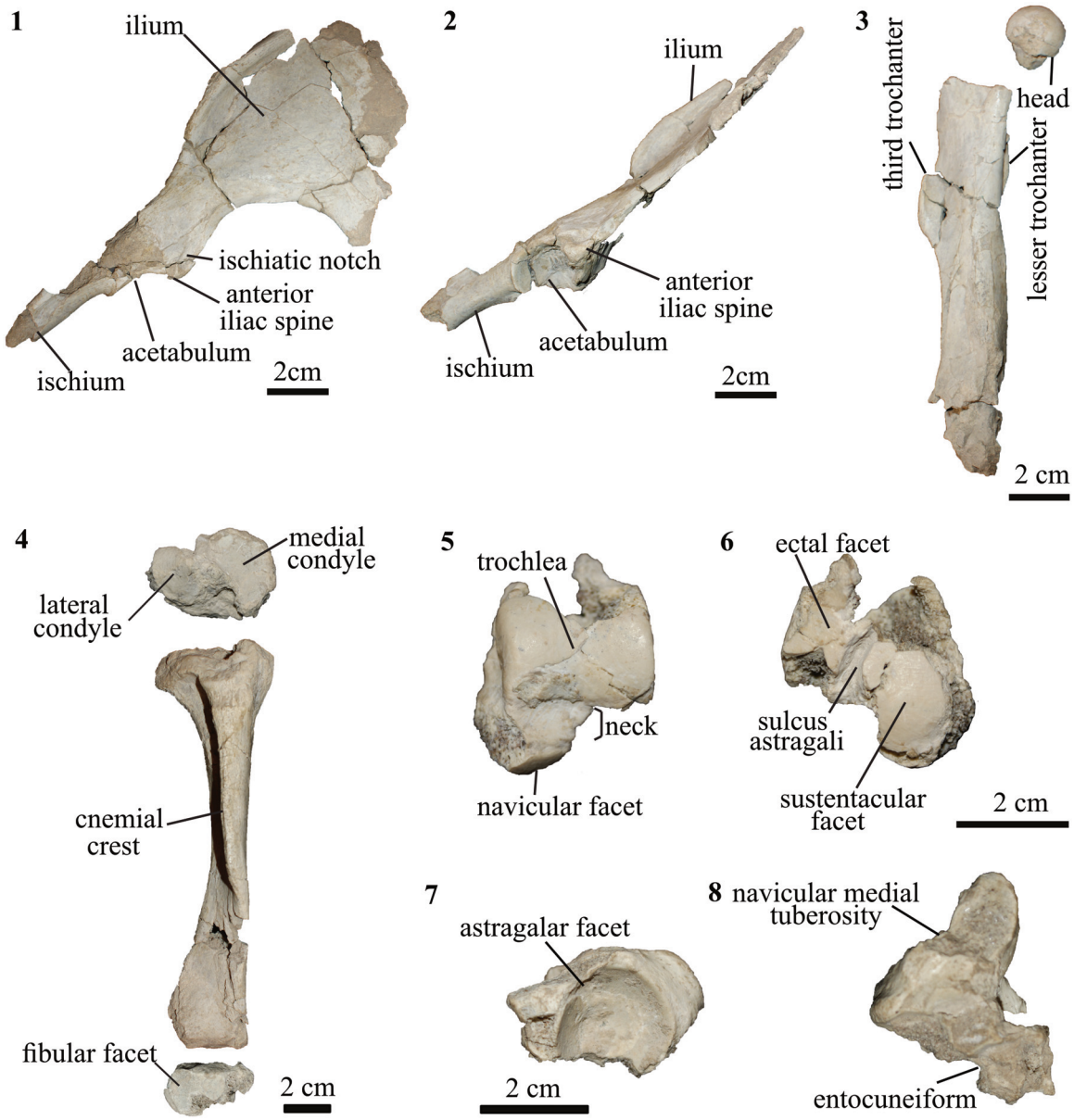

FIGURE 6. Hindlimb of *T. externa* (MPEF-PV 8166). right pelvis in **1** dorsal and **2** lateral views; **3** right femur in anterior view; **4** right tibia in proximal (top), anterior (middle) and distal (bottom) views; left astragalus in **5** dorsal and **6** plantar views; **7** right navicular in proximal view; **8** navicular and entocuneiform in plantar views.

neck is short (Figure 6.5). In dorsal view, the neck represents about half of the trochlear width, similar to AMNH 142463. The navicular facet is convex and anteromedial to the facets for the tibia (Figure 6.5).

The sustentacular facet is elongated anteroposteriorly and covers about half of the astragalus plantar width (Figure 6.6). The proximomedial portion of the sustentacular and the proximal and distal edges of the ectal facets are broken; a well-defined sulcus astragali separates the two. The ectal facet is restricted to the plantar plane. In ventral view, the medial portion of the navicular facet extends proximally and almost contacts the sustentacular facet (Figure 6.6). There is no cotylar fossa, and the medial astragalar facet is thin and constricted to the medial edge of the trochlea. In MPEF-PV 8166 the most posterior portion of the astragalar body is broken and therefore uninformative regarding the presence of an astragalar foramen, as described for AMNH 142463 and AMNH

TABLE 5. Isotemnid astragali measurements in mm.

Specimen No.	Locality	Maximum length	Trochlear width	Maximum width	Head width
MPEF-PV 8166	Cañadón Vaca		27.7		
AMNH 142463	Cañadón Vaca		35.9	41.4	
AMNH FM 14501	"Notostylops beds"	32.8	21.8	32.1	17.7
AMNH 28690	Cañadón Vaca	22	12	20.6	
AMNH 142464	Cañadón Vaca	20.5	8.9	16.7	9.3

28690 (Simpson, 1936, 1967; Shockey and Flynn, 2007).

Navicular. MPEF-PV 8166 preserves a right navicular articulated with a fragment of the entocuneiform (Figure 6.7-8). The astragalar facet is circular and deeply concave as described for *Pleurostylodon* (AMNH 28904) and an indeterminate isotemnid (AMNH 28690; Shockey and Flynn, 2007). The plantar process is present and elongated, with a rounded end. The navicular medial tuberosity is high and conspicuous as in *Colbertia*, *Allalmeia* (Lorente et al., 2014), and AMNH 28690 (Shockey and Flynn, 2007). The cuboid facet is oblique and faces distolaterally, suggesting that the cuboid extended more distally than the navicular. *Thomashuxleya* seems to have the reverse alternate tarsus condition in which the "astragolocuboid contact is lost and calcaneonavicular contact is achieved," following Cifelli (1993, p. 206), although it is not possible to determine if there was a calcaneal-navicular contact as the proximal border is broken.

Metapodials and phalanges. There is a complete first metapodial, which is long, narrow, and flat. The condyles are asymmetrical, with the lateral one more projected distally than the medial one. The lateral border is concave, and the medial one convex. The proximal epiphysis has a triangular shape and is wide transversally.

Three intermediate phalanges are complete, short, and wide. Two of them are symmetrical, and the remaining phalanx is smaller and asymmetrical. In addition, two ungual phalanges were recovered.

Body Mass Estimates

We recovered a wide range of body mass estimates depending on the equation used. The widest range of body mass estimates were obtained with dental measurements (Appendix 1). The second upper molar width gives the highest body mass estimation (1501 ± 583.8 kg), and the second lower molar length gives the lowest (289 ± 92.2 kg). Among craniomandibular measurements the posterior jaw length yielded the lowest estimate (26 ± 9.5 kg), and the maximum width of the mandibular angle yielded the highest (209 ± 84.6 kg). Regression equations based on postcranial measurements also show considerable variation, but not as much: the highest value is given by the anteroposterior diameter of the femur (304 ± 69.9 kg) and the lowest by the transverse diameter of the tibia's proximal epiphysis (72 ± 15.1 kg). The astragalus yielded an estimate of 84 ± 24.2 kg. The arithmetic mean and standard deviation of all the measurements combined were 354.8 kg and 356.2 kg, respectively. The body mass estimations of all the 19 variables analysed have a geometric mean of 235.9 kg and after the bootstrap the 95% confidence interval ranges between 158.1 kg and 354.7 kg. The median is 304 kg, the mode 396 kg, and the kurtosis (a descriptor of the tails of the distribution), is 2.97. As shown in Appendix 1, craniomandibular variables gave a mean of 126 kg and standard deviation of 92.7 kg; dental variables yielded (respectively) 556.4 kg and 390.3 kg; limbs yielded 143.2 kg and 92.9 kg. The estimates using multivariate regression equations yielded a mean of 180.5 kg and a standard deviation of 4.9 kg (Appendix 2).

Bone Histology

The cross-section shows some sediment in the medullary cavity (Figure 7.1) but can nonetheless be interpreted and represented schematically. *Thomashuxleya* femora display a large open medullary cavity surrounded by the cortex (Figure 7.2), which is not particularly thick in comparison with other large SANUs (Houssaye et al., 2016, figure 3). The image does not allow assessment of the relative thickness of the spongious transition zone.

Secondary bone of large mammals is typically represented by dense Harvesian bone (Kolb et al., 2015b). The bone sample of *Thomashuxleya* is characterized by a compact cortex and a spongiosa medullary cavity (Figure 7.1). The sample shows strong remodelling resulting in dense Haversian bone in the inner cortex (Figure 7.3-4). The primary fibrolamellar bone shows strong laminar

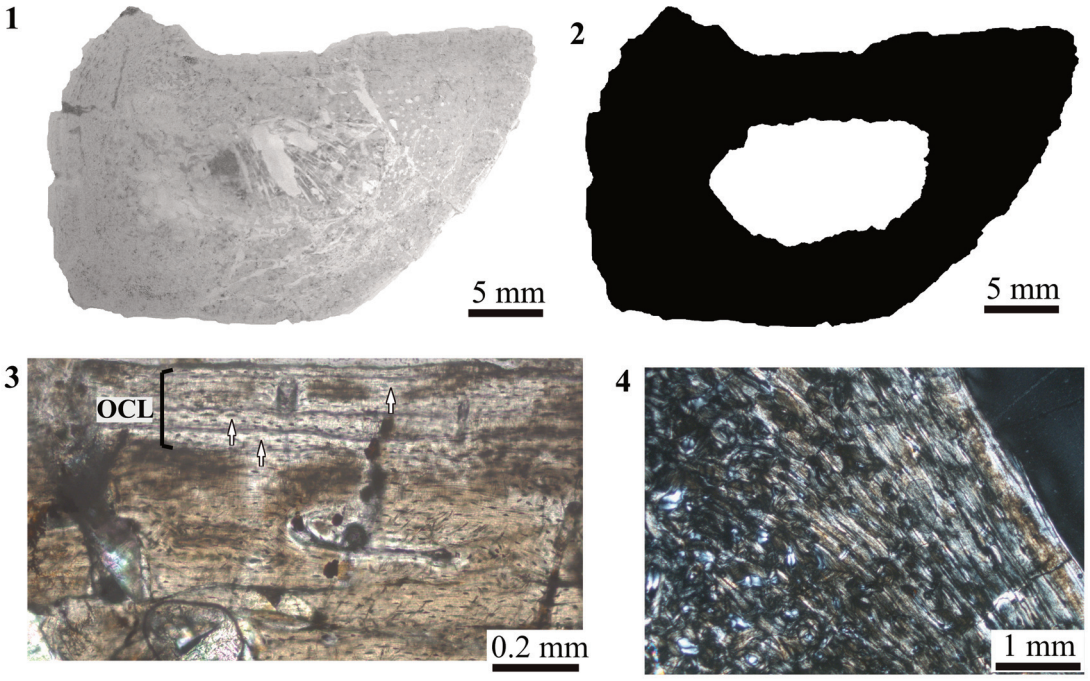

FIGURE 7. Bone histology and microstructure of *T. externa* (MPEF-PV 8166). **1** Cross section of the midshaft of the right femur; **2** same as 1 after conversion to a binary image (black represents bone and white the cavities); **3** bone histology under linear polarized light, with black arrows pointing the lines of arrested growth (LAGs). OCL= Outer circumferential layer. **4** Bone histology under cross polarized light.

and longitudinal vascularization. Towards the medullary region, resorption cavities are large and common. An outer circumferential layer (OCL) (Ponton et al., 2004) consisting of avascular lamellar bone is present. The OCL indicates that, despite incompletely fused femoral epiphyses, the specimen reached skeletal maturity (Kolb et al., 2015a; Martinez-Maza et al., 2014). A minimum of three lines of arrested growth (LAGs) could be identified within the OCL (Figure 7.3).

Phylogenetic Analysis

Relationships of *Thomashuxleya* within Notoungulata. The new *Thomashuxleya* specimen (MEPF-PV 866) provided information to code seven craniodental character states previously unknown for the genus in the character matrix of Deraco and García-López (2015) (see characters [and states] in Morphobank project 2084, 34[1], 35[0], 56[1], 83[0], 96[0], 97[0], 101[0]). The parsimony analysis yielded 281 trees, 420 steps long, with a consistency index (CI) of 0.383 and retention index (RI) of 0.765. A strict consensus of these trees (Figure 8) shows the same topology as that obtained by Deraco and García-López (2015; figure 5), with Notoungulata showing a basal polytomy including *Henricosbornia*, *Simpsonotus*, *Pampatemnus deuteros*, Notostylopidae (including *Pyrotherium*), Toxodontia and Typotheria. The synapomorphies of the main clades within Notoungulata and Toxodontia are the same as listed by Deraco and García-López (2015; figure 5), and therefore they are not repeated here.

Within Toxodontia, *Pampatemnus infernalis* appears as the most basal taxon. The sister clade shows a polytomy including *Pleurostylodon*, a (*Ryphodon [Thomashuxleya, Periphragnis])* clade, and another consisting of the remaining members of Toxodontia (Figure 8). The synapomorphies supporting the clade *(Ryphodon [Thomashuxleya, Periphragnis])* are also the same as listed by Deraco and García-López (2015; figure 5). *Thomashuxleya* has two autapomorphies: the posterolabial fossette on the upper molars disappearing before the closure of the central fossette (34[1]), and the mandibular foramen located at the level of the alveolar border (139[1]).

Relationships of *Thomashuxleya* within placentals. We applied parsimony (MP) using TNT to the combined morphology and protein dataset, including collagens recovered from extant species and Pleistocene fossils (Welker et al., 2015), amino acids for extant taxa (Meredith et al., 2011), and morphology for extinct and extant taxa (O'Leary et

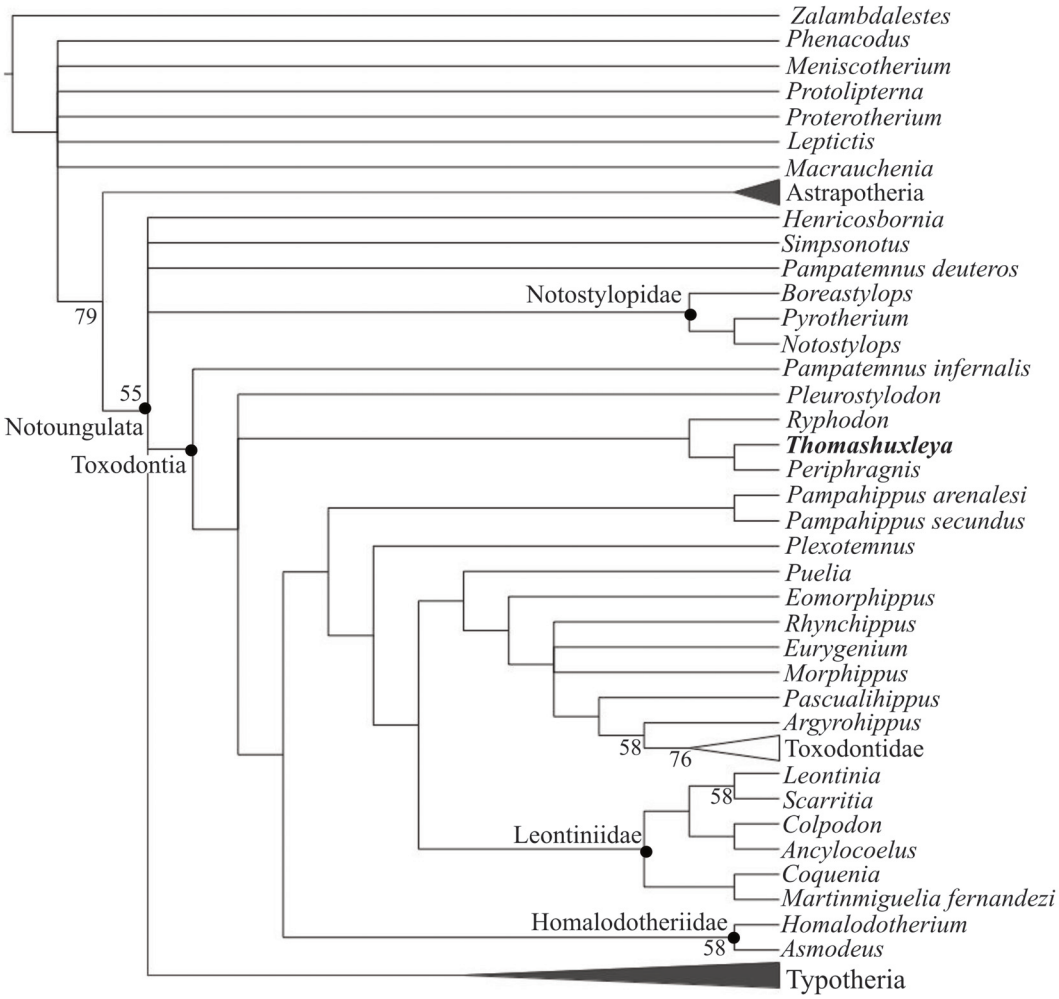

FIGURE 8. Strict consensus of 281 trees, 420 steps in length showing the phylogenetic relationships of *Thomashuxleya* within Notoungulata based on the morphological dataset of Deraco and García-López (2015). Numbers indicate bootstrap values above 50.

al., 2013) including our revised anatomical characters for *Thomashuxleya.* This recovered the basic structure of the now well-corroborated tree of placental mammals (Murphy et al., 2001; Tarver et al., 2016). MP analysis with the extended implied weighting yielded 510 trees, 122374 steps long, with a consistency index (CI) of 0.345 and retention index (RI) of 0.638. A strict consensus of these trees (Figure 9) divides meridiungulates between Afrotheria and Laurasiatheria. *Thomashuxleya* and *Carodnia* (sampled for morphology only) are within Afrotheria as sister taxa of tethytheres (i.e., Proboscidea and Sirenia), with a bootstrap value of 10 and 69, respectively. *Toxodon* and *Macrauchenia* (sampled for collagen sequences from Welker et al., 2015) are in a polytomy among perissodactyls, including *Mesohippus* and the fossil *Equus* sp. with a bootstrap value of 56. *Protolipterna* and *Didolodus* appear in the same clade with *Hyopsodus* and *Phenacodus,* as early divergent members of Euungulata (i.e., perissodactyls and artiodactyls), with a bootstrap value of 88.

We then constrained MP to support the monophyly of each of two clades (but not the two clades together): Notoungulata (*Toxodon* and *Thomashuxleya*) and Litopterna (*Macrauchenia* and *Protolipterna*). This yielded 620 trees of 122391 steps, with a CI of 0.345 and RI of 0.638. In the strict consensus, *Carodnia* is within Afrotheria as sister taxa to tethytheres. The remaining SANUs form a clade with *Hyopsodus* and *Phenacodus,* as sister taxon to Euungulata (Figure 10). The Wilcoxon ranks test shows that there is not a significant difference (p value > 0.05; Table 6) between the Notoungulata

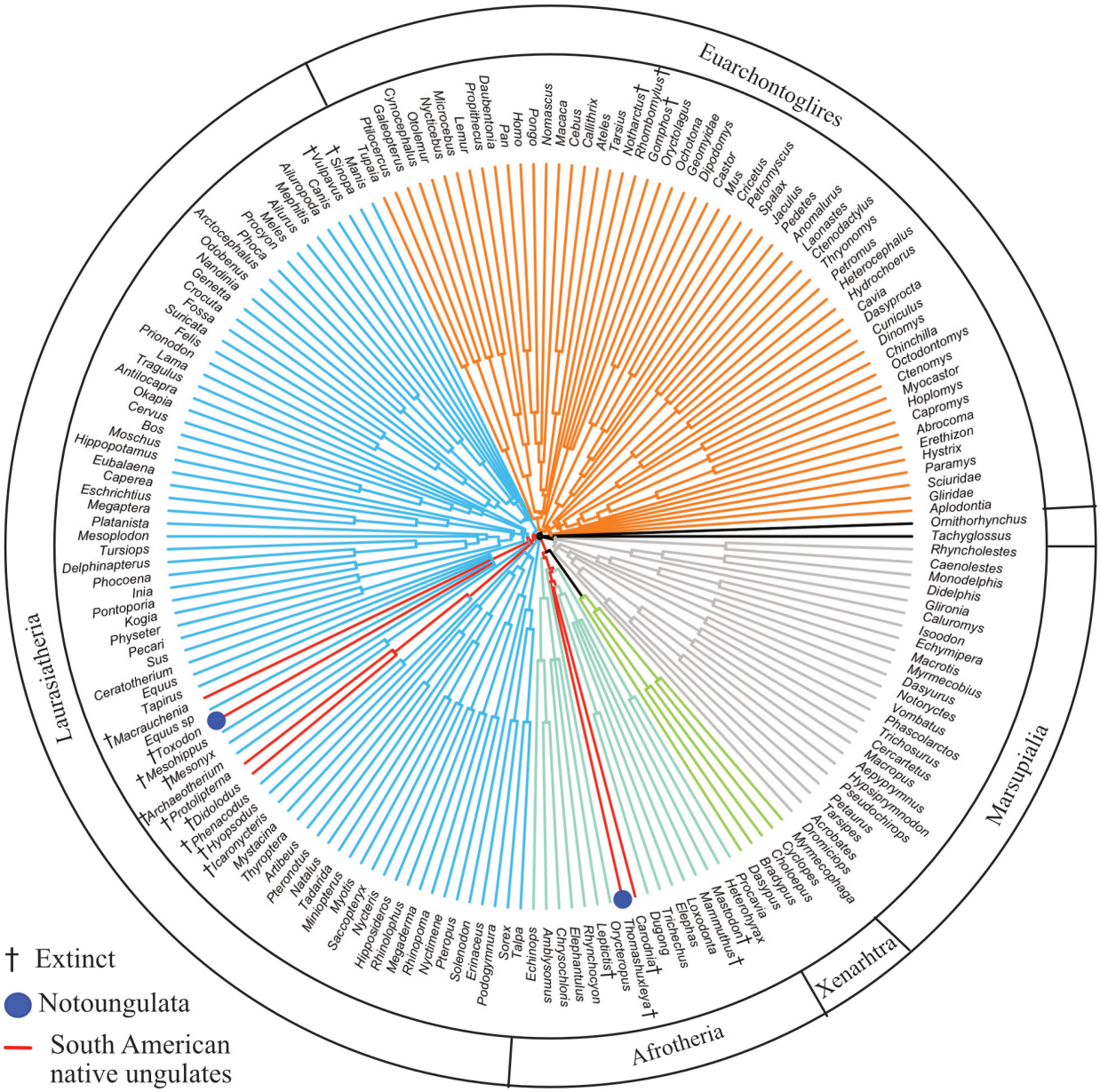

FIGURE 9. Strict consensus of 510 trees, 122374 steps in length from unconstrained parsimony analysis of combined proteomic and morphological data.

and Litopterna constraint and the globally optimal topology.

In order to test the different hypothesis regarding the relationships of SANUs, we also constrained all SANUs to form a clade (Meridiungulata). This hypothesis was proposed by McKenna (1975) based on biogeography, but it has not received support by the morphological data (e.g., Horovitz, 2004; Muizon and Cifelli, 2000). The "Meridungulata" constraint yielded 340 trees of 122424 steps, with a CI of 0.345 and RI 0.638. The strict consensus results in a polytomy with all SANUs plus *Hyopsodus* and *Phenacodus* forming the sister taxon of Euungulata. Again, a Wilcoxon rank sum test indicates there is not a significant difference (p value > 0.05; Table 6) between the "Meridiungulata" constraint and the globally optimal topology.

The unconstrained Bayesian analysis yielded an average standard deviation of split frequencies (SDSF) of 0.010 after 3,000,000 generations. This value is well under the recommended SDSF value of 0.05 (Ronquist et al., 2011); however, a number of other metrics identified in Tracer (Rambaut et

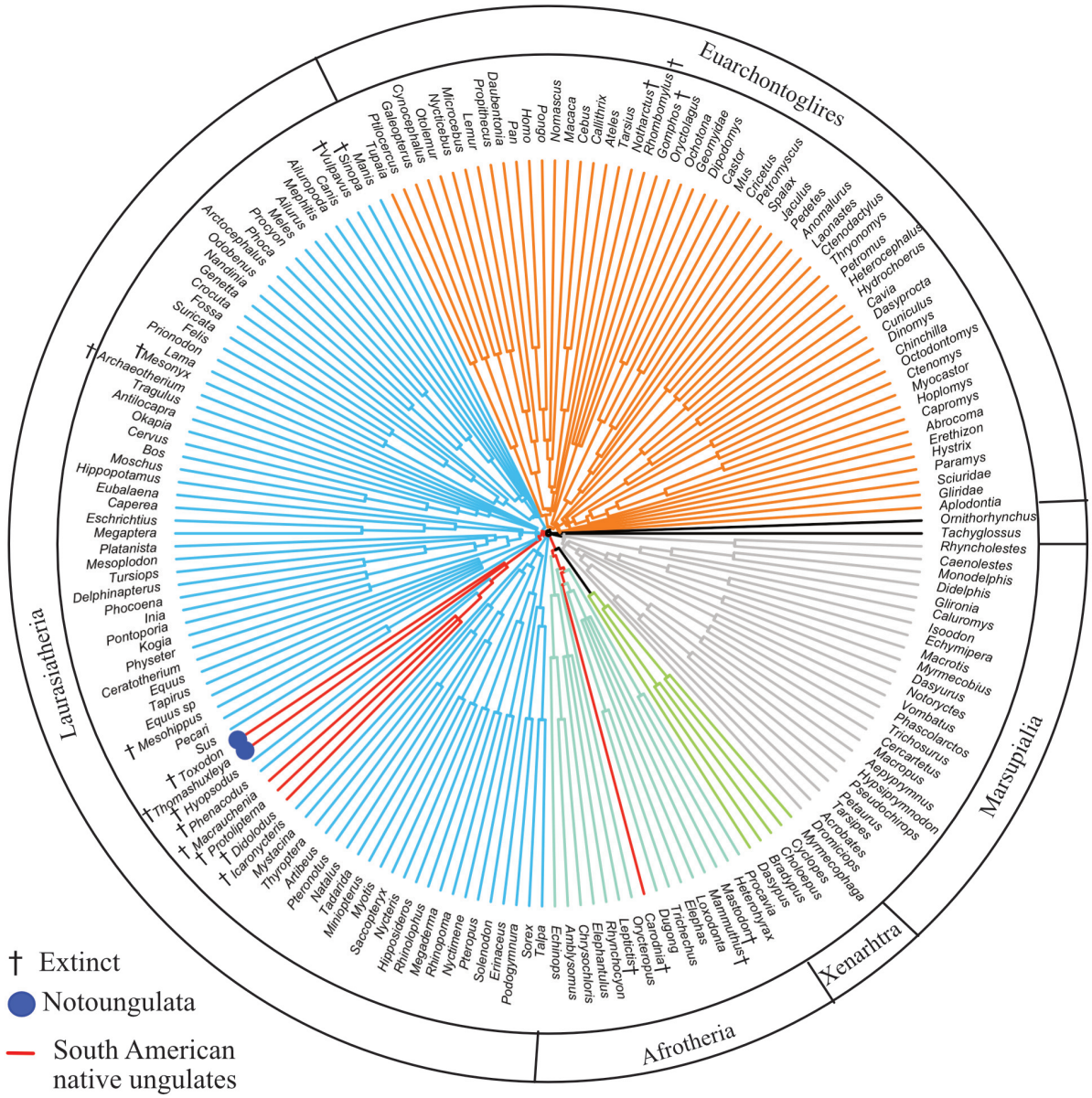

FIGURE 10. Strict consensus of 620 trees, 122391 steps in length from parsimony analysis of combined proteomic and morphological data constraining monophyly of each of two clades (but not both together): Notoungulata (i.e., *Thomashuxleya* and *Toxodon*) and Litopterna (i.e., *Protolipterna* and *Macrauchenia*).

al., 2014) indicate that independent runs did not converge on an optimal topology. The posterior probabilities of the South American fossil taxa with other placentals are low (Figure 11). The unconstrained Bayesian topology shows *Thomashuxleya* as the sister taxon of Xenarthra with a posterior probability of 0.62, *Protolipterna* and *Didolodus* as the sister group to Afrotheria (0.88), and *Carodnia* in a clade with *Loxodonta* (0.79). Finally, *Toxodon* and *Macrauchenia* form a clade which appears as the sister taxon of Perissodactyla with a posterior probability of 0.63.

The same dataset analysed constrained to support Notoungulata (*Thomashuxleya* and *Toxodon*) and Litopterna (*Macrauchenia* and *Protolipterna*), as above for MP, yielded an average standard deviation of split frequencies of 0.034 after 3,500,000 generations. The 50% majority rule consensus of the post burn-in topologies (Figure 12) shows Notoungulata and Litopterna as sister clades with a posterior probability of 1. The clade

TABLE 6. Results from the Wilcoxon signed ranks test comparing topologies carried out in PAUP. Meridungulata = constraint with all SANUs within a clade; N/L= Notoungulata *(Thomashuxleya, Toxodon)* and Litopterna *(Macrauchenia, Protolipterna)* monophyly constraints for each clade (but not both together); p values greater than 0.05 indicate no difference between optimal and competing topology.

Topology	Tree length	Rank sums	N	z	p
	122374	(best)			
N/L	122391	52385.0/--48640.0	449	-0.77	0.4390
Meridungulata	122424	214600.5/-193555.5	903	-1.49	0.14

(Notoungulata, Litopterna) appears as sister group of Perissodactyla (0.62) and *Carodnia* is within Afrotheria as sister taxon of *Loxodonta* (0.95) (Figure 12).

DISCUSSION

Cranioskeletal Anatomy

The completeness of MPEF-PV 8166 offers a unique opportunity to study the skeletal anatomy of *T. externa* in detail, and provides the first unambiguous associations of cranial and postcranial material from one individual. Dental similarities are substantial among the isotemnids *Thomashuxleya*, *Pleurolystodon*, *Anisotemnus*, and *Periphragnis* (Simpson, 1967), but the dental morphology along with size allowed us to refer MPEF-PV 8166 to *T. externa*. We noted morphological differences in several postcranial elements of MPEF-PV 8166 when compared with other specimens previously referred to this species. In particular, we noted differences in the scapulae, humeri, ulnae, and radii in comparison with AMNH 28905, which was used in O'Leary et al. (2013) to code postcranial characters of this species.

Although incomplete, the astragalus of MPEF-PV 8166 is of particular importance due to its association with craniodental remains. It is slightly smaller than AMNH 142463 referred to *T. externa* by Shockey and Flynn (2007). When compared with other astragali referred to Isotenmidae (Table 5), we found some differences that might indicate species specific characters within this group, such as the relatively high medial and lateral borders of the trochlea, and the relative width of the trochlea in relationship with the astragalar length. *Thomashuxleya* astragali (MPEF-PV 8166 and AMNH 142463) are considerably larger than other specimens variably assigned to this genus (e.g., AMNH 28690, AMNH 142464, and AMNH FM 14501), which therefore probably do not belong to *Thomashuxleya*.

Body Size

Regression equations obtained from dental variables yielded the highest estimates of body mass of MPEF-PV 8166 (Appendix 1), with an arithmetic mean of 556.4 kg. Other subsets of measurements differed in their estimates: craniomandibular variables gave a mean of 126 kg, limbs yielded a mean of 143.2 kg, multivariate regression equations that included dental variables yielded a mean of 180.5 kg (Appendix 2), and the body mass estimate of the astragalus was 84 ± 24.2 kg.

For Isotemnidae, Elissamburu (2012) favored estimations obtained from dental measurements. The dental dimensions can be influenced by differences in function and diet, which challenges their use to estimate the body mass in fossil mammals with no living descendants. Damuth (1990) noted that Paleogene ungulates from North America tend to have larger teeth relative to their body mass than extant ungulates. Considering the values obtained from the postcranial bones, we believe dental dimensions overestimate the body mass of MEPF-PV 8166 (Appendix 1).

Proximal limb bones are good estimators of body mass because they are weight-bearing elements, subject to biomechanical constrains (Scott, 1990). Elissamburu (2012) considered some postcranial measurements to be good estimators of body mass for *Thomashuxleya*, but not for closely related taxa such as *Pleurostylodon*, which is odd given the comparable dimensions and anatomy of both taxa. MEPF-PV 8166 and other specimens referred to *Thomashuxleya* show robust limbs. MEPF-PV 8166 exhibits some morphological features which are suggestive of scratch-digging capabilities, such as a high spine of the scapula, a large humeral deltopectoral crest that extends distally, and a long ulnar olecranon (Shockey et al., 2007). Fossorial habits have been inferred in mesotheriids (Shockey et al., 2007), and other notoungulates (e.g., *Protypotherium*) show features that suggest digging capabilities (Croft and Anderson, 2008). Fossorial habits may be an ancestral attribute in notoungulates (Shockey et

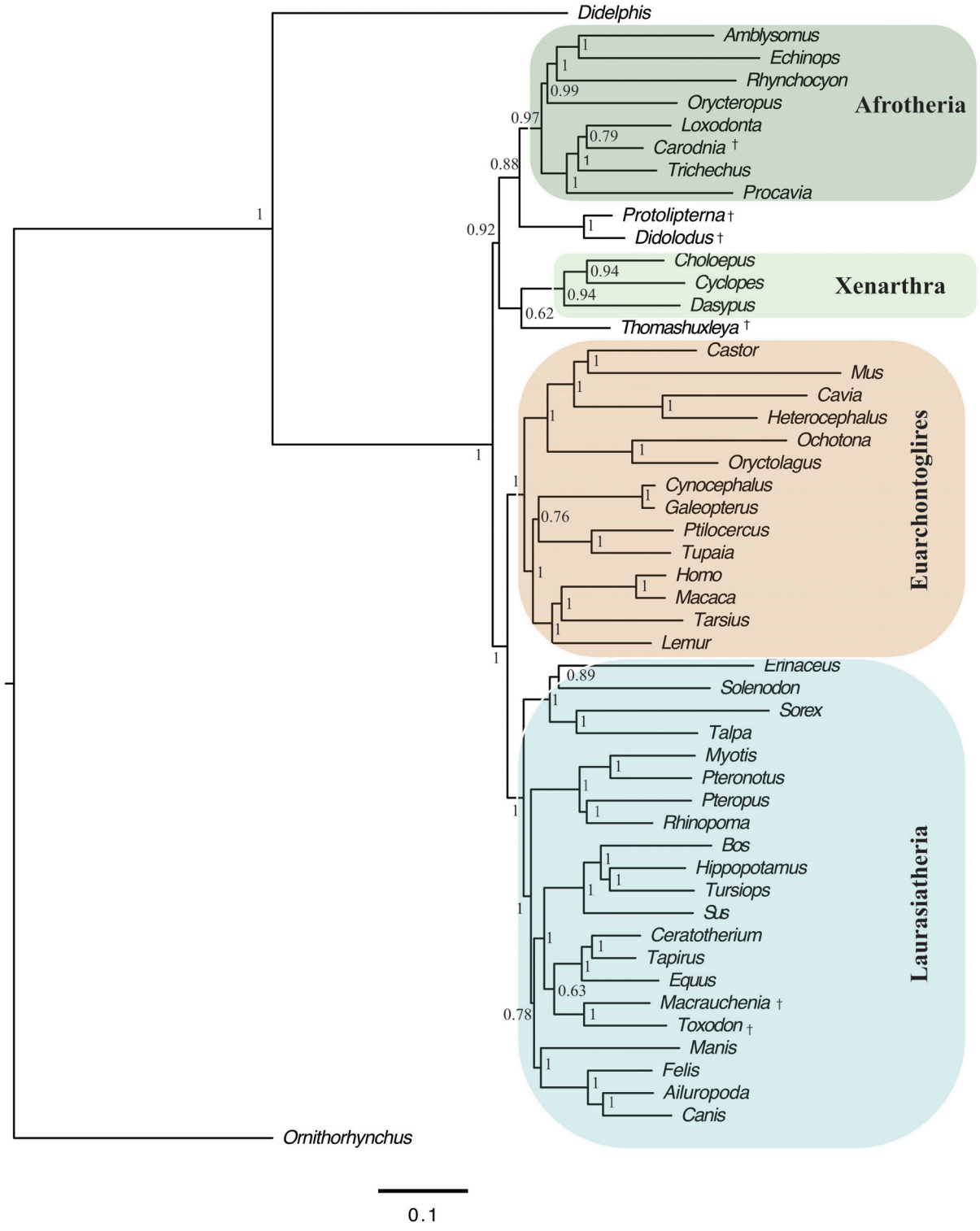

FIGURE 11. Optimal Bayesian tree (i.e., 50% majority rule of post-burn-in trees) of combined proteomic and morphological data. Numbers represent Bayesian posterior probabilities; daggers indicate fossil taxa.

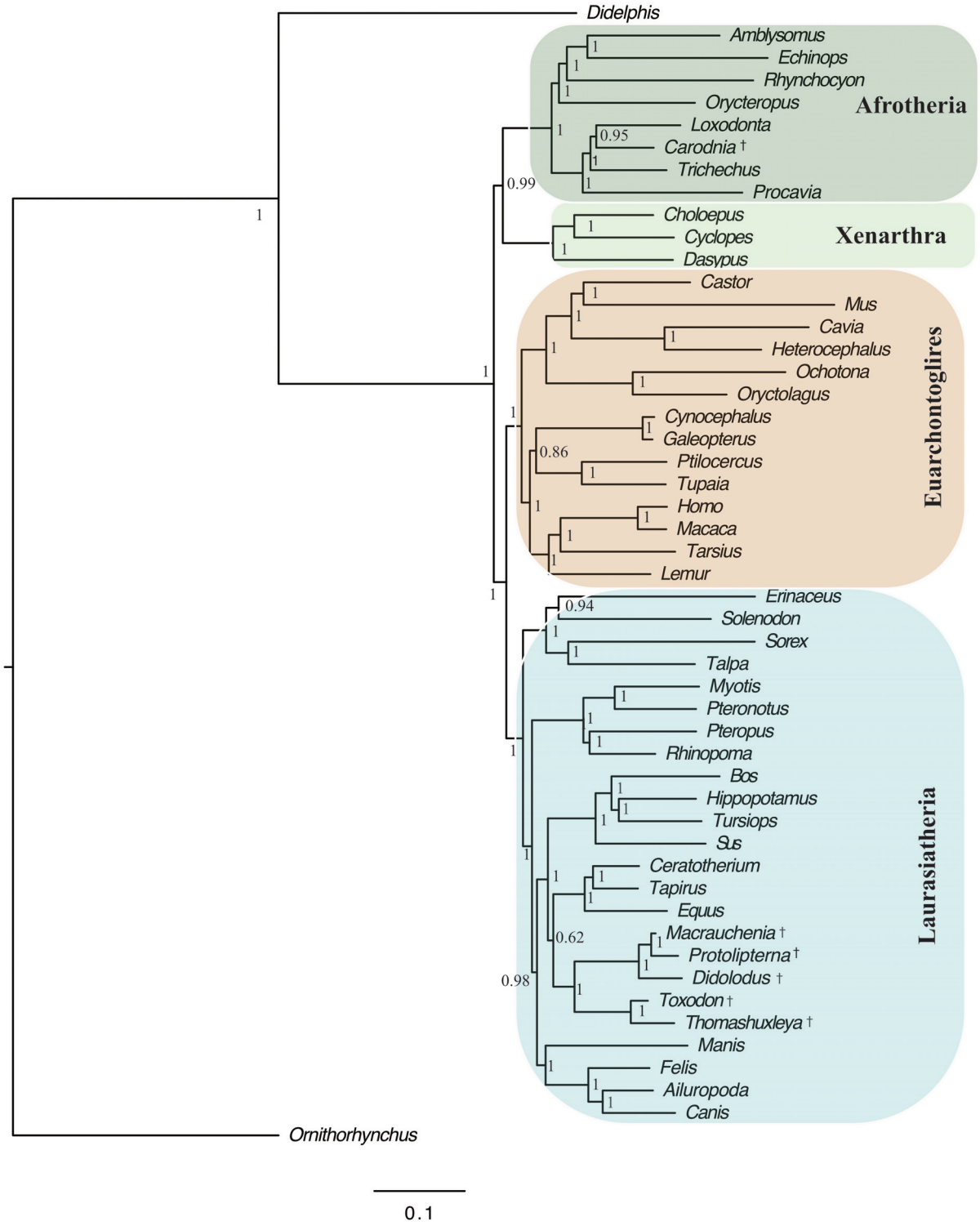

FIGURE 12. Optimal Bayesian tree (i.e., 50% majority rule of post-burn-in trees) of combined proteomic and morphological analysis constraining monophyly of each of two clades (but not both together): Notoungulata (i.e., *Thomashuxleya* and *Toxodon*) and Litopterna (i.e., *Protolipterna* and *Macrauchenia*). Numbers represent Bayesian posterior probabilities; daggers indicate fossil taxa.

al., 2007; Croft and Anderson, 2008), and if this is the case, limb bones could also overestimate the body size in notoungulates. The estimates obtained from postcranial measurements (mean 143.2 kg) are higher than the estimate of 70-90 kg for *Thomashuxleya* of Croft (2016). This estimate was based on a value of ca.1.5 m of head-body length based on Simpson's skeletal reconstruction (Croft, personal commun., 2017). In extant ungulates, the regression of head-body length shows the highest correlation with body mass and lowest percent of prediction error (Damuth, 1990).

The body mass estimate from the astragalus (84 ± 24.2 kg) is congruent with the estimate of 70-90 kg of Croft (2016) based on the estimated head-body length of *Thomashuxleya*. Astragalar regression equations of Tsubamoto (2014) are based on a broad taxonomic sample of mammals, whereas the regression equations using limb bones presented by Scott (1990) are based on living ungulates (artiodactyls and perissodactyls). Of the variety of body mass estimates for MEPF-PV 8166, we favor the one from the astragalus as it is based on a broader taxonomic sample of living mammals, and taken into account that morphological features in the limb bones associated with scratch-digging capabilities might bias the body mass estimate of MEPF-PV 8166.

T. externa is one of the largest mammalian taxa of the Vacan (Cifelli, 1985), only comparable in size with the astrapothere *Albertogaudrya*, according to the length of the lower molars. *T. externa* is the earliest known, anatomically well-documented todoxodontian notoungulate (Billet, 2011; Deraco and García-López, 2015). Basal notoungulates such as *Henricosbornia*, which also occur in the Vacan but with an origin in at least the Itaboraian (early Eocene; ~53-50 Ma; Gelfo et al., 2009; Woodburne et al., 2014a), were much smaller. For example, the m2 length of *Henricosbornia waitehor* from the Rio Chico Formation (Simpson, 1935) comprises less than a quarter of the m2 length in MPEF-PV 8166. With an estimated body mass of ~84 kg, *Thomashuxleya* demonstrates a large range of notoungulate body masses by the middle Eocene, and its postcranial morphology can be expected to reflect weight-bearing adaptations.

To our knowledge, of the more than 150 species recognized for notoungulates, bone histology is documented in only four (de Ricqlès et al., 2009; Tomassini et al., 2014, 2015, 2017; Forasiepi et al., 2015; Kolb et al., 2015b). As in *Thomashuxleya*, the toxodontians *Toxodon* and *Nesodon* showed Haversian bone with a compact cortex, a feature associated with the increased loading in large-bodied mammals (Straehl et al., 2013; Forasiepi et al., 2015; Kolb et al., 2015b; Tomassini et al., 2015). The presence of an outer circumferential layer (OCL) in the histological section of MPEF-PV 8166 indicates the specimen represents a skeletally mature individual of *T. externa*. At least some wear is evident on all of its dental loci, although compared to other Vacan specimens (and indeed Paleogene SANUs in general; see Strömberg et al., 2013) the degree of wear is fairly low.

Houssaye et al. (2016) analysed the bone microstructure of several SANUs including the toxodontid *Nesodon*. The femora of this taxon showed a large open medullary cavity surrounded by a spongious zone. A qualitative and quantitative analysis of the bone microstructure strongly suggest graviportality for *Nesodon* (Houssaye et al., 2016), based on the relatively high bone compactness and cortex thickness, and its position in a bone microstructure morphospace close to graviportal living mammals such as the rhinos *Ceratherium* and *Dicerorhinus*.

Systematics

The craniodental anatomy of MEPF-PV 8166 is similar to other specimens previously referred to *Thomashuxleya.* The completeness of the new *Thomashuxleya* specimen enable us to revise and add to data known for this taxon in a phylogenetic analysis within Notoungulata and within Placentalia. The craniodental anatomy of MEPF-PV 866 supports the placement of *Thomashuxleya* as an early divergent taxon within Toxodontia (Billet, 2011; Deraco and García-López, 2015). Some alleged synapomorphies that have previously been used to link SANUs with Afrotheria (Agnolin and Chimento, 2011) have already been convincingly refuted (Billet and Martin, 2011; Kramarz and Bond, 2014). Other studies group early members of Litopterna and South American "condylarths" with certain North American "condylarths"(Muizon and Cifelli, 2000; Gelfo, 2007) apparently a part of Laurasiatheria (Halliday et al., 2017). O'Leary et al. (2013) placed *Thomashuxleya* and *Carodnia* within Afrotheria, and *Didolodus* and *Protolipterna* within Laurasiatheria. Halliday et al. (2017) included *Protolipterna* and the notoungulate *Simpsonotus* in a comprehensive phylogenetic study of Paleocene placentals. In their study, *Protolipterna* was closely related to archaic artiodactyls, but the position of *Simpsonotus* was inconsistent, varying among different placental clades.

Welker et al. (2015) presented a new source of data to address this question in a pioneering study that used collagen protein sequences from two Pleistocene species to test the phylogenetic affinities of meridiungulates. They hypothesized that at least some of South America's endemic mammalian groups are close relatives of Perissodactyla. Previous authors (e.g., Billet, 2011; Cifelli, 1993; Gelfo, 2007; Horovitz, 2004; Muizon and Cifelli, 2000; Simpson, 1936, 1967) have shown that the two most speciose groups (notoungulates and litopterns) are ungulate-grade placentals; thanks to the novel data from Welker et al. (2015), we can now attempt a greater level of precision.

To fully evaluate the impact of the new material (if any) on the estimation of the relationships of *Thomashuxleya*, at least some integration of biomolecular and gross anatomical data is necessary. The matrix of O'Leary et al. (2013) is, to date, the largest available anatomical matrix that also samples at least some meridiungulates, and we have improved on their coding based on the new material described here. Further progress will be gained once the comprehensive matrix of O'Leary et al., 2013 is revised in both definitions and character codings; our study has made a start on the latter. The multiple analyses we perform is also a case study in which different data sources are integrated and results are evaluated from multiple perspectives. We believe that the combination of morphological and molecular data can provide more precise and robust hypotheses for several extinct clades of mammals (e.g., Asher et al., 2005; Muizon et al., 2015; Pattinson et al., 2015), and we further note that combination of molecular and morphological datasets can in principle increase support for clades not present when one or both are analysed in isolation (Gatesy and Baker, 2005; Lee and Camens, 2009; Thompson et al., 2012).

On the other hand, we do not maintain that combination of phylogenetic data from multiple sources (e.g., collagens from recent taxa, morphology from ancient fossils) will in every case yield a well-supported topology. The variety of optimality criteria we have applied to our analysis of phylogenetic data including meridiungulates and modern taxa does not confirm either the relationship proposed by Welker et al. (2015) with Perissodactyla, nor does it rule out alternatives that place one or more SANUs close to Afrotheria, Euungulata, or even Xenarthra. The strict consensus of our most parsimonious trees split Notoungulata, placing *Thomashuxleya* within Afrotheria and *Toxodon* within Laurasiatheria (Figure 9). The post-burnin, majority rule consensus of our optimal Bayesian trees place *Thomashuxleya* as the sister taxa of Xenarthra (with a very low posterior probability) and *Didolodus*, *Protolipterna*, and *Carodnia* in or near Afrotheria (also with low posterior probabilities; Figure 11). The monophyly of Notoungulata and Litopterna is supported by morphological data of the extensive fossil record of these two groups. The MP and Bayesian analyses constrained to support the monophyly of Notoungulata (*Toxodon* and *Thomashuxleya*) and Litopterna (*Macrauchenia* and *Protolipterna*) recovered these clades within Laurasiatheria (Figure 10 and 12), a result that approximates the hypothesis of Welker et al. (2015) that one or more meridiungulate groups are closely related to Perissodactyla.

There are a number of causes potentially behind this lack of a confident resolution of the phylogenetic relationships of meridiungulates with other placentals. First, although the new *Thomashuxleya* specimen is one of the oldest and most complete notoungulate yet known, it is still a highly derived taxon, and its potential synapomorphies with any extant relatives have been at least partly overwritten by homoplasy. This possibility is demonstrably not the case for many vertebrate groups with an extensive Paleogene fossil record (e.g., primates as shown by Pattinson et al., 2015), but it is naive to expect that such a scenario has never happened during the course of mammalian evolution. Muizon et al. (2015) performed a phylogenetic analysis of placental interordinal relationships using morphological characters and including SANUs and a large sample of other Paleogene fossils. They pointed out the high level of homoplasy detected in their dataset, and our data also clearly demonstrate homoplasy (RI of 0.638 and CI of 0.345 in our unconstrained tree).

Second, some part of the anatomy, which we have not yet sampled (e.g., inner ear), may yet contain key phylogenetic information with the potential to resolve the ambiguity discussed here (Macrini et al., 2010, 2013). An ear bone referred to an early divergent notoungulate shows that this region exhibits a mixture of plesiomorphic and derived features for Notoungulata (Billet and Muizon, 2013). The ear region of notoungulates exhibits similarities with hyracoids (Billet and Muizon, 2013), but further investigation is required to determine their phylogenetic implications. Finally, and non-exclusively, the early radiation of Notoungulata and other SANUs occurred very rapidly on parts of the continent which are not yet well sampled. Early Paleogene localities (e.g., Tiupampa, Itaborai)

older than Cañadón Vaca exist, but have not yet yielded well-preserved, associated remains of notoungulates. Although it is a Xenungulate and not a notoungulate, *Carodnia* is a notable exception, comprising another large, Eocene meridiungulate known from associated cranial and postcranial remains from Itaborai, Brazil. Accordingly, phylogenetic uncertainty may dissipate with the inclusion of additional anatomical characters (e.g., those derived from CT imaging) and with the discovery of more complete notoungulate material predating the Eocene. Further extraction of durable protein sequences from other meridiungulates, even those that predate the Neogene, remains theoretically possible and is clearly among the most promising avenues for further research into meridiungulate systematics (cf., Welker et al., 2015).

CONCLUSIONS

MPEF-PV 8166 is one of the oldest, most complete associated notoungulate skeletons yet documented in the literature. We refer this specimen to *T. externa* based on dental morphology and size. The presence of an associated dentition with postcrania enables us to recognize variation in skeletal elements previously assigned to this taxon. *T. externa* weighed approximately 84 ± 24.2 kg. Dental measurements provided larger estimates for body mass than skeletal elements. *T. externa* demonstrates that notoungulates acquired large size by the middle Eocene, and its bone histology shows that MPEF-PV 8166 was a skeletally mature individual with the capacity to withstand heavy loading, despite its incompletely fused femoral epiphyses. Our phylogenetic analysis raises a number of possibilities regarding its affinities. With *Thomashuxleya* constrained to be part of a monophyletic Notoungulata, MP recovers *Thomashuxleya* near the base of euungulates, close (but not on the stem) to Perissodactyla, whereas Bayesian analysis places it on the stem to Perissodactyla. Unconstrained MP and a Bayesian analysis splits meridiungulates into two groups: Pleistocene taxa known for collagen proteins with euungulates, and Paleogene taxa with afrotherians and xenarthrans.

ACKNOWLEDGEMENTS

We thank A. Carlini, P. Carlini, M. Cenizo, M. Ciancio, D. Croft, J. Gelfo, F. Goin, and M. Sánchez-Villagra for their help in the field and collecting the specimen described here. We are particularly grateful to A. Carlini for his generous hospitality and leadership during our stays in Argentina. M. Sánchez-Villagra kindly took some measurements and provided pictures of the skull. We are grateful to A. Carlini, M. Sánchez-Villagra, A. Forasiepi, E. Amson, and C. Pimiento, M. Geiger, and the Evolutionary Morphology and Palaeobiology of Vertebrates group in Zürich for valuable comments. We thank T. Scheyer and C. Kolb for assistance in the preparation and discussion of the histology sections. S. Lukac made the reconstruction of Thomashuxleya. We thank J. Gelfo, M. Lorente, D. Croft and an anonymous reviewer for their comments that greatly improved the manuscript. J. Carrillo was supported by Swiss National Fund P1ZHP3_165068, and SNF 31003A-149605 to M.R. Sánchez-Villagra, and the University of Cambridge Newton Trust and the Leverhulme Trust to R.J. Asher.

REFERENCES

Agnolin, F.L. and Chimento, N.R. 2011. Afrotherian affinities for endemic South American “ungulates.” *Mammalian Biology - Zeitschrift für Säugetierkunde,* 76 **(**2):101-108.
doi: dx.doi.org/10.1016/j.mambio.2010.12.001

Ameghino, F. 1897. Les mammifères crétacés de l’Argentine: deuxiême contribution â la connaissance de la faune mammalogique des couches â *Pyrotherium*. *Boletin Instituto Geografico Argentino,* 18:406-521.

Ameghino, F. 1901. Notices préliminaries sur des ongulés nouveaux des terrains Crétacés de Patagonie. *Boletín de la Academia Nacional de Ciencias de Córdoba,* 16:1-349.

Ameghino, F. 1902. Notice préliminaires sur des mammiferes nouveaux des terrains crétacés de Patagonie. *Boletín de la Academia Nacional de Ciencias de Córdoba,* 17:5-70.

Ameghino, F. 1904a. Nuevas especies de mamíferos, cretáceos y terciarios de la República Argentina. *Anales de la Sociedad Científica Argentina*, 56-58:1-142.

Ameghino, F. 1904b. La perforación astragaliana en los mamíferos no es un carácter originariamente primitivo. *Anales del Museo Nacional de Buenos Aires,* 3:349-460.

Asher, R.J. 2007. A web-database of mammalian morphology and a reanalysis of placental phylogeny. *BMC Evolutionary Biology,* 7:108.
doi: 10.1186/1471-2148-7-108

Asher, R.J., Emry, R.J., and McKenna, M.C. 2005. New material of *Centetodon* (Mammalia, Lipotyphla) and the importance of (missing) DNA sequences in systematic paleontology. *Journal of Vertebrate Paleontology*, 25(4):911-923.

Barnosky, A.D. and Lindsey, E.L. 2010. Timing of quaternary megafaunal extinction in South America in relation to human arrival and climate change. *Quaternary*

International, 217:10-29.
doi: dx.doi.org/10.1016/j.quaint.2009.11.017

Bellosi, E.D. and Krause, J.M. 2014. Onset of the Middle Eocene global cooling and expansion of open-vegetation habitats in central Patagonia. *Andean Geology*, 41 (1):29-48.

Bergqvist, L.P. Furtado, M.R., de Souza, C.P., and Powell, J.E. 2007. *Colbertia magellanica* (Bacia de Itaboraí, Brasil) e *Colbertia lumbrerense* (Grupo Salta, Argentina): a morfologia pós-craniana confrontada, p. 765-775. In Carvalho, I.S., Cassab, R.C., Schwanke, C., Carvahlo, A.A.C.S., Fernandes, M., Rodrigues, M.A.C,. Carvalho, M.S.S., and Oliveira, M.E.Q. (eds.), *Paleontologia: Cenários de Vida. Vol 1.* Editora Interciencia.

Billet, G. 2010. New observations on the skull of pyrotherium (pyrotheria, mammalia) and new phylogenetic hypotheses on South American ungulates. *Journal of Mammalian Evolution,* 17:21-59. doi: 10.1007/s10914-009-9123-0

Billet, G. 2011. Phylogeny of the notoungulata (mammalia) based on cranial and dental characters. *Journal of Systematic Palaeontology,* 9:481-497.
doi: 10.1080/14772019.2010.528456

Billet, G. and Martin, T. 2011. No evidence for an afrotherian-like delayed dental eruption in South American notoungulates. *Naturwissenschaften,* 98(6): 509-517.
doi: 10.1007/s00114-011-0795-y

Bininda-Emonds, O.R. P., Cardillo, M., Jones, K.E., MacPhee, R.D.E., Beck, R.M.D., Grenyer, R., Proce, S.A., Vos, A., Gittleman, J.L., and Purvis, A. 2007. The delayed rise of present-day mammals. *Nature,* 446:507-513. d
oi:10.1038/nature05634

Buckley, M. 2015. Ancient collagen reveals evolutionary history of the endemic South American 'ungulates'. *Proceedings of the Royal Society B,* 282:20142671.
doi: dx.doi.org/10.1098/rspb.2014.2671

Carlini, A.A., Ciancio, M., and Scillato-Yané, G.J. 2005. Los Xenarthra de Gran Barranca: mas de 20 a de historia. *Actas del XVI Congreso Geológico Argentino*,4:419-424.

Cassini, G.H., Cerdeño, E., Villafañe, A.L., and Muñoz, N.A. 2012. Paleobiology of Santacrucian native ungulates (Meridiungulata: Astrapotheria, Litopterna and Notoungulata), p. 243-286. In Vizcaíno, S.F., Kay, R.F., and Bargo, M.S. (eds.), *Early Miocene Paleobiology in Patagonia: High Latitude Paleocommunities of the Santa Cruz Formation*. Cambridge University Press, Cambridge.

Cassini, G.H., Mendoza, M., Vizcaíno, S.F., and Bargo, M.S. 2011. Inferring habitat and feeding behaviour of early Miocene notoungulates from Patagonia. *Lethaia,* 44:153-165.
doi:10.1111/j.1502-3931.2010.00231.x

Cerdeño, E., Vera, B., Schmidt, G.I., Pujos, F., and Quispe, B.M. 2012. An almost complete skeleton of a new Mesotheriidae (Notoungulata) from the late Miocene of Casira, Bolivia. *Journal of Systematic Palaeontology*, 10(2):341-360.
doi: 10.1080/14772019.2011.569576

Cifelli, R.L. 1985. Biostratigraphy of the Casamayoran, early Eocene, of Patagonia. *American Museum Novitates,* 2820.

Cifelli, R.L. 1993. The phylogeny of the native South American ungulates, p. 195-216. In Szalay, F.S., Novacek, M.J., and McKenna, M.C. (eds.), *Mammal Phylogeny Placentals*. Springer-Verlag, New York.

Cione, A.L., Tonni, E.P., and Soibelzon, L. 2003. The broken zig-zag: late Cenozoic large mammal and tortoise extinction in South America. *Revista del Museo Argentino de Ciencias Naturales,* 51(1):1-19.

Croft, D. A. 1999. Placentals: endemic South American ungulates, p. 890-906. In Singer, R. (ed.), *The Encyclopedia of Paleontology*. Fitzroy-Dearborn Publisher, Chicago.

Croft, D.A. 2016. *Horned Armadillos and Rafting Monkeys. The Fascinating Fossil Mammals of South America*. Indiana University Press, Bloomington and Indianapolis.

Croft, D.A. and Anderson, L.C. 2008. Locomotion in the extinct notoungulate *Protypotherium. Paleontologia Electronica,* 11(1):1-20.

Croft, D.A. Flynn, J.J., and Wyss, A.R. 2004. Notoungulata and Litopterna of the early Miocene Chucal fauna, northern Chile. *Fieldiana Geology*, 50:1-52.

Damuth, J. 1990. Problems in estimating body masses of archaic ungulates using dental measurements, p. 229-253. In Damuth, J. and MacFadden, B.J. (eds.), *Body Size in Mammalian Paleobiology: Estimation and Biological Implications*. Cambridge University Press, Cambridge.

Deraco, V. and García-López, D.A. 2015. A new Eocene Toxodontia (Mammalia, Notoungulata) from northwestern Argentina. *Journal of Vertebrate Paleontology,* e1037884.
doi: 10.1080/02724634.2015.1037884

de Ricqlès, A., Taquet, P., and de Buffrenil, V. 2009. "Rediscovery" of Paul Gervais' paleohistological collection. *Geodiversitas,* 31:943-971.
doi:10.5252/g2009n4a943

Elissamburu, A. 2012. Estimación de la masa corporal en géneros del Orden Notoungulata. *Estudios Geológicos,* 68:91-111.
doi:10.3989/egeol.40336.133

Farris, J.S. 1989. The retention index and the rescaled consistency index. *Cladistics*, 5:417-419.

Foley, N.M., Springer, M.S., and Teeling, E.C. 2016. Mammal madness: is the mammal tree of life not yet resolved? *Philosophical transactions of the Royal Society of London. Series B, Biological Sciences,* 331:20150140.
doi:10.1098/rstb.2015.0140

Forasiepi, A., Cerdeño, E., Bond, M., Schmidt, G., Naipauer, M., Straehl, F., Martinelli, A., Garrido, A., Schmitz, M., and Crowley, J. 2015. New toxodontid (Notoungulata) from the Early Miocene of Mendoza, Argentina. *Paläontologische Zeitschrift,* 89(3): 611-

634.
doi:10.1007/s12542-014-0233-5

Gatesy, J. and Baker, R.H. 2005. Hidden likelihood support in genomic data: can forty-five wrongs make a right? *Systematic Biology*, 54(3):483-492.
doi: 10.1080/10635150590945368

Geiger, M., Forasiepi, A.M., Koyabu, D., and Sánchez-Villagra, M.R. 2014. Heterochrony and post-natal growth in mammals – an examination of growth plates in limbs. *Journal of Evolutionary Biology*, 27(1):98-115. doi: 10.1111/jeb.12279

Gelfo, J.N. 2007. The 'Condylarth' *Raulvaccia peligrensis* (Mammalia: Didolodontidae) from the Paleocene of Patagonia, Argentina. *Journal of Vertebrate Paleontology,* 27(3): 651-660.

Gelfo, J.N., Goin, F.J., Woodburne, M.O., and Muizon, C.D. 2009. Biochronological relationships of the earliest South American Paleogene mammalian faunas. *Palaeontology,* 52:251-269.
doi:10.1111/j.1475-4983.2008.00835.x

Giannini, N. and García-López D. 2014. Ecomorphology of mammalian fossil lineages: identifying morphotypes in a case study of endemic South American ungulates. *Journal of Mammalian Evolution,* 21:195-212.
doi:10.1007/s10914-013-9233-6

Goloboff, P.A. 2014. Extended implied weighting. *Cladistics,* 30(3):260-272. doi:10.1111/cla.12047

Goloboff, P.A., Carpenter, J.M., Arias, J.S., and Miranda-Esquivel, D.R. 2008b. Weighting against homoplasy improves phylogenetic analysis of morphological datasets. *Cladistics,* 24(5):758-773.
doi:10.1111/j.1096-0031.2008.00209.x

Goloboff, P.A., Farris, J.S., and Nixon, K.C. 2008a. TNT, a free program for phylogenetic analysis. *Cladistics,* 24(5):774-786.
doi:10.1111/j.1096-0031.2008.00217.x

Halliday, T.J.D., Upchurch, P., and Goswami, A. 2017. Resolving the relationships of Paleocene placental mammals. *Biological Reviews*, 92(1):521-550.
doi:10.1111/brv.12242

Horovitz, I. 2004. Eutherian mammal systematics and the origins of South American ungulates as based on postcranial osteology. *Bulletin of Carnegie Museum of Natural History,* 36:63-79.
doi:10.2992/0145-9058(2004)36[63:EMSATO]2.0.CO;2

Houssaye, A., Fernandez, V., and Billet, G. 2016. Hyperspecialization in some South American endemic ungulates revealed by long bone microstructure. *Journal of Mammalian Evolution,* 23:221-235. doi: 10.1007/s10914-015-9312-y

Janis, C. 1990. Correlation of cranial and dental variables with body size in ungulates and macropodoids, p. 255-299. In Damuth, J. and MacFadden, B.J. (eds.), *Body Size in Mammalian Palaeobiology: Estimation and Biological Implications*. Cambridge University Press, Cambridge.

Kay, R.F., Madden, R.H., Vucetich, M.G., Carlini, A.A., Mazzoni, M.M., Re, G.H., Heizler, M., and Sandeman, H. 1999. Revised geochronology of the Casamayoran South American land mammal age: climatic and biotic implications. *Proceedings of the National Academy of Sciences,* 96:13235-13240.
doi:10.1073/pnas.96.23.13235

Kolb, C., Scheyer, T., Lister, A., Azorit, C., de Vos, J., Schlingemann, M., Rossner, G., Monaghan, N., and Sánchez-Villagra, M.R. 2015a. Growth in fossil and extant deer and implications for body size and life history evolution. *BMC Evolutionary Biology,* 15:19.
doi:10.1186/s12862-015-0295-3

Kolb, C., Scheyer, T.M., Veitschegger, K., Forasiepi, A.M., Amson, E., Van der Geer, A.A.E. Van den Hoek Ostende, L.W., Hayashi, S., and Sánchez-Villagra, M.R. 2015b. Mammalian bone palaeohistology: a survey and new data with emphasis on island forms. *PeerJ,* 3:e1358.
doi:10.7717/peerj.1358

Kramarz, A. and Bond, M. 2014. Critical revision of the alleged delayed dental eruption in South American "ungulates." *Mammalian Biology - Zeitschrift für Säugetierkunde,* 79(3):170-175.
doi:dx.doi.org/10.1016/j.mambio.2013.11.001

Lanfear, R., Calcott, B., Ho, S.Y.W., and Guindon, S. 2012. PartitionFinder: combined selection of partitioning schemes and substitution models for phylogenetic analyses. *Molecular Biology and Evolution,* 29(6):1695-1701.
doi:dx.doi.org/10.1093/molbev/mss020

Lee, M.S.Y. and Camens, A.B. 2009. Strong morphological support for the molecular evolutionary tree of placental mammals. *Journal of Evolutionary Biology*, 22(11):2243-2257.
doi:10.1111/j.1420-9101.2009.01843.x

Lorente, M., Gelfo, J.N., and López, G.M. 2014. Postcranial anatomy of the early notoungulate *Allalmeia atalaensis* from the Eocene of Argentina. *Alcheringa: An Australasian Journal of Palaeontology,* 38:398-411.
doi:10.1080/03115518.2014.885199

Lorente, M. 2015. *Desarrollo de modelos de asociación y clasificaciones de restos postcraneanos aislados de ungulados nativos del Paleoceno-Eoceno de América del Sur*. Unpublished PhD thesis, Facultad de Ciencias Naturales y Museo de La Plata, Universidad de La Plata, La Plata, Argentina

MacFadden, B.J. 2005. Diet and habitat of toxodont megaherbivores (Mammalia, Notoungulata) from the late Quaternary of South and Central America. *Quaternary Research,* 64:113-124.
doi:dx.doi.org/10.1016/j.yqres.2005.05.003

Madden, R.M. 1990. *Miocene Toxodontidae (Notoungulata, Mammalia) from Colombia, Ecuador and Chile*. Unpublished PhD thesis, Department of Biological Anthropology and Anatomy, Duke University

Madden, R.M. 2015. Hypsodonty in the South American fossil record, p. 12-59. In Madden, R.M. (ed.), *Hypsodonty in Mammals: Evolution, Geomorphology and*

the Role of Earth Surface Processes. Cambridge University Press, Cambridge.

Maddison, W.P. and Maddison, D.R. 2016. Mesquite: a modular system for evolutionary analysis. Version 3.10 mesquiteproject.org

Martinez-Maza, C., Alberdi, M.T., Nieto-Diaz, M., and Prado, J.L. 2014. Life-history traits of the Miocene *Hipparion concudense* (Spain) inferred from bone histological structure. *PLoS ONE,* 9:e103708. doi:10.1371/journal.pone.0103708

McKenna, M.C. and Bell, S.K. 1997. *Classification of Mammals above the Species Level*. Columbia University Press, New York.

Mendoza, M., Janis, C.M., and Palmqvist, P. 2006. Estimating the body mass of extinct ungulates: a study on the use of multiple regression. *Journal of Zoology,* 270:90-101. doi:10.1111/j.1469-7998.2006.00094.x

Meredith, R.W., Janečka, J.E., Gatesy, J., Ryder, O.A., Fisher, C.A., Teeling, E.C., Goodbla, A., Eizirik, E., Simão, T.L.L., Stadler, T., Rabosky, D.L., Honeycutt, R.L., Flynn, J.J., Ingram, C.M., Steiner, C., Williams, T.L., Robinson, T.J., Burk-Herrick, A.B., Westerman, M.,Ayoub, N.A., Springer, M.S., and Murphy, W.J. 2011. Impacts of the Cretaceous terrestrial revolution and KPG extinction on mammal diversification. *Science*, 334(6055):521-524. doi:10.1126/science.1211028

Muizon, C. de, and Cifelli, R. 2000. The "condylarths" (archaic Ungulata, Mammalia) from the early Palaeocene of Tiupampa (Bolivia): implications on the origin of the South American ungulates. *Geodiversitas*, 22(1):47-150.

Muizon, C. de, Billet, G., Argot, C., Ladevèze, S., and Goussard, F. 2015. *Alcidedorbignya inopinata*, a basal pantodont (Placentalia, Mammalia) from the early Palaeocene of Bolivia: anatomy, phylogeny and palaeobiology. *Geodiversitas*, 37(4):397-634. doi:10.5252/g2015n4a1

Murphy, W J., Eizirik, E., Johnson, W.E., Zhang, Y.P., Ryder, O.A., and O'Brien, J. 2001. Molecular phylogenetics and the origins of placental mammals. *Nature*, 409(6820):614-618. doi:10.1038/35054550

O'Leary, M.A., Bloch, J.I., Flynn, J.J., Gaudin, T.J., Giallombardo, A., Giannini, N.P., Goldberg, S.L., Kraatz, B.P., Luo, Z-X., Meng, J., Ni, X., Novacek, M.J., Perini, F.A., Randall, Z.S., Rougier, G.W., Sargis, E.J., Silcox, M.T., Simmons, N.B., Spaulding, M., Velazco, P.M., Weksler, M., Wible, J.R., and Cirranello, A.L. 2013. The Placental mammal ancestor and the post-K-Pg radiation of placentals. *Science*, 339:662-667. doi: 10.1126/science.1229237

Pascual, R. 2006. Evolution and geography: the biogeographic history of South American land mammals. *Annals of the Missouri Botanical Garden*, 93:209-230. doi: 10.3417/0026-6493(2006)93[209:eagtbh]2.0.co;2

Patterson, B. 1977. A primitive pyrothere (mammalia, notoungulata) from the early Tertiary of Northwestern Venezuela. *Fieldiana Geology*, 33(22):1-40. doi:10.5962/bhl.title.5225

Pattinson, D.J., Thompson, R.S., Piotrowski, A.K., and Asher, R.J. 2015. Phylogeny, paleontology, and primates: do incomplete fossil bias the tree of life? *Systematic Biology*, 64(2): 169-186. doi:10.1093/sysbio/syu077

Ponton, F., Elżanowski, A., Castanet, J., Chinsamy, A., Margerie, E.D., Ricqlès, A.D., and Cubo, J. 2004. Variation of the outer circumferential layer in the limb bones of birds. *Acta Ornithologica*, 39:137-140. doi: 10.3161/068.039.0210

R Core Team. 2016. R: A language and environment for statistical computing. R Foundation for Statistical Computing, Vienna, Austria.URL www.R-project.org/.

Rambaut, A., Suchard, M.A., Xie, D., and Drummond, A.J. 2014. Tracer v1.6. beast.bio.ed.ac.uk/Tracer

Ronquist, F., Huelsenbeck, J., and Teslenko, M. 2011. MrBayes 3.2 Manual: Tutorials and model summaries, downloaded 25 november 2016. mrbayes.sourceforge.net/manual.php

Ronquist, F., Teslenko, M., vand der Mark, P., Ayres, D.L., Darling, A., Höhna, S., Larget, B., Liu, L., Suchard, M.A., and Huelsenbeck, J.P. 2012. MrBayes 3.2: efficient Bayesian phylogenetic inference and model choice across a large model space. *Systematic Biology*, 61(3):539-542. doi:10.1093/sysbio/sys029

Roth, S. 1903. Los ungulados sudamericanos. *Anales del Museo de La Plata* 5.

Scott, K.M. 1990. Postcranial dimensions of ungulates as predictors of body mass, p. 301-335. In Damuth, J. and MacFadden, B.J. (eds.), *Body Size in Mammalian Paleobiology: Estimation and Biological Implications*. Cambridge University Press, Cambridge.

Scott, W.B. 1912. Mammalia of the Santa Cruz Beds. Volume VI, Paleontology. Part II Toxodonta, p. 111-238. In Scott, W.B. (ed.), *Reports of the Princeton University Expeditions to Patagonia, 1896-1899*. Princeton University, E. Schweizerbart'sche Verlagshandlung (E. Nägele), Stuttgart.

Shockey, B.J. and Flynn, J.J. 2007. Morphological diversity in the postcranial skeleton of Casamayoran (?middle to late Eocene) notoungulata and foot posture in notoungulates. *American Museum Novitates*, 3601.

Shockey, B.J., Croft, D.A., and Anaya, F. Analysis of function in the absence of extant functional homologues: a case study using mesotheriid notoungulates (Mammalia). *Paleobiology*, 33(2): 227-247. doi:10.1666/05052.1

Simpson, G.G. 1935. Descriptions of the oldest known South American mammals, from the Rio Chico Formation. *American Museum Novitates*, 793.

Simpson, G.G. 1936. Skeletal remains and restoration of Eocene Entelonychia from Patagonia. *American Museum Novitates*, 826.

Simpson, G.G. 1948. The beginning of the age of mammals. Part 1. *Bulletin of the American Museum of Natural History*, 91:1-232.

Simpson, G.G. 1967. The beginning of the age of mammals in South America. Part 2. *Bulletin of the American Museum of Natural History*, 137:1-260.

Simpson, G.G. 1978. Early mammals in South America: Fact, controversy, and mystery. *Proceedings of the American Philosophical Society.* 122:318–328.

Simpson, G.G. 1980. *Splendid Isolation. The Curious History of South American Mammals*. Yale University Press, New Haven and London.

Smith, J.B. and Dodson, P. 2003. A proposal for a standard terminology of anatomical notation and orientation in fossil vertebrate dentitions. *Journal of Vertebrate Paleontology*, 23(1):1-12. doi:dx.doi.org/10.1671/0272 4634(2003)23[1:APFAST]2.0.CO;2

Straehl, F.R., Scheyer, T.M., Forasiepi, A.M., MacPhee, R.D., and Sánchez-Villagra, M.R. 2013. Evolutionary patterns of bone histology and bone compactness in xenarthran mammal long bones. *PLoS ONE*, 8:e69275. doi:10.1371/journal.pone.0069275

Strömberg, C.A.E., Dunn, R.E., Madden, R.H., Kohn, M.J., and Carlini, A.A. 2013. Decoupling the spread of grasslands from the evolution of grazer-type herbivores in South America. *Nature Communications*, 4:178. doi:10.1038/ncomms2508

Song, S., Liu, L., Edwards, S.V., and Wu, S. 2012. Resolving conflict in eutherian mammal phylogeny using phylogenomics and the multispecies coalescent model. *Proceedings of the National Academy of Sciences*, 109(37):14942-14947. doi: 10.1073/pnas.1211733109

Swofford, D.L. 2002. PAUP*. *Phylogenetic Analysis Using Parsimony (*and other methods). Version 4.* Sinauer Associates, Sunderland, Massachusetts.

Tarver, J.E., dos Reis, M., Mirarab, S., Moran, R.J., Parker, S., O'Reilly, J.E., King, B.L., O'Connell, M.J., Asher, J.R., Warnow, T., Peterson, K., Donoghue, P.C.J., and Pisani, D. 2016. The interrelationships of placental mammals and the limits of phylogenetic inference. *Genome Biology and Evolution*, 8(2): 330-344. doi: 10.1093/gbe/evv261

Thompson, R.S., Bärmann, E.V., and Asher, R.J. 2012. The interpretation of hidden support in combined data phylogenetics. *Journal of Zoological Systematics and Evolutionary Research*, 50(4):251-263. doi:10.1111/j.1439-0469.2012.00670.x

Tomassini, R.L., Garrone, M.C., and Montalvo, C.I. 2017. New light on the endemic South American pachyrukhine *Paedotherium* Burmeister, 1888 (Notoungulata, Hegetotheriidae): taphonomic and paleohistological analysis. *Journal of South American Earth Sciences*, 73:33-41.doi: 10.1016/ j.jsames.2016.11.004

Tomassini, R.L., Miño-Boilini, A.R., Zurita, A.E., Montalvo, C.I., and Cesaretti, N. 2015. Modificaciones fosildiagenéticas en *Toxodon platensis* Owen, 1837 (Notoungulata, Toxodontidae) del Pleistoceno tardío de la provincia de Corrientes, Argentina. *Revista Mexicana de Ciencias Geológicas*, 32(2):283-292.

Tomassini, R.L., Montalvo, C.I., Manera, T., and Visconti G. 2014. Mineralogy, geochemistry and paleohistology of Pliocene mammals from the Monte Hermoso Formation (Argentina). *Paedotherium bonaerense* (Notoungulata, Hegetotheriidae) as a case study. *Ameghiniana*, 51:385-395. doi:10.5710/AMGH.01.07.2014.2737

Townsend, K.E.B. and Croft, D.A. 2008. Diets of notoungulates from the Santa Cruz Formation, Argentina: new evidence from enamel microwear. *Journal of Vertebrate Paleontology*, 28:217-230. doi:10.1671/0272-4634(2008)28[217:DONFTS]2.0.CO;2

Tsubamoto, T. 2014. Estimating body mass from the astragalus in mammals. *Acta Palaeontologica Polonica*, 59:259-265. doi: 10.4202/app.2011.0067

Welker, F., Collins, M.J., Thomas, J.A., Wadsley, M., Brace, S., Cappellini, E., Turvey, S.T., Reguero, M., Gelfo, J.N., Kramarz, A., Burger, J., Thomas-Oates, J., Ashford, D.A.,Ashton, P.D., Rowsell, K., Porter, D.M., Kessler, B., Fischer, R., Baessmann, C.,Kaspar, S., Olsen, J.V., Kiley, P., Elliott, J.A., Kelstrup, C.D., Mullin, V., Hofreiter, M., Willerslev, E., Hublin, J.J., Orlando, L., Barnes, I., and MacPhee, R.D.E. 2015. Ancient proteins resolve the evolutionary history of Darwin's South American ungulates. *Nature*, 522:81-84. doi: 10.1038/nature14249

Wilf, P., Cúneo, N.R., Escapa, I.H., Pol, D., and Woodburne, M.O. 2013. Splendid and seldom isolated: the paleobiogeography of Patagonia. *Annual Review of Earth and Planetary Sciences*, 41:561-603. doi:10.1146/annurev-earth-050212-124217

Woodburne, M.O., Goin, F.J., Bond, M., Carlini, A.A., Gelfo, J.N., López, G.M., Iglesias, A., and Zimicz, A.N. 2014a. Paleogene land mammal faunas of South America: a response to global climatic changes and indigenous floral diversity. *Journal of Mammalian Evolution*, 21:1-73. doi: 10.1007/s10914-012-9222-1

Woodburne, M.O., Goin, F.J., Raigemborn, M.S., Heizler, M., Gelfo, J.N., and Oliveira, E.V. 2014b. Revised timing of the South American early Paleogene land mammal ages. *Journal of South American Earth Sciences*, 54:109-119. doi: dx.doi.org/10.1016/j.jsames.2014.05.003

APPENDIX 1.

Definitions, measurements (in mm, unless otherwise stated) and equations used (Janis, 1990; Scott, 1990; Tsubamoto, 2014) to estimated the body mass (BM) in kg of MPEF-PV 8166. PE= Percent of error.

Variable	Acronym	Definition	Type	Dataset	Value	Equation	R^2	% PE	Slope	Intercept	BM	BM + PE	BM - PE
Lower molar row length	LMRL	Measured along the base of the teeth	Dental	All ungulates	75.6	log BM= 3.265*log(LMRL)-0.536	0.94	31.9	3.27	-0.54	396	522	269
First lower molar length	FLML	Measured at the occlusal surface of the tooth	Dental	All ungulates	20.1	log BM= 3.263*log(FLML)+1.337	0.93	34.6	3.26	1.34	389	524	254
First lower molar width	FLMW		Dental	All ungulates	15.6	log BM= 2.909*log(FLMW)+2.030	0.92	38.4	2.91	2.03	316	437	194
First lower molar area	FLMA	FLMA= FLML*FLMW	Dental	All ungulates	313.3	log BM= 1.553*log(FLMA)+1.701	0.93	33.2	1.55	1.7	378	503	252
Second lower molar length	SLML	Measured at the occlusal surface of the tooth	Dental	All ungulates	22.5	log BM= 3.201*log(SLML)+1.130	0.94	31.9	3.2	1.13	289	381	197
Second lower molar area	SLMA	SLMA= SLML*Second Lower Molar Width	Dental	All ungulates	343.7	log BM= 1.563*log(SLMA)+1.541	0.94	33.5	1.56	1.54	320	427	213
Third lower molar area	TLMA	TLMA= Third lower molar length *Third lower molar width	Dental	All ungulates	508.9	log BM= 1.580*log(TLMA)+1.404	0.93	33.1	1.58	1.4	479	638	321
Second upper molar length	SUML	Measured at the occlusal surface of the tooth	Dental	All ungulates	27.9	log BM= 3.184*log(SUML)+1.091	0.93	34.7	3.18	1.09	494	666	323
Second upper molar width	SUMW	Measured at the occlusal surface of the tooth	Dental	All ungulates	36.9	log BM= 3.004*log(SUMW)+1.469	0.92	38.9	3	1.47	1501	2085	917
Second upper molar area	SUMA	SUMA=SUML*SUMW	Dental	All ungulates	1029.5	log BM=1.568*log(SUMA)+1.277	0.94	32.7	1.57	1.28	1002	1329	674
Posterior jaw length	PJL	Measured as the horizontal distance from the back of the jaw condyle to the posterior border of m3	Crania	All ungulates	65.3	log BM= 2.412*log(PJL)+0.031	0.93	36.5	2.41	0.03	26	35	16
Maximum width of the mandibular angle	WMA	Measured from the junction of the posterior part of m3 with the jaw to the maximally distant point on the angle of the jaw	Crania	All ungulates	105.5	log BM= 2.803*log(WMA)-0.352	0.92	40.5	2.8	-0.35	209	293	124
Length of the ridge for the masseteric attachment	MFL	Measured from the posterior portion of the jaw glenoid to the most anterior extent of the scar for the origin of the masseter muscle	Crania	All ungulates	153	log BM= 2.950*log(MFL)-1.289	0.94	35	2.95	-1.29	143	193	93
Humerus functional length (cm)	H1	The distance between the most proximal point of the head and the most distal point of the trochlea	Postcranial	All ungulates	19.85	log BM= 3.4026*log(H1)-2.3707	0.92	28	3.4	-2.37	111	142	80
Humerus trochlear diameter (cm)	H4	The transverse distance of the distal articular surface	Postcranial	All ungulates	4.76	log BM= 2.4815*log(H4)+0.4516	0.95	22	2.48	0.45	136	166	106

Variable	Acronym	Definition	Type	Dataset	Value	Equation	R^2	% PE	Slope	Intercept	BM	BM + PE	BM - PE
Anteroposterior diameter of the femur (cm)	F6	The transverse diameter of the diaphysis at its midpoint	Postcranial	All ungulates	3.62	log BM=2.8210*log(F6)+0.9062	0.94	23	2.82	0.91	304	373	234
Mediolateral diameter of the shaft (cm)	F7	The anteroposterior diameter of the diaphysis at its midpoint	Postcranial	All ungulates	2.55	log BM=2.6016*log (F7)+0.9119	0.94	26	2.6	0.91	93	117	69
Diametro transverso proximal de la tibia (cm)	T2	The transverse diameter of the tibia's proximal epiphysis	Postcranial	All ungulates	5.5	log BM=2.8491*log(T2)-0.2495	0.95	21	2.85	-0.25	72	88	57
Transverse width of tibial trochlea	Li1		Astragalus	Various mammals	27.7	ln BM= 2.789*ln(Li1)+2.078	0.98	28.83	2.79	2.08	84	109	60

APPENDIX 2.

Selected measurement (in cm) and multivariate equations used (Mendoza et al., 2006) to estimated the body mass in kg (BM) of MPEF-PV 8166.

Adj. R^2	%MPE	mid PE	LMRL	LPRL	JMA	JMC	JD	JMB	BM	BM+ mid PE	BM -mid PE
0.98	21-25	23	7.56	5.86	6.53	10.55	4.88		177	217	167
0.98	21-25	23	7.56	5.86	6.53	10.55	4.88	11.6	184	226	174

CHAPTER 2

Neotropical mammal diversity and the Great American Biotic Interchange: spatial and temporal variation in South America's fossil record

Juan D. Carrillo, Analía Forasiepi, Carlos Jaramillo, and Marcelo R. Sánchez-Villagra. 2015.
Frontiers in Genetics, 5:451.doi:10.3389/
fgene.2014.00451

frontiers in GENETICS

REVIEW ARTICLE
published: 05 January 2015
doi: 10.3389/fgene.2014.00451

Neotropical mammal diversity and the Great American Biotic Interchange: spatial and temporal variation in South America's fossil record

Juan D. Carrillo[1,2]*, Analía Forasiepi[3], Carlos Jaramillo[2] and Marcelo R. Sánchez-Villagra[1]

[1] *Paläontologisches Institut und Museum, University of Zurich, Zurich, Switzerland*
[2] *Smithsonian Tropical Research Institute, Panama City, Panama*
[3] *Instituto Argentino de Nivología, Glaciología y Ciencias Ambientales (IANIGLA), CCT-CONICET Mendoza, Mendoza, Argentina*

Edited by:
James Edward Richardson, Royal Botanic Garden Edinburgh, UK

Reviewed by:
William Daniel Gosling, University of Amsterdam, Netherlands
Bruce D Patterson, Field Museum of Natural History, USA

****Correspondence:***
Juan D. Carrillo, Paläontologisches Institut und Museum, University of Zurich, Karl-Schmid-Strasse 4, 8006 Zürich, Switzerland
e-mail: juan.carrillo@pim.uzh.ch

The vast mammal diversity of the Neotropics is the result of a long evolutionary history. During most of the Cenozoic, South America was an island continent with an endemic mammalian fauna. This isolation ceased during the late Neogene after the formation of the Isthmus of Panama, resulting in an event known as the Great American Biotic Interchange (GABI). In this study, we investigate biogeographic patterns in South America, just before or when the first immigrants are recorded and we review the temporal and geographical distribution of fossil mammals during the GABI. We performed a dissimilarity analysis which grouped the faunal assemblages according to their age and their geographic distribution. Our data support the differentiation between tropical and temperate assemblages in South America during the middle and late Miocene. The GABI begins during the late Miocene (~10–7 Ma) and the putative oldest migrations are recorded in the temperate region, where the number of GABI participants rapidly increases after ~5 Ma and this trend continues during the Pleistocene. A sampling bias toward higher latitudes and younger records challenges the study of the temporal and geographic patterns of the GABI.

Keywords: Miocene, Pliocene, biogeography, mammalia, South America

INTRODUCTION

The Neotropics [Neotropical region *sensu lato* of Morrone (2014)] supports an extremely large diversity of living mammals. Currently there are around 1500 recognized species which represent in the order of 30% of the total world mammal diversity. Included are endemic groups such as marsupials (opossums), xenarthrans (sloths, armadillos, and anteaters), caviomorph rodents (capybaras, spiny rats, chinchillas), platyrrhine monkeys, and phyllostomid bats (Patterson and Costa, 2012). The variety of biomes found in the Neotropics (lowland rainforest, savannas, mountain forest, scrublands, and deserts) could provide a partitioned environment enhancing species richness (Tews et al., 2004).

The current Neotropical mammal fauna is the result of a long evolutionary history. The Cenozoic (66–0 Ma) in South America was characterized by long term geographical isolation with the evolution of an endemic fauna (Simpson, 1980). Sporadic dispersal events from other geographic areas interrupted this isolation introducing novel clades into South America including caviomorph rodents during the middle Eocene (~41 Ma) and platyrrhine monkeys during the late Oligocene (~26 Ma) (Pascual, 2006; Antoine et al., 2012; Croft, 2012; Goin et al., 2012). The isolation of South America's mammal fauna ceased by ~10–7 Ma, when proximity, and then permanent connection was established with Central America. This connection initiated a massive faunal exchange between North America (NA) and South America (SA). This event is known as the Great American Biotic Interchange (GABI) (Simpson, 1980; Webb, 1985). The classic interpretation places the onset of the GABI by ~3.0 Ma, with some early migrations during the late Miocene from SA to NA by ~9 Ma and from NA to SA by ~7 Ma. Other studies using dated molecular phylogenies across a wide range of taxa indicate an important part of the interchange may have predated the permanent land connection by ~3 Ma (Koepfli et al., 2007; Cody et al., 2010; Eizirik et al., 2010; Eizirik, 2012). The core of the GABI is composed by a series of major migration "waves" during the Pliocene–Pleistocene (2.5–0.012 Ma) (Webb, 2006; Woodburne, 2010). Recently, several NA mammals have been reported from the late Miocene deposits, ~10 Ma, within the Amazon basin. These include a dromomerycine artiodactyl, gomphotheres, peccaries, and tapirs which suggest a more intense earlier connection (Campbell et al., 2000, 2010; Frailey and Campbell, 2012; Prothero et al., 2014). However, the taxonomy and age of some of these fossils have been questioned (Alberdi et al., 2004; Lucas and Alvarado, 2010; Lucas, 2013). In Amazonia, Pleistocene terraces are built from older Cenozoic deposits (Latrubesse et al., 1997), resulting in non-contemporaneous associations (Cozzuol, 2006). Even with these concerns in mind, in the last decades the presence of northern forms in South America is becoming better understood.

During the late Miocene (11.6–5.3 Ma) and early Pliocene (5.3–3.6 Ma), the GABI was taxonomically balanced, as predicted by the MacArthur–Wilson species equilibrium hypothesis, with similar number of NA and SA families participating in the interchange (Webb, 1976; Marshall et al., 1982). During the Pleistocene, NA mammals appeared to have diversified exponentially in SA, resulting in an overall prevalence of NA over SA–derived mammals. This could be the result of competitive displacement (Webb, 1976, 1991; Marshall et al., 1982), but this has not been subjected to rigorous analyses. In contrast, ecological replacement has been demonstrated for extinct metatherians and placental carnivores (Prevosti et al., 2013).

Vrba (1992) analyzed the GABI in the context of the "habitat theory" (i.e., physical environmental changes are the main drivers of "distribution drift") and highlighted the importance of environmental changes over biotic interactions as the major cause of the biotic turnover. Webb (1991) proposed that the Pleistocene glaciations and the widespread development of savannas in the Neotropics facilitated dispersals during the GABI of savanna-adapted mammals. Woodburne (2010) agreed with Webb's model and related the pulses of faunistic movements to the glaciations and sea level changes of the Pliocene and Pleistocene. However, most recent evidence does not support the widespread expansion of savannas in the tropics during glacial times (Behling et al., 2010). The GABI was dynamic with bidirectional migrations (Carlini et al., 2008b; Castro et al., 2014) and with reciprocal exchanges within a single lineage (e.g., procyonids; Baskin, 1989; Forasiepi et al., 2014; and felids; Prevosti, 2006).

Potential biogeographic barriers or corridors along with environmental changes controlled patterns of movements (Webb, 1991; Woodburne, 2010). The Andes are currently an important biogeographic feature in South America extending for about 8000 km from Venezuela to Argentina, reaching average heights of about 4000 masl and maximum elevations up to 7000 masl (Ramos, 1999). The present day elevations of the northern and the north central Andes (north of 20°S) were reached during or soon after the late Miocene (Mora et al., 2009) and may have constituted a colonization corridor during the GABI (Patterson et al., 2012 and references therein).

A full understanding of the GABI is difficult because of the difference in fossil sampling between low and high latitudes (**Figure 1**). Even with the major recent advances in Neotropical paleontology (Kay et al., 1997; Campbell, 2004; MacFadden, 2006; Sánchez-Villagra et al., 2010; Antoine et al., 2012), our knowledge of this large portion of territory that comprises the neotropics, twice the size of Europe and almost as large as North America is scarce (Croft, 2012).

In this contribution, we investigate biogeographic patterns for the middle and late Miocene (15.9–5.3 Ma) in SA at the initiation of the GABI. We review the temporal and geographical distribution of fossil mammals during the GABI and discuss the special significance of the fossil record from northern SA to understand the patterns and dynamics of the interchange.

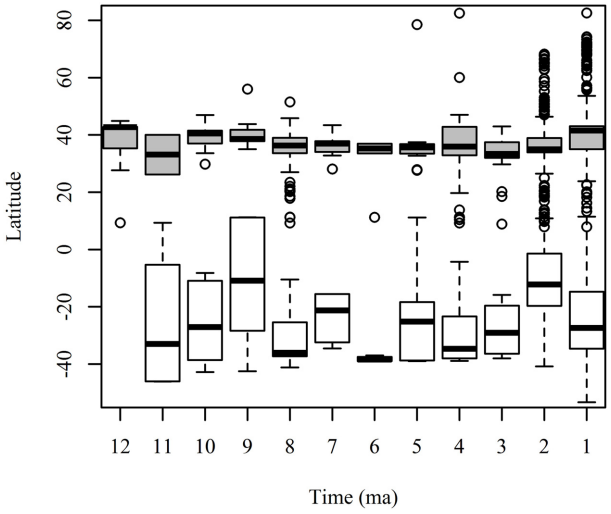

FIGURE 1 | Number of collections in the Paleobiology Database (PBDB) across latitude for land mammals in North America (gray boxes) and South America (white boxes) for each 1 ma period in the last 12 ma. The boxplot shows the mean and standard deviation of the latitude of the PBDB collections for each time interval.

MATERIALS AND METHODS

Species lists from several middle and late Miocene–Pliocene mammal associations (La Venta, Fitzcarrald, Quebrada Honda, Collon Curá, Urumaco, Acre, Mesopotamian, Cerro Azul, Chiquimil, Andalhuala, Monte Hermoso, Inchasi and Uquía) were compiled from several sources (Goin et al., 2000; Cozzuol, 2006; Reguero and Candela, 2011; Brandoni, 2013; Tomassini et al., 2013; Tejada-Lara et al., in press) and other references available in the Paleobiology Database (PBDB) (Alroy, 2013), to which we added 450 references with records of Neogene fossil mammals from the Americas (**Figures 2**, **3**; Supplementary Material 1–2). We obtained latitude and paleolatitude from each locality from the PBDB (**Table 1**) and estimated the distance in km among localities using Google Earth. Localities were coded for presence/absence at the generic level (Supplementary Table 1). The biochronology refers to the South American Land Mammal Ages (SALMA) and the calibration of the boundaries of Tomassini et al. (2013, modified from Cione et al., 2007) and Cione and Tonni (1999, 2001). Genera were used as taxonomic unit (including taxonomic identifications with *cf.* and *aff.* qualifiers). Lower taxonomical levels are still unresolved for several localities and data are incomparable.

We analyzed closely contemporaneous fossil mammal associations from SA using the Bray-Curtis binary dissimilarity index. This reaches a maximum value of 1 when there are no shared taxa between the two compared communities. The Vegan package (Okasanen et al., 2013) was used to perform a cluster analysis with average grouping method and a Nonmetric Multidimensional Scaling (NMDS) set to two dimensions (axes) and 1000 runs. We compared tropical and temperate Miocene localities, and in order to account for differences in the sample size, we set the number of taxa equal to the assemblage with the lowest richness within the subgroup and calculate Bray-Curtis dissimilarity by resampling with replacement 1000 times all the localities. The Vegan package was used to obtain genera accumulation curves for

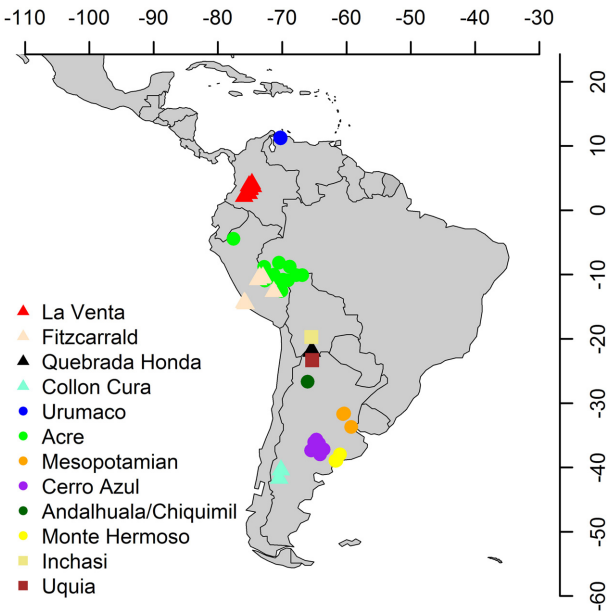

FIGURE 2 | Middle and late Miocene – Pliocene main fossil sites for land mammals in South America. Triangles, middle Miocene; circles, late Miocene; squares, Pliocene.

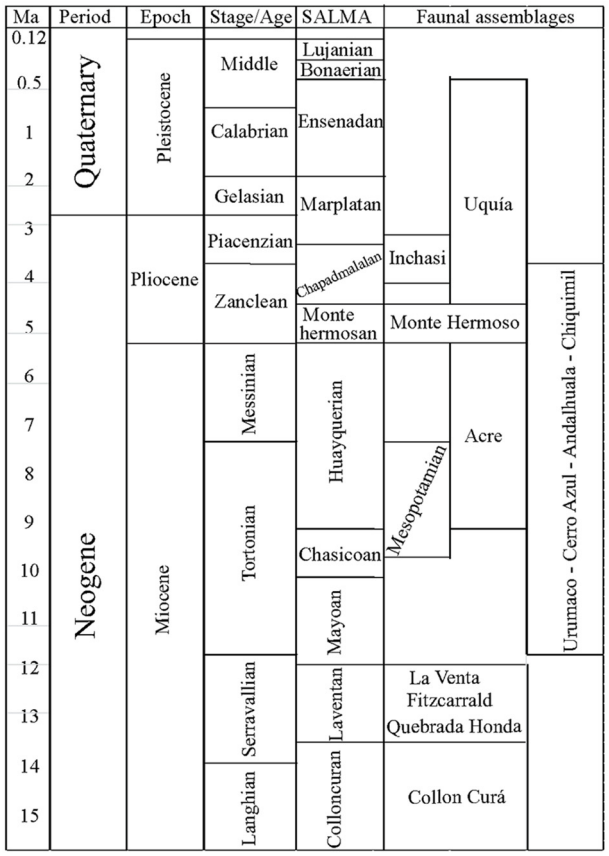

FIGURE 3 | Chronostratigraphy, South American Land Mammal Ages (SALMAs) and temporal distribution of the faunal assemblages discussed in the text. Colloncuran:15.7–14 Ma (Madden et al., 1997) Laventan: 13.5–11.8 Ma. (Madden et al., 1997); Mayoan: 11.8–10 Ma. (Flynn and Swisher, 1995); Chasicoan: 10– ~8.5 (Flynn and Swisher, 1995); Huayquerian = ~8.5–5.28 Ma. Lower age following (Cione and Tonni, 2001; Reguero and Candela, 2011) and upper age following (Tomassini et al., 2013); Montehermosan = 5.28 –4.5/5.0 Ma. (Tomassini et al., 2013); Chapadmalalan = 4.5/5.0–3.3 (Tomassini et al., 2013); Marplatan = 3.3 – ~2.0 Ma. Lower age following (Tomassini et al., 2013) and upper age following (Cione and Tonni, 1999; Cione et al., 2007); Ensenadan = ~2.0–<0.78(0.5?) Ma. (Cione and Tonni, 1999; Cione et al., 2007); Bonaerian = <0.78(0.5?)–0.13 Ma. (Cione and Tonni, 1999); Lujanian = 0.13–0.08 Ma (Cione and Tonni, 1999).

tropical assemblages, using the random method. All analyses were performed in R (R Core Team, 2013).

We obtained records for late Miocene to late Pliocene land mammals for NA and SA from the PBDB. We classified each genus as North or South American if the taxon or its ancestor were in either NA or SA before 10 Ma. We compared the geographic distribution (tropical vs. temperate) and time of first appearance datum (FAD) of GABI migrants in the continent (Supplementary Material 3 and Supplementary Table 2). In order to account for the age uncertainty of each FAD, we generate 1000 different random values between the maximal and minimal age estimate and calculate the mean and standard deviation of the age estimate for each record.

STUDY SITES

We selected faunal associations from the tropical and temperate regions of South America which all together span from the middle Miocene (~15 Ma) to the late Pliocene (~2 Ma), a critical time period for the GABI. The study sites cover a wide latitudinal gradient across the continent (**Table 1**).

La Venta

La Venta is one of the best-studied fossil assemblages from the Neotropics and among vertebrates includes freshwater fishes, crocodiles, turtles and different mammal clades (Kay et al., 1997). These come from the Honda Group in the central Magdalena valley, Colombia (**Figure 2**). Its age is constrained by radiometric and paleomagnetic data. The assemblage of La Venta served as the basis for defining the Laventan SALMA (middle Miocene, 13.5–11.8 Ma) (Madden et al., 1997).

Fitzcarrald

The localities of the Fitzcarrald assemblage are found along the Inuya and Mapuya rivers in the Amazon of Peru (**Figure 2**) from the Ipururo Formation, interpreted as middle Miocene (Laventan Age) (Antoine et al., 2007; Tejada-Lara et al., in press). The vertebrate assemblage includes fishes, turtles, crocodiles, snakes and 24 mammalian taxa (Negri et al., 2010; Tejada-Lara et al., in press).

Quebrada Honda

Quebrada Honda is located in southern Bolivia at ~21°S latitude, 20 km north of the Argentine frontier and at an elevation of about 3500 m (**Figure 2**). The fossil-bearing deposits crop out in the valley of the Honda River and its tributaries. Paleomagnetic and radioisotopic data provide an extrapolated age of 13–12.7 Ma for

Table 1 | Modern and ancient latitude and elevation of the faunal assemblages used in this study.

Faunal association	Latitude	Paleolatitude	Elevation	Paleoelevation	Biome
La Venta	∼3° N	∼2.6° N	∼380 m	"Lowland"	Tropical
Fitzcarrald	∼10.5° S	∼12° S	< 300 m	"Lowland"	Tropical
Quebrada Honda	∼22° S	∼22° S	∼3500 m	∼2600 ± 600 m	Temperate
Collón Curá	∼40° S	∼41° S	∼800 m	?	Temperate
Urumaco	∼11° N	∼11° N	<100 m	"Lowland"	Tropical
Acre	∼10° S	∼10.5° S	<300 m	"Lowland"	Tropical
Mesopotamian	∼32° S	∼32° S	<100 m	"Lowland"	Temperate
Cerro Azul	∼37° S	∼37° S	∼150 m	"Lowland"	Temperate
Chiquimil	∼27° S	∼27° S	1000–2500 m	?	Temperate
Andalhuala	∼27° S	∼27° S	1000–2500 m	?	Temperate
Monte Hermoso	∼38° S	∼38° S	<100 m	"Lowland"	Temperate
Inchasi	∼19° S	∼20° S	∼3220 m	?	Temperate
Uquía	∼23° S	∼23° S	∼2800 m	∼1400–1700 m	Temperate

the fossil bearing beds (MacFadden et al., 1990). Multiple proxies to estimate paleoelevation of the Central Andean Altiplano have yielded values between 1000 and 2000 m for the middle Miocene (Garzione et al., 2008); however, a most recent study using clumped isotope thermometry on paleosol carbonates inferred an earlier uplift for the Altiplano, with Quebrada Honda at about 2600 ± 600 m and a mean annual temperature of ∼9 ± 5° C (Garzione et al., 2014). The assemblage includes about 30 mammals representing metatherians, xenarthrans, rodents, astrapotheres, litopterns and notoungulates and correspond to the Laventan SALMA (Croft, 2007).

Collón Curá

The Collón Curá Formation is largely exposed at the west of Nord-Patagonian Massif (Neuquén and Río Negro provinces, and Norwest Chubut Province). The rich vertebrate association is represented by reptiles, birds, and principally mammals: metatherians, xenarthrans, rodents, notoungulates, litopterns, and astrapotheres (Kramarz et al., 2011). The fossil mammals collected in the vicinities of the Collón Curá river by Santiago Roth in the late 19th Century are the basis for the definition of the Colloncuran SALMA, although a critical review of most of the findings is still pending. Several radiometric dates for the Collón Curá Formation indicate ages between 15.5 and 10 Ma for the vertebrate association (e.g., Rabassa, 1974, 1978; Marshall et al., 1977; Bondesio et al., 1980; Mazzoni and Benvenuto, 1990; Madden et al., 1997).

Urumaco

The Urumaco sequence is found in the Falcón State in northwestern Venezuela (**Figure 2**). It includes the Querales, Socorro, Urumaco, Codore and San Gregorio formations, which together span from the middle Miocene to late Pliocene (Quiroz and Jaramillo, 2010). The Urumaco sequence shows a high diversity of crocodilians (Scheyer et al., 2013) and xenarthrans (Carlini et al., 2006a,b, 2008a,c). We focus our analysis on the Urumaco Formation. Linares (2004), on the basis of a mammal list of undescribed material suggested a middle to late Miocene age. Until a detail taxonomic revision is conducted, the biostratigraphic correlation of the Urumaco association remains tentative.

Acre

The Acre region in the southwestern Amazonia includes several fossiliferous localities which would represent different time intervals considering the geological and palinological evidence (Cozzuol, 2006). Fossil vertebrates come from the Solimões Formation of the state of Acre, Brazil and Peruvian and Bolivian localities from the Madre de Dios Formation (Negri et al., 2010) (**Figure 2**). The vertebrate assemblage is very diverse and includes fishes, snakes, lizards, birds, turtles, crocodiles, and mammals including whales, dolphins, manatees and a diverse assemblage of terrestrial forms. The Acre mammal assemblage has been referred to late Miocene, Huayquerian SALMA (Cozzuol, 2006; Ribeiro et al., 2013) or included also in the Pliocene, Montehermosan SALMA (Cozzuol, 2006). Campbell et al. (2001) reported $^{40}A/^{39}A$ dates of 9.01 ± 0.28 Ma for the base of the Madre de Dios Formation and 3.12 ± 0.02 Ma near the top.

Mesopotamian

The continental mammals of the Mesopotamian assemblage come from the lower levels of the Ituzaingó Formation, which crops out along the cliffs of the Paraná River in Corrientes and Entre Ríos provinces, north-east Argentina (**Figure 2**). The vertebrate assemblage is rich and includes fishes, crocodiles, birds and mammals (Cione et al., 2000; Brandoni and Noriega, 2013). It differs taxonomically from other associations in Argentina at the same latitudes and this was explained by a southern extension of the northern realm (Cozzuol, 2006). The age of the Mesopotamian assemblage has been largely debated (Cione et al., 2000 and references therein); it is currently assigned to the late Miocene, Huayquerian SALMA (Cione et al., 2000) or also extended into the Chasicoan SALMA (Brandoni, 2013; Brunetto et al., 2013). The dating of 9.47 Ma for the upper levels of the lower Paraná Formation (Pérez, 2013) represents a maximum limit for the Mesopotamian assemblage.

Cerro Azul

Several localities in central east Argentina (La Pampa and Buenos Aires provinces) have provided abundant fossil vertebrates from the Cerro Azul and Epecuén formations which are considered geologically correlated (Goin et al., 2000). This assemblage includes reptiles, birds and a rich mammal association. These units are assigned to the late Miocene, Huayquerian SALMA (Goin et al., 2000; Montalvo et al., 2008; Verzi and Montalvo, 2008; Verzi et al., 2011) on the basis of mammal biostratigraphy. This association is currently the most complete list for this age (Goin et al., 2000). The possibility of extension into the late Pliocene cannot be discarded for some localities assigned to the Cerro Azul Formation (Prevosti and Pardiñas, 2009).

Chiquimil

The Chiquimil Formation is exposed in north-west Argentina (Catamarca Province) and is divided in three members. The Chiquimil A (Riggs and Patterson, 1939; Marshall and Patterson, 1981) or El Jarillal Member (Herbst et al., 2000; Reguero and Candela, 2011) provided a rich fossil record. The mammalian association has been assigned to the late Miocene, Huayquerian SALMA (Reguero and Candela, 2011). A dating in the middle section of the Chiquimil Formation indicated ∼6.68 Ma (Marshall and Patterson, 1981).

Andalhuala

The Andalhuala Formation is exposed in the Santa María Valley in north-west Argentina (Catamarca Province). This is a classical fossiliferous unit of the South American Neogene with abundant and diverse fossil remains, including plants, invertebrates, and vertebrates (Riggs and Patterson, 1939; Marshall and Patterson, 1981). Basal levels of the Andalhuala Formation have been dated to ∼7.14 Ma (Latorre et al., 1997) and ∼6.02 Ma (Marshall and Patterson, 1981) while a tuff sample close to the upper part of the sequence was dated to ∼3.53 Ma (Bossi et al., 1993). The mammal association has been referred to the Montehermosan–Chapadmalalan SALMAs (Reguero and Candela, 2011).

Monte Hermoso

The Monte Hermoso Formation is exposed in the Atlantic coast at the south west of Buenos Aires Province, Argentina. This unit has provided fishes, anurans, reptiles, birds, and a diverse mammal association. Recent biostratigraphic and biochronological analyses (Tomassini and Montalvo, 2013; Tomassini et al., 2013) have recognized a single biozone (the *Eumysops laeviplicatus* Range Zone) in the Montehermosan Formation which is the base for the Montehermosan SALMA. The Montehermosan was restricted to the early Pliocene between <5.28 and 4.5/5.0 Ma by considering the dating of 5.28 Ma in levels with Huayquerian mammals and paleomagnetic correlations in the upper Chapadmalal Formation (Tomassini et al., 2013).

Inchasi

The locality of Inchasi is found in the eastern cordillera in the department of Potosí, Bolivia at an elevation of about 3220 masl and ∼19°S latitude (**Figure 2**). The mammal assemblage includes 10 mammals, representing xenarthra, rodentia, and native ungulates (Litopterna and Notoungulata) (Anaya and MacFadden, 1995). Paleomagnetic analysis indicates an age of about 4–3.3 Ma. The analysis of the mammal association first suggested Montehermosan and/or Chapadmalalan ages (MacFadden et al., 1993). A later revision (Cione and Tonni, 1996) correlated Inchasi with the Chapadmalalan, although probably older than the classical Chapalmalalan sections at the Atlantic coast.

Uquía

The Uquía Formation crops out in the Quebrada de Humahuaca, Jujuy province, north western Argentina at an elevation of ∼2800 masl and ∼23°S latitude (**Figure 2**). The Uquía Formation is divided in three units: the Lower Unit was assigned to the late Chapadmalalan, the Middle Unit to the Marplatan (Vorhuean, Sanandresian), and the Upper Unit to the Ensenadan (Reguero et al., 2007; Reguero and Candela, 2011). ^{40}K–^{40}Ar data from a volcanic tuff ("Dacitic tuff") in the Lower Unit provided ∼3.0 Ma. Another tuff (U1) dated as 2.5 Ma is the boundary between the Middle and Upper Unit. The geological and paleontological evidence suggested that during the late Pliocene the area was a wide intermountain valley at about 1700–1400 masl (Reguero et al., 2007).

RESULTS

MIDDLE AND LATE MIOCENE–PLIOCENE MAMMAL FAUNAS FROM SA

In the NMDS analysis (stress value = 0.083), the analyzed South American localities are primarily grouped by age and secondarily by geographic position (**Figure 4A**). The NMDS1 clearly separates middle Miocene, late Miocene and Pliocene localities and for the middle and late Miocene assemblages, the NMDS2 separates tropical from temperate localities. For the middle Miocene (Colloncuran, Laventan), the cluster analysis separates the tropical assemblages of La Venta (∼2.6°N paleolatitude) and Fitzcarrald (∼12.5°S paleolatitude) from the southern Collón Curá (∼41.3°S paleolatitude) and Quebrada Honda (∼22.3°S paleolatitude). For the late Miocene (Huayquerian–Montehermosan), Urumaco (∼10.9°N paleolatitude) appears outside the groups formed by Acre (∼10.5°S paleolatitude) and Mesopotamian (∼32.5°S paleolatitude), another cluster includes the Argentinean assemblages of Andalhuala (∼26.8°S paleolatitude), Chiquimil (∼27.0°S paleolatitude), Cerro Azul (∼37.0°S paleolatitude), and Monte Hermoso (∼38.9°S paleolatitude). Finally, the early Pliocene (Chapadmalalan– Marplatan) temperate associations from Inchasi (∼19.9°S paleolatitude) and Uquía (∼23.4°S paleolatitude) cluster together, although there are no tropical assemblages to compare with. If we compare only faunal assemblages from the same time period (middle Miocene, late Miocene and Pliocene), there is a positive relationship between the Bray-Curtis dissimilarity and the distance of each pair of assemblages studied (**Figure 4B**).

The Bray-Curtis dissimilarity values with resampling calculated for the tropical, temperate and tropical vs. temperate assemblages for the middle and late Miocene shows that all the assemblages are very different (**Figure 4C**). The Bray-Curtis dissimilarity between middle Miocene tropical (La Venta and Fitzcarrald) and temperate (Quebrada Honda and Collón Curá) assemblages compared to the dissimilarity between tropical vs. temperate are found to be statistically significant. Dissimilarity

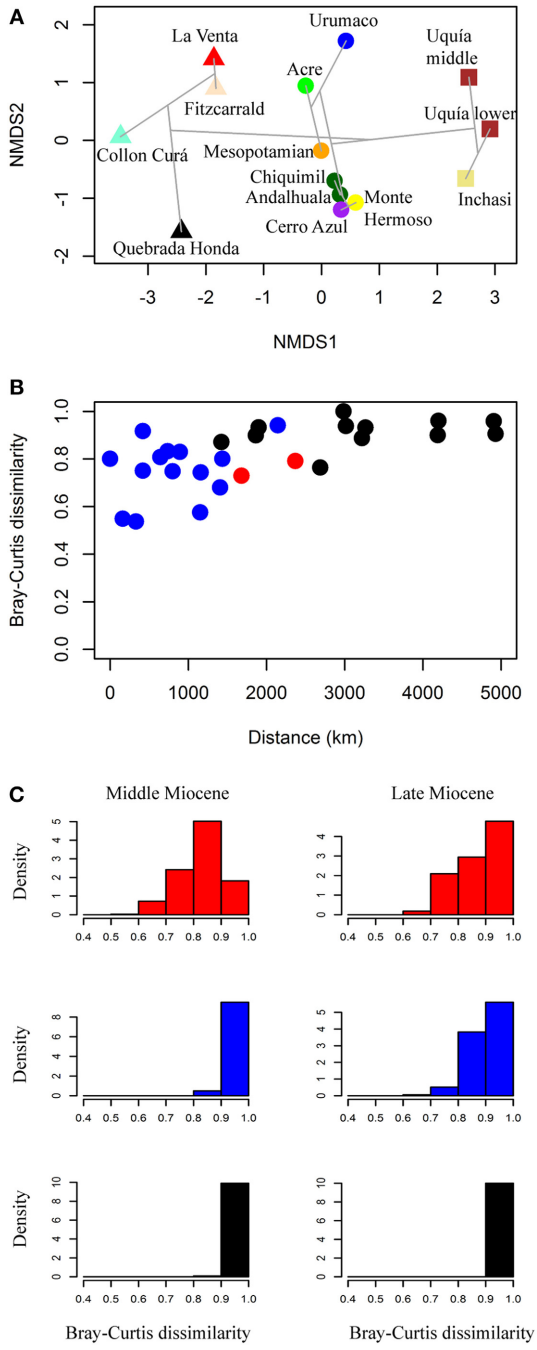

FIGURE 4 | (A) NMDS plot of the faunal associations using Bray-Curtis dissimilarity; triangles, middle Miocene; circles, late Miocene; squares, Pliocene. The gray lines show the clustering result. **(B)** Bray-Curtis dissimilarity relationship with distance in km, between each locality pair. We include only localities pairs which are within the same time interval (middle Miocene, late Miocene, Pliocene), red, tropical–tropical pair; blue, temperate–temperate pair; black, tropical–temperate pair. **(C)** Density histograms of the Bray-Curtis dissimilarity values among the different faunal associations analyzed for the middle and late Miocene, red, only tropical faunas, blue, only temperate faunas, black, tropical vs. temperate faunas.

values of middle Miocene tropical (mean = 0.830) are lower than middle Miocene tropical vs. temperate (mean = 0.956) (Mann-Whitney U, $p < 2.2$ e-16); whereas middle Miocene temperate dissimilarity (mean = 0.964) is higher than middle Miocene tropical vs. temperate dissimilarity (Mann-Whitney U, $p \leq 2.87$ e-15). For the late Miocene, dissimilarity of tropical assemblages (Acre and Urumaco) is lower (mean = 0.873) than tropical vs. temperate (mean = 0.969) (Mann-Whitney U, $p < 2.2$ e-16). We also found difference between temperate assemblages (Mesopotamian, Chiquimil, Andalhuala, Cerro Azul, and Monte Hermoso; mean = 0.899) and tropical vs. temperate dissimilarity (Mann Whitney U, $p < 2.2$e-16).

The number of PBDB collections was used to generate accumulation curves for the tropical assemblage (**Figure 5**). Each collection represents a geographic and stratigraphic point where the fossils have been found and provide a good proxy for sampling effort. We excluded from the analysis the Acre collection with unknown stratigraphic provenance. The accumulation curves show that generic richness for tropical assemblages is underestimated, even for the better known assemblage of La Venta.

TEMPORAL AND SPATIAL DISTRIBUTION PATTERNS OF GABI

The cumulative first appearance datum (FAD) of non-native taxa for both NA and SA continents (**Figure 6A**, Supplementary Table 2) shows that first migrations are recorded in the temperate region (cumulative FAD mean = 2 by 10 Ma), represented by the ground sloths *Thinobadistes* (Mylodontidae) and *Pliometanastes* (Megalonychidae) recorded at McGehee Farm, Florida (Hirschfeld and Webb, 1968; Webb, 1989). During the late Miocene (12–5 Ma), the number of FAD is similar between the tropics (cumulative FAD mean = 6 by 5 Ma) and temperate (cumulative FAD mean = 7 by 5 Ma). In the tropics, the oldest records of migrants are those from the Acre region in Peru (Campbell et al., 2010; Prothero et al., 2014) of disputable age (Alberdi et al., 2004; Lucas and Alvarado, 2010; Lucas, 2013). During the Pliocene (between 3 and 4 Ma) there is an increase in the number of FAD at higher latitudes (cumulative FAD mean =

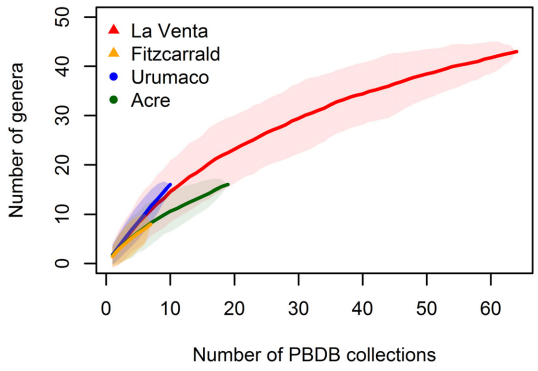

FIGURE 5 | Accumulation curves estimated with random method for the tropical faunal associations, shaded areas represent the 95% confidence interval.

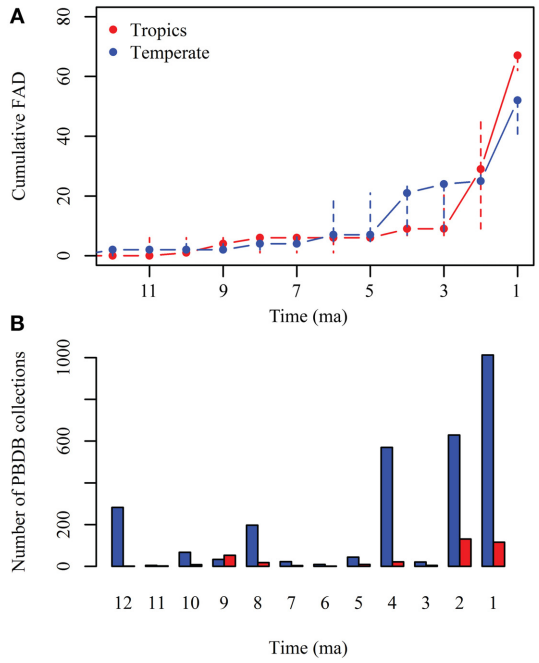

FIGURE 6 | (A) Cumulative first appearance datum (FAD) of GABI participants in North and South America for each million year since 12 Ma; red, FADs record in the tropics; blue, FADs record in the temperate regions. Solid circles represent the mean and dashed lines the standard deviation. **(B)** Number of collections with records of land mammals in the Paleobiology Database (PBDB) for each million year since 12 Ma; red, collections in the tropics; blue= collections in the temperate region.

21), but this is not recorded in the tropics (cumulative FAD mean = 9). Finally, during the Pleistocene (2–1 Ma) a higher number of FADs are recorded in tropical and temperate regions. Most of the collections in the PBDB with records of land mammals in the Americas are in the temperate region and are younger than 4 Ma (**Figure 6B**).

DISCUSSION

MIDDLE AND LATE MIOCENE–PLIOCENE MAMMAL FAUNAS FROM SA

The NMDS1 shows that a strong temporal component establishes the dissimilarity relationships among the faunas. In addition, an important influence of the geographic position is reflected in the distribution of the faunas along the NMDS2 axis. There is a positive relationship between the Bray-Curtis dissimilarity values and the distance between faunas (**Figures 4 A,B**).

For the middle Miocene, Colloncuran–Laventan faunal associations, a differentiation between the tropical assemblages of La Venta and Fitzcarrald, and the southern Quebrada Honda and Collón Curá was observed (**Figure 4A**). The middle latitude fauna Quebrada Honda appears unique, although it is closer to the slightly older and temperate Collón Curá than to the contemporaneous tropical faunas of La Venta and Fitzcarrald (Croft, 2007; Tejada-Lara et al., in press). The reconstructed paleoenvironment for the middle Miocene Monkey Beds assemblage at La Venta considered an estimated annual rainfall between 1500 and 2000 mm using diet, locomotion and body size indices of the mammal community (Kay and Madden, 1997a,b).

For the late Miocene assemblages, the NMDS indicates a high dissimilarity between the tropical faunas of Urumaco and Acre. For the Urumaco mammal assemblage, xenarthrans and rodents are the most conspicuous elements, but further studies on other clades promise to document a higher diversity than currently recognized. The temperate assemblages of Chiquimil, Andalhuala, Cerro Azul, and Monte Hermoso cluster together and the Mesopotamian is between this group and Acre (**Figure 4A**).

After taking into account the differences in sample size, we found that the dissimilarity values of tropical assemblages (mean = 0.830 for middle Miocene, and mean = 0.879 for late Miocene) and late Miocene temperate assemblages (mean = 0.899 for late Miocene) are lower than the values for tropical vs. temperate assemblages (mean = 0.956 for middle Miocene and mean = 0.969 for late Miocene) (**Figure 4C**). Consequently, the Bray-Curtis dissimilarity between faunas of the same age and biome is lower than between faunas of different biomes (tropical vs. temperate); although, the mean dissimilarity values in all cases are high (>0.8).

As shown by the accumulation curves (**Figure 5**), the generic richness of the tropical assemblages studied are underestimated. A more comprehensive knowledge of tropical faunas is needed to better understand the paleodiversity patterns and paleobiogeography in the new world.

TEMPORAL AND SPATIAL DISTRIBUTION PATTERNS OF GABI

The cumulative FAD across time of GABI participants in each continent shows that the GABI was a gradual process that began in the late Miocene (~10 ma) (**Figure 6A**). The early phase of GABI (pre GABI *sensu* Woodburne, 2010) is characterized by a small number of migrants, with a mean cumulative FAD = 6 between 4 and 5 Ma in the tropics and a cumulative FAD = 7 in the temperate region. The land connection between the two continents occurred at the Isthmus of Panama, located within the tropical zone. Therefore, it would be expected that the Neotropics record the earliest GABI immigrants, but older immigrants have been found at higher latitudes.

The findings reported by Campbell and colleagues (Campbell et al., 2010; Frailey and Campbell, 2012; Prothero et al., 2014) in the Acre region of the Amazon basin, assigned to late Miocene (~9 Ma) sediments would represent the oldest NA immigrants. However, the dromomerycine artiodactyl, peccaries, tapirs, and gomphotheres have not been found in other late Miocene localities in SA and these findings await further clarifications. In SA, the most frequent pre-GABI elements are procyonids recorded in several late Miocene–Pliocene (Huayquerian–Chapadmalalan) SA localities since ~7.3 Ma (Cione et al., 2007; Reguero and Candela, 2011; Forasiepi et al., 2014). The evidence of the fossil record combined with the living species distribution suggests that much of the evolutionary history of procyonids occurred in the Neotropics, possibly in SA (Eizirik, 2012). Molecular studies have predicted that the diversification of the group occurred in the early Miocene (~20 Ma), with most of the major genus-level lineages occurring in the Miocene (Koepfli et al., 2007; Eizirik et al., 2010; Eizirik, 2012). This scenario requires a bias in the

fossil record, claims an evolutionary history for procyonids in SA that largely precedes the GABI, and suggests an arrival into SA long before previously thought as for several other mammalian clades (Almendra and Rogers, 2012; and references therein).

Since 4 Ma, the number of FAD at higher latitudes rapidly increases and this trend continues during the Pleistocene. In contrast, the number of FAD in the tropics remains low during the Pliocene (cumulative FAD mean = 9 by 2–3 Ma), but rapidly increases during the Pleistocene. A large difference in the number of PBDB collections across time and latitude is observed for land mammals for the last 12 Ma (**Figure 6B**). Most records come from higher latitudes and are younger than 4 Ma, by the time the FAD increases; this suggest that temporal and geographic patterns of GABI are influenced by the sampling bias toward high latitudes and the higher number of Pliocene–Pleistocene records.

The migration of northern taxa into SA after the completion of the land bridge by ~3 Ma was correlated with supposed expansion of savannas and grasslands in the Neotropics during glacial periods (Webb, 1991, 2006; Leigh et al., 2014). The expansion of savannas during glacial times has been questioned (Behling et al., 2010). If this is the case, the Andes could have served as route of migration of northern taxa toward temperate environments in SA (Webb, 1991), as NA taxa seem to have been more successful in temperate biomes whereas SA taxa dominate in the tropics (Webb, 1991, 2006; Leigh et al., 2014).

CONCLUSIONS

The dissimilarity analysis primarily grouped the faunal assemblages by age and secondarily by geographic distribution. The dissimilarity values among the fossil faunal assemblages analyzed support the differentiation between tropical and temperate assemblages in SA during the middle Miocene (Colloncuran–Laventan) and late Miocene (Huayquerian–Montehermosan). The mid-latitude, middle Miocene assemblage of Quebrada Honda has higher affinities with the slightly older and temperate Collón Curá than with the tropical assemblages of La Venta and Fitzcarrald. For the late Miocene, the temperate assemblages of Chiquimil, Andalhuala, Cerro Azul, and Monte Hermoso cluster together, while the Mesopotamian is between this group and the tropical assemblages of Acre and Urumaco.

The cumulative FAD across time and latitude shows that faunisitc movements related to GABI began during the late Miocene (~10 Ma) with the oldest records found at higher latitudes. The number of FAD remained relatively low until 4–5 Ma when FAD starts to increase, peaking during the Pleistocene.

The study of paleodiversity patterns and paleobiogeography in the Americas is challenged by the sampling bias toward higher latitudes and the still scarce data from tropical faunas. The interpretation of the temporal and geographic patterns of GABI is likely influenced by these sampling issues.

AUTHOR CONTRIBUTIONS

Conceived and designed: Juan D. Carrillo, Analía Forasiepi, Carlos Jaramillo, Marcelo R. Sánchez-Villagra. Compiled bibliographic data: Juan D. Carrillo, Analía Forasiepi F, Carlos Jaramillo. Analyzed data: Juan D. Carrillo, Carlos Jaramillo. Wrote the paper: Juan D. Carrillo, Analía Forasiepi. All authors contributed to the final interpretation and editing of the manuscript.

ACKNOWLEDGMENTS

We are grateful to V. Rull, and the topic editors T. Pennington and J. E. Richardson for the invitation to contribute to this volume and two anonymous reviews for the valuable comments. We thank A. A. Carlini, M. Bond, F. Prevosti, and the group of Evolutionary Morphology and Paleobiology of Vertebrates (Zurich), in particular G. Aguirre-Fernández and M. Stange, for valuable comments. A. Cardenas and J. Alroy contributed to the data available at the PBDB. Thanks go to Smithsonian Institution, The Anders Foundation, Gregory D. and Jennifer Walston Johnson, NSF OISE-EAR-DRL 0966884 and NSF EAR 0957679 and to A. A. Carlini and J. D. Carrillo-Briceño for the support during our work in Urumaco. We thank the authorities at the Instituto del Patrimonio Cultural of the República Bolivariana de Venezuela and the Alcaldía Municipio de Urumaco for their generous support. Juan Carrillo was supported by Swiss National Fund SNF 31003A-149605 to M. R. Sánchez-Villagra.

SUPPLEMENTARY MATERIAL

The Supplementary Material for this article can be found online at: http://www.frontiersin.org/journal/10.3389/fgene.2014.00451/abstract

REFERENCES

Alberdi, M. T., Prado, J. L., and Salas, R. (2004). The Pleistocene Gomphotheriidae (Proboscidea) from Peru. *Neues Jahrb. Geol. Paläont. Abh.* 231, 423–452.

Almendra, A. L., and Rogers, D. S. (2012). "Biogeography of Central American mammals. Patterns and processes," in *Bones, Clones and Biomes. The History and Geography of Recent Neotropical Mammals,* eds B. D. Patterson and L. P. Costa (Chicago; London: The University of Chicago Press), 203–228. doi: 10.7208/chicago/9780226649214.003.0010

Alroy, J., (2013). *North American Fossil Mammal Systematics.* Paleobiology Database. Available online at: http://paleobiodb.org/cgi-bin/bridge.pl?page=OSA_3_North_American_mammals

Anaya, F., and MacFadden, B. J. (1995). Pliocene mammals from Inchasi, Bolivia: the endemic fauna just before the Great American Interchange. *Bull. Fla. Mus. Nat. Hist.* 39, 87–140.

Antoine, P. O., Marivaux, L., Croft, D. A., Billet, G., Ganerod, M., Jaramillo, C., et al. (2012). Middle Eocene rodents from Peruvian Amazonia reveal the pattern and timing of caviomorph origins and biogeography. *Proc. Biol. Sci.* 279, 1319–1326. doi: 10.1098/rspb.2011.1732

Antoine, P. O., Salas-Gismondi, R., Baby, P., Benammi, M., Brusset, S., De Franceschi, D., et al. (2007). The middle Miocene (Laventan) Fitzcarrald fauna, Amazonian Peru. *Cuad. Museo Geominero* 8, 19–24.

Baskin, J. A. (1989). Comments on New World Tertiary Procyonidae (Mammalia, Carnivora). *J. Vertebr. Paleontol.* 9, 110–117. doi: 10.1080/02724634.1989.10011743

Behling, H., Bush, M., and Hooghiemstra, H. (2010). "Biotic development of Quaternary Amazonia: a palynological perspective," in *Amazonia: Landscape and Species Evolution* (Chichester: Wiley-Blackwell Publishing Ltd.), 335–345.

Bondesio, P., Rabassa, J., Pascual, R., Vucetich, M. G., and Scillato-Yané, G. (1980). "La Formación Collón Curá de Pilcaniyeu viejo y sus alrededores (Río Negro, República Argentina). Su antigüedad y las condiciones ambientales según su distribución de litogénesis y sus vertebrados," in *2° Congreso Argentino de Paleontología y Bioestratigrafía y 1° Congreso Latinoamericano de Paleontología, Actas*, Vol. 3 (Buenos Aires: Asociación Paleontológica Argentina), 85–99.

Bossi, G. E., Muruaga, C., Sanagua, J., Hernando, A., Quiroga, G., and Ahumada, A. (1993). "Geología y estratigrafía de la cuenca neógena Santa María-Hualfín (Dptos. Santa María y Belén), Provincia de Catamarca," in *Actas, Congreso Geológico Argentino, 12th and Congreso de Exploración de Hidrocarburos, 2nd, Mendoza*, Vol. 2 (Buenos Aires, Asociación Geológica Argentina), 156–165.

Brandoni, D. (2013). "Los mamíferos continentales del "Mesopotamiense" (Mioceno tardío) de Entre Ríos, Argentina. Diversidad, edad y paleogeografía," in El Neógeno de la Mesopotamia argentina, Publicación especial 14, eds D. Brandoni and J. I. Noriega (Buenos Aires: Asociación Paleontológica Argentina), 179–191.

Brandoni, D., and Noriega, J. I. (2013). *El neógeno de la Mesopotamia Argentina*, Publicación Especial 14. Buenos Aires: Asociación Paleontológica Argentina.

Brunetto, E., Noriega, J. I., and Brandoni, D. (2013). "Sedimentología, estratigrafía y edad de la Formación Ituzaingó en la Provincia de Entre Ríos, Argentina," in *El Neógeno de la Mesopotamia argentina,* Publicación Especial, eds D. Brandoni, and J. I. Noriega (Buenos Aires, Argentina: Asociación Paleontológica Argentina), 13–27.

Campbell, K. E. Jr. (2004). *The Paleogene Mammalian Fauna of Santa Rosa, Amazonian Peru.* Los Angeles, CA: Natural History Museum of Los Angeles County.

Campbell, K. E. Jr., Frailey, C. D., and Romero-Pittman, L. (2000). *The late Miocene Gomphothere Amahuacatherium Peruvium (Proboscidea: Gomphotheriidae) from Amazonian Peru: Implications for the Great American Faunal Interchange*. Lima, Peri: Instituto Geologico Minero Metalurgico.

Campbell, K. E. Jr., Heizler, M., Frailey, C. D., Romero-Pittman, L., and Prothero, D. R. (2001). Upper Cenozoic chronostratigraphy of the southwestern Amazon Basin. *Geology* 29, 595–598. doi: 10.1130/0091-7613(2001)029<0595:UCCOTS>2.0.CO;2

Campbell, K. E. Jr., Prothero, D. R., Romero-Pittman, L., Hertel, F., and Rivera, N. (2010). Amazonian magnetostratigraphy: Dating the first pulse of the Great American Faunal Interchange. *J. South Am. Earth Sci.* 29, 619–626. doi: 10.1016/j.jsames.2009.11.007

Carlini, A. A., Brandoni, D., and Sánchez, R. (2006a). First Megatheriines (Xenarthra, Phyllophaga, Megatheriidae) from the Urumaco (Late Miocene) and Codore (Pliocene) Formations, Estado Falcón, Venezuela. *J.Syst. Palaeontol.* 4, 269–278. doi: 10.1017/S1477201906001878

Carlini, A. A., Brandoni, D., and Sánchez, R. (2008a). Additions to the knowledge of Urumaquia robusta (Xenarthra, Phyllophaga, Megatheriidae) from the Urumaco Formation (Late Miocene), Estado Falcón, Venezuela. *Paläontol. Z.* 82, 153–162. doi: 10.1007/BF02988406

Carlini, A. A., Scillato-Yané, G. J., and Sánchez, R. (2006b). New Mylodontoidea (Xenarthra, Phyllophaga) from the Middle Miocene-Pliocene of Venezuela. *J. Syst. Palaeontol.* 4, 255–267. doi: 10.1017/S147720190600191X

Carlini, A. A., Zurita, A., and Aguilera, O. A. (2008b). North American Glyptodontines (Xenarthra, Mammalia) in the Upper Pleistocene of northern South America. *Paläontol. Z.* 82, 125–138. doi: 10.1007/BF02988404

Carlini, A. A., Zurita, A., Scillato-Yané, G. J., Sánchez, R., and Aguilera, O. A. (2008c). New Glyptodont from the Codore Formation (Pliocene), Falcón State, Venezuela, its relationship with the *Asterostemma* problem, and the paleobiogeography of the Glyptodontinae. *Paläontol. Z.* 82, 139–152. doi: 10.1007/BF02988405

Castro, M. C., Carlini, A. A., Sánchez, R., and Sánchez-Villagra, M. R. (2014). A new Dasypodini armadillo (Xenarthra: Cingulata) from San Gregorio Formation, Pliocene of Venezuela: affinities and biogeographic interpretations. *Naturwissenschaften* 101, 77–86. doi: 10.1007/s00114-013-1131-5

Cione, A. L., Azpelicueta, M. D. L. M., Bond, M., Carlini, A. A., Casciotta, J. R., Cozzuol, M. A., et al. (2000). Miocene vertebrates from Entre Ríos province, eastern Argentina. *Insugeo Ser. Correl. Geol.* 14, 191–237.

Cione, A. L., and Tonni, E. P. (1996). Reassesment of the Pliocene-Pleistocene continental time scale of Southern South America. Correlation of the type Chapadmalalan with Bolivian sections. *J. South Am. Earth Sci.* 9, 221–236. doi: 10.1016/0895-9811(96)00008-9

Cione, A. L., and Tonni, E. P. (1999). "Biostratigraphy and chronological scale of upper-most Cenozoic in the Pampean area, Argentina," in *Quaternary of South America and Antartic Peninsula,* Vol. 3, eds J. Rabassa and M. Salemme (Rotterdam: Balkema), 23–51.

Cione, A. L., and Tonni, E. P. (2001). Correlation of Pliocene to Holocene southern south american and european vertebrate-bearing units. *Boll. Soc. Paleontol. Ital.* 40, 167–173.

Cione, A. L., Tonni, E. P., Bargo, S., Bond, M., Candela, A. M., Carlini, A. A., et al. (2007). "Mamíferos continentales del Mioceno tardío a la actualidad en la Argentina: cincuenta años de estudios," in *Asociación Paleontológica Argentina, Publicación Especial 11 Ameghiana 50° aniversario* (Buenos Aires: Asociación Paleontológica Argentina), 257–278.

Cody, S., Richardson, J. E., Rull, V., Ellis, C., and Pennington, T. (2010). The Great American Biotic Interchange revisited. *Ecography* 33, 326–332. doi: 10.1111/j.1600-0587.2010.06327.x

Cozzuol, M. A. (2006). The Acre vertebrate fauna: Age, diversity, and geography. *J. South Am. Earth Sci.* 21, 185–203. doi: 10.1016/j.jsames.2006.03.005

Croft, D. A. (2007). The Middle Miocene (Laventan) Quebrada Honda fauna, southern Bolivia and a description of its Notoungulates. *Palaeontology* 50, 277–303. doi: 10.1111/j.1475-4983.2006.00610.x

Croft, D. A. (2012). "Punctuated isolation. The making and mixing of South American's mammals," in *Bones, Clones and Biomes. The History and Geography of Recent Neotropical Mammals*, eds B. D. Patterson and L. P. Costa (Chicago; London: The University of Chicago Press), 9–19.

Eizirik, E. (2012). "A molecular view on the evolutionary history and biogeography of Neotropical carnivores (Mammalia, Carnivora)," in *Bones, Clones and Biomes.* The *H*istory and *G*eography of *R*ecent *N*eotropical *M*ammals, eds B. D. Patterson and L. P. Costa (Chicago; London: The University of Chicago Press), 123–142. doi: 10.7208/chicago/9780226649214.003.0007

Eizirik, E., Murphy, W. J., Koepfli, K. P., Johnson, W. E., Jerry, W., and Dragoo, J. W. (2010). Pattern and timing of diversification of the mammalian order Carnivora inferred from multiple nuclear gene sequences. *Mol. Phylogenet. Evol.* 56, 49–63. doi: 10.1016/j.ympev.2010.01.033

Flynn, J. J., and Swisher, C. C. III. (1995). "Cenozoic South American land mammal ages; correlation to global geochronologies," in *Geochronology, Time Scales and Global Stratigraphic Correlation,* eds W. Berggren, D. Kent, M. Aubry, and J. Herdenbol (Tulsa, OK: Soc. Sediment. Geol. Spec. Pub), 317–333.

Forasiepi, A. M., Soibelzon, L. H., Suarez-Gomez, C., Sánchez, R., Quiroz, L. I., Jaramillo, C., et al. (2014). Carnivorans at the Great American Biotic Interchange: new discoveries from the northern neotropics. *Naturwissenschaffen* 101, 965–974. doi: 10.1007/s00114-014-1237-4

Frailey, C. D., and Campbell, K. E. (2012). Two New Genera of Peccaries (Mammalia, Artiodactyla, Tayassuidae) from Upper Miocene Deposits of the Amazon Basin. *J. Paleontol.* 86, 852–877. doi: 10.1666/12-012.1

Garzione, C. N., Auerbach, D. J., Jin-Sook Smith, J., Rosario, J. J., Passey, B. H., Jordan, T. E., et al. (2014). Clumped isotope evidence for diachronous surface cooling of the Altiplano and pulsed surface uplift of the Central Andes. *Earth Planet. Sci. Lett.* 393, 173–181. doi: 10.1016/j.epsl.2014.02.029

Garzione, C. N., Hoke, G., Libarkin, J. C., Withers, S., MacFadden, B., Eiler, J., et al. (2008). Rise of the Andes. *Science* 320, 1304–1307. doi: 10.1126/science.1148615

Goin, F. J., Gelfo, J. N., Chornogubsky, L., Woodburne, M. O., and Martin, T. (2012). "Origins, radiations, and distributions of south american mammals," in *Bones, Clones and Biomes. The History and Geography of Recent Neotropical Mammals*, eds B. D. Patterson and L. P. Costa (Chicago; London: The University of Chicago Press), 20–50. doi: 10.7208/chicago/9780226649214.003.0003

Goin, F. J., Montalvo, C. I., and Visconti, G. (2000). Los marsupiales (Mammalia) del Mioceno de la Formación Cerro Azul (Provincia de la Pampa, Argentina). *Estudios Geol.* 56, 101–126. doi: 10.3989/egeol.00561-2158

Herbst, R., Anzótegui, L. M., Esteban, G., Mautino, L. R., Morton, S., and Nasif, N. (2000). "Síntesis paleontológica del Mioceno de los valles Calchaquíes, noroeste argentino," in *El Neógeno de Argentina,* eds F. G. Aceñolaza and R. Herbst (Tucumán: INSUGEO, Serie Correlación Geológica), 263–288.

Hirschfeld, S. E., and Webb, S. D. (1968). Plio-Pleistocene megalonychid sloth of North America. *Bull. Fla. State Mus.* 12, 213–296.

Kay, R. F., and Madden, R. H. (1997a). Mammals and rainfall: paleoecology of the middle Miocene at La Venta (Colombia, South America). *J. Human Evol.* 32, 161–199. doi: 10.1006/jhev.1996.0104

Kay, R. F., and Madden, R. H. (1997b). "Paleogeography and paleoecology," in *Vertebrate Paleontology in the Neotropics. The Miocene fauna of La Venta, Colombia*, eds R. F. Kay, R. H. Madden, R. L. Cifelli, and J. J. Flynn (Washington; London: Smithsonian Institution Press), 520–550.

Kay, R. F., Madden, R. H., Cifelli, R. L., and Flynn, J. J. (1997). *Vertebrate Paleontology in the Neotropics. The Miocene Fauna of La Venta, Colombia.* Washington; London: Smithsonian Institution Press.

Koepfli, K. P., Gompper, M. E., Eizirik, E., Ho, C. C., Linden, L., and Maldonado, J. E. (2007). Phylogeny of the Procyonidae (Mammalia: Carnivora): molecules, morphology and the Great American Interchange. *Mol. Phylogenet. Evol.* 43, 1076–1095. doi: 10.1016/j.ympev.2006.10.003

Kramarz, A. G., Forasiepi, A. M., and Bond, M. (2011). "Vertebrados Cenozoicos," in *Relatorio del XVIII Congreso Geológico Argentino. Geología y Recursos*

Naturales de la Provincia del Neuquén, eds H. A. Leanza, C. Arregui, O. Carbone, J. C. Danieli, and J. M. Vallés (Buenos Aires: Asociación Geológica Argentina), 557–572.

Latorre, C., Quade, J., and Mcintosh, W. C. (1997). The expansion of C4 grasses and global change in the late Miocene: Stable isotope evidence from the Americas. *Earth Planet. Sci. Lett.* 146, 83–96. doi: 10.1016/S0012-821X(96)00231-2

Latrubesse, E. M., Bocquentin, J., Santos, C. R., and Ramonell, C. G. (1997). Paleonvironmental model for the late Cenozoic southwestern Amazonia: paleontology and geology. *Acta Amazonica* 27, 103–118.

Leigh, E. G., O'Dea, A., and Vermeij, G. J. (2014). Historical biogeography of the Isthmus of Panama. *Biol. Rev.* 89, 148–172. doi: 10.1111/brv.12048

Linares, O. J. (2004). Bioestratigrafía de la fauna de mamíferos de las formaciones Socorro, Urumaco y Codore (Mioceno medio-Plioceno temprano) de la región de Urumaco, Falcón, Venezuela. *Paleobiologia Neotropical* 1, 1–26.

Lucas, S. G. (2013). The palaeobiogeography of South American gomphotheres. *J. Palaeogeogr.* 2, 19–40. doi: 10.3724/sp.j.1261.2013.00015

Lucas, S. G., and Alvarado, G. E. (2010). Fossil Proboscidea from the upper Cenozoic of Central America: taxonomy, evolutionary and paleobiogeographic significance. *Revista Geológica de America Central* 42, 9–42.

MacFadden, B. J. (2006). Extinct mammalian biodiversity of the ancient New World tropics. *Trends Ecol. Evol.* 21, 157–165. doi: 10.1016/j.tree.2005.12.003

MacFadden, B. J., Anaya, F., and Argollo, J. (1993). Magnetic polarity stratigraphy of Inchasi: a Pliocene mammal-bearing locality from the Bolivian Andes deposited just before the Great American Interchange. *Earth and Planetary Science Letters* 114, 229–241. doi: 10.1016/0012-821X(93)90027-7

MacFadden, B. J., Anaya, F., Perez, H., Naeser, C. W., Zeitler, P. K., and Campbell Jr, K. E. (1990). Late Cenozoic Paleomagnetism and Chronology of Andean Basins of Bolivia: Evidence for Possible Oroclinal Bending. *The Journal of Geology* 98, 541–555. doi: 10.1086/629423

Madden, R. H., Guerrero, J., Kay, R. F., Flynn, J. J., Swisher, C. C., and Walton, A. H. (1997). "The Laventan stage and age," in *Vertebrate paleontology in the Neotropics. The Miocene fauna of La Venta, Colombia,* eds R. F. Kay, R. H. Madden, R. L. Cifelli and J. J. Flynn (Washington; Londonm: Smithsonian Instituion Press), 499–519.

Marshall, L. G., Pascual, R., Curtis, G. H., and Drake, R. E. (1977). South American Geochronology: Radiometric Time Scale for Middle to Late Tertiary Mammal-Bearing Horizons in Patagonia. *Science* 195, 1325–1328. doi: 10.1126/science.195.4284.1325

Marshall, L. G., and Patterson, B. (1981). Geology and geochronology of the mammal-bearing Tertiary of the Valle de Santa Maria and Río Corral Quemado, Catamarca Province, Argentina. *Fieldiana Geology* 9, 1–80.

Marshall, L. G., Webb, S. D., Sepkoski, J. J., and Raup, D. M. (1982). Mammalian Evolution and the Great American Interchange. *Science* 215, 1351–1357. doi: 10.1126/science.215.4538.1351

Mazzoni, M. M., and Benvenuto, A. (1990). Radiometric ages of Tertiary ignimbrites and the Collón Cura Formation, Northwestern Patagonia. in *9° Congreso Geológico Argentino, Actas,* Vol. 1 (Buenos Aires: Asociación Paleontológica Argentina), 731–746.

Montalvo, C. I., Melchor, R. N., Visconti, G., and Cerdeño, E. (2008). Vertebrate taphonomy in loess-palaeosol deposits: a case study from the late Miocene of central Argentina. *Geobios* 41, 133–143. doi: 10.1016/j.geobios.2006.09.004

Mora, A., Baby, P., Roddaz, M., Parra, M., Brusset, S., and Hermoza, W., et al. (2009). "Tectonic history of the andes and sub-andean zones: implications for the development of the Amazon drainage basin," in *Amazonia: Landscape and Species Evolution* (Wiley-Blackwell Publishing Ltd.), 38–60.

Morrone, J. J. (2014). Cladistic biogeography of the Neotropical region: identifying the main events in the diversification of the terrestrial biota. *Cladistics* 30, 202–214. doi: 10.1111/cla.12039

Negri, F. R., Bocquentin-Villanueva, J., Ferigolo, J., and Antoine, P.-O. (2010). "A review of tertiary mammal faunas and birds from Western Amazonia," in *Amazonia: Landscape and Species Evolution* (Chichester: Wiley-Blackwell Publishing Ltd.), 243–258.

Okasanen, J., Guillaume Blanchet, F., Kindt, R., Legendre, P., Minchin, P. R., and O'hara, R. B., et al. (2013). *Vegan: Community Ecology Package.* R package version 2.0-10. Available online at: http://CRAN.R-project.org/package=vegan

Pascual, R. (2006). Evolution and geography: The biogeographic history of south american land mammals. *Ann. Mo. Bot. Gard.* 93, 209–230. doi: 10.3417/0026-6493(2006)93[209:EAGTBH]2.0.CO;2

Patterson, B. D., and Costa, L. P. (2012). "Introduction to the history and geography of Neotropical mammals," in *Bones, Clones and Biomes. The History and Geography of Recent Neotropical Mammals,* eds B. D. Patterson and L. P. Costa (Chicago; London: The University of Chicago Press), 1–5. doi: 10.7208/chicago/9780226649214.003.0001

Patterson, B. D., Solari, S., and Velazco, P. M. (2012). "The role of the Andes in the diversification and biogeography of Neotropical mammals," in *Bones, Clones and Biomes. The History and Geography of Recent Neotropical Mammals*, eds B. D. Patterson, and L. P. Costa (Chicago; London: The University of Chicago Press), 351–378. doi: 10.7208/chicago/9780226649214.003.0015

Pérez, L. M. (2013). "Nuevo aporte al conocimiento de la edad de la Formación Paraná, Mioceno de la Provincia de Entre Ríos, Argentina," in *El Neógeno de la Mesopotamia Argentina*, eds D. Brandoni and J. I. Noriega (Buenos Aires: Asociación Paleontológica Argentina, Publicación Especial), 7–12.

Prevosti, F., Forasiepi, A., and Zimicz, N. (2013). The evolution of the cenozoic terrestrial mammalian predator guild in South America: competition or replacement? *J. Mammal. Evol.* 20, 3–21. doi: 10.1007/s10914-011-9175-9

Prevosti, F. J. (2006). New material of Pleistocene cats (Carnivora, Felidae) from Southern South America, with comments on biogeography and the fossil record. *Geobios* 39, 679–694. doi: 10.1016/j.geobios.2005.01.004

Prevosti, F. J., and Pardiñas, U. F. J. (2009). Comment on "The oldest South American Cricetidae (Rodentia) and Mustelidae (Carnivora): late Miocene faunal turnover in central Argentina and the Great American Biotic Interchange" by D. H. Verzi and C. I. Montalvo [Palaeogeography, Palaeoclimatology, Palaeoecology 267 (2008) 284–291]. *Palaeogeogr. Palaeoclimatol. Palaeoecol.* 280, 543–547. doi: 10.1016/j.palaeo.2009.05.021

Prothero, D. R., Campbell, K. E., Beatty, B. L., and Frailey, C. D. (2014). New late Miocene dromomerycine artiodactyl from the Amazon Basin: implications for interchange dynamics. *J. Paleontol.* 88, 434–443. doi: 10.1666/13-022

Quiroz, L. I., and Jaramillo, C. A. (2010). "Stratigraphy and sedimentary environments of Miocene shallow to marginal marine deposits in the Urumaco trough, Falcón basin, western Venezuela," in *Urumaco and Venezuelan Paleontology. The Fossil Record of the Northern Neotropics,* eds M. R. Sánchez-Villagra, O. A. Aguilera, and A. A. Carlini (Bloomington; Indianapolis: Indiana University Press), 153–172.

Rabassa, J. (1974). *Geología de la Región Pilcaniyeu-Comallo.* Bariloche: Fundación Bariloche, Departamento Recursos Naturales Energéticos, Publicación.

Rabassa, J. (1978). "Estratigrafía de la región Pilcaniyeu-Comallo, provincia de Río Negro," in *7° Congreso Geológico Argentino, Actas*, Vol. 1 (Neuquén), 731–746.

Ramos, V. (1999). Plate tectonic setting of the Andean Cordillera. *Episodes* 22, 183–190.

R Core Team. (2013). *R: A Language and Environment for Statistical Computing.* Vienna, Austria: R Foundation for Statistical Computing. Available online at: http://www.R-project.org/.

Reguero, M. A., and Candela, A. M. (2011). "Late Cenozoic mammals from the Northwest of Argentina," in *Cenozoic geology of the Central Andes of Argentina,* eds. J. A. Salfity and R. A. Marquillas (Salta: INCE, Instituto del Cenozoico), 411–426.

Reguero, M. A., Candela, A. M., and Alonso, R. N. (2007). Biochronology and biostratigraphy of the Uquía Formation (Pliocene-early Pleistocene, NW Argentina) and its significance in the Great American Biotic Interchange. *J. South Am. Earth Sci.* 23, 1–16. doi: 10.1016/j.jsames.2006.09.005

Ribeiro, A. M., Madden, R. H., Negri, F. R., Kerber, L., Hsiou, A. S., and Rodrigues, K. A. (2013). "Mamíferos fósiles y biocronología en el suroeste de la Amazonia, Brasil," in *El Neógeno de la Mesopotamia Argentina,* Publicación Especial 14, eds D. Brandoni and J. I. Noriega (Buenos Aires: Asociación Paleontológica Argentina), 207–221.

Riggs, E., and Patterson, B. (1939). Stratigraphy of late Miocene and Pliocene deposits of the Province of Catamarca (Argentina) with notes on the faunae. *Physics* 14, 143–162.

Sánchez-Villagra, M. R., Aguilera, O. A., and Carlini, A. A. (2010). *Urumaco & Venezuelan Paleontology. The fossil record of the Northern Neotropics.* Bloomington; Indianapolis: Indiana University Press.

Scheyer, T. M., Aguilera, O. A., Delfino, M., Fortier, D. C., Carlini, A. A., Sanchez, R., et al. (2013). Crocodylian diversity peak and extinction in the late Cenozoic of the northern Neotropics. *Nat. Commun.* 4, 1907. doi: 10.1038/ncomms2940

Simpson, G. G. (1980). *Splendid Isolation. The Curious History of South American Mammals.* New Haven; London: Yale University Press.

Tejada-Lara, J. V., Salas-Gismondi, R., Pujos, F., Baby, P., Benammi, M., Brusset, S., et al. (in press). Life in proto-Amazonia: middle Miocene mammals from the Fitzcarrald Arch (Peruvian Amazonia). *Paleontology.*

Tews, J., Brose, U., Grimm, V., Tielbörger, K., Wichmann, M. C., Schwager, M., et al. (2004). Animal species diversity driven by habitat heterogeneity/diversity: the importance of key stone structures. *J. Biogeogr.* 31, 79–92. doi: 10.1046/j.0305-0270.2003.00994.x

Tomassini, R. L., and Montalvo, C. I. (2013). Taphonomic modes on fluvial deposits of the Monte Hermoso Formation (early Pliocene), Buenos Aires province, Argentina. *Palaeogeogr. Palaeoclimatol. Palaeoecol.* 369, 282–294. doi: 10.1016/j.palaeo.2012.10.035

Tomassini, R. L., Montalvo, C. I., Deschamps, C. M., and Manera, T. (2013). Biostratigraphy and biochronology of the Monte Hermoso Formation (early Pliocene) at its type locality, Buenos Aires Province, Argentina. *J. South Am. Earth Sci.* 48, 31–42. doi: 10.1016/j.jsames.2013.08.002

Verzi, D. H., and Montalvo, C. I. (2008). The oldest South American Cricetidae (Rodentia) and Mustelidae (Carnivora): late Miocene faunal turnover in central Argentina and the Great American Biotic Interchange. *Palaeogeogr. Palaeoclimatol. Palaeoecol.* 267, 284–291. doi: 10.1016/j.palaeo.2008.07.003

Verzi, D. H., Vieytes, E. C., and Montalvo, C. I. (2011). Dental evolution in neophanomys (Rodentia, Octodontidae) from the late Miocene of central Argentina. *Geobios* 44, 621–633. doi: 10.1016/j.geobios.2011.02.008

Vrba, E. S. (1992). Mammals as a key to evolutionary theory. *J. Mammal.* 73, 1–28. doi: 10.2307/1381862

Webb, S. D. (1976). Mammalian Faunal Dynamics of the Great American Interchange. *Paleobiology* 2, 220–234.

Webb, S. D. (1985). "Late Cenozoic mammal dispersal between the Americas," in *The Great American Biotic Interchange*, eds F. G. Stehli and S. D. Webb (New York; London: Plenum Press), 357–386. doi: 10.1007/978-1-4684-9181-4_14

Webb, S. D. (1989). "Osteology and relationships of *Thinobadistes segnis*, the first Mylodont sloth in North America," in *Advances in Tropical Mammalogy,* eds K. H. Redford and J. F. Eisenberg (Gainsville: The Sandhill Crane Press), 469–532.

Webb, S. D. (1991). Ecogeography and the Great American Interchange. *Paleobiology* 17, 266–280.

Webb, S. D. (2006). The Great American Biotic Iinterchange: patterns and processes. *Ann. Mo. Bot. Gard.* 93, 245–257. doi: 10.3417/0026-6493(2006)93[245:TGABIP]2.0.CO;2

Woodburne, M. (2010). The Great American Biotic Interchange: dispersals, tectonics, climate, sea level and holding pens. *J. Mammal. Evol.* 17, 245–264. doi: 10.1007/s10914-010-9144-8

Conflict of Interest Statement: The authors declare that the research was conducted in the absence of any commercial or financial relationships that could be construed as a potential conflict of interest.

Received: 30 August 2014; accepted: 10 December 2014; published online: 05 January 2015.

Citation: Carrillo JD, Forasiepi A, Jaramillo C and Sánchez-Villagra MR (2015) Neotropical mammal diversity and the Great American Biotic Interchange: spatial and temporal variation in South America's fossil record. Front. Genet. ***5****:451. doi: 10.3389/fgene.2014.00451*

This article was submitted to Evolutionary and Population Genetics, a section of the journal Frontiers in Genetics.

Supplementary Material

Neotropical mammal diversity and the Great American Biotic Interchange: spatial and temporal variation in South America's fossil record

Juan D. Carrillo[1,3]*, Analía Forasiepi[2], Carlos Jaramillo[3] , Marcelo R. Sánchez-Villagra[1]

[1] Paläontologisches Institut und Museum, Universität Zürich, Zurich, Switzerland

[2] IANIGLA, CCT-CONICET Mendoza, Av. Ruiz Leal s/n, 5500 Mendoza, Argentina

[3] Smithsonian Tropical Research Institute, Panama, Panama

*** Correspondence:** Juan D. Carrillo, Paläontologisches Institut und Museum, Universität Zürich , Karl-Schmid-Strasse 4 8006, Zurich,Switzerland.

Juan.carrillo@pim.uzh.ch

1. Supplementary Material 1

Taxonomic lists of the mammal faunal assemblages analyzed

La Venta: *Anadasypus, Aotus, Boreostemma, Eodolichotis, Eumops, Glossotheriopsis, Granastrapotherium, Hondathentes, Huilatherium, Kiotomops, Lagonimico, Marmosa, Micodon, Microscleromys, Microsteiromys, Miocallicebus, Nanoastegotherium, Neoglyptatelus, Neonematherium, Neosaimiri, Noctilio, Notonycteris, Nuciruptor, Olenopsis, Pachybiotherium, Palynephyllum, Patasola, Pedrolypeutes, Pericotoxodon, Potamops, Prodolichotis, Prolicaphrium, Pseudoprepotherium, Rhodanodolichotis, Ricardomys, Scirrotherium, Scleromys, Stirtonia, Theosodon, Thylamys, Thyroptera, Xenastrapotherium.*

Fitzcarrald: *Acarechimys, Boreostemma, Drytomomys, Granastrapotherium, Megathericulus, Miocochilius, Neoepiblema, Neoglyptatelus, Parapropalaehoplophorus, Pericotoxodon, Potamarchus, Prodolichotis, Scleromys, Tetramerorhinus, Theosodon, Urumacotherium, Xenastrapotherium.*

Quebrada Honda: *Acarechimys, Acyon, Guiomys, Hapalops, Hemihegetotherium, Hiskatherium, Hondalagus, Mesoprocta, Miocochilius, Paratrigodon, Plesiotypotherium, Prolagostomus, Prozaedyus, Quebradahondomys.*

Collón Curá: *Abderites, Acarechimys, Acdestis, Alloiomys, Amphibradys, Anisolophus, Arctodictis, Branisamyopsis, Diellipsodon, Eocardia, Eonaucum, Epipatriarchus, Eucholaeops, Eucinepeltus, Eutrachytherus, Galileomys, Glossoptheriopsis, Hegetotherium, Homalodotherium,*

Hyperoxotodon, Icochilus, Interatherium, Maruchito, Massoiamys, Megastus, Megathericulus, Neoreomys, Neosteiromys, Nesciotherium, Nesodon, Pachyrukhos, Palyeidodon, Patagosmilus, Pitheculites, Planops, Pliolagostomus, Prepotherium, Proeutatus, Prolagostomus, Propithecia, Protacaremys, Prothylacynus, Prototrigodon, Protypotherium, Prozaedius, Pseudonotictis , Pseuhapalops, Scleromys, Steiromys, Stenotatus, Stereotoxodon, Stilotherium, Theosodon, Vetelia.

Urumaco: *Bolivartherium, Bounodus, Cardiatherium, Eumegamys, Gyrinodon, Lestodon, Mirandabradys, Ocnerotherium, Olenopsis, Phoberomys, Potamarchus, Tetrastylus, Urumacotherium, Urumaquia.*

Acre: *Abothrodon, Acrecebus, Amahuacatherium, Anadasypus, Asterostemma, Cardiatherium, Cullinia, Didelphis, Eumegamys, Gyriabrus, Gyrinodon, Hapalops, Kraglievichia, Lutreolina, Mesenodon, Mesotoxodon, Minitoxodon, Neoepiblema, Neoglyptatelus, Neotoxodon, Neotrigodon, Noctilio, Octodontobradys, Palaeotoxodon, Paraglyptodon, Paratrigodon, Phoberomys, Planops, Plesiotoxodon, Pliomorphus, Plohophorus, Potamarchus, Proterotherium, Protomegalonyx, Pseudoprepotherium, Purperia, Ranculcus, Scirrotherium, Simplimus, Solimoea, Stenodon, Stirtonia, Surameryx, Sylvochoerus, Telicomys, Tetrastylus, Toxodontherium, Trigodon, Trigodonops, Urumacotherium, Waldochoerus, Xenastrapotherium, Scleromys.*

Mesopotamian: *Amphiocnus, Berthawyleria, Borhyaena, Brachytherium, Cardiatherium, Cardiomys, Carlesia, Caviodon, Chasicotatus, Chironectes, Chlamyphractus, Comaphorus, Cullinia, Cyonasua, Dasypus, Diadiaphorus, Dilobodon, Dinotoxodon, Drytomomys, Eleutherocercus, Eomegatherium, Eumegamys, Eumegamysops, Eumysops, Eutemnodus, Eutomodus, Eutypotherium, Gyriabrus, Haplodontherium, Haplostropha, Hoplophorus, Isostylomys, Kraglievichia, Lagostomus, Macroeuphractus, Megabradys, Megalonychops, Munizia, Myocastor, Neobrachytherium, Neoepiblema, Neohapalops, Notictis, Octomylodon, Ortotherium, Oxyodontherium, Pachynodon, Palaeocavia, Palaeohoplophorus, Palaeotoxodon, Paradoxomys, Parahoplophorus, Paranabradys, Paranamys, Paranauchenia, Parodimys, Philander, Phoberomys, Pliodolichotis, Pliomegatherium, Pliomorphus, Plohophorus, Potamarchus, Prodolichotis, Proeuphractus, Promacrauchenia, Promegatherium, Promylodon, Pronothrotherium, Protabrocoma, Proterotherium, Protoglyptodon, Protomegalonyx, Protypotherium, Pseudoeuryurus, Pyramiodontherium, Ranculcus, Scalabrinitherium, Scirrotherium, Sphenotherus, Stenotephanos, Strabosodon, Strophostephanos, Stylocynus, Tetrastylus, Thylacosmilus, Torcellia, Toxodontherium, Urotherium, Xotodon, Zygolestes.*

Cerro Azul: *Aspidocalyptus, Borhyaenidium, Cardiomys, Chasichimys, Chasicotatus, Chorobates, Clyomys, Coscinocercus, Cyonasua, Doellotatus, Elassotherium, Eoauchenia, Eosclerocalyptus, Epecuenia, Eumysops, Hemihegetotherium, Hyperdidelphys, Lagostomus, Lutreolina, Macrauchenia, Macrochorobates, Macroeuphractus, Microtragulus, Neophanomys, Orthomyctera, Paedotherium, Palaeocavia, Palaeoctodon, Paleuphractus, Phtoramys, Pisanodon, Pithanotomys, Plesiomegatherium, Pliolestes, Plohophorus, Proeuphractus, Promacrauchenia, Pseudotypotherium, Tetrastylus, Thylacosmilus, Thylamys, Thylatheridium, Xenodontomys,*

Zygolestes.

Chiquimil: *Cardiomys, Chasicotatus, Chorobates, Diadiaphorus, Eosclerocalyptus, Gyriabrus, Lagostomopsis, Macrochorobates, Nephanomys, Orthomyctera, Paedotherium, Paleuphractus, Paraeuphractus, Paranamys, Potamarchus, Proscelidodon, Protabrocoma, Pseudohegetotherium, Stromaphorus, Tetrastylus, Toxodontherium, Tremacyllus, Typotheriopsis, Vassallia, Vetelia, Xotodon.*

Andalhuala: *Cardiomys, Chapalmalania, Chasicotatus, Chorobates, Cyonasua, Eosclerocalyptus, Glyptodontidium, Hemihegetotherium, Hesperocynus, Hyperdidelphys, Lagostomopsis, Lutreolina, Macrochorobates, Macroeucphractus, Microtragulus, Neobrachytherium, Neophanomys, Orthomyctera, Palaeocavia, Paraeuphractus, Phlyctaenopyga, Pithanotomys, Prodolichotis, Promacrauchenia, Pronothrotherium, Protabrocoma, Pyramiodontherium, Sphenotherus, Stromaphorus, Tetrastylus, Thylacosmilus, Toxodontherium, Treamcyllus, Typotheriopsis, Urotherium, Xotodon.*

Monte Hermoso: *Actenomys, Alitoxodon, Argyrolagus, Auliscomys, Cardiomys, Caviodon, Chorobates, Cyonasua, Diheterocnus, Diplasiotherium, Doellotatus, Eleutherocercus, Eoauchenia, Eosclerocalyptus, Epitherium, Eucelophorus, Eumysops, Holozaedyus, Hyperdidelphys, Lagostomus, Lestodon, Lutreolina, Macrochorobates, Macroeuphractus, Microcavia, Microtragulus, Myrmecophaga, Necromys, Neocavia, Neopachtus, Neophanomys, Notocynus, Orthomyctera, Paedotherium, Palaeocavia, Palaeodaedicurus, Pampatherium, Parahyaenodon, Paramyocastor, Phtoramys, Phugatherium, Phyctaenopyga, Pithanotomys, Plaina, Plohophoroides, Plohophorus, Prodolichotis, Promacrauchenia, Proscelidodon, Pseudoplataeomys, Pseudotypotherium, Reithrodon, Ringueletia, Sparassocynus, Telicomys, Thylacosmilus, Thylamys, Thylaohorops, Thylatheridium, Toxodon, Trachycalyptus, Tremacyllus, Trigodon, Xotodon.*

Inchasi: *Caviodon, Glossotherium, Hypsitherium, Paraglyptodon, Phugatherium, Plohophorus, Posnanskytherium, Promacrauchenia, Proscelidodon, Vassallia.*

Uquía: Lower: *Ctenomys, Doellotatus, Microcavia, Paraglyptodon, Scelidotheridium, Vassallia;* Middle: *Chaetophractus, Ctenomys, Erethizon, Hippidion, Hydrochoeropsis, Lestodon, Megatherium, Panochthus, Paraglyptodon, Platygonus, Pyramiodontherium, Urotherium, Windhausenia, Xiphuroides.*

2. Supplementary Material 2

Search queries used and Paleobiology Database (PBDB) ID's of the collections belonging to the different mammal assemblages used in the analysis.

Queries:

Taxonomic level: genus

Taxon or taxa to include: Mammalia

Taxon or taxa to exclude: Cetacea, Sirenia

La Venta

Date of download: 13.04.2014

PBDB collection ID's: 13630, 13650, 13653, 13678, 13680, 13681, 13682, 13684, 13685, 13686, 13687, 13739, 13740, 13741, 13743, 13747, 13749, 13750, 13754, 13757, 13758, 94555, 117981, 132559, 132580, 133441, 133648, 133688, 133689, 133692, 133693, 133780, 134806, 135348, 135373, 136211, 136233, 139894, 140007, 140012, 140046, 140051, 140179, 140181, 140183, 140634, 141256, 141257, 142428, 142486, 142494, 143489, 143779, 143781, 143785, 143787, 143788, 143789, 143791, 143795, 144401, 145175, 145191, 145194, 145234, 145432, 145559, 145614, 145617, 146527

Fitzcarrald

Date of download: 19.11.2014

PBDB collection ID's: 107992, 107993, 144792, 144793, 144794, 144795, 144950,163839,163840,163841, 163842, 163843, 163844

Quebrada Honda

Date of download: 13.04.2014

PBDB collection ID's: 38071, 133664, 133629

Collón Curá

Date of download: 04.07.2014

PBDB collection ID's: 28611, 141175, 142148

Urumaco

Date of download: 19.04.2014

PBDB collection ID's: 92751, 144849, 145271, 145364, 145365, 145380, 146290, 146407, 146416, 146421, 146422, 146423, 146425, 146426, 146427, 146428, 146429, 146430, 146431, 146432, 146433, 146446, 146447, 146448, 146449, 146450, 146451, 152543, 146452

Acre

Date of download: 28.05.2014

PBDB collection ID's: 134808, 136714, 136716, 136717, 137876, 148207, 156532, 137877, 137878, 137879, 137880 , 137881 , 137882 , 137883, 137884 , 144064, 144066, 144515, 134868, 55602, 67383, 67384, 67385, 67386

Mesopotamian

Date of download: 13.04.2014

PBDB collection ID's: 55600, 140472, 140696

Cerro Azul

Date of download: 04.07.2014

PBDB collection ID's: 87198, 140925, 140932, 141939, 151498, 151499, 151500, 152063, 152065, 152066, 152067

Chiquimil

Date of download: 04.07.2014

PBDB collection ID: 157794

Andalhuala

Date of download: 04.07.2014

PBDB collection ID: 157795

Monte Hermoso

Date of download: 11.06.2014

PBDB collection ID's: 13503, 140627, 141247, 145757, 152062, 152064, 152081, 152084, 152085, 152086, 152087, 152088

Inchasi

Date of download: 12.06.2014

PBDB collection ID: 71112

Uquía

Date of download: 11.06.2014

PBDB collection ID's: Uquía lower 141894; Uquía middle 141896

3. Supplementary Material 3

Search queries used to get records of GABI participants in North and South America from the Paleobiology Database (PBDB).

Date of download: 16.08.2014

NORTH AMERICAN-ORIGIN MAMMALS

Taxon or taxa to include: Peradectinae, Herpetotheriinae, Peradectes, Armintodelphys , Leptictida,Lagomorpha,Alagomyidae,Laredomyidae,Ischyromyidae,Allomyidae,Aplodontoidea, Sciuroidea, Castoroidea, Castorimorpha, Cricetidae, Myodonta, Protoptychidae, Geomyoidea, Muridae, Palaeoryctidae, Cimolestidae, Apatemyidae, Taeniodonta, Tillodontia, Pantodonta, Pantolestidae, Epoicotheriidae, Metacheiromyidae, Feliformia, Amphicyonidae, Cyonidea, Lycophocyon, Palaearctonyx,Procynodictis, Canidae, Mustelida, Musteloidea,Nothocyon, Ursida, Ursidae, Creodonta, Perissodactyla, Achaenodontidae, Achtiaria,Ancodonta, Antiacodontidae, Antiacodontinae, Caenotheriidae, Cetancodontamorpha, Choeropotamoidea, Delahomeryx, Dichobunoidea, Dulcidon, Entelodontoidea, Eolantianus, Eschatiidae, Eurytheriidae, Helohyinae, Hexacodus, Hidrosotherium, Hsanotherium, Leptochoerinae, Lophiomerycidae, Myanmarius, Neoselenodontia, Nonruminantia, Palaeodonta, Protolabididae, Raoellidae, Raphenacodus, Ruminantiamorpha, Simpsonodus, Suiformes, Suoidea, Tragulohyus, Tylopoda, Whippomorpha, Proboscidea, Erinaceomorpha, Soricomorpha, Solenodontidae, Talpidae, Lipotyphla, Dinocerata, Acreodi, Emballonuridae, Tadarida, Molossops, Molossus, Nyctinomops, Mormoopidae, Pteropodidae, Vespertilionidae

Taxon or taxa to exclude: Hystricognathi, Cavina, Pinnipedia, Cetacea, Sirenia, Desmostylia, Wangliidae, Diclidurus

Time span: Miocene-Holocene

Continent: South America

SOUTH AMERICAN-ORIGIN MAMMALS

Taxon or taxa to include: Gondwanatheria, Ameridelphia, Microbiotheria, Paucituberculata, Pucadelphydae, Didelphinae, Caluromyinae, Marmosinae, Derorhynchinae, Eobrasiliinae, Sparassocynus, Hyladelphinae, Thylamyinae, Caroloameghiniinae, Polydolopimorphia, Sparassodonta, Borhyaenoidea, Xenarthra, Hystricognathi, Cavina, Platyrrhini, Litopterna, Notoungulata, Astrapotheria, Xenungulata, Pyrotheria, Meridiungulata, Diclidurus, Furipteridae, Eumops, Kiotomops, Mormopterus, Promops, Noctilionidae, Phyllostomidae, Thyropteridae

Taxon or taxa to exclude: Alphadontinae, Peradectinae, Herpetotheriinae, Peradectes, Armintodelphys, Iugomortiferum, Cimolestes,

Time span: Miocene-Holocene

Continent: North America

4. Supplementary Material 4

The R code used to perform the different analyses

```
#NMDS analysis with bray-Curtis distance and average cluster dendogram
#load presence/abscence matrix from the Supplementary Table 1
Supp1<-read.csv("Supplementary_Table1.csv",row.names=1)
Supp.1<-as.matrix(Supp1)
str(Supp.1)

# load Vegan package#
library(vegan)
# Get a distance matrix for the faunas with Bray-Curtis distance
dist.Bray<-vegdist(Supp.1, method="bray", binary=TRUE)
str(dist.Bray)
# Get a cluster plot only
dist.Bray.av<-hclust(dist.Bray, method="average")
plot(dist.Bray.av,ylab="Bray curtis dissimilarity")

## Perform NMDS analysis, k value=2 and 1000 runs
nmds.data<-metaMDS(Supp.1, distance="bray",k=2, trymax=1000,autotransform=TRUE,
wascores=TRUE, expand=TRUE)
nmds.data$converge
nmds.data$stress

# Plot of the NMDS with the clusterdendrogram - Figure 4 A
dist.Bray.av.groups[]<-cutree(dist.Bray.av,k=3)
ave.lev<-levels(factor(dist.Bray.av.groups))

 q<-ordiplot(nmds.data, type="n")
for(i in 1:length(ave.lev)){
points(nmds.data, col=dist.Bray.av.groups[],
pch=16,cex=2)
}
text(nmds.data,pos=3)
ordicluster(q,dist.Bray.av, col="darkgrey")

#Analysis of Bray-Curtis dissimilarity values taking into account differences in sample size
```

```
#Data for histograms showed in Figure 4C
#load taxonomic lists from Supplementary Material 1
# Middle Miocene faunal assemblages
Fitzcarrald.gen<-read.csv("Fitzcarrald.csv",sep=";")
str(Fitzcarrald.gen)
Fitzcarrald.gen$Fauna<-rep("Fitzcarrald",17)
LaVenta.gen<-read.csv("LaVenta.csv")
str(LaVenta.gen)
LaVenta.gen$Fauna<-rep("La Venta", 42)
QuebradaHonda.gen<-read.csv("QuebradaHonda.csv")
str(QuebradaHonda.gen)
QuebradaHonda.gen$Fauna<-rep("Quebrada Honda", 14)
CollonCura.gen<-read.csv("CollonCura.csv",sep=";")
str(CollonCura.gen)
CollonCura.gen$Fauna<-rep("Collon Cura", 54)

#Loops to estimate Bray-Curtis dissimilarity 1000 times for each pair of faunas
# From the fauna with more taxa (e.g. La Venta) each time is randomly chosen the same number of taxa as the
#fauna with fewer taxa (e.g. Fitzcarrald)
# La Venta- Fitzcarrald - tropical middle Miocene
nrand<-1000
xy.boot =numeric(nrand)
for(i in 1:nrand){
gen<-as.vector(sample(LaVenta.gen$genus,17, replace=TRUE))
name<-rep("La Venta",17)
t<-as.data.frame(cbind(gen,name))
gen<-as.vector(Fitzcarrald.gen$genus)
name<-rep("Fitzcarrald",17)
p<-as.data.frame(cbind(gen,name))
q<-rbind(t,p)
tab<-table(q$name,q$gen)
xy.boot[i]=vegdist(tab, method="bray", binary=TRUE)
}
mean(xy.boot)
sd(xy.boot)
Lv.Fitz<-xy.boot
mean(Lv.Fitz)

#Collon Cura - Quebrada Honda - temperate middle Miocene
nrand<-1000
```

```
xy.boot =numeric(nrand)
for(i in 1:nrand){
gen<-as.vector(sample(CollonCura.gen$genus,14, replace=TRUE))
name<-rep("Collon Cura",14)
t<-as.data.frame(cbind(gen,name))
gen<-as.vector(QuebradaHonda.gen$genus)
name<-rep("Quebrada Honda",14)
p<-as.data.frame(cbind(gen,name))
q<-rbind(t,p)
tab<-table(q$name,q$gen)
xy.boot[i]=vegdist(tab, method="bray", binary=TRUE)
}
mean(xy.boot)
sd(xy.boot)
Col.Qh<-xy.boot
mean(Col.Qh)

#middle miocene temperate vs tropical
nrand<-1000
xy.boot =numeric(nrand)
for(i in 1:nrand){
gen<-as.vector(sample(CollonCura.gen$genus,14, replace=TRUE))
name<-rep("Collon Cura",14)
t<-as.data.frame(cbind(gen,name))
gen<-as.vector(sample(QuebradaHonda.gen$genus,14,replace=TRUE))
name<-rep("Quebrada Honda",14)
p<-as.data.frame(cbind(gen,name))
gen<-as.vector(sample(LaVenta.gen$genus,14, replace=TRUE))
name<-rep("La Venta",14)
o<-as.data.frame(cbind(gen,name))
gen<-as.vector(Fitzcarrald.gen$genus)
name<-rep("Fitzcarrald",14)
r<-as.data.frame(cbind(gen,name))
q<-rbind(t,p,o,r)
tab<-table(q$name,q$gen)
f<-as.matrix(vegdist(tab, method="bray", binary=TRUE))
xy.boot[i]=mean(f[1:2,3:4])
 }
mean(xy.boot)
sd(xy.boot)
```

```
trop.temp.midmio<-xy.boot
mean(trop.temp.midmio)

#Acre-Urumaco, tropical late miocene
Acre.gen<-read.csv("Acre-ranges.csv")
str(Acre.gen)
Acre.gen$Fauna<-rep("Acre",53)
Urumaco.gen<-read.csv("Urumaco-ranges.csv",sep=";")
str(Urumaco.gen)
Urumaco.gen$Fauna<-rep("Urumaco", 14)
nrand<-1000
xy.boot =numeric(nrand)
for(i in 1:nrand){
gen<-as.vector(sample(Acre.gen$genus,14, replace=TRUE))
name<-rep("Acre",14)
t<-as.data.frame(cbind(gen,name))
gen<-as.vector(Urumaco.gen$genus)
name<-rep("Urumaco",14)
p<-as.data.frame(cbind(gen,name))
q<-rbind(t,p)
tab<-table(q$name,q$gen)
xy.boot[i]=vegdist(tab, method="bray", binary=TRUE)
}
mean(xy.boot)
sd(xy.boot)
Acr.Uru<-xy.boot
mean(Acr.Uru)

#temperate late miocene -Mesopotamian, Chiquimil,Andalhuala,Cerro Azul,Monte Hermoso
Mesopotamia.gen<-read.csv("Mesopotamian-ranges.csv")
str(Mesopotamia.gen)
Mesopotamia.gen$Fauna<-rep("Mesopotamian", 91)
Chiquimil.gen<-read.csv("Chiquimil-ranges.csv")
str(Chiquimil.gen)
Chiquimil.gen$Fauna<-rep("Chiquimil", 26)
Andalhuala.gen<-read.csv("Andalhuala-ranges.csv")
str(Andalhuala.gen)
Andalhuala.gen$Fauna<-rep("Andalhuala", 36)
CerroAzul.gen<-read.csv("CerroAzul-ranges.csv")
str(CerroAzul.gen)
```

```
CerroAzul.gen$Fauna<-rep("Cerro Azul", 44)
MonteHermoso.gen<-read.csv(„MonteHermoso-ranges.csv")
str(MonteHermoso.gen)
MonteHermoso.gen$Fauna<-rep(„Monte Hermoso", 64)

nrand<-1000
xy.boot =numeric(nrand)
for(i in 1:nrand){
gen<-as.vector(sample(Mesopotamia.gen$genus,26, replace=TRUE))
name<-rep("Mesopotamian",26)
t<-as.data.frame(cbind(gen,name))
gen<-as.vector(sample(Andalhuala.gen$genus,26,replace=TRUE))
name<-rep("Andalhuala",26)
p<-as.data.frame(cbind(gen,name))
gen<-as.vector(sample(CerroAzul.gen$genus,26, replace=TRUE))
name<-rep("CerroAzul",26)
o<-as.data.frame(cbind(gen,name))
gen<-as.vector(sample(MonteHermoso.gen$genus,26, replace=TRUE))
name<-rep("MonteHermoso",26)
s<-as.data.frame(cbind(gen,name))
gen<-as.vector(Chiquimil.gen$genus)
name<-rep("Chiquimil",26)
r<-as.data.frame(cbind(gen,name))
q<-rbind(t,p,o,s,r)
tab<-table(q$name,q$gen)
xy.boot[i]=vegdist(tab, method="bray", binary=TRUE)
}
mean(xy.boot)
sd(xy.boot)
te.lat.mio<-xy.boot
mean(te.lat.mio)

#All late miocene trop vs temp
nrand<-1000
xy.boot =numeric(nrand)
for(i in 1:nrand){
gen<-as.vector(sample(Mesopotamia.gen$genus,14, replace=TRUE))
name<-rep("Mesopotamian",14)
t<-as.data.frame(cbind(gen,name))
gen<-as.vector(sample(Andalhuala.gen$genus,14,replace=TRUE))
```

```
name<-rep("Andalhuala",14)
p<-as.data.frame(cbind(gen,name))
gen<-as.vector(sample(CerroAzul.gen$genus,14, replace=TRUE))
name<-rep("CerroAzul",14)
o<-as.data.frame(cbind(gen,name))
gen<-as.vector(sample(MonteHermoso.gen$genus,14, replace=TRUE))
name<-rep("MonteHermoso",14)
s<-as.data.frame(cbind(gen,name))
gen<-as.vector(sample(Chiquimil.gen$genus,14,replace=TRUE))
name<-rep("Chiquimil",14)
r<-as.data.frame(cbind(gen,name))
gen<-as.vector(sample(Acre.gen$genus,14, replace=TRUE))
name<-rep("Acre",14)
w<-as.data.frame(cbind(gen,name))
gen<-as.vector(Urumaco.gen$genus)
name<-rep("Urumaco",14)
z<-as.data.frame(cbind(gen,name))
q<-rbind(t,p,o,s,r,w,z)
tab<-table(q$name,q$gen)
f<-as.matrix(vegdist(tab, method="bray", binary=TRUE))
xy.boot[i]= mean(f[1:5,6:7])
}
mean(xy.boot)
sd(xy.boot)
lat.mio<-xy.boot
mean(lat.mio)

#Mann U test for the dissimilarity values of the tropical and temperate  middle and late Miocene faunas
wilcox.test(Lv.Fitz,trop.temp.midmio)
wilcox.test(Col.Qh, trop.temp.midmio)
wilcox.test(Acr.Uru,lat.mio)
wilcox.test(te.lat.mio,lat.mio)

# Analysis of cumulative first appearance (FAD) during the GABI in tropics vs temperate – Data for figure 6A
# Load First appearance data from Supplementary Table  2
all.fad<-read.csv(Supplementary_Table2)
#Separate tropical and temperate fad
trop.fad<-subset(all.fad, paleolatdec<=23 & paleolatdec>= -23)
str(trop.fad)
plot(trop.fad$ma_mid, trop.fad$paleolatdec)
```

```
temp.fad<-subset(all.fad, paleolatdec< -23 | paleolatdec> 23)
str(temp.fad)
plot(temp.fad$ma_mid, temp.fad$paleolatdec)

# Generate the resampling of the age of each fad record given their estimated age range (max and min age)
# The function for the loop
fun1<-function(df,i,N){runif(N,min=df$ma_min[i], max=df$ma_max[i])}
trop.resam<-foreach(i= 1:67)%do% fun1(trop.fad,i,1000)

# For the tropics
trop.fad$mean.resample<-as.numeric(foreach(i= 1:67)%do%
mean(fun1(trop.fad,i,1000)))
trop.fad$sd.resample<-as.numeric(foreach(i= 1:67)%do%
sd(fun1(trop.fad,i,1000)))

#Calculate the mean and standard deviation (sd) for the fad in the tropics
str(trop.fad)
tropics.mean<-trop.fad$mean.resample
tropics.sd1<-(trop.fad$mean.resample+trop.fad$sd.resample)
tropics.sd2<-(trop.fad$mean.resample - trop.fad$sd.resample)

tropics.meancut<-cut(tropics.mean,breaks, right=TRUE)
tropics.meanfreq<-table(tropics.meancut)
tropics.sd1cut<-cut(tropics.sd1,breaks, right=TRUE)
tropics.sd1freq<-table(tropics.sd1cut)
tropics.sd2cut<-cut(tropics.sd2,breaks, right=TRUE)
tropics.sd2freq<-table(tropics.sd2cut)

trop.meancumfreq<-c(0,cumsum(rev(tropics.meanfreq)))
trop.sd1cumfreq<-c(0,cumsum(rev(tropics.sd1freq)))
trop.sd2cumfreq<-c(0,cumsum(rev(tropics.sd2freq)))

#For temperate fad
temp.fad$mean.resample<-as.numeric(foreach(i= 1:52)%do%
mean(fun1(temp.fad,i,1000)))
temp.fad$sd.resample<-as.numeric(foreach(i= 1:52)%do%
sd(fun1(temp.fad,i,1000)))
#Calculate mean and standard deviation sd for the fad in temperate
str(temp.fad)
temp.mean<-temp.fad$mean.resample
```

```
temp.sd1<-(temp.fad$mean.resample+temp.fad$sd.resample)
temp.sd2<-(temp.fad$mean.resample - temp.fad$sd.resample)

breaks2<-seq(15,0,by= -1)
temp.meancut<-cut(temp.mean,breaks2, right=TRUE)
temp.meanfreq<-table(temp.meancut)
temp.sd1cut<-cut(temp.sd1,breaks2, right=TRUE)
temp.sd1freq<-table(temp.sd1cut)
temp.sd2cut<-cut(temp.sd2,breaks2, right=TRUE)
temp.sd2freq<-table(temp.sd2cut)

temp.meancumfreq<-c(0,cumsum(rev(temp.meanfreq)))
temp.sd1cumfreq<-c(0,cumsum(rev(temp.sd1freq)))
temp.sd2cumfreq<-c(0,cumsum(rev(temp.sd2freq)))
# Plot for the fad during GABI shown in Figure 6A
plot(breaks,trop.meancumfreq, xlim=c(12,0), type="b", col="red", pch=16,
xlab="Time (ma)", ylab= "Cumulative FAD", ylim=c(0,100))
segments(breaks,trop.meancumfreq,breaks,trop.sd1cumfreq,col="red",lty=2)
segments(breaks,trop.meancumfreq,breaks,trop.sd2cumfreq,col="red",lty=2)
points(breaks,temp.meancumfreq, type="b", col="blue", pch=16)
segments(breaks,temp.meancumfreq,breaks,temp.sd1cumfreq,col="blue",lty=2)
segments(breaks,temp.meancumfreq,breaks,temp.sd2cumfreq,col="blue",lty=2)
```

Supplementary Table 1. Matrix used to calculate de Bray-Curtis dissimilarity index among the different assemblages analysed; 0 = absent, 1 = present.

Assemblage	*Abothrodon*	*Acrecebus*	*Amahuacatherium*	*Anadasypus*	*Asterostemma*
Acre	1	1	1	1	1
Andalhuala	0	0	0	0	0
Cerro Azul	0	0	0	0	0
Chiquimil	0	0	0	0	0
Collon Cura	0	0	0	0	0
Fitzcarrald	0	0	0	0	0
Inchasi	0	0	0	0	0
La Venta	0	0	0	1	0
Mesopotamian	0	0	0	0	0
Monte Hermoso	0	0	0	0	0
Quebrada Honda	0	0	0	0	0
Uquia Lower	0	0	0	0	0
Uquia Middle	0	0	0	0	0
Urumaco	0	0	0	0	0

Cardiatherium	*Cullinia*	*Didelphis*	*Eumegamys*	*Gyriabrus*	*Gyrinodon*	*Hapalops*	*Kraglievichia*
1	1	1	1	1	1	1	1
0	0	0	0	0	0	0	0
0	0	0	0	0	0	0	0
0	0	0	0	1	0	0	0
0	0	0	0	0	0	0	0
0	0	0	0	0	0	0	0
0	0	0	0	0	0	0	0
0	0	0	0	0	0	0	0
1	1	0	1	1	0	0	1
0	0	0	0	0	0	0	0
0	0	0	0	0	0	1	0
0	0	0	0	0	0	0	0
0	0	0	0	0	0	0	0
1	0	0	1	0	1	0	0

Lutreolina	*Mesenodon*	*Mesotoxodon*	*Minitoxodon*	*Neoepiblema*	*Neoglyptatelus*	*Neotoxodon*
1	1	1	1	1	1	1
1	0	0	0	0	0	0
1	0	0	0	0	0	0
0	0	0	0	0	0	0
0	0	0	0	0	0	0
0	0	0	0	1	1	0
0	0	0	0	0	0	0
0	0	0	0	0	1	0
0	0	0	0	1	0	0
1	0	0	0	0	0	0
0	0	0	0	0	0	0
0	0	0	0	0	0	0
0	0	0	0	0	0	0
0	0	0	0	0	0	0

Neotrigodon	*Noctilio*	*Octodontobradys*	*Palaeotoxodon*	*Paraglyptodon*	*Paratrigodon*	*Phoberomys*
1	1	1	1	1	1	1
0	0	0	0	0	0	0
0	0	0	0	0	0	0
0	0	0	0	0	0	0
0	0	0	0	0	0	0
0	0	0	0	0	0	0
0	0	0	0	1	0	0
0	1	0	0	0	0	0
0	0	0	1	0	0	1
0	0	0	0	0	0	0
0	0	0	0	0	1	0
0	0	0	0	1	0	0
0	0	0	0	1	0	0
0	0	0	0	0	0	1

Planops	*Plesiotoxodon*	*Pliomorphus*	*Plohophorus*	*Potamarchus*	*Proterotherium*	*Protomegalonyx*
1	1	1	1	1	1	1
0	0	0	0	0	0	0
0	0	0	1	0	0	0
0	0	0	0	1	0	0
1	0	0	0	0	0	0
0	0	0	0	1	0	0
0	0	0	1	0	0	0
0	0	0	0	0	0	0
0	0	1	1	1	1	1
0	0	0	1	0	0	0
0	0	0	0	0	0	0
0	0	0	0	0	0	0
0	0	0	0	0	0	0
0	0	0	0	1	0	0

Pseudoprepotherium	*Purperia*	*Ranculcus*	*Scirrotherium*	*Scleromys*	*Simplimus*	*Solimoea*
1	1	1	1	1	1	1
0	0	0	0	0	0	0
0	0	0	0	0	0	0
0	0	0	0	0	0	0
0	0	0	0	0	0	0
0	0	0	0	0	0	0
0	0	0	0	0	0	0
1	0	0	1	0	0	0
0	0	1	1	0	0	0
0	0	0	0	0	0	0
0	0	0	0	0	0	0
0	0	0	0	0	0	0
0	0	0	0	0	0	0
0	0	0	0	0	0	0

Stenodon	*Stirtonia*	*Surameryx*	*Sylvochoerus*	*Telicomys*	*Tetrastylus*	*Toxodontherium*	*Trigodon*
1	1	1	1	1	1	1	1
0	0	0	0	0	1	1	0
0	0	0	0	0	1	0	0
0	0	0	0	0	1	1	0
0	0	0	0	0	0	0	0
0	0	0	0	0	0	0	0
0	0	0	0	0	0	0	0
0	1	0	0	0	0	0	0
0	0	0	0	0	1	1	0
0	0	0	0	1	0	0	1
0	0	0	0	0	0	0	0
0	0	0	0	0	0	0	0
0	0	0	0	0	0	0	0
0	0	0	0	0	1	0	0

Trigodonops	*Urumacotherium*	*Waldochoerus*	*Xenastrapotherium*	*Aspidocalyptus*	*Borhyaenidium*
1	1	1	1	0	0
0	0	0	0	0	0
0	0	0	0	1	1
0	0	0	0	0	0
0	0	0	0	0	0
0	1	0	1	0	0
0	0	0	0	0	0
0	0	0	1	0	0
0	0	0	0	0	0
0	0	0	0	0	0
0	0	0	0	0	0
0	0	0	0	0	0
0	1	0	0	0	0

Cardiomys	*Chasichimys*	*Chasicotatus*	*Chorobates*	*Clyomys*	*Coscinocercus*	*Cyonasua*
0	0	0	0	0	0	0
1	0	1	1	0	0	1
1	1	1	1	1	1	1
1	0	1	1	0	0	0
0	0	0	0	0	0	0
0	0	0	0	0	0	0
0	0	0	0	0	0	0
0	0	0	0	0	0	0
1	0	1	0	0	0	1
1	0	0	1	0	0	1
0	0	0	0	0	0	0
0	0	0	0	0	0	0
0	0	0	0	0	0	0
0	0	0	0	0	0	0

Doellotatus	*Elassotherium*	*Eoauchenia*	*Eosclerocalyptus*	*Epecuenia*	*Eumysops*
0	0	0	0	0	0
0	0	0	1	0	0
1	1	1	1	1	1
0	0	0	1	0	0
0	0	0	0	0	0
0	0	0	0	0	0
0	0	0	0	0	0
0	0	0	0	0	0
0	0	0	0	0	1
1	0	1	1	0	1
0	0	0	0	0	0
1	0	0	0	0	0
0	0	0	0	0	0
0	0	0	0	0	0

Hemihegetotherium	*Hyperdidelphys*	*Lagostomus*	*Macrauchenia*	*Macrochorobates*
0	0	0	0	0
1	1	0	0	1
1	1	1	1	1
0	0	0	0	1
0	0	0	0	0
0	0	0	0	0
0	0	0	0	0
0	0	0	0	0
0	0	1	0	0
0	1	1	0	1
1	0	0	0	0
0	0	0	0	0
0	0	0	0	0
0	0	0	0	0

Macroeuphractus	*Microtragulus*	*Neophanomys*	*Orthomyctera*	*Paedotherium*	*Palaeocavia*
0	0	0	0	0	0
0	1	1	1	0	1
1	1	1	1	1	1
0	0	0	1	1	0
0	0	0	0	0	0
0	0	0	0	0	0
0	0	0	0	0	0
0	0	0	0	0	0
1	0	0	0	0	1
1	1	1	1	1	1
0	0	0	0	0	0
0	0	0	0	0	0
0	0	0	0	0	0
0	0	0	0	0	0

Palaeoctodon	*Paleuphractus*	*Phtoramys*	*Pisanodon*	*Pithanotomys*	*Plesiomegatherium*	*Pliolestes*
0	0	0	0	0	0	0
0	0	0	0	1	0	0
1	1	1	1	1	1	1
0	1	0	0	0	0	0
0	0	0	0	0	0	0
0	0	0	0	0	0	0
0	0	0	0	0	0	0
0	0	0	0	0	0	0
0	0	0	0	0	0	0
0	0	1	0	1	0	0
0	0	0	0	0	0	0
0	0	0	0	0	0	0
0	0	0	0	0	0	0
0	0	0	0	0	0	0

Proeuphractus	*Promacrauchenia*	*Pseudotypotherium*	*Thylacosmilus*	*Thylamys*	*Thylatheridium*
0	0	0	0	0	0
0	1	0	1	0	0
1	1	1	1	1	1
0	0	0	0	0	0
0	0	0	0	0	0
0	0	0	0	0	0
0	1	0	0	0	0
0	0	0	0	1	0
1	1	0	1	0	0
0	1	1	1	1	1
0	0	0	0	0	0
0	0	0	0	0	0
0	0	0	0	0	0
0	0	0	0	0	0

Xenodontomys	*Zygolestes*	*Acarechimys*	*Boreostemma*	*Drytomomys*	*Granastrapotherium*
0	0	0	0	0	0
0	0	0	0	0	0
1	1	0	0	0	0
0	0	0	0	0	0
0	0	1	0	0	0
0	0	1	1	1	1
0	0	0	0	0	0
0	0	0	1	0	1
0	1	0	0	1	0
0	0	0	0	0	0
0	0	1	0	0	0
0	0	0	0	0	0
0	0	0	0	0	0
0	0	0	0	0	0

Megathericulus	*Miocochilius*	*Parapropalaehoplophorus*	*Pericotoxodon*	*Prodolichotis*	*Scleromys*
0	0	0	0	0	0
0	0	0	0	1	0
0	0	0	0	0	0
0	0	0	0	0	0
1	0	0	0	0	1
1	1	1	1	1	1
0	0	0	0	0	0
0	0	0	1	1	1
0	0	0	0	1	0
0	0	0	0	1	0
0	1	0	0	0	0
0	0	0	0	0	0
0	0	0	0	0	0
0	0	0	0	0	0

Tetramerorhinus	*Theosodon*	*Aotus*	*Eodolichotis*	*Eumops*	*Glossotheriopsis*	*Hondathentes*
0	0	0	0	0	0	0
0	0	0	0	0	0	0
0	0	0	0	0	0	0
0	0	0	0	0	0	0
0	1	0	0	0	0	0
1	1	0	0	0	0	0
0	0	0	0	0	0	0
0	1	1	1	1	1	1
0	0	0	0	0	0	0
0	0	0	0	0	0	0
0	0	0	0	0	0	0
0	0	0	0	0	0	0
0	0	0	0	0	0	0
0	0	0	0	0	0	0

Huilatherium	*Kiotomops*	*Lagonimico*	*Marmosa*	*Micodon*	*Microscleromys*	*Microsteiromys*
0	0	0	0	0	0	0
0	0	0	0	0	0	0
0	0	0	0	0	0	0
0	0	0	0	0	0	0
0	0	0	0	0	0	0
0	0	0	0	0	0	0
0	0	0	0	0	0	0
1	1	1	1	1	1	1
0	0	0	0	0	0	0
0	0	0	0	0	0	0
0	0	0	0	0	0	0
0	0	0	0	0	0	0
0	0	0	0	0	0	0

Miocallicebus	*Nanoastegotherium*	*Neonematherium*	*Neosaimiri*	*Notonycteris*	*Nuciruptor*
0	0	0	0	0	0
0	0	0	0	0	0
0	0	0	0	0	0
0	0	0	0	0	0
0	0	0	0	0	0
0	0	0	0	0	0
0	0	0	0	0	0
1	1	1	1	1	1
0	0	0	0	0	0
0	0	0	0	0	0
0	0	0	0	0	0
0	0	0	0	0	0
0	0	0	0	0	0
0	0	0	0	0	0

Olenopsis	*Pachybiotherium*	*Palynephyllum*	*Patasola*	*Pedrolypeutes*	*Potamops*	*Prolicaphrium*
0	0	0	0	0	0	0
0	0	0	0	0	0	0
0	0	0	0	0	0	0
0	0	0	0	0	0	0
0	0	0	0	0	0	0
0	0	0	0	0	0	0
0	0	0	0	0	0	0
1	1	1	1	1	1	1
0	0	0	0	0	0	0
0	0	0	0	0	0	0
0	0	0	0	0	0	0
0	0	0	0	0	0	0
0	0	0	0	0	0	0
1	0	0	0	0	0	0

Rhodanodolichotis	*Ricardomys*	*Thyroptera*	*Amphiocnus*	*Berthawyleria*	*Borhyaena*
0	0	0	0	0	0
0	0	0	0	0	0
0	0	0	0	0	0
0	0	0	0	0	0
0	0	0	0	0	0
0	0	0	0	0	0
0	0	0	0	0	0
1	1	1	0	0	0
0	0	0	1	1	1
0	0	0	0	0	0
0	0	0	0	0	0
0	0	0	0	0	0
0	0	0	0	0	0
0	0	0	0	0	0

Brachytherium	*Carlesia*	*Caviodon*	*Chironectes*	*Chlamyphractus*	*Comaphorus*	*Dasypus*
0	0	0	0	0	0	0
0	0	0	0	0	0	0
0	0	0	0	0	0	0
0	0	0	0	0	0	0
0	0	0	0	0	0	0
0	0	0	0	0	0	0
0	0	1	0	0	0	0
0	0	0	0	0	0	0
1	1	1	1	1	1	1
0	0	1	0	0	0	0
0	0	0	0	0	0	0
0	0	0	0	0	0	0
0	0	0	0	0	0	0
0	0	0	0	0	0	0

Diadiaphorus	*Dilobodon*	*Dinotoxodon*	*Eleutherocercus*	*Eomegatherium*	*Eumegamysops*
0	0	0	0	0	0
0	0	0	0	0	0
0	0	0	0	0	0
1	0	0	0	0	0
0	0	0	0	0	0
0	0	0	0	0	0
0	0	0	0	0	0
0	0	0	0	0	0
1	1	1	1	1	1
0	0	0	1	0	0
0	0	0	0	0	0
0	0	0	0	0	0
0	0	0	0	0	0
0	0	0	0	0	0

Eutemnodus	*Eutomodus*	*Eutypotherium*	*Haplodontherium*	*Haplostropha*	*Hoplophorus*
0	0	0	0	0	0
0	0	0	0	0	0
0	0	0	0	0	0
0	0	0	0	0	0
0	0	0	0	0	0
0	0	0	0	0	0
0	0	0	0	0	0
0	0	0	0	0	0
1	1	1	1	1	1
0	0	0	0	0	0
0	0	0	0	0	0
0	0	0	0	0	0
0	0	0	0	0	0
0	0	0	0	0	0

Isostylomys	*Megabradys*	*Megalonychops*	*Munizia*	*Myocastor*	*Neobrachytherium*	*Neohapalops*
0	0	0	0	0	0	0
0	0	0	0	0	1	0
0	0	0	0	0	0	0
0	0	0	0	0	0	0
0	0	0	0	0	0	0
0	0	0	0	0	0	0
0	0	0	0	0	0	0
0	0	0	0	0	0	0
1	1	1	1	1	1	1
0	0	0	0	0	0	0
0	0	0	0	0	0	0
0	0	0	0	0	0	0
0	0	0	0	0	0	0
0	0	0	0	0	0	0

Noticitis	*Octomylodon*	*Ortotherium*	*Oxyodontherium*	*Pachynodon*	*Palaeohoplophorus*
0	0	0	0	0	0
0	0	0	0	0	0
0	0	0	0	0	0
0	0	0	0	0	0
0	0	0	0	0	0
0	0	0	0	0	0
0	0	0	0	0	0
0	0	0	0	0	0
1	1	1	1	1	1
0	0	0	0	0	0
0	0	0	0	0	0
0	0	0	0	0	0
0	0	0	0	0	0
0	0	0	0	0	0

Paradoxomys	*Parahoplophorus*	*Paranabradys*	*Paranamys*	*Paranauchenia*	*Parodimys*
0	0	0	0	0	0
0	0	0	0	0	0
0	0	0	0	0	0
0	0	0	1	0	0
0	0	0	0	0	0
0	0	0	0	0	0
0	0	0	0	0	0
0	0	0	0	0	0
1	1	1	1	1	1
0	0	0	0	0	0
0	0	0	0	0	0
0	0	0	0	0	0
0	0	0	0	0	0
0	0	0	0	0	0

Philander	*Pliodolichotis*	*Pliomegatherium*	*Promegatherium*	*Promylodon*	*Pronothrotherium*
0	0	0	0	0	0
0	0	0	0	0	1
0	0	0	0	0	0
0	0	0	0	0	0
0	0	0	0	0	0
0	0	0	0	0	0
0	0	0	0	0	0
0	0	0	0	0	0
1	1	1	1	1	1
0	0	0	0	0	0
0	0	0	0	0	0
0	0	0	0	0	0
0	0	0	0	0	0
0	0	0	0	0	0

Protabrocoma	*Protoglyptodon*	*Protypotherium*	*Pseudoeuryurus*	*Pyramiodontherium*
0	0	0	0	0
1	0	0	0	1
0	0	0	0	0
1	0	0	0	0
0	0	1	0	0
0	0	0	0	0
0	0	0	0	0
0	0	0	0	0
1	1	1	1	1
0	0	0	0	0
0	0	0	0	0
0	0	0	0	0
0	0	0	0	1
0	0	0	0	0

Scalabrinitherium	*Sphenotherus*	*Stenotephanos*	*Strabosodon*	*Strophostephanos*	*Stylocynus*
0	0	0	0	0	0
0	1	0	0	0	0
0	0	0	0	0	0
0	0	0	0	0	0
0	0	0	0	0	0
0	0	0	0	0	0
0	0	0	0	0	0
0	0	0	0	0	0
1	1	1	1	1	1
0	0	0	0	0	0
0	0	0	0	0	0
0	0	0	0	0	0
0	0	0	0	0	0
0	0	0	0	0	0

Torcellia	*Urotherium*	*Xotodon*	*Acyon*	*Guiomys*	*Hiskatherium*	*Hondalagus*	*Mesoprocta*
0	0	0	0	0	0	0	0
0	1	1	0	0	0	0	0
0	0	0	0	0	0	0	0
0	0	1	0	0	0	0	0
0	0	0	0	0	0	0	0
0	0	0	0	0	0	0	0
0	0	0	0	0	0	0	0
0	0	0	0	0	0	0	0
1	1	1	0	0	0	0	0
0	0	1	0	0	0	0	0
0	0	0	1	1	1	1	1
0	0	0	0	0	0	0	0
0	1	0	0	0	0	0	0
0	0	0	0	0	0	0	0

Plesiotypotherium	*Prolagostomus*	*Prozaedyus*	*Quebradahondomys*	*Bolivartherium*	*Bounodus*
0	0	0	0	0	0
0	0	0	0	0	0
0	0	0	0	0	0
0	0	0	0	0	0
0	1	0	0	0	0
0	0	0	0	0	0
0	0	0	0	0	0
0	0	0	0	0	0
0	0	0	0	0	0
0	0	0	0	0	0
0	0	0	0	0	0
1	1	1	1	0	0
0	0	0	0	0	0
0	0	0	0	0	0
0	0	0	0	1	1

Lestodon	*Mirandabradys*	*Ocnerotherium*	*Urumaquia*	*Actenomys*	*Alitoxodon*	*Argyrolagus*
0	0	0	0	0	0	0
0	0	0	0	0	0	0
0	0	0	0	0	0	0
0	0	0	0	0	0	0
0	0	0	0	0	0	0
0	0	0	0	0	0	0
0	0	0	0	0	0	0
0	0	0	0	0	0	0
0	0	0	0	0	0	0
1	0	0	0	1	1	1
0	0	0	0	0	0	0
0	0	0	0	0	0	0
1	0	0	0	0	0	0
1	1	1	1	0	0	0

Auliscomys	*Diheterocnus*	*Diplasiotherium*	*Epitherium*	*Eucelophorus*	*Holozaedyus*	*Microcavia*
0	0	0	0	0	0	0
0	0	0	0	0	0	0
0	0	0	0	0	0	0
0	0	0	0	0	0	0
0	0	0	0	0	0	0
0	0	0	0	0	0	0
0	0	0	0	0	0	0
0	0	0	0	0	0	0
0	0	0	0	0	0	0
1	1	1	1	1	1	1
0	0	0	0	0	0	0
0	0	0	0	0	0	1
0	0	0	0	0	0	0
0	0	0	0	0	0	0

Myrmecophaga	*Necromys*	*Neocavia*	*Neopachtus*	*Notocynus*	*Palaeodaedicurus*	*Pampatherium*
0	0	0	0	0	0	0
0	0	0	0	0	0	0
0	0	0	0	0	0	0
0	0	0	0	0	0	0
0	0	0	0	0	0	0
0	0	0	0	0	0	0
0	0	0	0	0	0	0
0	0	0	0	0	0	0
0	0	0	0	0	0	0
1	1	1	1	1	1	1
0	0	0	0	0	0	0
0	0	0	0	0	0	0
0	0	0	0	0	0	0
0	0	0	0	0	0	0

Parahyaenodon	*Paramyocastor*	*Phugatherium*	*Phyctaenopyga*	*Plaina*	*Plohophoroides*
0	0	0	0	0	0
0	0	0	0	0	0
0	0	0	0	0	0
0	0	0	0	0	0
0	0	0	0	0	0
0	0	0	0	0	0
0	0	1	0	0	0
0	0	0	0	0	0
0	0	0	0	0	0
1	1	1	1	1	1
0	0	0	0	0	0
0	0	0	0	0	0
0	0	0	0	0	0
0	0	0	0	0	0

Parahyaenodon	*Paramyocastor*	*Phugatherium*	*Phyctaenopyga*	*Plaina*	*Plohophoroides*
0	0	0	0	0	0
0	0	0	0	0	0
0	0	0	0	0	0
0	0	0	0	0	0
0	0	0	0	0	0
0	0	0	0	0	0
0	0	1	0	0	0
0	0	0	0	0	0
0	0	0	0	0	0
1	1	1	1	1	1
0	0	0	0	0	0
0	0	0	0	0	0
0	0	0	0	0	0
0	0	0	0	0	0

Proscelidodon	*Pseudoplataeomys*	*Reithrodon*	*Ringueletia*	*Sparassocynus*	*Thylaohorops*
0	0	0	0	0	0
0	0	0	0	0	0
0	0	0	0	0	0
1	0	0	0	0	0
0	0	0	0	0	0
0	0	0	0	0	0
1	0	0	0	0	0
0	0	0	0	0	0
0	0	0	0	0	0
1	1	1	1	1	1
0	0	0	0	0	0
0	0	0	0	0	0
0	0	0	0	0	0
0	0	0	0	0	0

Toxodon	*Trachycalyptus*	*Tremacyllus*	*Glossotherium*	*Hypsitherium*	*Posnanskytherium*	*Vassallia*
0	0	0	0	0	0	0
0	0	0	0	0	0	0
0	0	0	0	0	0	0
0	0	1	0	0	0	1
0	0	0	0	0	0	0
0	0	0	0	0	0	0
0	0	0	1	1	1	1
0	0	0	0	0	0	0
0	0	0	0	0	0	0
1	1	1	0	0	0	0
0	0	0	0	0	0	0
0	0	0	0	0	0	1
0	0	0	0	0	0	0
0	0	0	0	0	0	0

Chaetophractus	*Ctenomys*	*Erethizon*	*Hippidion*	*Hydrochoeropsis*	*Megatherium*	*Panochthus*
0	0	0	0	0	0	0
0	0	0	0	0	0	0
0	0	0	0	0	0	0
0	0	0	0	0	0	0
0	0	0	0	0	0	0
0	0	0	0	0	0	0
0	0	0	0	0	0	0
0	0	0	0	0	0	0
0	0	0	0	0	0	0
0	0	0	0	0	0	0
0	0	0	0	0	0	0
0	0	0	0	0	0	0
0	1	0	0	0	0	0
1	1	1	1	1	1	1
0	0	0	0	0	0	0

Platygonu	*Windhausenia*	*Xiphuroides*	*Scelidotheridium*	*Chapalmalania*	*Glyptodontidium*
0	0	0	0	0	0
0	0	0	0	1	1
0	0	0	0	0	0
0	0	0	0	0	0
0	0	0	0	0	0
0	0	0	0	0	0
0	0	0	0	0	0
0	0	0	0	0	0
0	0	0	0	0	0
0	0	0	0	0	0
0	0	0	0	0	0
0	0	0	0	0	0
0	0	0	1	0	0
1	1	1	0	0	0
0	0	0	0	0	0

Hesperocynus	*Lagostomopsis*	*Macroeucphractus*	*Paraeuphractus*	*Phlyctaenopyga*	*Stromaphorus*
0	0	0	0	0	0
1	1	1	1	1	1
0	0	0	0	0	0
0	1	0	1	0	1
0	0	0	0	0	0
0	0	0	0	0	0
0	0	0	0	0	0
0	0	0	0	0	0
0	0	0	0	0	0
0	0	0	0	0	0
0	0	0	0	0	0
0	0	0	0	0	0
0	0	0	0	0	0

Treamcyllus	*Typotheriopsis*	*Nephanomys*	*Pseudohegetotherium*	*Vetelia*	*Abderites*	*Acdestis*
0	0	0	0	0	0	0
1	1	0	0	0	0	0
0	0	0	0	0	0	0
0	1	1	1	1	0	0
0	0	0	0	1	1	1
0	0	0	0	0	0	0
0	0	0	0	0	0	0
0	0	0	0	0	0	0
0	0	0	0	0	0	0
0	0	0	0	0	0	0
0	0	0	0	0	0	0
0	0	0	0	0	0	0
0	0	0	0	0	0	0
0	0	0	0	0	0	0

Alloiomys	*Amphibradys*	*Anisolophus*	*Arctodictis*	*Branisamyopsis*	*Diellipsodon*	*Eocardia*
0	0	0	0	0	0	0
0	0	0	0	0	0	0
0	0	0	0	0	0	0
0	0	0	0	0	0	0
1	1	1	1	1	1	1
0	0	0	0	0	0	0
0	0	0	0	0	0	0
0	0	0	0	0	0	0
0	0	0	0	0	0	0
0	0	0	0	0	0	0
0	0	0	0	0	0	0
0	0	0	0	0	0	0
0	0	0	0	0	0	0
0	0	0	0	0	0	0

Eonaucum	*Epipatriarchus*	*Eucholaeops*	*Eucinepeltus*	*Eutrachytherus*	*Galileomys*
0	0	0	0	0	0
0	0	0	0	0	0
0	0	0	0	0	0
0	0	0	0	0	0
1	1	1	1	1	1
0	0	0	0	0	0
0	0	0	0	0	0
0	0	0	0	0	0
0	0	0	0	0	0
0	0	0	0	0	0
0	0	0	0	0	0
0	0	0	0	0	0
0	0	0	0	0	0
0	0	0	0	0	0

Glossoptheriopsis	*Hegetotherium*	*Homalodotherium*	*Hyperoxotodon*	*Icochilus*	*Interatherium*
0	0	0	0	0	0
0	0	0	0	0	0
0	0	0	0	0	0
0	0	0	0	0	0
1	1	1	1	1	1
0	0	0	0	0	0
0	0	0	0	0	0
0	0	0	0	0	0
0	0	0	0	0	0
0	0	0	0	0	0
0	0	0	0	0	0
0	0	0	0	0	0
0	0	0	0	0	0
0	0	0	0	0	0

Maruchito	*Massoiamys*	*Megastus*	*Neoreomys*	*Neosteiromys*	*Nesciotherium*	*Nesodon*
0	0	0	0	0	0	0
0	0	0	0	0	0	0
0	0	0	0	0	0	0
0	0	0	0	0	0	0
1	1	1	1	1	1	1
0	0	0	0	0	0	0
0	0	0	0	0	0	0
0	0	0	0	0	0	0
0	0	0	0	0	0	0
0	0	0	0	0	0	0
0	0	0	0	0	0	0
0	0	0	0	0	0	0
0	0	0	0	0	0	0
0	0	0	0	0	0	0

Pachyrukhos	*Palyeidodon*	*Patagosmilus*	*Pitheculites*	*Pliolagostomus*	*Prepotherium*	*Proeutatus*
0	0	0	0	0	0	0
0	0	0	0	0	0	0
0	0	0	0	0	0	0
0	0	0	0	0	0	0
1	1	1	1	1	1	1
0	0	0	0	0	0	0
0	0	0	0	0	0	0
0	0	0	0	0	0	0
0	0	0	0	0	0	0
0	0	0	0	0	0	0
0	0	0	0	0	0	0
0	0	0	0	0	0	0
0	0	0	0	0	0	0
0	0	0	0	0	0	0

Propithecia	*Protacaremys*	*Prothylacynus*	*Prototrigodon*	*Prozaedius*	*Pseudonotictis*
0	0	0	0	0	0
0	0	0	0	0	0
0	0	0	0	0	0
0	0	0	0	0	0
1	1	1	1	1	1
0	0	0	0	0	0
0	0	0	0	0	0
0	0	0	0	0	0
0	0	0	0	0	0
0	0	0	0	0	0
0	0	0	0	0	0
0	0	0	0	0	0
0	0	0	0	0	0
0	0	0	0	0	0

Pseuhapalops	*Steiromys*	*Stenotatus*	*Stereotoxodon*	*Stilotherium*
0	0	0	0	0
0	0	0	0	0
0	0	0	0	0
0	0	0	0	0
1	1	1	1	1
0	0	0	0	0
0	0	0	0	0
0	0	0	0	0
0	0	0	0	0
0	0	0	0	0
0	0	0	0	0
0	0	0	0	0
0	0	0	0	0
0	0	0	0	0

Supplementary Table 2. First appearance datum (FAD) of GABI participants in North and South America, data from the PBDB.

collection_no	collection.authorizer	order_name	family_name	occurrence.genus_name	occurrence.reference_no	collection.reference_no	collection_name	country	latdec	lngdec	paleolatdec	paleolngdec	epoch	ma_max	ma_min	ma_mid
18036	J. Alroy	Xenarthra	Megalonychidae	Megalonyx	6209	6209	Axtel	United States	35	-101.9	35.3	-100		10.3	4.9	7.6
18560	J. Alroy	Xenarthra	Mylodontidae	Thinobadistes	3572	1919	McGehee Farm	United States	29.65	-82.6	29.9	-80.1	Miocene	13.6	10	12
18560	J. Alroy	Xenarthra	Megalonychidae	Pliometanastes	1919	1919	McGehee Farm	United States	29.65	-82.6	29.9	-80.1	Miocene	13.6	10	12
18738	J. Alroy	Xenarthra	Mylodontidae	Glossotherium	1175	1175	Rancho El Ocote (Medial)	Mexico	21.2	-100.7	21.5	-99.1	Miocene	10.3	4.9	7.6
18746	J. Alroy	Xenarthra	Megalonychidae	Megalonyx	6213	1482	Tehuichila	Mexico	20.7	-98.7	21	-97.1		10.3	4.9	7.6
19638	J. Alroy	Chiroptera	Molossidae	Eumops	1295	2040	McRae Wash	United States	32	-110.2	32.1	-110	Pliocene	4.9	1.8	3.4
19650	J. Alroy	Rodentia	Erethizontidae	Erethizon	6294	1797	Wolf Ranch	United States	32	-110.2	32.1	-110	Pliocene	4.9	1.8	3.4
19656	J. Alroy	Hicanodonta	Sclerocalyptidae	Glyptotherium	1584	1584	111 Ranch (Lower)	United States	33	-109.6	33.1	-109	Pliocene	4.9	1.8	3.4
19747	J. Alroy	Xenarthra	Megatheriidae	Eremotherium	2615	2615	Brighton Canal	United States	27.3	-81.3	27.4	-80.7	Pleistocene	4.9	1.8	3.4
19749	J. Alroy	Xenarthra		Pachyarmatherium	1391	2621	El Jobean Pit	United States	26.9	-82	27	-81.4	Pleistocene	4.9	1.8	3.4
19752	J. Alroy	Xenarthra	Dasypodidae	Dasypus	3567	3567	Haile XVA	United States	29.8	-82.1	29.9	-81.5	Pliocene	4.9	1.8	3.4
19752	J. Alroy	Xenarthra	Pampatheriidae	Holmesina	3567	3567	Haile XVA	United States	29.8	-82.1	29.9	-81.5	Pliocene	4.9	1.8	3.4
19763	J. Alroy	Rodentia	Caviidae	Neochoerus	927	927	Sommer's Pit	United States	26.1	-81.5	26.2	-80.9		4.9	1.8	3.4
20077	J. Alroy	Rodentia	Caviidae	Neochoerus	1178	2594	Rancho Viejo	Mexico	21.03	-100.8	21.2	-100		4.9	1.8	3.4
20117	J. Alroy	Xenarthra	Nothrotheriidae	Nothrotherium	1186	1186	Vallecito Creek (CU 49)	United States	32.9	-117.1	32.7	-116	Pleistocene	4.9	1.8	3.4
20152	J. Alroy	Xenarthra	Megalonychidae	Meizonyx	3576	3575	Barranca del Sisimico	El Salvador	13.7	-88.8	13.7	-88.7	Pleistocene	1.8	0.3	1.1
20152	J. Alroy	Notoungulata	Toxodontidae	Mixotoxodon	3575	3575	Barranca del Sisimico	El Salvador	13.7	-88.8	13.7	-88.7	Pleistocene	1.8	0.3	1.1
20322	J. Alroy	Xenarthra	Nothrotheriidae	Nothrotheriops	2499	2245	El Golfo de Santa Clara	Mexico	31.7	-114.5	31.6	-114		4.9	1.8	3.4
20322	J. Alroy	Xenarthra	Myrmecophagidae	Myrmecophaga	3105	2245	El Golfo de Santa Clara	Mexico	31.7	-114.5	31.6	-114		4.9	1.8	3.4
20384	J. Alroy	Chiroptera	Phyllostomidae	Desmodus	2611	3580	Inglis IA	United States	29	-82.68	29.1	-82.1		4.9	1.8	3.4
20384	J. Alroy	Xenarthra	Mylodontidae	Paramylodon	2499	3580	Inglis IA	United States	29	-82.68	29.1	-82.1		4.9	1.8	3.4
20495	J. Alroy	Rodentia	Caviidae	Hydrochoerus	19165	19165	Terapa	Mexico	29.68	-109.7	29.7	-110	Pleistocene	0.3	0	0.2
20495	J. Alroy	Xenarthra	Pampatheriidae	Pampatherium	28655	19165	Terapa	Mexico	29.68	-109.7	29.7	-110	Pleistocene	0.3	0	0.2
70114	J. Alroy	Hicanodonta	Sclerocalyptidae	Glyptotherium	23536	23536	Arroyo El Tanque (17 m)	Mexico	21.1	-100.8	21.2	-100		4.9	1.8	3.4
70114	J. Alroy	Xenarthra	Pampatheriidae	Vassallia	23536	23536	Arroyo El Tanque (17 m)	Mexico	21.1	-100.8	21.2	-100		4.9	1.8	3.4
71264	J. Alroy	Didelphimorphia	Didelphidae	Marmosa	24062	24062	Cueva de Abra Travertine	Mexico	22.4	-98	22.4	-98	Pleistocene	0.13	0	0.1
71264	J. Alroy	Chiroptera	Phyllostomidae	Artibeus	24062	24062	Cueva de Abra Travertine	Mexico	22.4	-98	22.4	-98	Pleistocene	0.13	0	0.1

71278	J. Alroy	Xenarthra	Glyptodontidae	Glyptodon	24004	24004	El Hatillo	Panama	7.917	-80.63	7.92	-80.6	Pleistocene	0.13	0	0.1
71278	J. Alroy	Xenarthra	Glyptodontidae	Lomaphorus	24004	24004	El Hatillo	Panama	7.917	-80.63	7.92	-80.6	Pleistocene	0.13	0	0.1
71278	J. Alroy	Xenarthra	Mylodontidae	Scelidotherium	24004	24004	El Hatillo	Panama	7.917	-80.63	7.92	-80.6	Pleistocene	0.13	0	0.1
71294	J. Alroy	Notoungulata	Toxodontidae	Toxodon	23961	23961	Ciudad Real	Guatemala	14.45	-90.57	14.5	-90.6	Pleistocene	0.13	0	0.1
71312	J. Alroy	Xenarthra	Megatheriidae	Megatherium	23972	23972	Rio de la Pasion	Guatemala	16.25	-90.03	16.3	-90	Pleistocene	0.13	0	0.1
71312	J. Alroy	Xenarthra	Mylodontidae	Mylodon	23972	23972	Rio de la Pasion	Guatemala	16.25	-90.03	16.3	-90	Pleistocene	0.13	0	0.1
104046	M. Uhen	Xenarthra	Mylodontidae	Mylodon	15425	15425	Allen's Farm	United States	29.21	-81	29.2	-81	Pleistocene	0.13	0	0.1
13503	J. Alroy	Carnivora	Procyonidae	Parahyaenodon	47205	6117	Monte Hermoso	Argentina	-38	-61	-38.1	-59.6		6.8	4	5.4
13907	J. Alroy	Carnivora	Felidae	Leopardus	6166	6166	15 km N Mar del Plata	Argentina	-38	-57.55	-38	-57		3	1.2	2.1
36611	J. Alroy	Artiodactyla	Camelidae	Palaeolama	9817	9817	900 m SW of Punta Hermengo (lower)	Argentina	-38.3	-57.85	-38.3	-57.6	Pleistocene	1.2	0.8	1
55600	M. Uhen	Carnivora	Procyonidae	Cyonasua	15016	15016	Parana, Pueblo Brugo to Diamante, Ituzaingo Fm.	Argentina	-33.7	-59.25	-33.8	-57.1	Miocene	9	6.8	7.9
63335	D. Croft	Rodentia	Cricetidae	Reithrodon	17632	17632	Bajo San José Lower Section, Buenos Aires, Argentina	Argentina	-38.5	-61.77	-38.5	-61.8	Pleistocene	0.78	0.1	0.5
63335	D. Croft	Artiodactyla	Tayassuidae	Tayassu	17632	17632	Bajo San José Lower Section, Buenos Aires, Argentina	Argentina	-38.5	-61.77	-38.5	-61.8	Pleistocene	0.78	0.1	0.5
63335	D. Croft	Rodentia	Cricetidae	Lundomys	17632	17632	Bajo San José Lower Section, Buenos Aires, Argentina	Argentina	-38.5	-61.77	-38.5	-61.8	Pleistocene	0.78	0.1	0.5
63335	D. Croft	Rodentia	Cricetidae	Akodon	17632	17632	Bajo San José Lower Section, Buenos Aires, Argentina	Argentina	-38.5	-61.77	-38.5	-61.8	Pleistocene	0.78	0.1	0.5
63335	D. Croft	Carnivora	Felidae	Herpailurus	17632	17632	Bajo San José Lower Section, Buenos Aires, Argentina	Argentina	-38.5	-61.77	-38.5	-61.8	Pleistocene	0.78	0.1	0.5
63515	C. Bell	Chiroptera	Vespertilionidae	Eptesicus	18256	18256	Mene de Inciarte Tar Seep	Venezuela	10.79	-72.24	10.8	-72.2	Pleistocene	0.13	0	0.1
63515	C. Bell	Artiodactyla	Cervidae	Mazama	26437	18256	Mene de Inciarte Tar Seep	Venezuela	10.79	-72.24	10.8	-72.2	Pleistocene	0.13	0	0.1
63515	C. Bell	Chiroptera	Vespertilionidae	Rhogeessa	18256	18256	Mene de Inciarte Tar Seep	Venezuela	10.79	-72.24	10.8	-72.2	Pleistocene	0.13	0	0.1
63515	C. Bell	Rodentia	Cricetidae	Sigmodon	31501	18256	Mene de Inciarte Tar Seep	Venezuela	10.79	-72.24	10.8	-72.2	Pleistocene	0.13	0	0.1
63515	C. Bell	Rodentia	Muridae	Heteromys	31501	18256	Mene de Inciarte Tar Seep	Venezuela	10.79	-72.24	10.8	-72.2	Pleistocene	0.13	0	0.1
70673	D. Croft	Rodentia	Cricetidae	Calomys	19694	19694	Tarija	Bolivia	-21.5	-64.73	-21.6	-64.3	Pleistocene	2.59	0.8	1.7
70673	D. Croft	Rodentia	Cricetidae	Oxymycterus	19694	19694	Tarija	Bolivia	-21.5	-64.73	-21.6	-64.3	Pleistocene	2.59	0.8	1.7
70673	D. Croft	Carnivora	Canidae	Chrysocyon	19694	19694	Tarija	Bolivia	-21.5	-64.73	-21.6	-64.3	Pleistocene	2.59	0.8	1.7
70673	D. Croft	Carnivora	Ursidae	Arctodus	19694	19694	Tarija	Bolivia	-21.5	-64.73	-21.6	-64.3	Pleistocene	2.59	0.8	1.7

70673	D. Croft	Rodentia	Cricetidae	Andinomys	19694	19694	Tarija	Bolivia	-21.5	-64.73	-21.6	-64.3	Pleistocene	2.59	0.8	1.7
70673	D. Croft	Rodentia	Cricetidae	Nectomys	19694	19694	Tarija	Bolivia	-21.5	-64.73	-21.6	-64.3	Pleistocene	2.59	0.8	1.7
70673	D. Croft	Proboscidea	Gomphotheriidae	Haplomastodon	19694	19694	Tarija	Bolivia	-21.5	-64.73	-21.6	-64.3	Pleistocene	2.59	0.8	1.7
70673	D. Croft	Carnivora	Canidae	Theriodictis	19694	19694	Tarija	Bolivia	-21.5	-64.73	-21.6	-64.3	Pleistocene	2.59	0.8	1.7
70673	D. Croft	Carnivora	Procyonidae	Nasua	19694	19694	Tarija	Bolivia	-21.5	-64.73	-21.6	-64.3	Pleistocene	2.59	0.8	1.7
70673	D. Croft	Rodentia	Cricetidae	Kunsia	19694	19694	Tarija	Bolivia	-21.5	-64.73	-21.6	-64.3	Pleistocene	2.59	0.8	1.7
70673	D. Croft	Proboscidea	Gomphotheriidae	Notiomastodon	19694	19694	Tarija	Bolivia	-21.5	-64.73	-21.6	-64.3	Pleistocene	2.59	0.8	1.7
70673	D. Croft	Rodentia	Cricetidae	Phyllotis	19694	19694	Tarija	Bolivia	-21.5	-64.73	-21.6	-64.3	Pleistocene	2.59	0.8	1.7
70673	D. Croft	Proboscidea	Gomphotheriidae	Cuvieronius	19636	19694	Tarija	Bolivia	-21.5	-64.73	-21.6	-64.3	Pleistocene	2.59	0.8	1.7
70673	D. Croft	Artiodactyla	Cervidae	Charitoceros	19694	19694	Tarija	Bolivia	-21.5	-64.73	-21.6	-64.3	Pleistocene	2.59	0.8	1.7
70673	D. Croft	Carnivora	Felidae	Puma	19694	19694	Tarija	Bolivia	-21.5	-64.73	-21.6	-64.3	Pleistocene	2.59	0.8	1.7
70704	D. Croft	Carnivora	Felidae	Panthera	19694	19694	Nuapua 1, Chuquisaca, Bolivia	Bolivia	-20.8	-63.07	-20.8	-63.1	Pleistocene	0.78	0.1	0.5
71265	J. Alroy	Artiodactyla	Cervidae	Antifer	23979	23979			-33.2	-65.34	-31.9	-71.5	Pleistocene	0.13	0	0.1
71274	J. Alroy	Artiodactyla	Cervidae	Morenelaphus	24014	24014	Pintado	Uruguay	-30.4	-56.45	-30.4	-56.5	Pleistocene	0.78	0	0.4
71274	J. Alroy	Artiodactyla	Cervidae	Ozotoceros	24014	24014	Pintado	Uruguay	-30.4	-56.45	-30.4	-56.5	Pleistocene	0.78	0	0.4
71285	J. Alroy	Lagomorpha	Leporidae	Sylvilagus	24107	24107	Los Hoyos	Colombia	3.8	-74.3	3.8	-74.3	Pleistocene	0.78	0	0.4
71289	J. Alroy	Artiodactyla	Cervidae	Blastocerus	24007	24007	Arroyo Toropi-Level 1	Argentina	-27.8	-58.3	-27.8	-58	Pleistocene	0.78	0	0.4
71291	J. Alroy		Soricidae	Cryptotis	24108	24108	Curiti	Colombia	7.1	-73.2	7.1	-73.2	Pleistocene	0.78	0	0.4
71302	J. Alroy	Carnivora	Canidae	Speothos	24084	24084	Joao Cativo-Site 2	Brazil	-3.5	-39.58	-3.48	-39.4	Pleistocene	2.59	0	1.3
71303	J. Alroy	Carnivora	Mustelidae	Lontra	24010	24010	Lujan	Argentina	-34.1	-57.13	-34.1	-57.1	Pleistocene	0.78	0	0.4
71303	J. Alroy	Carnivora	Mustelidae	Lyncodon	24010	24010	Lujan	Argentina	-34.1	-57.13	-34.1	-57.1	Pleistocene	0.78	0	0.4
71303	J. Alroy	Artiodactyla	Camelidae	Eulamaops	24010	24010	Lujan	Argentina	-34.1	-57.13	-34.1	-57.1	Pleistocene	0.78	0	0.4
71303	J. Alroy	Carnivora	Canidae	Dusicyon	24010	24010	Lujan	Argentina	-34.1	-57.13	-34.1	-57.1	Pleistocene	0.78	0	0.4
71304	J. Alroy	Carnivora	Mustelidae	Galictis	24008	24008	Arroyo Loberia	Argentina	-38	-57.72	-38.1	-57.4	Pleistocene	2.59	0	1.3
71322	J. Alroy	Proboscidea	Gomphotheriidae	Stegomastodon	23916	23916	Nuapua 1	Bolivia	-20.9	-63.07	-20.9	-62.8	Pleistocene	1.2	0.8	1
71330	J. Alroy	Rodentia	Muridae	Colomys	24113	24113	Santa Clara del Mar	Argentina	-37.8	-57.42	-37.8	-57.4	Pleistocene	0.13	0	0.1
71334	J. Alroy	Lagomorpha	Leporidae	Kerodon	23910	23910	Toca da Cima dos Pilao	Brazil	-9.02	-42.7	-9.02	-42.7	Pleistocene	0.13	0	0.1
71347	J. Alroy	Artiodactyla	Camelidae	Vicugna	23974	23974	Centinela del Mar	Argentina	-36	-58	-36	-58	Pleistocene	0.78	0	0.4
92299	M. Uhen	Carnivora	Mustelidae	Pteronura	31109	31109	South Bank of Ensenada Creek	Argentina	-32.1	-60.44	-32.1	-60.4	Pleistocene	0.13	0	0.1
133630	C. Jaramillo	Carnivora	Canidae	Dusicyon	43044	43044	La Carolina	Ecuador	-2.22	-80.93	-2.22					

133633	C. Jaramillo	Artiodactyla	Cervidae	Agalmaceros		43044	43044	Quebrada de Ot?n	Ecuador	-0.88	-78.4	0.33	-78	Pleistocene	2.59	0	1.3
136521	C. Jaramillo	Carnivora	Mustelidae	Pteronura		43673	43673	Gruta do Curupira	Brazil	-15.2	-56.75	-15.2	-56.8	Pleistocene	0.13	0	0.1
137876	C. Jaramillo	Artiodactyla	Tayassuidae	Sylvochoerus		44103	44103			-9.76	-72.77	-9.14	-71	Miocene	11.6	5.3	8.5
137877	C. Jaramillo	Artiodactyla	Tayassuidae	Waldochoerus		44103	44103	VF2	Peru	-11	-72.68	-11.3	-70.9	Miocene	11.6	5.3	8.5
140653	C. Jaramillo	Artiodactyla	Cervidae	Epieurycerus		45580	45580	La Plata (Ensenada)	Argentina	-34.9	-57.93	-34.9	-57.9	Pleistocene	0.78	0.1	0.5
140934	C. Jaramillo	Rodentia	Cricetidae	Eligmodontia		45758	23867	Quequén Salado - Indio Rico	Argentina	-38.7	-60.6	-38.8	-60.6	Pleistocene	0.78	0	0.4
141182	C. Jaramillo	Rodentia	Cricetidae	Oligoryzomys		45821	45827	La Angostura	Argentina	-26.9	-65.7	-26.9	-65.7	Pleistocene	0.03	0	0
141182	C. Jaramillo	Rodentia	Cricetidae	Neotomys		45821	45827	La Angostura	Argentina	-26.9	-65.7	-26.9	-65.7	Pleistocene	0.03	0	0
141182	C. Jaramillo	Rodentia	Cricetidae	Tafimys		45821	45827	La Angostura	Argentina	-26.9	-65.7	-26.9	-65.7	Pleistocene	0.03	0	0
141182	C. Jaramillo	Rodentia	Cricetidae	Abrothrix		45821	45827	La Angostura	Argentina	-26.9	-65.7	-26.9	-65.7	Pleistocene	0.03	0	0
141896	C. Jaramillo	Perissodactyla	Equidae	Hippidion		46088	46088	Esquina Blanca - Middle Unit	Argentina	-23.3	-65.33	-23.4	-64.6		3	1.2	2.1
141896	C. Jaramillo	Artiodactyla	Tayassuidae	Platygonus		46088	46088	Esquina Blanca - Middle Unit	Argentina	-23.3	-65.33	-23.4	-64.6		3	1.2	2.1
142016	C. Jaramillo	Carnivora	Ursidae	Arctotherium		46109	46109	Tarija-1	Bolivia	-21.5	-64.75	-21.6	-64.3	Pleistocene	1.2	0.8	1
142016	C. Jaramillo	Perissodactyla	Tapiridae	Tapirus		46109	46109	Tarija-1	Bolivia	-21.5	-64.75	-21.6	-64.3	Pleistocene	1.2	0.8	1
142016	C. Jaramillo	Carnivora	Mustelidae	Conepatus		46109	46109	Tarija-1	Bolivia	-21.5	-64.75	-21.6	-64.3	Pleistocene	1.2	0.8	1
142016	C. Jaramillo	Perissodactyla	Equidae	Equus		46109	46109	Tarija-1	Bolivia	-21.5	-64.75	-21.6	-64.3	Pleistocene	1.2	0.8	1
142016	C. Jaramillo	Artiodactyla	Camelidae	Palaeolama		46109	46109	Tarija-1	Bolivia	-21.5	-64.75	-21.6	-64.3	Pleistocene	1.2	0.8	1
142016	C. Jaramillo	Artiodactyla	Camelidae	Lama		46109	46109	Tarija-1	Bolivia	-21.5	-64.75	-21.6	-64.3	Pleistocene	1.2	0.8	1
142016	C. Jaramillo	Carnivora	Canidae	Canis		46109	46109	Tarija-1	Bolivia	-21.5	-64.75	-21.6	-64.3	Pleistocene	1.2	0.8	1
142016	C. Jaramillo	Carnivora	Felidae	Smilodon		46109	46109	Tarija-1	Bolivia	-21.5	-64.75	-21.6	-64.3	Pleistocene	1.2	0.8	1
142016	C. Jaramillo	Perissodactyla	Equidae	Onohippidium		46109	46109	Tarija-1	Bolivia	-21.5	-64.75	-21.6	-64.3	Pleistocene	1.2	0.8	1
142016	C. Jaramillo	Artiodactyla	Tayassuidae	Dicotyles		46109	46109	Tarija-1	Bolivia	-21.5	-64.75	-21.6	-64.3	Pleistocene	1.2	0.8	1
142016	C. Jaramillo	Artiodactyla	Camelidae	Hemiauchenia	NA		46109	Tarija-1	Bolivia	-21.5	-64.75	-21.6	-64.3	Pleistocene	1.2	0.8	1
142016	C. Jaramillo	Carnivora	Canidae	Protocyon		46109	46109	Tarija-1	Bolivia	-21.5	-64.75	-21.6	-64.3	Pleistocene	1.2	0.8	1
142016	C. Jaramillo	Carnivora	Felidae	Felis		46109	46109	Tarija-1	Bolivia	-21.5	-64.75	-21.6	-64.3	Pleistocene	1.2	0.8	1
142338	C. Jaramillo	Rodentia	Cricetidae	Holochilus		46210	46210	Tarija-2	Bolivia	-21.5	-64.75	-21.6	-64.3	Pleistocene	2.59	0.8	1.7
142544	C. Jaramillo	Artiodactyla	Tayassuidae	Catagonus		46285	46285	Tarija-3	Bolivia	-21.6	-64.77	-21.6	-64.5	Pleistocene	1.2	0.8	1
143054	C. Jaramillo	Artiodactyla	Cervidae	Hippocamelus		46381	46381	Pueblo Viejo (Tarija)	Bolivia	-21.5	-64.78	-21.5	-64.5	Pleistocene	1.2	0.8	1
144515	C. Jaramillo	Proboscidea	Gomphotheriidae	Amahuacatherium		46734	46734	Aurinsa	Peru	-12.6	-70.11	-12.9	-67.9	Miocene	10	9	9.5
144977	C. Jaramillo	Carnivora	Felidae	Homotherium		46869	46869	El Breal de Orocual	Venezuela	9.847	-63.33	9.82	-63.2	Pleistocene	1	0.5	0.8

145366	C. Jaramillo	Carnivora	Canidae	Urocyon	46993	46993	Inciarte asphalt pit	Venezuela	10.8	-72.24	10.8	-72.2	Pleistocene	0.13	0	0.1
145505	C. Jaramillo	Artiodactyla	Cervidae	Odocoileus	46859	46859	Cupisnique Desert (including Pampa de los Fósiles and Piedra Escrita sites	Peru	-7.5	-79.5	-7.5	-79.5	Pleistocene	0.03	0	0
147999	C. Jaramillo	Carnivora	Felidae	Smilodon	47573	47573	Mar del Plata (Ensenadan)	Argentina	-38	-57.59	-38	-57.3	Pleistocene	1.2	0.8	1
152062	C. Jaramillo	Rodentia	Cricetidae	Necromys	48757	48757	Farola (FL1)	Argentina	-39	-61.7	-39.1	-60.3		6.8	4	5.4
152062	C. Jaramillo	Rodentia	Cricetidae	Auliscomys	48757	48757	Farola (FL1)	Argentina	-39	-61.7	-39.1	-60.3		6.8	4	5.4
153674	C. Jaramillo	Rodentia	Cricetidae	Scapteromys	49750	49750	Las Brusquitas - Vorohue	Argentina	-38.2	-57.74	-38.3	-56.6	Pliocene	4	3	3.5
156532	C. Jaramillo	Artiodactyla	Palaeomerycidae	Surameryx	51301	51301	LACM 5159	Brazil	-10.9	-69.57	-11.2	-67.8	Miocene	11.6	5.3	8.5

CHAPTER 3

Giant rodents from the Neotropics: diversity and dental variation of late Miocene neoepiblemid remains from Urumaco, Venezuela

Phoberomys pattersoni. Artwork: Jorge González

Juan D. Carrillo, and Marcelo R. Sánchez-Villagra. 2015.
Paläontologisches Zeitschrift, 89:1057-1071.doi: 10.1007/s12542-015-0267-3

Paläontol Z (2015) 89:1057–1071
DOI 10.1007/s12542-015-0267-3

RESEARCH PAPER

Giant rodents from the Neotropics: diversity and dental variation of late Miocene neoepiblemid remains from Urumaco, Venezuela

Juan D. Carrillo[1] · **Marcelo R. Sánchez-Villagra**[1]

Received: 9 December 2014 / Accepted: 27 April 2015 / Published online: 10 May 2015

Abstract Caviomorphs constitute a large evolutionary radiation of South America rodents, exhibiting a wide range of body size and ecomorphological disparity. The geological history of caviomorphs has been recorded mainly from high latitudes, besides isolated discoveries from the Neotropics. The late Miocene fauna from Urumaco, Venezuela, is noteworthy for its location and for preserving the giant rodent *Phoberomys pattersoni*. Previous studies of isolated postcranial remains suggested that the rodent diversity from Urumaco was higher than is currently recognized. Based on new remains we document dental variation that indicates the presence of at least two giant rodent taxa in Urumaco, including *Neoepiblema*. Quantitative analysis of dentition of the different neoepiblemid species supports the differentiation between *Neoepiblema* and *Phoberomys* and suggests that several recognized species of *Phoberomys* could represent different ontogenetic stages of one or few taxa within the genus.

Keywords Mammalia · Caviomorpha · South America · Neogene · Body size · Paleobiology

Kurzfassung Die Caviomorpha stellen eine grosse evolutionäre Radiation südamerikanischer Nagetiere dar. Die geologische Geschichte der Caviomorpha ist, neben isolierten Entdeckungen in der Neotropis, hauptsächlich von den hohen Breiten überliefert. Die spätmiozäne Fauna von Urumaco, Venezuela, ist bemerkenswert für ihre Lage und für die Erhaltung von *Phoberomys pattersoni*. Vorhergehende Studien isolierter postcranialer Überreste deuteten darauf hin, dass die Diversität der Riesennager von Urumaco größer war als gegenwärtig angenommen. Basierend auf neuen Überresten dokumentieren wir dentale Variation, die auf die Anwesenheit von mindestens zwei verschiedenen Riesennager-Taxa in Urumaco, einschliesslich *Neoepiblema*, hinweist. Eine quantitative Analyse des Gebisses der verschiedenen neoepiblemiden Arten unterstützt die Unterscheidung zwischen *Neoepiblema* und *Phoberomys*, und deutet darauf hin, daß verschiedene anerkannte Arten von *Phoberomys* unterschiedliche ontogenetische Stadien eines oder mehrerer Taxa innerhalb einer Gattung repräsentieren könnten.

Schlüsselwörter Mammalia · Caviomorpha · Südamerika · Neotropis · Neogen · Körpergröße · Paläobiologie

Abbreviations

AMU-CURS	Alcaldía del Municipio de Urumaco, Falcón, Venezuela
CIAAP-UNEM	Centro de Investigaciones Antropológicas Arqueológicas y Paleontológicas, Universidad Nacional Experimental Francisco de Miranda, Coro, Venezuela
MCNC	Museo Nacional de Ciencias, Caracas, Venezuela
MLP	Museo de La Plata, La Plata, Argentina
MACN	Museo Argentino de Ciencias Naturales, Buenos Aires, Argentina
SALMA	South American land mammal age
M-m	Molar

✉ Marcelo R. Sánchez-Villagra
m.sanchez@pim.uzh.ch

Juan D. Carrillo
juan.carrillo@pim.uzh.ch

[1] Paläontologisches Institut und Museum, Universität Zürich, Karl-Schmid-Strasse 4, 8006 Zurich, Switzerland

P-p	Premolar
AP	Anteroposterior length
AW	Anterior width
PW	Posterior width
MW	Medium width

Introduction

Caviomorphs constitute a large radiation of South America rodents, exhibiting a wide range of body size and morphological disparity, including terrestrial, fossorial, semiaquatic, scansorial and arboreal representatives (Mares and Ojeda 1982; Weisbecker and Schmid 2007). The group likely arrived from Africa by rafting, with the first appearance of a stem caviomorph recorded in the middle Eocene of the Peruvian Amazonia (Yahuarango Formation; 41.6–40.94 Ma; Antoine et al. 2012). The molecular evidence and fossil record support the appearance of main clades ('superfamilies/families') within Caviomorpha during the late Eocene to early Oligocene (Vucetich et al. 1999; Fabre et al. 2012; Voloch et al. 2013), whereas most of the living 'families' radiated between the middle and late Miocene (Vucetich et al. 1999; Opazo 2005; Pérez and Pol 2012; Upham and Patterson 2012).

The long history of caviomorphs has been recorded, as is the general case from South America, from high latitudes (e.g., Wood and Patterson 1959; Vucetich et al. 1993, 1999, 2010a, b, 2014; Kramarz and Bellosi 2005; Flynn et al. 2008; Rinderknecht and Blanco 2008; Nasif et al. 2013), but the northern Neotropics have also provided significant discoveries (MacFadden 2006). The tropical faunas of Santa Rosa (late Eocene; Campbell 2004) and Contamana (middle Eocene; Antoine et al. 2012) of Peru, La Venta in the middle Miocene (Laventan SALMA) of Colombia (Kay et al. 1997), Urumaco in the late Miocene of Venezuela (Sánchez-Villagra et al. 2010) and Acre (Solimões Formation) in the middle to late Miocene of Amazonia (Cozzuol 2006; Ribeiro et al. 2013) are noteworthy, because of the diversity they preserve. The new tropical fossil assemblages of Fitzcarrald in middle Miocene (Laventan) sediments of the Peruvian Amazonia (Tejada-Lara et al. 2015) and Castilletes middle Miocene-early Pliocene in northern Colombia (Moreno et al. 2015) add important data to the Neotropical fossil record. The Greater Antilles have also been a source of significant discoveries (MacPhee 2011; MacPhee and Flemming 2003). As in northern South America, the most remarkable aspect of some Caribbean rodents has been their very large size (Silva Taboada et al. 2007).

Among the caviomorphs the Neoepiblemidae, including *Neoepiblema*, *Eusigmomys* and *Phoberomys* (Negri and Ferigolo 1999), are among the largest ones. Phylogenetic analyses suggest a close relationship between *Phoberomys* and *Dinomys*, the pacarana, among extant taxa (Sánchez-Villagra et al. 2003; Horovitz et al. 2006), but the phylogenetic relationships of these and other extinct and large caviomorphs are in need of study (Kramarz et al. 2013). Phylogenetic analyses based on molecular data support the close affinities between Dinomyidae and Chinchillidae (Opazo 2005; Huchon et al. 2007; Blanga-Kanfi et al. 2009; Fabre et al. 2012; Upham and Patterson 2012).

Phoberomys pattersoni is the largest neoepiblemid and is known based on an almost completed skeleton from the late Miocene deposits of the Urumaco Formation (Mones 1980; Bondesio and Bocquentin-Villanueva 1988; Sánchez-Villagra et al. 2003; Horovitz et al. 2006). Body mass estimates resulted in extreme sizes ranging from 220 to 450 kg (Millien and Bovy 2010; Geiger et al. 2013). Previous studies suggested that giant rodent diversity from Urumaco was higher than is currently recognized, either based on a few craniodental remains (Horovitz et al. 2006, 2010) or on isolated femora that cannot be used for definitive taxonomic assignations (Geiger et al. 2013). The taxonomy of these rodents is based largely on dental features (Table 1). There are size and morphological intraspecific variations in euhypsodont teeth, which are important to consider in order to understand the taxonomy and ontogeny of these rodents (Vucetich et al. 2005; Deschamps et al. 2007), an aspect that has been largely ignored so far because of the lack of appropriate samples.

Another caviomorph rodent documented for the Urumaco Formation includes an unidentified species of the dinomyid *Eumegamys* (Pascual and Díaz de Gamero 1969). Furthermore, faunal lists from Urumaco have included dental remains referred to *Tetrastylus*, *Telicomys* and Potamarchinae cf. *Potamarchus* and *Olenopsis* (Linares 2004). However, a revision of the referred specimens has not been done and most of these records are in need of verification (Horovitz et al. 2010). Geiger et al. (2013) distinguished four different morphotypes of giant caviomorphs from Urumaco based on an analysis of the femoral morphological variation and growth.

Neoepiblemids have been recorded in middle and late Miocene deposits of Brazil, Argentina and Peru (Horovitz et al. 2010; Tejada-Lara et al. 2015) (Fig. 1). An almost complete cranium and several mandibular remains of *Neoepiblema ambrosettianus* have been described for the late Miocene of Acre, Brazil (Bocquentin-Villanueva et al. 1990; Negri and Ferigolo 1999). Rodents are one of the most diverse groups registered in the Acre region with ten genera and twelve species, eleven of which are neoepiblemids and dinomyids (Ribeiro et al. 2013;

Table 1 Summary of dental traits, age and geographic distribution of the recognized members of *Phoberomys* and *Neoepiblema*

Taxon	Dental traits	Locality	Age	Reference
Phoberomys Kraglievich 1926	M3 with seven to eight laminae united labially, p4 with four laminae, the first two or three united labially and the third or fourth or just the fourth free			Bondesio and Bocquentin-Villanueva (1988)
Phoberomys insolita Kraglievich 1940	M3 with eight laminae united labially	Mesopotamia, Argentina	Late Miocene (Huayquerian)	Kraglievich 1940
Phoberomys pattersoni Mones 1980	M3 with seven laminae united labially. P4 with four laminae, the two anterior ones united labially, the posterior ones free	Urumaco, Venezuela	Late Miocene	Bondesio and Bocquentin-Villanueva (1988), Mones (1980)
Phoberomys lozanoi Kraglievich 1926	M3 with eight laminae united labially, the eighth one is poorly developed and not visible in oclusal view	Mesopotamia, Argentina	Late Miocene (Huayquerian)	Kraglievich (1940)
Phoberomys burmeisteri Kraglievich 1926	p4 with four laminae, the two anterior ones united labially and two posterior ones free	Mesopotamia, Argentina and Acre, Brazil	Late Miocene (Huayquerian)	Kraglievich (1926, 1932)
Phoberomys praecursor Kraglievich (1932	p4 with four laminae, the three anterior ones united labially and fourth one free	Mesopotamia, Argentina	Late Miocene (Huayquerian)	Kraglievich (1932)
Phoberomys bordasi Patterson 1942	p4 with four laminae, the three anterior ones united labially and the fourth free	Acre, Brazil	Late Miocene (Huayquerian)	Patterson (1942)
Phoberomys minima Kraglievich 1940	Lower molars smaller than *P. lozanoi* and larger than *Neoepiblema*	Mesopotamia, Argentina and Acre, Brazil	Late Miocene (Huayquerian)	Kraglievich (1940)
Neoepiblema Ameghino 1889	M3 with four laminae united labially, p4-m3 with three laminae, the first two united labially and the third free. In the p4 the third prism free or united lingually to the second			Negri and Ferigolo (1999)
Neoepiblema ambrossetianus Ameghino 1889	Molars larger than *N. horridula*. Second and third laminae of P4-M3 more transversal than *N. horridula*	Mesopotamia, Argentina and Acre, Brazil	Late Miocene (Huayquerian)	Negri and Ferigolo (1999), Bocquentin-Villanueva et al. (1990)
Neoepiblema horridula Ameghino 1889	As for the genus	Mesopotamia, Argentina and Acre, Brazil	Late Miocene (Huayquerian)	Ameghino (1889)

Kerber et al. 2015). The late Miocene sediments from the Paraná region, Argentina, include terrestrial mammals from the Ituzaingó Formation, which counts under its rodent fauna several members of the Neoepiblemidae (*Phoberomys* and *Neoepiblema*) (Cione et al. 2000; Nasif et al. 2013). Additional records of Neoepiblemidae include *Neoepiblema* sp. in Fitzcarrald, Peru (Tejada-Lara et al. 2015), and the San Gregorio Formation, Pliocene of Venezuela (Vucetich et al. 2010c).

In this work we describe new dental and cranial remains of giant rodents from the Urumaco Formation providing evidence of a higher rodent diversity and morphological disparity than previously recognized. We quantify the dental size variation in *Phoberomys* and *Neoepiblema*, and we show that the morphological variation in neoepiblemid rodents from Urumaco does not just represent intraspecific variation within *P. pattersoni*, the only species from this group previously described for the Urumaco fauna.

Materials and methods

We investigated the dentition of neoepiblemid specimens from Urumaco, Venezuela, and Mesopotamia, Argentina, as well as different taxa described in the literature. In order to have a clear view of the occlusal surface of the dentition, we sectioned the upper and lower dentition of ten specimens from Urumaco. We first stabilized the samples surrounding the teeth with the resin Technovit® 5071, and we cut the dentition with a sawblade along the anteroposterior axis, at about 50 mm from the occlusal surface. For each tooth available, we measured the anteroposterior length (AP), anterior width (AW), posterior width (PW) and medium width (MW). For the M3, as it has multiple laminae, we only measured the AP and PW. Measurements were taken with calipers to the nearest 0.1 mm. For the dental terminology we follow Negri and Ferigolo (1999) and Bondesio and Bocquentin-Villanueva (1988). Our use

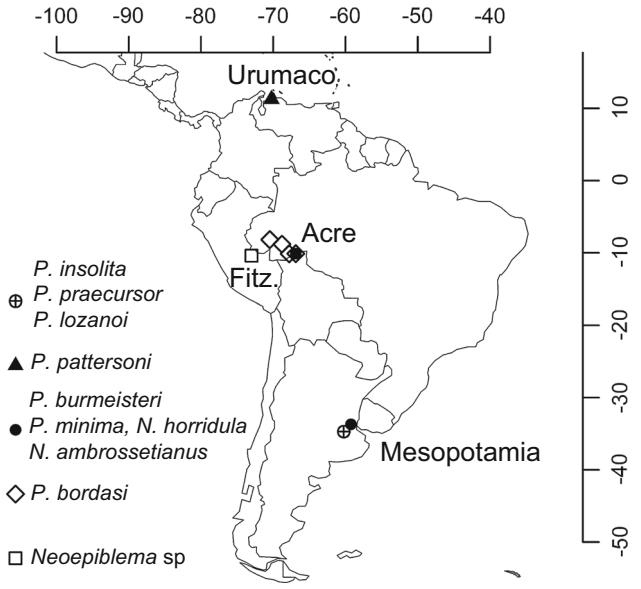

Fig. 1 Distribution of *Phoberomys* and *Neoepiblema* in South America. *Fitz* Fitzcarrald. Data downloaded from the Paleobiology database on 26 November 2014 using group names = *Phoberomys*, *Neoepiblema*, region = South America

of the term "laminae" is equivalent to "prisms" as used by Mones (1980).

For the quantitative analysis of the dentition, we performed a bivariate plot of the logarithm (log) of AW vs. log of AP. We grouped in the analysis the P4–M2 for the upper dentition and m1–m3 for the lower dentition because they are morphologically indistinguishable when dealing with isolated teeth. We did a linear regression for each set of teeth. The plots and regressions were made with R (R core team 2014).

Systematic paleontology

Rodentia Bowdich, 1821
Hystricognathi, Tullberg, 1899
Chinchilloidea Bennett, 1833
Neoepiblemidae, Kraglievich, 1926

Neoepiblema Ameghino, 1889
Neoepiblema sp.

Material AMU-CURS 381, partial left dentary with p4–m3.

Provenance NW San Rafael (11°14′52″N, 70°14′06″W), Urumaco Formation, upper member (Fig. 2).

Description AMU-CURS 381 has three laminae in the p4, the two anterior ones united labially and the third one free, as *Neoepiblema* (Negri and Ferigolo 1999). The mandibular symphysis extends posteriorly up to the middle anterior portion of p4, as described for *N. ambrosettianus* (Mones and Toledo 1989), but also true for *P. pattersoni* (AMU-CURS 53 and AMU-CURS 170, see below). AMU-CURS 381 have only three laminae in p4, in contrast with *Phoberomys* that has four, the first two connected labially (Bondesio and Bocquentin-Villanueva 1988). The m1–m3 of AMU-CURS 381 have three laminae, all of them free (Fig. 3a); in contrast to the other species of *Neoepiblema* that have three laminae in the lower molars, the second connected labially to the first and the third free (Negri and Ferigolo 1999). AMU-CURS 381 differs from some specimens referred to *Neoepiblema ambrosettianus* in having the third prism of the p4 free and not connected lingually to the second (Mones and Toledo 1989; Bocquentin-Villanueva et al. 1990).

We assigned AMU-CURS 381 to *Neoepiblema* based on the morphology and number of laminae of the p4. The fact that the m1–m3 of AMU-CURS 381 have three free laminae suggests that the labial connection between the first and second prism in m1–m3 is a variable character for *Neoepiblema*

Phoberomys Kraglievich, 1926
Phoberomys sp. A

Material AMU-CURS 382, partial left mandible with p4 only preserved at the alveolar level and m1–m3 poorly preserved. UNEFM-VF 014, with this catalog number, there are two partial mandibles, one right dentary with p4–m3, which we refer to *Phoberomys* sp. A, and a second right dentary with m1–m3 identified as *Phoberomys* sp.

Provenance AMU-CURS 382 comes from NW San Rafael (11°14′52″N, 70°14′06″W), Urumaco Formation, upper member (Fig. 2). UNEFM-VF 014 comes from Urumaco Formation, Urumaco.

Description AMU-CURS 382 and UNEFM-VF 014 exhibit features described for both *Phoberomys* and *Neoepiblema.* The p4 has four laminae, the two anterior ones connected labially and the third and fourth free, as in *P. pattersoni* and *P. burmeisteri* (Kraglievich 1926, 1932; Bondesio and Bocquentin-Villanueva 1988) (Fig. 3b). Due to its preservation it is difficult to observe the number and pattern of laminae in m1 and m2 for AMU-CURS 382; however, it is possible to state they are three, and they all seem to be free as in *Phoberomys*. In UNEFM-VF 014, the m1–m2 have three free laminae. The m3 has three laminae, the two anterior ones connected labially, as in *Neoepiblema* (Negri and Ferigolo 1999). The molar dimensions of these specimens are small compared to specimens referred to *P. pattersoni* (Table 2).

In contrast with AMU-CURS 382 and UNEF-VF 014, the p4 of *P. bordasi* and *P. praecursor* has the three anterior laminae united labially and the fourth free (Kraglievich 1932; Patterson 1942). These specimens differ

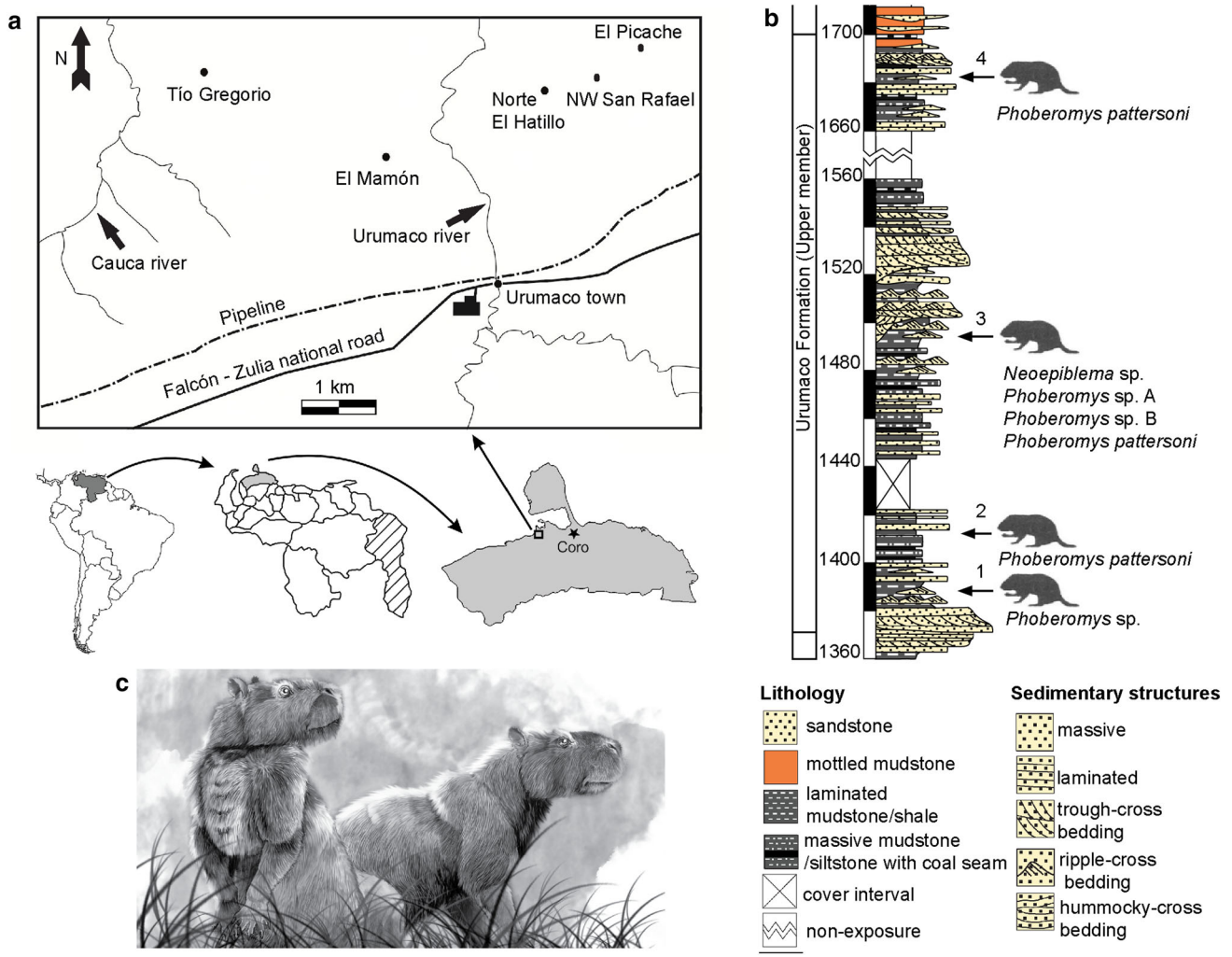

Fig. 2 Geographic and stratigraphic occurrence of neoepiblemids from Urumaco; **a** fossil localities and **b** stratigraphic profile of the upper member of the Urumaco Formation; the taxonomic occurrence of neoepiblemid taxa is indicated for each locality: (1) El Hatillo, (2) El Mamón, (3) El Picache/NW San Rafael and (4) Tío Gregorio/Cerro José La Paz. Modified from Quiroz and Jaramillo (2010) and Scheyer et al. (2013); **c** restoration of *P. pattersoni*. Artwork by Jorge González, modified from Horovitz et al. (2010)

from *Neoepiblema* in that the p4 of the latter has only three laminae (Negri and Ferigolo 1999). We therefore assigned AMU-CURS 382 and UNEFM–VF 014 to *Phoberomys* based on the morphology and laminae of the p4. The labial connection between the first and second laminae in m3 is a variable character in *Phoberomys* and neoepiblemids in general, as was mentioned above for AMU-CURS 381 referred to *Neoepiblema* sp.

Phoberomys sp. B

Material AMU-CURS 380—maxilla with right M1–M3 and left M3. AMU-CURS 35, partial maxilla with right P4–M3 and left P4–M1. MCN 66–72 V, isolated M3.

Provenance AMU-CURS 380 comes from NW San Rafael (11°14′52″N, 70°14′06″W), Urumaco Formation, upper member. AMU-CURS 35 comes from El Picache, Urumaco Formation, upper member (Fig. 2). MCN 66–72 V is from Urumaco Formation, Urumaco.

Description AMU-CURS 380 shows some diagenetic deformation, as the maxilla is slightly folded toward the left side. It preserves the right M1–M3 and the left M3. It is not possible to observe clearly the morphology of laminae in M1, but it has three laminae connected labially in M2. AMU-CURS 35 shows the P4–M2 with three laminae connected labially.

AMU-CURS 380, AMU-CURS 35 and MCN 66–72 V differ from other specimens of *Phoberomys* in the number of laminae of M3. The M3 of these specimens have six laminae (Fig. 3f, g), all connected labially, and it narrows posteriorly. In contrast, the M3 of other *Phoberomys* species have seven to eight laminae connected labially (Bondesio and Bocquentin-Villanueva 1988). The relative

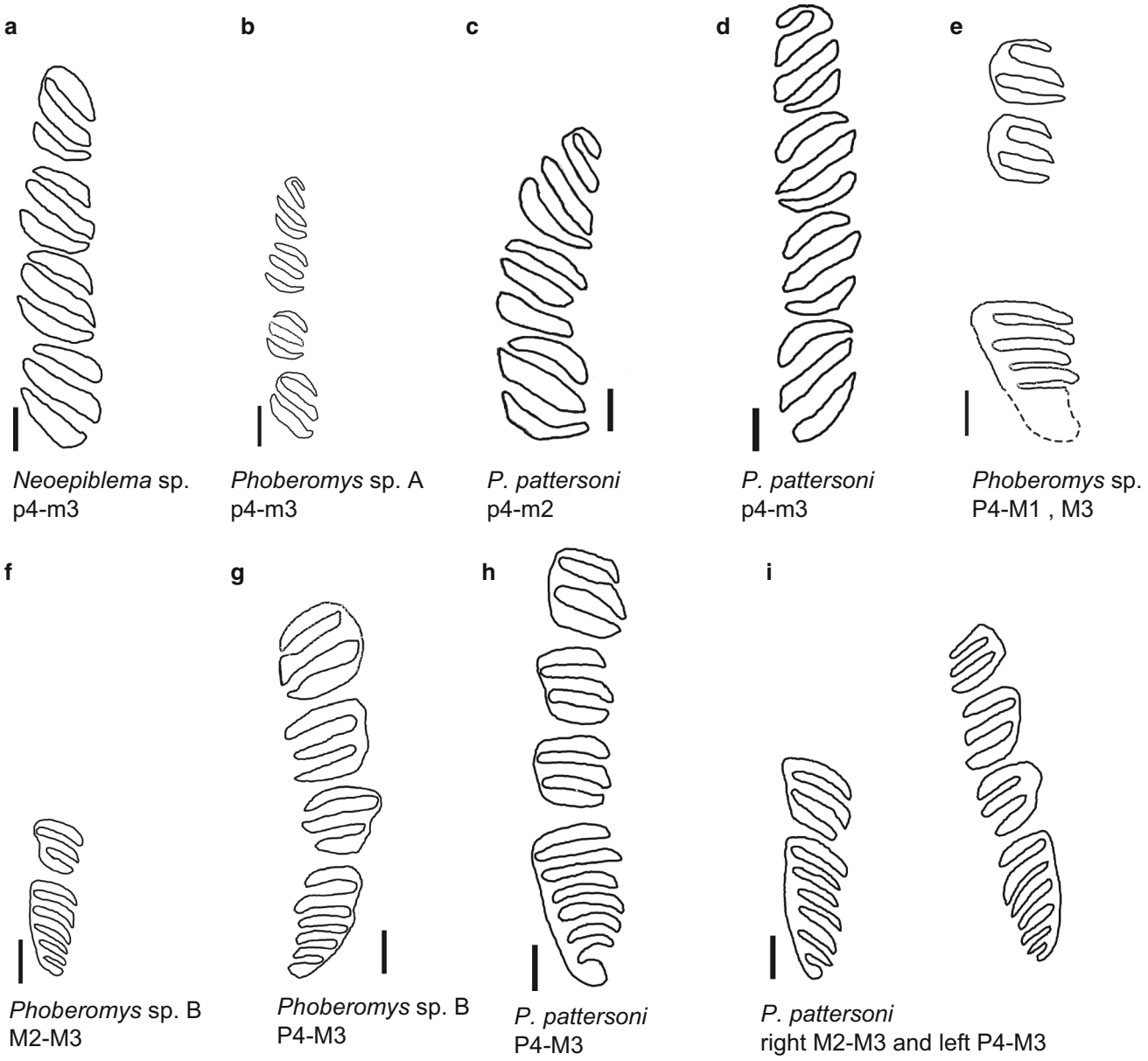

Fig. 3 Occlusal surface morphology of the neoepiblemids from Urumaco. **a** Lower dentition *Neopiblema* sp. (AMU-CURS 381); **b** lower dentition *Phoberomys* sp. A, (AMU-CURS 382); **c** lower dentition *P. pattersoni* (AMU-CURS 454); **d** lower dentition *P. pattersoni* (AMU-CURS 170); **e** upper dentition *Phoberomys* sp. (AMU-CURS 161); *dashed lines* represent the portion of M3 where the occlusal morphology could not be observed; **f** upper dentition *Phoberomys* sp. B (AMU-CURS 380); **g** upper dentition *Phoberomys* sp. B (AMU-CURS 35); **h** upper dentition *P. pattersoni* (AMU-CURS 255); **i** upper dentition *P. pattersoni* (AMU-CURS 53). *Scale bar* 10 mm

dimensions of the dentition of these specimens are small compared to other specimens referred to *Phoberomys* (Table 2).

Phoberomys sp.

Material AMU-CURS 161—complete cranium compressed in the dorsal-ventral plane.

Provenance AMU-CURS 161 comes from Norte El Hatillo, Urumaco Formation, upper member (Fig. 2).

Description AMU-CURS 161 is tentatively assigned to *Phoberomys* because it presents more than four laminae connected labially in the M3, although is not possible to assess the total number of laminae because of the preservation of the posterior portion of the M3. *Phoberomys* has 7–8 laminae in M3 (Bondesio and Bocquentin-Villanueva 1988); in contrast *Neoepiblema* have only four laminae (Negri and Ferigolo 1999). The P4–M1 of AMU-CURS 161 have three laminae connected labially as in all

Table 2 Dental measurements of neoepiblemids

Taxon	Catalog number	Tooth	Left				Right			
			Length	Width			Length	Width		
			AP	AW	PW	MW	AP	AW	PW	MW
Phoberomys sp.	AMU-CURS 161	P4					15.6	12.9	16.1	15.7
		M1					18.2	17.2	14.8	15
		M2					17.5	19.6	16.4	?
		M3					27.3	20.7	11.4	NA
	UNEFM TG4	P4					28.6	28.5	22.1	?
		M1					21.1	21.6	20.6	21
		M2					19.3	23.5	20.3	22.2
		M3					41.1	22	13.1	NA
	UNEFM 1438	M1	17.7	16.2	13.7	15				
		M2	19.3	17	14.1	18				
	MACN-Pv 2645	p4					11.6	7.4	7.6	8.3
	UNEFM-VF 014	m1					20.7	14.8	14.7	16.7
		m2					22.6	16.8	19.3	17.6
		m3					26.2	18.3	17.6	21.8
	MACN-Pv 3475	m1–m3					25.4	20.6	20.9	23.7
	CIAAP 1438[b]	M1	16.9	17						
		M2	18.3	18.3						
		m2					22.6	16.5		
Phoberomys sp. A	AMU-CURS 382	p4	17	?	12.8	?				
		m1	15.2	9.9	11.7	?				
		m2	15.9	8.6	10.7	10.8				
		m3	19.7	10.4	10.5	9.6				
	UNEFM-VF 014	p4					15	14.8	10.9	11.9
		m1					14	11.7	12	12.2
		m2					15.4	12.2	11.7	13.5
		m3					15.3	11.5	11.8	13.2
Phoberomys sp. B	AMU-CURS 380	M1	15.4	13	9.9	?				
		M2	13	12.8	8.3	11.7				
		M3	23.1	12.2	5.5	NA				
	AMU-CURS 35	P4	24.1	13.9	18.1	14.1				
		M1	20.5	17.2	15.4	17				
		M2	16.6	16.9	?	?				
		M3	28.2	13.5	7.6	NA				
	MCNC 66–72 V	M3	15.1	9.1	6.7	NA				
P. insolita	MACN-Pv 13480	P4–M2	17	20.2	20.3	21.4				
	MACN-Pv 4068	P4–M2	21.5	22.2	19.6	21.8				
	MACN-Pv 3290	P4–M2					22.2	21.9	22	22.7
P. pattersoni	AMU-CURS 255	P4	21.3	13.5	12.8	?	21.4	11	11	?
		M1	19.2	16.6	14.8	?	18.6	13.2	14.4	?
		M2	17	16.2	14.1	?	18.5	15.5	15	?
		M3	33.5	14.3	6.4	NA	36.6	20.4	9.9	NA
	MCNC 12-72 V	M3	33.6	17.1	7.1	NA				
	AMU-CURS 39	P4	25.2	22.4	24.6	22.5	26.5	19.8	22.7	22.7
		M1	26.5	21	22.3	24.4	19.9	19.5	20.3	22.4
		M2	22.2	20	21	23.6	19.6	22.5	19.1	20.8
		M3	48	22.4	20.4	NA	49.3	22.4	13.3	NA
		p4					32.7	14.2	21.1	21.4
		m1					?	?	?	23.4
		m2					26	25.2	22.6	?
		m3					29.3	26.8	27.4	26.2

Table 2 continued

Taxon	Catalog number	Tooth	Left				Right			
			Length	Width			Length	Width		
			AP	AW	PW	MW	AP	AW	PW	MW
	AMU-CURS 53	P4	26.1	15.1	17.3	?	?	?	17.6	?
		M1	22.9	?	15.5	?	21.8	17.6	16	?
		M2	22	18.8	14	17.1	21.8	17.7	12.5	17
		M3	38.5	15	10.5	NA	42.3	18.4	9	NA
		p4	26.4	14.6	15.2	?				
		m1	25.9	14.9	13	?				
		m2	25.6	15.2	13.6	?				
		m3	26.4	15.5	11.4	?				
	AMU-CURS 454	p4	31.9	12.6	28.3	13.4				
		m1	23.5	18.2	20.4	21.4				
		m2	25.5	19.4	23.9	22.2				
		m3	27.5	24.1	17.5	?				
	AMU-CURS 170	p4					25.5	11.6	14.7	15.3
		m1					23.7	15.2	18.5	18.8
		m2					24.3	15.2	18.5	18.8
		m3					27.6	17.8	14.4	16.5
	MCNC 104–72 V	m3	36.9	22.4	22	26.6				
	UNEFM-VF 020[b]	P4					27.9	20.8		
		M1					20.6	21		
		M2					18.6	21		
		M3					41	20.7		
P. praecursor	MACN-Pv 9026	p4	28.7	11.8	22.2	19.4				
P. burmeisteri	MACN-A 5831 (Type)	P4–M2	21	23.8	26	31.4				
	MLP 15-254	p4					33.3	24.2	22.5	22.3
	MLP 15-257	p4					32.8	21.1	24.5	22
	MACN-Pv 4729	p4					30.8	12.8	19.5	20.2
	MLP 12-246	m1	23.8	20.3	21	20.5				
		m2	25.3	20.8	21.6	21.8				
		m3	32	22.2	23	21.2				
	MACN-Pv 2494	m3					36.8	24.4	28	28.8
	MACN-Pv 6620	m1–m3	28.6	20.5	22.5	20.4				
	MACN-Pv 3288	m1–m3					26.6	20.2	24	23.7
P. lozanoi	MLP 36[c]	M3	34	14.5	8.5	NA				
P. bordasi	AMNH 22666[f]	p4					16.4	4	13.3	13.7
		m1					16.5	12	14.5	15.7
P. minima	MACN-Pv 3461	P4–M2	13.7	12.8	12.7	15.7				
Neoepiblema sp.	MLP 73-I-10-2	P4–M2					11.7	9	10.5	9.9
	AMU-CURS 381	p4	22	15	14	14.6				
		m1	18.8	14.7	16.6	14.5				
		m2	18.3	17	18.6	19				
		m3	23.5	18.5	17	19.7				
	MLP 15-420a	m1–m3	10.3	5.8	7.7	8.3				
	MLP 15-419a	m1–m3	10.5	7.7	8.9	8.6				
	MLP 15-421	m1–m3	12.4	8.5	11.6	9.7				
	MLP 41-XII-13-4102	m1–m3					13.4	11.7	11.7	11.6

Table 2 continued

Taxon	Catalog number	Tooth	Left				Right			
			Length	Width			Length	Width		
			AP	AW	PW	MW	AP	AW	PW	MW
N. horridula	MACN-Pv 2609	P4					12.4	8.5	8.7	10.2
		M1					11.8	9.2	8	9.8
		M2					11.9	9.2	7.8	9.8
		M3					15.7	9	4.6	NA
	MLP 69-XII-2-20 (Type)	M3					12.6	5.6	7.2	NA
	MACN-Pv 13414	M3	14.9	8.8	5.9	NA				
	MACN-Pv 15318	M3					10	5.9	3.4	NA
	MLP 73-I-10-4	P4–M2					7.1	4	4.8	4.7
	MACN-Pv 13365	P4–M2	10.5	8	7.6	8.4				
	MACN-Pv 13362	P4–M2					10	7.9	9.4	10.2
	MACN-Pv 9036	P4–M2	11.6	8.9	7.4	8.6				
	MACN-Pv 4504	P4–M2	9.8	8.6	7.3	8.8				
	MACN A 5874	P4–M2	8	7.7	7.4	7.7				
	MACN-Pv 3458	P4–M2	11.5	8.5	7.9	8.6				
		M3	15.6	8.8	6.4	NA				
N. ambrossetianus	MACN-Pv 4575	P4–M2					12.4	13.7	20	17.3
	MACN-Pv 4580	m1					8.3	4.5	6.2	5.9
		m2					7.8	5.4	6.4	6.5
	MACN-Pv 13473 (Type)	m1	13.5	7.7	10.4	10				
		m2	15.1	8.3	11.4	11.6				
	MACN-Pv 4576	m1–m3					14.7	14.1	17.6	16
	MACN-Pv 4542	m1–m3					11	8.1	9.7	8.1
	MACN-Pv 4031	m1–m3					11.1	7.7	8.4	11.4
	MACN-Pv 8885	m1–m3	13.7	9.5	11.1	11.5				
	MACN-Pv 3404	m1–m3					12.1	9.2	11.4	11.2
	MACN-A 5829	m1–m3	8.8	6.4	7.3	7.2				
	MACN-A 5830	m1–m3	8.4	6.9	9.8	9.2				
	MACN-Pv 2484	m1–m3	11.3	7.4	8.9	8.6				
	MACN-Pv 4480	m1–m3					6	4	4.5	5
	MACN-Pv 3276	m1–m3	11.3	7.2	8.4	8.8				
	MPEG PV-82[d]	p4	15	9	10	12				
		m1	15.5		13					
		m2	15.1		12					
		m3	15.3	8	13					
	UFAC 4515[e]	P4	16	11.7	12	15	16	11.8	12	15.2
		M1	15	12.8	14.4	11	15	13.1	11.5	14.7
		M2	15	13.1	12	14.6	15	12.8	12	14.2
		M3	22.2	12.2	10.2	NA	22	11.5	10.4	NA
	UFAC 1716[a]	M2					14	10.5		
		M3					21	10		
		p4	13.5	10						
		m1	12.5	11						
		m2	13	17						
		m3	10	11						
	UFAC 1490[a]	p4					16	9		
		m1					13.5	10		
		m2					13.5	10		
		m3					15.5	11		

Table 2 continued

Taxon	Catalog number	Tooth	Left				Right			
			Length	Width			Length	Width		
			AP	AW	PW	MW	AP	AW	PW	MW
	UFAC 1658[a]	p4	17	11						
	UFAC 1810[a]	p4					16	11.5		
		m1					16	13.5		
		m2					16	12		
		m3					19	11		

AP anterior-posterior length, *AW* anterior width, *PW* posterior width, *MW* medium width, *NA* not applicable

[a] Bocquentin-Villanueva et al. (1990)

[b] Horovitz et al. (2006)

[c] Kraglievich (1940)

[d] Mones and Toledo (1989)

[e] Negri and Ferigolo (1999)

[f] Patterson (1942)

neoepiblemids (Fig. 3e). The preservation prevents observing the morphology of laminae in M2. AMU-CURS 161 presents a strong diagenetic compression in the dorso-ventral plane and its bad preservation prevents observing most of the cranial sutures. The skull is long and narrow, with conspicuous sagittal and nuchal crests (Fig. 4). AMU-CURS 161 shares some traits with *Neoepiblema* such as the ventral root of the zygomatic process at the level of P4, and palatines present at the level of the middle portion of M3; these traits were included in the generic diagnosis of *Neoepiblema* by Negri and Ferigolo (1999), but they are also present in *P. pattersoni* (e.g., AMU-CURS 255, see below).

AMU-CURS 161 shares some traits with *N. ambrosettianus,* including: premaxilar elongated forming more than half of the diastema and a prominent sagittal crest projecting over the other elements of the cranium (Negri and Ferigolo 1999). The presence of a sagittal crest in a specimen originally referred to *P. pattersoni* by Bondesio, and Bocquentin-Villanueva (1988) (CIAAP 1438) was also mentioned by Horovitz et al. (2006), who referred the specimen to cf. *Phoberomys* while highlighting several differences between CIAAP 1438 and other specimens of *P. pattersoni*.

Phoberomys pattersoni, Mones 1980

Material AMU-CURS 255, complete cranium compressed in the dorsal-ventral plane and the anterior portion of the rostrum folded toward the lateral right plane. AMU-CURS 53, maxilla with right and left P4–M3 and partial left dentary with p4–m3. AMU-CURS 454, partial left mandible ramus with p4–m3, poorly preserved. AMU-CURS 170, a complete mandible with right and left p4–m3.

Provenance AMU-CURS 255 comes from El Picache, Urumaco Formation, upper member; AMU-CURS 39 and AMU-CURS 53 are from El Mamón, Urumaco Formation, upper member; AMU-CURS 454 comes from Cerro Jose La Paz (11°14′40″N, 70°09′44.3″W), Urumaco Formation, upper member and AMU-CURS 170 comes from Tío Gregorio, Urumaco Formation, upper member (Fig. 2).

Description AMU-CURS 255 is assigned to *P. pattersoni* based on the M3 with seven laminae connected labially (Fig. 3g) (Mones 1980; Bondesio and Bocquentin-Villanueva 1988) and the narrowing of the posterior portion of M3 at the level of the last three laminae (Mones 1980; Sánchez-Villagra et al. 2003). The P4–M2 have three laminae connected labially. The third lamina of P4 is concave anteriorly and has a "V" shape inflexion in its inner portion (Bondesio and Bocquentin-Villanueva 1988) (Fig. 3g). AMU-CURS 255 also presents a strong diagenetic distortion; it is compressed in the dorso-ventral plane, and the most anterior portion of the rostrum is folded toward the right lateral side (Fig. 4). Due to the preservation it is not possible to observe the cranial sutures. The skull does not show a well-developed sagittal crest as has been mentioned before for *P. pattersoni* (Sánchez-Villagra et al. 2003) and in contrast to *N. ambrossetianus* (Negri and Ferigolo 1999) and cf. *Phoberomys* (Horovitz et al. 2006). It is possible that the degree of development of the sagittal crest is related to age. AMU-CURS 255 has the anterior root of the zygomatic arch at the level of P4 as in *N. ambrossetianus* (Negri and Ferigolo 1999) and cf. *Phoberomys* (Horovitz et al. 2006).

AMU-CURS 53 is also assigned to *P. pattersoni* based on the number of laminae and morphology of the M3 (Fig. 3i). The P4–M2 have three laminae all connected

labially, as in all neoepiblemids. Although the specimen consists of a complete lower left dentition, the preservation of the specimen prevents the examination of diagnostic features of *P. pattersoni* in the p4. The m1–m3 have three laminae, apparently all free. AMU-CURS 454 and AMU-CURS 170 are identified as *P. pattersoni* based on the p4 morphology with four laminae, the two anterior ones connected labially and m1–m3 with three laminae, all free (Fig. 3c, d) (Bondesio and Bocquentin-Villanueva 1988). In AMU-CURS 53 and AMU-CURS 170, the mandibular symphysis extends posteriorly, reaching the anterior portion of the p4.

Quantitative analysis

The relationship between the anteroposterior length (AP) and anterior width (AW) of the upper and lower dentition in *Phoberomys* and *Neoepiblema* is different in the two genera, with *Neoepiblema* having a lower length to width ratio than *Phoberomys*, although the two taxa are within the same trajectory (Fig. 5a–d). For *Neoepiblema* we found that *N. horridula* is smaller than *N. ambrossetianus* and the dental morphospace of the two species does not overlap (Fig. 5a, b). Within *Phoberomys*, there is no clear differentiation of the dental morphospace among species (Fig. 5a–d).

For the M3 (Fig. 5a), there are two specimens assigned to *Phoberomys* sp. B (MCN 66–72 V and AMU-CURS 380), which overlaps with *Neoepiblema*; besides its small size, these specimens have six laminae in the M3. For the P4–M2 (Fig. 5b) and lower dentition (Fig. 5c, d), there is also a small overlap between the two genera. However, the overall pattern is the same, with *Neoepiblema* being smaller than *Phoberomys* and both genera falling within the same trajectory.

Discussion

Most of the neoepiblemid species currently recognized as valid are known from isolated or fragmentary upper or lower dentitions (for a summary of the systematic history of Neoepiblemidae, see Bondesio and Bocquentin-Villanueva, 1988: 32–33 and Negri and Ferigolo, 1999: 8–12). The most important characteristics considered for species definition within the group have been the number and morphology of laminae in premolars and molars and the relative molar size (e.g., Kraglievich 1940; Mones 1980; Patterson 1942). However, rodents with euhypsodont teeth have a wide range of ontogenetic and intraspecific morphological variation (Vucetich et al. 2005), which calls for caution for the definition of new taxa based on fragmentary material without an appropriate sample size. We found for example that the pattern of labial connections among the laminae in m1–m3 is a variable character in *Phoberomys* and *Neoepiblema* and should not be used as a characteristic to differentiate the two genera.

Until now, *P. pattersoni* and *Eumegamys* were the only big rodent taxa formally reported for the Urumaco Formation. We found evidence to support the recognition of a higher diversity of giant rodents from Urumaco and report for the first time the presence of *Neoepiblema* in this Formation. Vucetich et al. (2010c) reported *Neoepiblema* sp. for the San Gregorio Formation (late Pliocene) toward the top of the Urumaco sequence from an assemblage that also includes hydrochoerids and an octodontoid. The record of *Neoepiblema* in the Urumaco Formation confirms the presence of this taxon in the northern Neotropics since the late Miocene. The oldest record of *Neoepiblema* comes from the middle Miocene Fitzcarrald fauna (Tejada-Lara et al. 2015). Until now, no rodents from the Socorro Formation (middle Miocene) in the Uumaco sequence had been reported. In an expedition in January 2015, one of us (MRS-V) found a distal femur (AMU-CURS 641) of a giant rodent from the Socorro Formation. It is from East of Capirote (11°11′32.9″N, 70°11′22.4″W), the road to Quebrada Honda, the same locality reported by Head et al. (2006: 234) for snakes.

Previous work in the late Miocene deposits of Acre, in southern Brazil and Paraná, and in northern Argentina shows a high diversity of rodents. Given the postulated similarity of the Urumaco mammal assemblage with the Acre and, to a lesser extent, the Paraná assemblages (Cozzuol 2006; Carrillo et al. 2015), a higher diversity than recognized until now for Urumaco was only expected. This conclusion is supported by the previous study of morphological diversity in postcranial remains (Geiger et al. 2013).

The length-width relationship in the dentition shows a differentiation between the two neoepiblemid genera, with *Neoepiblema* having a lower length-to-width ratio than *Phoberomys.* Within *Neoepiblema, N. horridula* is smaller than *N. ambrossetianus*, and there is no overlap between the two species. In the case of *Phoberomys*, there is not a clear differentiation among the different species recognized within the genus, and they overlap along the trajectory of the dental morphospace, suggesting that some of these species could represent different ontogenetic stages of one or few taxa within *Phoberomys,* as has also been proposed for hydrochoerids (Vucetich et al. 2005; Deschamps et al. 2013). The possibility that the number of neoepiblemid species is lower than currently recognized has also been raised by other authors (Vucetich et al. 2010c; Nasif et al. 2013).

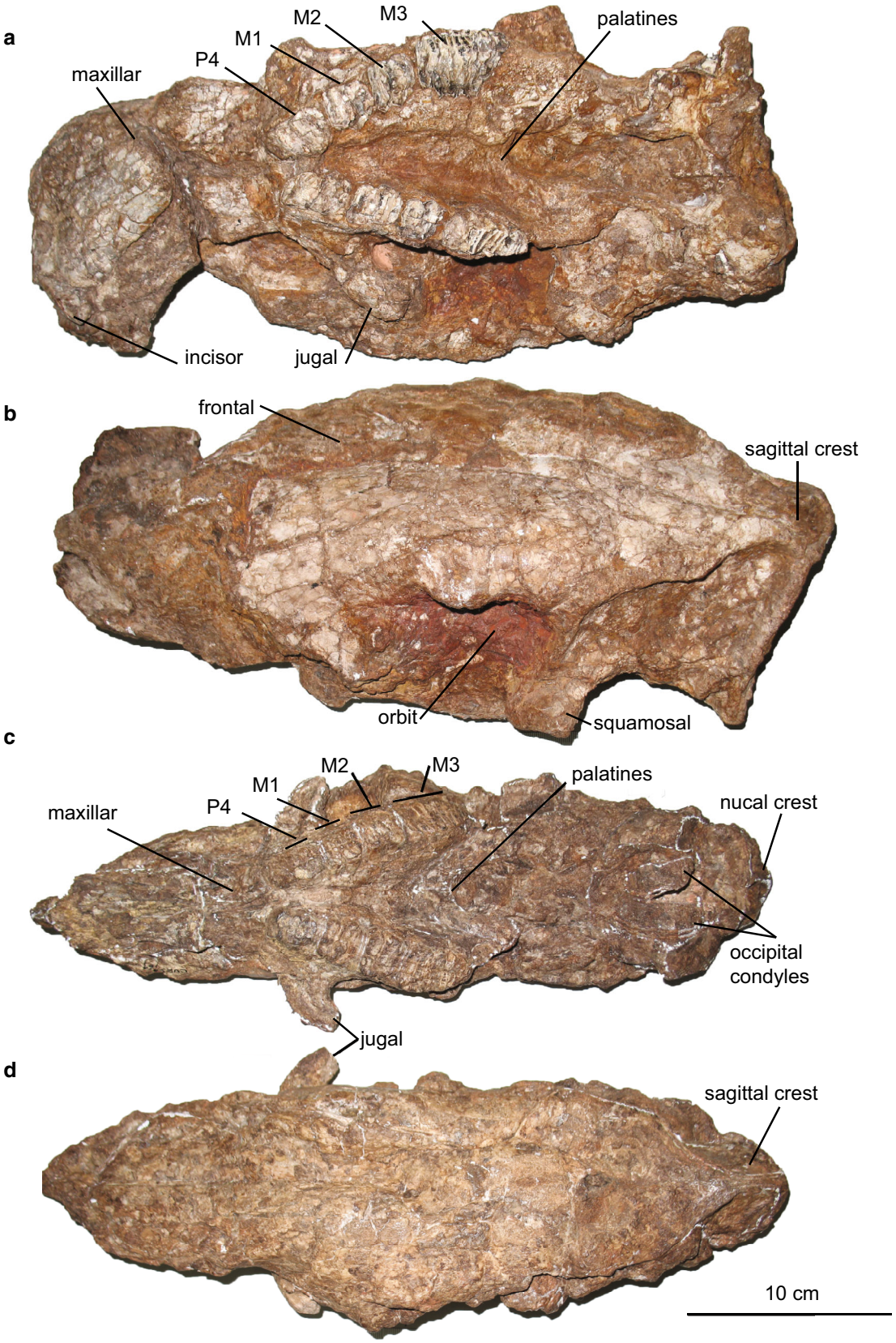

Fig. 4 Neoepiblemid skulls from Urumaco. *P. pattersoni* (AMU-CURS 255) **a** ventral view; **b** dorsal view. *Phoberomys* sp. (AMU-CUS 161) **c** ventral view; **d** dorsal view

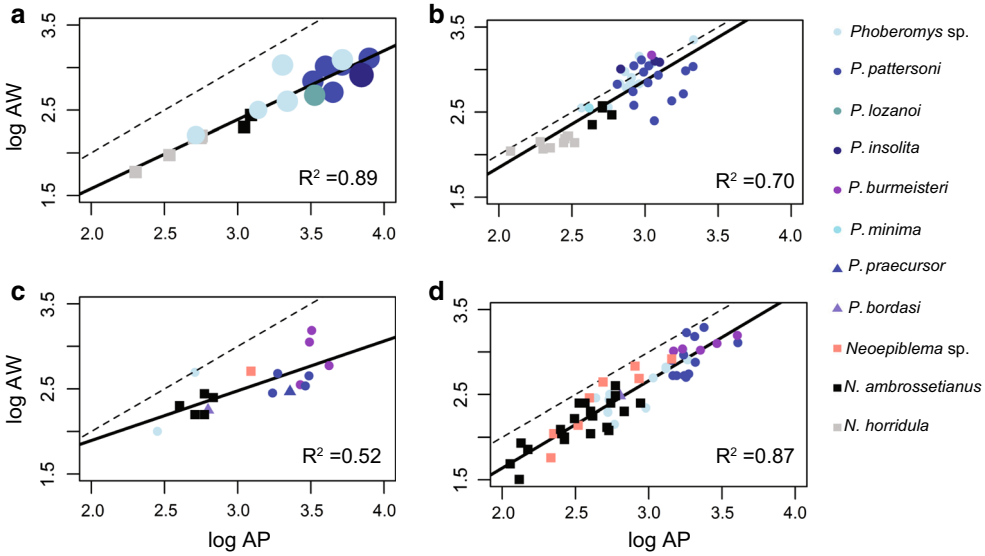

Fig. 5 Length-width relationship of the upper and lower dentition in Neoepiblemidae. **a** M3, the dot size is proportional to the number of laminae. **b** P4-M2. **c** p4, the dot size is proportional to the number of laminae. **d** m1-m3; *log AW* logarithm of anterior width, *log AP* logarithm of anterposterior length. *Solid line* regression line for log AW vs. log AP, R^2 value indicated in each panel; *dashed line* isometric line

In the upper dentition the M3 has been used to differentiate the different species of neoepiblemids (Table 1). The case of three small specimens referred to *Phoberomys* sp. B (AMU-CURS 380, AMU-CURS 35 and MCN 66–72 V) is interesting because they have six laminae on M3. The number of laminae on the M3 for *Phoberomys* ranges between seven and eight (Bondesio and Bocquentin-Villanueva 1988), and *Neoepiblema* has four laminae (Negri and Ferigolo 1999). We interpret the existence of six laminae in the M3 of small specimens assigned to *Phoberomys* as an indication of either the possibility of addition of at least one laminae in the M3 during growth or as a higher variability in this area of dental anatomy than currently recognized.

Conclusion

A higher diversity of giant rodents in the Urumaco Formation is reported with the finding of *Neoepiblema* sp. There have been questions about the validity of the several neoepiblemid species currently recognized. Our dental and quantitative analysis of Neoepiblemidae shows a differentiation between *Phoberomys* and *Neoepiblema*, although both genera fall within the same trajectory. Within *Neoepiblema*, *N. horridula* is smaller than *N. ambrossetianus*; the differentiation on size between the two species of *Neoepiblema* suggest that they are both valid taxa. In contrast, in *Phoberomys* there is not a clear differentiation among the different species recognized for the genus, suggesting that some could represent different ontogenetic stages of one or a few taxa.

Acknowledgments We thank the authorities at the Instituto del Patrimonio Cultural of the Republica Bolivariana de Venezuela and the Alcaldía Municipio de Urumaco for their generous support. Gina Ojeda (CIAAP-UNEFM), Hyram Moreno (MCNC), A. Kramarz (MACN) and M. Reguero (MLP) provided access to the collections under their care. We are thankful to R. Sánchez, A.A. Carlini and J.D. Carrillo-Briceño for their support and help during fieldwork in Urumaco and T. Scheyer and C. Kolb for help and advice with the teeth sectioning, and J.D. Carrillo-Briceño for geographic information. C. Kolb helped with the German abstract. We dedicate this work to Rodolfo Sánchez, to honor his more than 30 years of palaeontological exploration in Urumaco. He kindly provided stratigraphic information on most of the specimens reported here. We thank M.G Vucetich, C. Deschamps (La Plata) and members of the group of Evolutionary Morphology and Paleobiology of Vertebrates (Zurich) for their comments and discussions as well as M.E. Pérez and an anonymous reviewer for valuable comments that helped to improve the manuscript. J.D. Carrillo was supported by Swiss National Fund SNF 31003A-149605 to M.R. Sánchez-Villagra.

References

Ameghino, F. 1889. Contribución al conocimiento de los mamíferos fósiles de la República Argentina. *Boletín de la Academia Nacional de Ciencias de Córdoba* 6: 1–127.

Antoine, P.-O., L. Marivaux, D.A. Croft, G. Billet, M. Ganerod, C. Jaramillo, T. Martin, et al. 2012. Middle Eocene rodents from Peruvian Amazonia reveal the pattern and timing of caviomorph origins and biogeography. *Proceedings of the Royal Society B: Biological Sciences* 279(1732): 1319–1326. doi:10.1098/rspb.2011.1732.

Bennett, E.T. 1833. On the Chinchillidae, a family of herbivorous Rodentia, and on a new genus referrible to it. *The Transactions of the Zoological Society of London* 1(1): 35–64. doi:10.1111/j.1096-3642.1835.tb00602.x.

Blanga-Kanfi, S., H. Miranda, O. Penn, T. Pupko, R.W. DeBry, and D. Huchon. 2009. Rodent phylogeny revised: analysis of six

nuclear genes from all major rodent clades. *BMC Evolutionary Biology* 9: 71. doi:10.1186/1471-2148-9-71.

Bocquentin-Villanueva, J., J.P. Souza-Filho, and F.R. Negri. 1990. Neoepiblema acreensis, sp. n. (Mammalia, Rodentia) do Neógeno do Acre, Brasil. *Bol Mus Para Emílio Goeldi, sér Ciencias* 2: 65–72.

Bondesio, P., and J. Bocquentin-Villanueva. 1988. Novedosos restos de Neoepiblemidae (Rodentia, Hytricognathi) del Mioceno tardío de Venezuela: inferencias paleoambientales. *Ameghiniana* 25(1): 31–37.

Bowdich, T.E. 1821. *An analysis of the natural classifications of Mammalia for the use of students and travelers*. Paris: Smith.

Campbell, K.E. 2004. The Paleogene mammalian fauna of Santa Rosa, Amazonia Perú. *Natural History Museum of Los Angeles County, Sciences Series* 40: 1–163.

Carrillo, J.D., A. Forasiepi, C. Jaramillo, and M.R. Sánchez-Villagra. 2015. Neotropical mammal diversity and the Great American biotic interchange: spatial and temporal variation in South America's fossil record. *Frontiers in Genetics* 5: 451. doi:10.3389/fgene.2014.00451.

Cione, A.L., M.M. Azpelicueta, M. Bond, A.A. Carlini, J.R. Casciotta, M.A. Cozzuol, M. de la Fuente, et al. 2000. Miocene vertebrates from Entre Ríos province, eastern Argentina. *Insugeo, Serie de Correlación Geológica* 14: 191–237.

Cozzuol, M.A. 2006. The Acre vertebrate fauna: age, diversity, and geography. *Journal of South American Earth Sciences* 21(3): 185–203. doi:10.1016/j.jsames.2006.03.005.

Deschamps, C.M., I. Olivares, E.C. Vieytes, and M.G. Vucetich. 2007. Ontogeny and diversity of the oldest capybaras (Rodentia: Hydrochoeridae; late Miocene of Argentina). *Journal of Vertebrate Paleontology* 27(3): 683–692. doi:10.1671/0272-4634(2007)27[683:OADOTO]2.0.CO;2.

Deschamps, C.M., M.G. Vucetich, C.I. Montalvo, and M.A. Zárate. 2013. Capybaras (Rodentia, Hydrochoeridae, Hydrochoerinae) and their bearing in the calibration of the late Miocene–Pliocene sequences of South America. *Journal of South American Earth Sciences* 48: 145–158. doi:10.1016/j.jsames.2013.09.007.

Fabre, P.-H., L. Hautier, D. Dimitrov, and E.P. Douzery. 2012. A glimpse on the pattern of rodent diversification: a phylogenetic approach. *BMC Evolutionary Biology* 12(1): 88.

Flynn, J.J., R. Charrier, D.A. Croft, P.B. Gans, T.M. Herriott, J.A. Wertheim, and A.R. Wyss. 2008. Chronologic implications of new Miocene mammals from the Cura-Mallín and Trapa Trapa formations, Laguna del Laja area, south central Chile. *Journal of South American Earth Sciences* 26: 412–423. doi:10.1016/j.jsames.2008.05.006.

Geiger, M., L.A.B. Wilson, L. Costeur, R. Sánchez, and M.R. Sánchez-Villagra. 2013. Diversity and body size in giant caviomorphs (Rodentia) from the northern Neotropics—a study of femoral variation. *Journal of Vertebrate Paleontology* 33(6): 1449–1456. doi:10.1080/02724634.2013.780952.

Head, J.J., M.R. Sánchez-Villagra, and O.A. Aguilera. 2006. Fossil snakes from the Neogene of Venezuela (Falcón State). *Journal of Systematic Palaeontology* 4(3): 233–240. doi:10.1017/S1477201906001866.

Horovitz, I., M.R. Sánchez-Villagra, T. Martin, and O.A. Aguilera. 2006. The fossil record of *Phoberomys pattersoni* Mones 1980 (Mammalia, Rodentia) from Urumaco (Late Miocene, Venezuela), with an analysis of its phylogenetic relationships. *Journal of Systematic Palaeontology* 4(03): 293–306. doi:10.1017/S1477201906001908.

Horovitz, I., M.R. Sánchez-Villagra, M.G. Vucetich, and O.A. Aguilera. 2010. Fossil rodents from the late Miocene Urumaco and middle Miocene Cumaca Formations, Venezuela. In *Urumaco and Venezuelan paleontology. The fossil record of the Northern Neotropics. Life of the past*, ed. M.R. Sánchez-Villagra, O.A. Aguilera, and A.A. Carlini, 214–232. Bloomington and Indianapolis: Indiana University Press.

Huchon, D., P. Chevret, U. Jordan, C.W. Kilpatrick, V. Ranwez, P.D. Jenkins, J. Brosius, and J. Schmitz. 2007. Multiple molecular evidences for a living mammalian fossil. *Proceedings of the National Academy of Sciences* 104(18): 4795–7499. doi:10.1073/pnas.0701289104.

Kay, R.F., R.H. Madden, R.L. Cifelli, and J.J. Flynn. 1997. *Vertebrate paleontology in the neotropics. The Miocene fauna of La Venta, Colombia*. Washington and London: Smithsonian Institution Press.

Kerber, L., F.R. Negri, A.M. Ribeiro, M.G. Vucetich, and J.P. De Souza-Filho. 2015. Late Miocene potamarchine rodents from southwestern Amazonia, Brazil, with description of new taxa. *Acta Palaeontologica Polonica*. doi:10.4202/app.00091.2014 (in press).

Kraglievich, L. 1926. Los grandes roedores terciarios de la Argentina y sus relaciones con ciertos géneros pleistocenos de Las Antillas. *Anales del Museo Nacional de Historia Natural* 34: 121–235.

Kraglievich, L. 1932. Diagnosis de nuevos géneros y especies de roedores cávidos y eumegámidos fósiles de Argentina. *Anales de la Sociedad Cientifica Argentina* 114:155–181 and 211–237.

Kraglievich, L. 1940. Descripción detallada de diversos roedores argentinos terciarios clasificados por el autor. In: A. Torcelli and C.A. Marelli (eds), Obras completas y trabajos científicos inéditos de Lucas Kraglievich. Obras de Geología y Paleontología 2: 297–330.

Kramarz, A.G., and E.S. Bellosi. 2005. Hystricognath rodents from the Pinturas Formation, Early–Middle Miocene of Patagonia, biostratigraphic and paleoenvironmental implications. *Journal of South American Earth Sciences* 18: 199–212. doi:10.1016/j.jsames.2004.10.005.

Kramarz, A.G., M.G. Vucetich, and M. Arnal. 2013. A new early Miocene chinchilloid Hystricognath rodent; an approach to the understanding of the early chinchillid dental evolution. *Journal of Mammalian Evolution* 20(3): 249–261. doi:10.1007/s10914-012-9215-0.

Linares, O.J. 2004. Bioestratigrafía de la fauna de mamíferos de las Formaciones Socorro, Urumaco y Codore (Mioceno medio-Plioceno temprano) de la región de Urumaco, Falcón, Venezuela. *Paleobiologia Neotropical* 1: 1–26.

MacFadden, B.J. 2006. Extinct mammalian biodiversity of the ancient New World tropics. *Trends in Ecology and Evolution* 21(3): 157–165. doi:10.1016/j.tree.2005.12.003.

MacPhee, R.D.E. 2011. Basicranial morphology and relationships of Antillean Heptaxodontidae (Rodentia, Ctenohystrica, Caviomorpha). *Bulletin of the American Museum of Natural History*. doi:10.1206/0003-0090-363.1.1.

MacPhee, R. D. E., and C. Flemming. 2003. A possible Heptaxodontine and other Caviidan rodents from the Quaternary of Jamaica. *American Museum Novitates*:1-42. doi:10.1206/0003-0082(2003)422<0001:APHAOC>2.0.CO;2.

Mares, M.A., and R.A. Ojeda. 1982. Patterns of diversity and adaptation in South American hystricognath rodents. In *Mammalian Biology in South America*, eds. M.A. Mares, and H. Genoways, 393–432. The University of Pittsburgh. Special Publication Series (PymItuning Laboratory of Ecology).

Millien, V., and H. Bovy. 2010. When teeth and bones disagree: body mass estimation of a giant extinct rodent. *Journal of Mammalogy* 91(1): 11–18. doi:10.1644/08-MAMM-A-347R1.1.

Mones, A. 1980. Un neoepiblemidae del Plioceno medio (Formación Urumaco) de Venezuela (Mammalia: Rodentia: Caviomorpha). *Ameghiniana* 17(3): 277–279.

Mones, A., and P.M. Toledo. 1989. Primer hallazdo de Euphilus Ameghino, 1889 (Mammalia: Rodentia: Neoepiblemidae) en el Neogeno del Estado de Acre, Brasil. *Comunicaciones*

Paleontologicas del Museo de Historia Natural de Montevideo 21(2): 1–15.

Moreno, J.F., A.J.W. Hendy, L. Quiroz, N. Hoyos, D.S. Jones, V. Zapata, S. Zapata, et al. 2015. Revised stratigraphy of Neogene strata in the Cocinetas basin, La Guajira, Colombia. *Swiss Journal of Paleontology* 134(1): 1–39. doi:10.1007/s13358-015-0071-4.

Nasif, N.L., A.M. Candela, L. Rasia, M.C. Madozzo-Jaén, and R. Bonini. 2013. Actualización del conocimiento de los roedores del Mioceno tardío de la Mesopotamia argentina: aspectos sistemáticos, evolutivos y paleobiogeográficos. *Ascociación Paleontológica Argentina, Publicación Especial* 14: 153–169.

Negri, F.R., and J. Ferigolo. 1999. Anatomia craniana de *Neoepiblema ambrosettianus* (Ameghino, 1889) (Rodentia, Caviomorpha, Neoepiblemidae) do Mioceno Superior-Plioceno, Estado do Acre, Brasil e revisao das especies do genero. *Boletim do Museu Paraense Emilio Goeldi, Série Ciências da Terra* 11: 1–80.

Opazo, J.C. 2005. A molecular timescale for caviomorph rodents (Mammalia, Hytricognathi). *Molecular Phylogenetics and Evolution* 37(3): 932–937. doi:10.1016/j.ympev.2005.05.002.

Pascual, R., and M.L. Díaz de Gamero. 1969. Sobre la presencia del género *Eumegamys* (Rodentia, Caviomorpha) en la Formación Urumaco del Estado Falcón (Venezuela). *Su significación cronológica Asociación Venezolana de Geología, Minas y Petróleo, Boletín Informativo* 12: 367–388.

Patterson, B. 1942. Two tertiary mammals from northern South America. *American Museum Novitates* 1173: 1–7.

Pérez, M.E., and D. Pol. 2012. Major radiations in the evolution of caviid rodents: reconciling fossils, ghost lineages, and relaxed molecular clocks. *PLoS One* 10: e48380. doi:10.1371/journal.pone.0048380.

Quiroz, L., and C. Jaramillo. 2010. Stratigraphy and sedimentary environments of Miocene shallow to marginal marine deposits in the Urumaco trough, Falcón Basin, Western Venezuela. In *Urumaco and Venezuelan paleontology. The fossil record of the Northern Neotropics*, ed. M.R. Sánchez-Villagra, O.A. Aguilera, and A.A. Carlini, 153–172. Bloomington and Indianapolis: Indiana University Press.

R Core Team. 2014. R: a language and environment for statistical computing. R Foundation for Statistical Computing, Vienna, Austria. http://www.R-project.org/. Accessed 8 Sep 2014.

Ribeiro, A.M., R.H. Madden, F.R. Negri, L. Kerber, A.S. Hsiou, and K.A. Rodrigues. 2013. Mamíferos fósiles y biocronología en el suroeste de la Amazonia, Brasil. *Asociación Paleontológica Argentina, Publicación Especial* 14: 207–221.

Rinderknecht, A., and R.E. Blanco. 2008. The largest fossil rodent. *Proceedings of the Royal Society B: Biological Sciences* 275(1637): 923–928. doi:10.1098/rspb.2007.1645.

Sánchez-Villagra, M.R., O. Aguilera, and I. Horovitz. 2003. The anatomy of the world's largest extinct rodent. *Science* 301(5640): 1708–1710. doi:10.1126/science.1089332.

Sánchez-Villagra, M.R., O.A. Aguilera, and A.A. Carlini. 2010. *Urumaco and Venezuelan paleontology. The fossil record of the Northern Neotropics. Life of the past*. Bloomington and Indianapolis: Indiana University Press.

Scheyer, T.M., O.A. Aguilera, M. Delfino, D.C. Fortier, A.A. Carlini, R. Sánchez, J.D. Carrillo-Briceno, L. Quiroz, and M.R. Sánchez-Villagra. 2013. Crocodylian diversity peak and extinction in the late Cenozoic of the northern Neotropics. *Nature communications* 4: 1907. doi:10.1038/ncomms2940.

Silva Taboada, G., W. Suárez Duque, and D.F. Stephen. 2007. *Compendio de los mamíferos terrestres autóctonos de Cuba vivientes y extinguidos*. La Habana: Museo Nacional de Historia Natural.

Tejada-Lara, J., R. Salas-Gismondi, F. Pujos, M. Baby, M. Benammi, S. Brusset, D. De Franceschi, N. Espurt, M. Urbina, and P.-O. Antoine. 2015. Life in proto-Amazonia: middle Miocene mammals from the Fitzcarrald Arch (Peruvian Amazonia). *Palaeontology* 58(2): 341–378. doi:10.1111/pala.12147.

Tullberg, T. 1889. Über das System der Nagetiere, eine phylogenetische Studie. *Nova Acta Regiae Societatis Scientiarum Upsalensis* III:1–514.

Upham, N.S., and B.D. Patterson. 2012. Diversification and biogeography of the Neotropical caviomoprh lineage Octodontoidea (Rodentia: Hytricognathi). *Molecular Phylogenetics and Evolution* 63: 417–429. doi:10.1016/j.ympev.2012.01.020.

Voloch, C.M., J.F. Vilela, L. Loss-Oliveira, and C.G. Schrago. 2013. Phylogeny and chronology of the major lineages of New World hystricognath rodents: insights on the biogeography of the Eocene/Oligocene arrival of mammals in South America. *BMC Research Notes* 6: 160. doi:10.1186/1756-0500-6-160.

Vucetich, M.G., M.M. Mazzoni, and U.F.J. Pardiñas. 1993. Los roedores de la Formación Collón Curá (Mioceno Medio) y la ignimbrita Pilcaniyeu, Cañadón del Tordillo, Neuquén. *Ameghiniana* 30(4): 361–381.

Vucetich, M.G., D.H. Verzi, and J.-L. Hartenberger. 1999. Review and analysis of the radiation of the South American Hystricognathi (Mammalia, Rodentia). *Comptes Rendus de l'Academie des Sciences* 329: 763–769.

Vucetich, M.G., C.M. Deschamps, A.I. Olivares, and M.T. Dozo. 2005. Capybaras, size, shape, and time: a model kit. *Acta Palaeontologica Polonica* 50(2): 259–272.

Vucetich, M.G., E.C. Vieytes, M.E. Pérez, and A.A. Carlini. 2010a. The rodents from La Cantera and the early evolution of caviomorphs in South America. In *The paleontology of Gran Barranca*, ed. R.H. Madden, A.A. Carlini, M.G. Vucetich, and R.F. Kay, 193–205. Cambridge: University of Cambridge Press.

Vucetich, M.G., A.G. Kramarz, and A.M. Candela. 2010b. Colhuehuapian rodents from Gran Barranca and other Patagonian localities: state of the art. In *The paleontology of Gran Barranca*, ed. R.H. Madden, A.A. Carlini, M.G. Vucetich, and R.F. Kay, 206–219. Cambridge: University of Cambridge Press.

Vucetich, M.G., A.A. Carlini, O. Aguilera, and M.R. Sánchez-Villagra. 2010c. The tropics as reservoir of otherwise extinct mammals: the case of rodents from a new Pliocene faunal assemblage from Northern Venezuela. *Journal of Mammalian Evolution* 17(4): 265–273. doi:10.1007/s10914-010-9142-x.

Vucetich, M.G., M.T. Dozo, M. Amal, and M.E. Pérez. 2014. New rodents (Mammalia) from the late Oligocene of Cabeza Blanca (Chubut) and the first rodent radiation in Patagonia. *Historical Biology* 27(2): 236–257. doi:10.1080/08912963.2014.883506.

Weisbecker, V., and S. Schmid. 2007. Autopodial skeletal diversity in hystricognath rodents: functional and phylogenetic aspects. *Mammalian biology—Zeitschrift für Säugetierkunde* 72(1): 27–44. doi:10.1016/j.mambio.2006.03.005.

Wood, A.E., and B. Patterson. 1959. The rodents of the Deseadan Oligocene of Patagonia and the beginnings of South American rodent evolution. *Bulletin of the Museum of Comparative Zoology* 120: 281–428.

CHAPTER 4

The Neogene record of northern South American native ungulates

Life reconstruction of the San Gregorio Formation faunal assemblage, Falcón basin
Artwork: Stjepan Lukac

Juan D. Carrillo, Eli Amson, Carlos Jaramillo, Rodolfo Sánchez, Luis Quiroz, Carlos Cuartas, and Marcelo R. Sánchez-Villagra. Formated for *Smithsonian Contributions to Paleobiology*

THE NEOGENE RECORD OF NORTHERN SOUTH AMERICAN NATIVE UNGULATES

Juan D. Carrillo

Paläontologisches Institut und Museum, Universität Zürich

Karl-Schmid-Strasse 4, 8006 Zurich, Switzerland

juan.carrillo@pim.uzh.ch

Eli Amson

Humboldt-Universität, AG Morphologie und Formengeschichte, Bild Wissen Gestaltung ein interdisziplinäres Labor & Institut für Biologie

Philippstrasse 12/13, D-10115, Berlin, Germany

eli.amson@hu-berlin.de

Carlos Jaramillo

Smithsonian Tropical Research Institute

Apartado 0843-03092, Balboa, Ancon, Panama

jaramilloc@si.edu

Rodolfo Sánchez

Museo Paleontológico de la Alcaldía de Urumaco

rodolfosanchez128@gmail.com

Luis Quiroz

Department of Geological Sciences, University of Saskatchewan, Saskatoon, Saskatchewan S7N 5E2, Canada

luisignacioquiroz@gmail.com

Carlos Cuartas

Smithsonian Tropical Research Institute

Apartado 0843-03092, Balboa, Ancon, Panama

carlcuartas@gmail.com

Marcelo R. Sánchez-Villagra

Paläontologisches Institut und Museum, Universität Zürich

Karl-Schmid-Strasse 4, 8006 Zurich, Switzerland

m.sanchez@pim.uzh.ch

Abstract

South America was isolated during most of the Cenozoic and it was home to an endemic fauna. The South American Native Ungulates (SANUs) exhibited high taxonomical, morphological and ecological diversity, and they were widely distributed on the continent. However, most SANU fossil records come from high latitudes. This sampling bias challenges the study of their diversity dynamics and biogeography during important tectonic and biotic events, such as the Great American Biotic Interchange, the faunal exchange between North and South America after the formation of the Isthmus of Panama. We describe new SANU remains from the Neogene of the Cocinetas (northern Colombia) and Falcón (northwestern Venezuela) basins. In the Cocinetas basin, the middle Miocene fauna of the Castilletes Formation includes *Hilarcotherium miyou* sp. nov. (Astrapotheriidae), cf. *Huilatherium* (Leontiniidae), and *Neodolodus* cf. *colombianus* (Proterotheriidae). The late Pliocene fauna of the Ware Formation includes a Toxodontinae indet. and the putative oldest record of Camelidae in South America. In the Falcón basin, the Pliocene/Pleistocene faunas of the Codore and San Gregorio Formations include *Falcontoxodon aguilerai* gen. et sp. nov. and Proterotheriidae indet. We provide a phylogenetic analysis for Astrapotheriidae and Toxodontidae. The new data document a tropical provinciality within some SANU clades (e.g., Astrapotheriidae, Leontiniidae, Proterotheriidae) during the middle Miocene. This contrasts with the wide latitudinal distribution of clades of other mammals previously reported, including the sparassodont *Lycopsis padillai* and the sloth *Hyperleptus*?. The Pliocene/Pleistocene tropical faunas from northern South America are characterized by the predominance of native taxa, despite

their proximity to the Isthmus of Panama (which was fully emerged by that time). Only one North American ungulate herbivore immigrant is present, a Camelidae indet. The Pliocene and early Pleistocene faunas document an important landscape change in the region and suggest that environmental changes and biotic interactions affected the diversity dynamics and biogeographic patterns of SANUs during the Great American Biotic Interchange.

Table of contents

LIST OF TABLES

LIST OF FIGURES

Ages and the chronology of the Cocinetas and Falcón basins.

2. Geographic location of the Cocinetas and Falcón basins.

3. Geographic and stratigraphic occurrence of South American Native Ungulates in the Cocinetas basin.

4. Geographic and stratigraphic occurrence of *Falcontoxodon* gen. nov. and Proterotheriidae in the Falcón basin.

5. Mandible of *Hilarcotherium miyou* sp. nov. (Uruguaytheriinae, Astrapotheria).

6. Mandible of *Xenastrapotherium christi* (Uruguaytheriinae, Astrapotheria).

7. Partial skull and mandibular symphysis of *Hilarcotherium miyou* sp. nov.

8. Bivariate plots with dental measurements of Uruguaytheriinae (Astrapotheria).

9. Basicranium and vertebrae of Uruguaytheriinae indet. from the Castilletes Formation, and selected astrapotheres for comparison.

10. Scapulae and humeri of Uruguaytheriinae indet. from the Castilletes Formation, and selected astrapotheres for comparison.

11. Antebrachial bones of Uruguaytheriinae indet. from the Castilletes Formation, and selected astrapotheres for comparison.

12. Hypothesis of phylogenetic relationships within Astrapotheriidae.

13. Right m3 of Leontiniidae (Notoungulata).

14. Skull of *Falcontoxodon aguilerai* gen. et sp. nov. (Toxodontidae, Notoungulata).

15. *Gyrinodon quassus* (Toxodontidae, Notoungulata).

16. Mandible of *Falcontoxodon aguilerai* gen. et sp. nov.

17. Partial skull of *Falcontoxodon* aff. *aguilerai*.

18. Partial mandibles of *Falcontoxodon* sp.

19. Right foot of *Nesodon imbricatus* (Toxodontidae, Notoungulata).

20. Toxodontid astragali.

21. Astragalar morphospace in toxodontids.

22. Toxodontid calcanei and metatarsals.

23. Left M1 or M2 of Toxodontinae indet. from the Ware Formation.

24. Hypothesis of phylogenetic relationships within Toxodontidae.

25. Dental remains of Proterotheriidae (Litopterna) from the Cocinetas basin.

26. Postcrania of Proterotheriidae (Litopterna) from Ware and Codore Formations.

27. Right m1 or m2 of Camelidae indet. (Artiodactyla) from the Ware Formation.

28. Urumaco West chronostratigraphy.

29. Urumaco East chronostratigraphy.

30. Life reconstruction of the Castilletes Formation faunal assemblage, Cocinetas basin.

31. Key of the reconstruction shown in Figure 30.

32. Life reconstruction of the San Gregorio Formation faunal assemblage, Falcón basin.

33. Key of the reconstruction shown in Figure 32.

34. Life reconstruction of the Ware Formation faunal assemblage, Cocinetas basin.

35. Key of the reconstruction shown in Figure 34.

INTRODUCTION

South America was isolated during most of the Cenozoic and was home to a highly endemic fauna (Simpson, 1980; Wilf et al. 2013). This isolation was punctuated with dispersal events that introduced novel clades into the continent (Croft, 2012), such as the hystricognath rodents during the middle Eocene (ca. 41 MYA [Antoine et al. 2012]) and platyrrhine monkeys during the late Eocene (Bond et al. 2015) (Figure 1), migrations referred to as the Trans-Atlantic Dispersal Interval (TADI [Croft, 2016]). The isolation of South America's mammal fauna ceased during the late Neogene after the formation of the

Isthmus of Panama and the establishment of a land connection with North America, resulting in a faunal exchange between the continents known as the Great American Biotic Interchange (Figure 1).

Among mammals, the South American Native Ungulates ("SANUs"; Welker et al. 2015) are a conspicuous faunal element of the Cenozoic in the continent, with an extensive fossil record that extends from the early Paleocene (ca. 64 MYA, Tiupampan South American Land Mammal age [SALMA]; Gelfo et al. 2009; Woodburne et al. 2014a) to late Pleistocene (ca. 11-7 KYA, Cione et al. 2003; ca. 11-13 KYA, Barnosky and Lindsey, 2010). SANUs are recorded along a wide latitudinal range in South America reaching central and southern North America at least by late Pleistocene times (Lundelius et al. 2013). SANUs exhibit a high taxonomic diversity, wide body mass range and different degrees of hypsodonty (Madden, 2015; Bond, 2016; Gomes-Rodrigues et al. 2017).

Phylogenetic relationships among SANUs, and of SANUs to other placentals, have long been a subject of debate. SANUs include the clades Litopterna, Notoungulata, Astrapotheria, Xenungulata and Pyrotheria, which have been hypothesized to be monophyletic (classified in Meridiungulata; McKenna, 1975; McKenna and Bell, 1997) or non-monophyletic, having different affinities to multiple placentals (Billet and Martin, 2011; O'Leary et al. 2013; Kramarz and Bond, 2014; Buckley, 2015; Welker et al. 2015; Westbury et al. 2017). Proposed phylogenetic hypotheses include

Figure 1. Geologic time scale of the Cenozoic illustrating the South American Land Mammal Ages (SALMAs), the chronology of the Cocinetas and Falcón basins, the first appearance datums (FADs) of some South American clades, and the Cenozoic events of faunal exchange (Croft, 2016): TADI (Trans-Atlantic Dispersal Interval), the Great American Biotic Interchange, including the main dispersal events (GABI 1-4). The chronology of the latter follows Woodburne (2010): GABI 1= ca. 2.4-2.6 MYA, GABI 2= ca. 1.8 MYA, GABI 3= ca. 0.8-1.0 MYA, GABI 4= ca. 0.125 MYA.

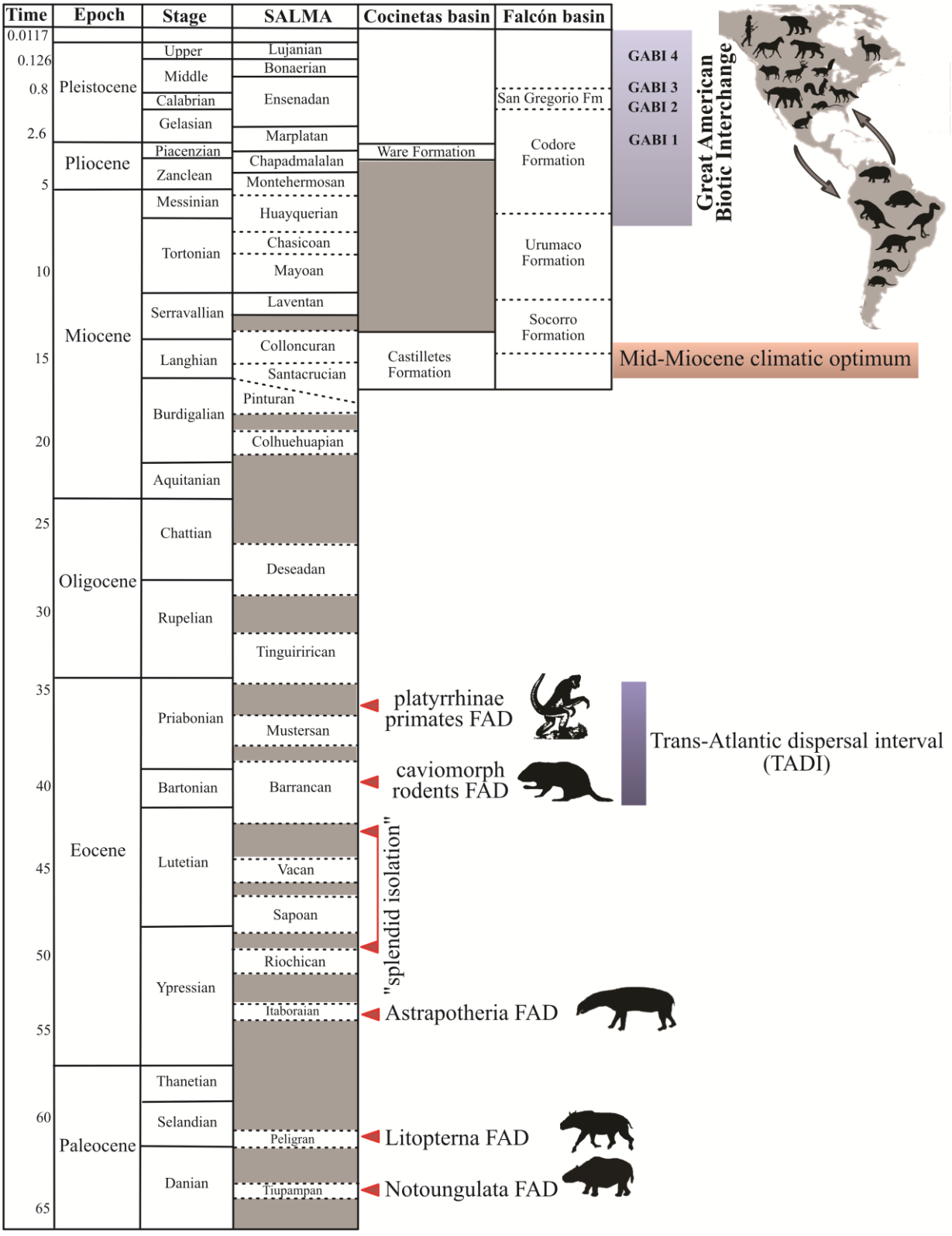

affinities of Litopterna and other closely related SANUs with an extinct group of North American ungulates known as Mioclaenideae (Cifelli, 1983; Muizon and Cifelli, 2000). Using postcranial data, Horovitz (2004) analyzed the

relationships of SANUs with several other placentals and found no support for their monophyly. SANUs were split between two separate clades of Holarctic ungulates ("Condylarthra"), one comprising Litopterna and Notoungulata and another comprising Astrapotheria. Using craniodental characters, Billet (2010, 2011) included Pyrotheria within Notoungulata and found this clade to be sister to Astrapotheria rather than Litopterna.

O'Leary et al. (2013) combined morphological characters and molecular sequences to evaluate the phylogenetic relationships within Placentalia, represented by 86 fossil and living species. According to this phylogeny, representatives of Notoungulata and Xenungulata are within Afrotheria, whereas representatives of Litopterna are within Laurasiatheria. In contrast, Welker et al. (2015) and Buckley (2015) used alpha 1 and 2 collagen chains to address the phylogenetic relationship of Notoungulata and Litopterna. Their results support that the conclusion that Notoungulata and Litopterna form a clade as sister taxon to Perissodactyla, within Laurasiatheria. The close relationship of Litopterna with Perissodactyla is also supported by mitogenomic data (Westbury et al. 2017). Carrillo and Asher (2017) combined amino acid, collagen sequences, and morphological characters, into a dataset including 182 fossil and living taxa in order to evaluate the relationship of Notoungulata and other SANUs within placentals. Their results yielded a limited number of possible phylogenetic relationships, but did not arbitrate between potential affinities with Afrotheria and Laurasiatheria.

Astrapotheria

Astrapotheria is a clade of SANUs recorded from the early Eocene (Itaboraian SALMA; (Soria and Powell, 1981; Soria, 1987; Kramarz and Bond, 2013; Woodburne et al. 2014a,b) to the middle Miocene (12.76-13.6 mya, Laventan SALMA; Johnson, 1984; Johnson and Madden, 1997; Goillot et al. 2011; Vallejo-Pareja et al. 2015). The clade had a large body mass range between ~60 kg (*Albertogaudrya;* Vizcaíno et al. 2012) and

~4117 kg (*Parastrapotherium herculeum*?; Kramarz and Bond, 2011). Astrapotheres are characterized by having canines developed as tusks, flattened astragalus, and calcaneus with secondary ectal facet and enlarged peroneal tubercle (Cifelli, 1993; Weston et al. 2004). In the more derived taxa the nasals are retracted, indicating the presence of a proboscis (Scott, 1937; Johnson, 1984; Johnson and Madden, 1997). Scott (1937) suggested amphibious habits for astrapotheres. Taphonomic evidence supports semi-aquatic habits (Scott, 1937; Johnson, 1984; Marshall et al. 1990; Weston et al. 2004), and microanatomical features of long bones could support specializations to graviportality and semi-aquatic habits in astrapotheres (Houssaye et al. 2016).

According to Cifelli (1993) two main clades are recognized within Astrapotheria: Trygonostylopidae and Astrapotheriidae. The latter comprises two clades: Astrapotheriinae, consisting of the southern taxa *Astrapotherium* and *Astrapothericulus*, and Uruguaytheriinae, which is composed of *Uruguaytherium, Granastrapotherium, Xenastrapotherium* and *Hilarcotherium.* The Uruguaytheriinae is supported by dental characters such as the absence of hypoflexid, absence of pillar in the lower molars, and absence of a labial cingulum (Johnson and Madden, 1997; Kramarz and Bond, 2009, 2011; Vallejo-Pareja et al. 2015).

Among Uruguaytheriinae, *Uruguaytherium beaulieui* is the oldest described taxon, being sister to the rest of the clade, and recorded in Uruguay but without precise provenance or known age (Kraglievich, 1928; Kramarz and Bond, 2011; Vallejo-Pareja et al. 2015). The earliest record of Uruguaytheriinae is a P4 of an undetermined genus collected in Alto Río Beu, near Santa Rosa, Ucayali, Peru (?late Oligocene; Antoine et al. 2016). Additional Uruguaytheriinae specimens are recorded in the early middle Miocene (Colloncuran SALMA) fauna of Cerdas, Bolivia (Croft et al. 2016). A neotropical clade within Uruguaytheriinae comprises *Hilarcotherium castanedaii, Granastrapotherium snorki,* and five species of *Xenastrapotherium* (*X. kraglievichi, X. aequatorialis, X. chaparralensis, X. amazonense, X. christi*)

(Kraglievich, 1928; Stehlin, 1928; Cabrera, 1929; Johnson and Madden, 1997; Vallejo-Pareja et al. 2015). *Hilarcotherium* is recorded in La Victoria Formation (middle Miocene), in the upper Magdalena valley, Colombia (Vallejo-Pareja et al. 2015). *Granastrapotherium* and *Xenastrapotherium* co-occurred in the middle Miocene (Laventan SALMA) faunas of La Venta and Fitzcarrald (Johnson and Madden, 1997; Goillot et al. 2011). *Xenastrapotherium* is widely distributed geographically and stratigraphically. It is recorded in Colombia, Venezuela, Ecuador, Brazil and Peru, in sediments ranging from early to middle late Miocene in age (Goillot et al. 2011; Antoine et al. 2016).

Notoungulata

Notoungulata is a clade of SANUs with a high taxonomic diversity that includes more than 140 genera and 13 families (Croft, 1999), large morphological disparity (Giannini and García-López, 2014; Bond, 2016), and diverse dental eruption patterns, degrees of hypsodonty (Madden, 2015; Gomes-Rodrigues et al. 2017) and diets (MacFadden, 2005; Croft and Weinstein, 2008; Townsend and Croft, 2008). Notoungulata is monophyletic (Roth, 1903; Cifelli, 1993; Billet, 2010, 2011) and is recorded during most of the Cenozoic in South America, from the early Paleocene (ca. 64 MYA Tiupampan) (Gelfo et al. 2009; Woodburne et al. 2014a) to the late Pleistocene (Cione et al. 2003; Barnosky and Lindsey, 2010). Together with Typotheria, Toxodontia is one of the main clades of Notoungulata. Toxodontia includes, among others, the clades Leontiniidae and Toxodontidae (Billet, 2011).

Leontiniidae are part of a clade within Toxodontia that also includes some Notohippidae and Toxodontidae (Cifelli, 1993; Billet, 2011). Leontiniidae is known from the late Eocene (Mustersan SALMA) (Bond and López, 1995; Ribeiro et al. 2010) to the middle Miocene (Laventan) (Villaroel and Colwell Danis, 1997). It attained its greater diversity during the late Oligocene (Deseadan SALMA) (Shockey et al. 2012; Cerdeño and Vera, 2015). Leontiniids have a medium to large body mass among Toxodontia. They are characterized by having mesodont (see

Mones, 1982) cheek teeth and a tendency to form tusk-like incisors (Shockey et al. 2012). In the Miocene, leontiniids are represented by *Colpodon* from the various localities in central Patagonia, Argentina (Colhuehuapian SALMA; ca. 20.0-20.2 MYA) and Laguna del Laja, Chile (early Miocene; ca. 19.5-19.8 MYA) (Ré et al. 2010; Ribeiro et al. 2010; Shockey et al. 2012), and *Huilatherium* from La Venta, Colombia (Laventan) (Villaroel and Colwell Danis, 1997). The phylogenetic relationships within Leontiniidae are not fully resolved, but the Miocene taxa *Colpodon* and *Huilatherium* are hypothesized to belong to the same clade (Shockey et al. 2012; Cerdeño and Vera, 2015).

Toxodontidae is a clade of medium to large herbivores characterized by a specialized anterior dentition, ever-growing tusks, and hypsodont molars (Madden 1997). Toxodonts were widespread in South America from the late Oligocene to late Pleistocene (Deseadan through Lujanian SALMAs) (Nasif et al. 2000). Within Toxodontidae two clades are recognized: Nesodontinae and Toxodontinae (Nasif et al. 2000; Forasiepi et al. 2015). Nesodontinae consists of early middle Miocene (Pinturan-Santacrucian SALMAs) toxodontids from southern South America, whereas Toxodontinae comprises middle Miocene to late Pleistocene (Santacrucian through Lujanian) taxa widely distributed on the continent (Forasiepi et al. 2015). Toxodontinae representatives reached Central (Webb and Perrigo, 1984; Lucas et al. 1997; Lucas, 2014) and North America (~30º N) (Lundelius et al. 2013) during the late Pleistocene as part of the Great American Biotic Interchange (see below).

Litopterna

Litopterna is a diverse clade of SANUs recorded in South America from the late Paleocene (Peligran SALMA) (Gelfo et al. 2009) to the late Pleistocene (Bond et al. 2001). Several clades are recognized within Litopterna: Protolipternidae, Notonychopidae, Adianthidae, Macraucheniidae, and Proterotheriidae (Cifelli, 1983, 1993; Schmidt, 2015; Forasiepi et al. 2016). The Sparnotheriodontidae has been variably treated as "Condylarthra" (Cifelli, 1983,

1993) or as a member of Litopterna (Soria, 2001).

The Proterotheriidae were small to medium-sized cursorial herbivores. They show different types of dentition, including brachyodont, mesodont, and protohypsodont (Soria, 2001; Villafañe et al. 2012; Schmidt, 2015). They are characterized by a reduction of the digits II and IV, acquiring a functional monodactyly (Cifelli and Villaroel, 1997; Ubilla et al. 2011; Schmidt, 2015). Proterotheriidae had a wide distribution, and it is recorded from the Paleocene (Itaboraian) to the late Pleistocene (Bonaerian-Lujanian). It attained its maximum diversity during the Miocene (Santacrucian through Huayquerian SALMAs) (Bond et al. 2001; Villafañe et al. 2006; Scherer et al. 2009; Ubilla et al. 2011; Schmidt, 2015).

There are three main clades recognized within Proterotheriidae: Anisolambdinae, Megadolodinae, and Proterotheriinae; only the latter two are recorded in the Neogene (Cifelli, 1983; Cifelli and Villaroel, 1997; Soria, 2001; Villafañe et al. 2006). The Megadolodinae is known from the La Venta fauna (middle Miocene; Laventan) of Colombia (McKenna, 1956; Cifelli and Villaroel, 1997) and the Urumaco Formation (late Miocene) of Venezuela (Carlini et al. 2006a). The Proterotheriinae is recorded from the late Oligocene to the late Pleistocene (Deseadan trough Lujanian) (Villafañe et al. 2006). They have a wide distribution (including northern South America) and reach their highest diversity during the Miocene (Santacrucian through Huayquerian) (Cifelli and Guerrero, 1997; Villafañe et al. 2006; Schmidt, 2011, 2015).

Study Sites

Cocinetas Basin

The Cocinetas basin is located in the eastern Guajira peninsula, in northern Colombia (Figure 2). The Neogene stratigraphy of the basin was revised by Moreno et al. (2015). The terrestrial mammal assemblages were collected from both the Castilletes and Ware Formations. The Castilletes Formation was deposited in a shallow marine to fluvio-deltaic environment and has been dated as 16.7-14.2 MYA based on $^{87}Sr/^{86}Sr$ isotope chronostratigraphy and macroinvertebrate biostratigraphy (late early to early middle

Figure 2. Geographic location of the Cocinetas and Falcón basins in Colombia and Venezuela, respectively.

Miocene, upper Burdigalian-Langhian; Santacrucian/Colloncuran SALMAs; Hendy et al. 2015; Moreno et al. 2015). The Ware Formation is dominated by fluvio-deltaic environment deposits at the base and shoreface and nearshore deposits at the top. It is dated as 3.4-2.78 MYA based on $^{87}Sr/^{86}Sr$ isotope chronostratigraphy and macroinvertebrate biostratigraphy (late Pliocene, Piacenzan, Chapadmalalan/ Marplatan SALMAs; (Hendy et al. 2015; Moreno et al. 2015).

The terrestrial mammalian fauna of the Castilletes Formation includes a sparassodont, a sloth, astrapotheres, litopterns, and notoungulates (Table 1; Amson et al. 2016; Suarez et al. 2016). The Castilletes Formation also records other terrestrial and marine fossils such as mollusks, echinoderms, arthropods, sharks, rays, bony fishes, snakes, turtles, crocodiles, cetaceans, and plants (Aguilera et al. 2013a; Cadena and Jaramillo, 2015a, 2015b; Hendy et al. 2015; Moreno et al. 2015; Moreno-Bernal et al. 2016; Aguirre-Fernández et al. 2017a). The mammalian fauna of the Ware Formation is characterized by an assemblage of sloths, cingulates, rodents, toxodontids, a procyonid, and a camelid (Table 1), the latter two being immigrants from North America (Forasiepi et al. 2014; Moreno et al. 2015; Amson et al. 2016; Moreno-Bernal et al. 2016; Pérez et al. 2017). The Ware Formation also records crocodiles (Moreno-Bernal et al. 2016), turtles, bony fishes, fossil wood, and a diverse marine assemblage (Aguilera et al. 2013b; Hendy et al. 2015; Jaramillo et al. 2015; Moreno et al. 2015).

Falcón Basin

The Falcón basin in northwestern Venezuela (Figure 2) has a long history of paleontological and geological studies (Sánchez-Villagra, 2010).

Table 1. Mammals from the Cocinetas basin. BM= Body mass in kg.

Castilletes Formation				
Clade		**Taxa**	**BM**	**Reference**
Sparassodonta	Borhyaenoidea	*Lycopsis padillai*	22	Suarez et al. (2016)
Xenarthra	Megatherioidea	*Hyperleptus*?		Amson et al. (2016)
Xenarthra	Glyptodontidae	Glyptodontidae indet.		Moreno et al. (2015)
Xenarthra	Pampatheriidae	Pampatheriidae indet.		Moreno et al. (2015)
Astrapotheria	Uruguaytheriinae	*Hilarcotherium miyou* n. sp.	~6456	This work
Notoungulata	Leontiniidae	cf. *Huilatherium*		This work
Litopterna	Proterotheriidae	*Neodolodus* cf. *colombianus*		This work
Ware Formation				
Clade		**Taxa**	**BS**	**Reference**
Xenarthra	Lestodontini	Gen. et sp. nov.		Amson et al. (2016)
Xenarthra	Scelidotheriinae	Gen. et. sp. indet.		Amson et al. (2016)
Xenarthra	Megalonychidae	Gen. et sp. nov.		Amson et al. (2016)
Xenarthra	Megatheriinae	*Pliomegatherium lelongi*	2417	Amson et al. (2016)
Xenarthra	Nothrotheriinae	cf. *Nothrotherium*	41	Amson et al. (2016)
Xenarthra	Glyptodontidae	Glyptodontidae indet.		Moreno et al. (2015)
Xenarthra	Pampatheriidae	Pampatheriidae indet.		Moreno et al. (2015)
Rodentia	Caviomorpha	?*Hydrochoeropsis wayuu*	~24	Pérez et al. (in press)
Rodentia	Caviomorpha	Erethizontidae indet.		Moreno et al. (2015)
Notoungulata	Toxodontidae	Toxodontinae indet.		This work
Artiodactyla	Camelidae	Camelidae indet.		This work
Carnivora	Procyonidae	*Chapalmalania sp.*		Forasiepi et al. (2014)
Litopterna	Proterotheriidae	Proterotheriidae indet.		This work

The Urumaco sequence includes four geological formations with reports of fossil mammals: Socorro, Urumaco, Codore (Sánchez-Villagra et al. 2010, and references therein), and San Gregorio (Table 2), which together extend from the middle Miocene to the late Pliocene (Quiroz and Jaramillo, 2010).

The Urumaco Formation is characterized by diverse faunal associations in terrestrial, freshwater, estuarine, and marine environments of late Miocene age (Sánchez-Villagra and Aguilera, 2006; Quiroz and Jaramillo, 2010). The terrestrial mammal fauna

Table 2. Mammals from the Falcón basin. BM= Body mass in kg.

Codore Formation				
Clade		**Taxa**	**BM**	**Reference**
Notoungulata	Toxodontidae	*Falcontoxodon aguilerai* n. sp.	796	This work
Litopterna	Proterotheriidae	Proterotheriidae indet.		This work
Xenarthra	Glyptodontidae	*Boreostemma pliocena*		Carlini et al. (2008)
	Pampatheriidae	Indet.		A. Carlini pers comm
San Gregorio Formation				
Clade		**Taxa**		**Reference**
Carnivora	Procyonidae	*Cyonasua* sp.		Forasiepi et al. (2014)
Notoungulata	Toxodontidae	*Falcontoxodon* sp.		This work
Rodentia	Caviomorpha	cf. *Caviodon*		Vucetich et al. (2010)
		Hydrochoeropsis? *wayuu*		Vucetich et al. (2010); Perez et al. (2016)
		Marisela gregoriana		Vucetich et al. (2010)
		Neoepiblema sp.		Vucetich et al. (2010)
Xenarthra	Dasypodidae	*Pliodasypus vergelianus*		Castro et al. (2014)
	Glyptodontidae	*Boreostemma?* sp. nov.		Zurita et al. (2011)
	Megatheriinae	aff. *Proeremotherium*		A. Carlini pers comm
	Pampatheriidae			A. Carlini pers comm

of Urumaco includes giant rodents (Sánchez-Villagra et al. 2003; Horovitz et al. 2006, 2010; Geiger et al. 2013; Carrillo and Sánchez-Villagra 2015) as well a high diversity of sloths (Carlini, Scillato-Yané, and Sánchez 2006; Carlini, Brandoni, and Sánchez 2006; Carlini, Brandoni, and Sánchez 2008; Rincón et al. 2015). The described SANUs include the megadolodine litoptern *Bounodus enigmaticus* (Carlini, Gelfo, and Sánchez 2006) and a toxodontine *incertae sedis* (Bond, Madden, and Carlini 2006). Linares (2004) provided a list of SANUs, none of which have been described (see Bond and Gelfo 2010).

The Codore Formation is early Pliocene in age. It is divided into three formal members: El Jebe, Chiguaje, and Algodones. The Jebe and Algodones were deposited in a fluvial environment, whereas the Chiguaje represents a marine transgression (Quiroz and Jaramillo, 2010)

and records cetaceans (Aguirre-Fernández et al. 2017a; 2017b). The terrestrial mammal fauna from Codore includes the glyptodon *Boreostemma pliocena* from the El Jebe Member (Carlini et al. 2008) and a pampathere (A. A. Carlini, Museo de La Plata, personal communication).

The San Gregorio Formation is late Pliocene-early Pleistocene in age (Quiroz and Jaramillo, 2010). Fossil mammals come from the Vergel Member at the base of the San Gregorio and consist of caviomorph rodents (Vucetich et al. 2010), cingulates (Zurita et al. 2011; Castro et al. 2014), and a procyonid (Forasiepi et al. 2014).

The Great American Biotic Interchange

The Great American Biotic Interchange (GABI) is one of the greatest events of biota exchange at a continental scale (Marshall et al. 1982; Webb, 1985, 1991). The traditional interpretation places the onset of the GABI by ca. 3 MYA, with some early mammal migrations ("heralds") during the late Miocene from South to North America by ca. 9 MYA and from North to South America by ca. 7 MYA (Webb, 2006; Woodburne, 2010; Leigh et al. 2014; Cione et al. 2015; O'Dea et al. 2016). Other studies using dated molecular phylogenies across a wide range of taxa in addition to mammals indicate that an important part of the interchange predated ca. 3 MYA (Koepfli et al. 2007; Cody et al. 2010; Eizirik, 2012; Leite et al. 2014; Bacon et al. 2015; Stange et al. 2017).

The mammalian fossil record in South America shows that although the first migrations are recorded during the late Miocene (ca.10-7 MYA), the number of GABI participants rapidly increases after ca. 5-3 MYA and this trend continues during the Pleistocene (Carrillo et al. 2015). Dated molecular phylogenies suggest a similar pattern for birds (Weir et al. 2009). For mammals, the core of the GABI is composed of a series of major migration "waves" during the Pleistocene (2.5-0.012 MYA) (Woodburne, 2010). Climatic and environmental changes possibly influenced migration patterns during the Pleistocene (Webb, 1991; Bacon et al. 2016). Empirical data on tropical paleoenvironments and paleofaunas from the Pliocene and Pleistocene are needed to test

this hypothesis.

The Neotropical fossil record is essential to better understand the diversity dynamics and paleobiogeography during the GABI. However, there is a strong fossil sampling bias in the continent, as our knowledge of the tropics is very scant when compared with that of the temperate faunas (Carrillo et al. 2015). The new findings from the Cocinetas and Falcón basins serve to characterize changes of mammal assemblages in northern South America just before and during the GABI.

MATERIALS AND METHODS

We took standard linear measurements with a caliper to the nearest 0.1 mm, and with a metric tape for large elements (> 15 cm). For orientation of the dentition we follow Smith and Dodson (2003), where the four cardinal directions are mesial, distal, lingual and labial (buccal). We follow the recommendations of Bengtson (1988) for the use of open nomenclature. SALMAs chronology follows Flynn and Swisher (1995), Madden et al. (1997), Cione and Tonni (1999, 2001), Tonni (2009), Kramarz et al.(2010), Shockey et al. (2012), Tomassini et al. (2013), and Woodburne et al. (2014a,b). Three-dimensional surface models of selected specimens of the described material will be available in MorphoMuseuM upon publication.

Comparative Anatomical Descriptions

Astrapotheriidae

The astrapothere material described here comes from the Castilletes Formation, in the Guajira Department, northern Colombia (Figure 3). Dental morphology and terminology follow Johnson (1984). We took craniodental measurements for astrapotheres following Johnson and Madden (1997) and Vallejo-Pareja et al. (2015). The craniodental material is described in comparison with other Uruguaytheriinae *sensu* Vallejo-Pareja et al. (2015), and postcranial elements are compared with astrapotheres whose postcranial anatomy is best known, in particular *Astrapotherium* and *Parastrapotherium* (Riggs, 1935; Scott, 1937).

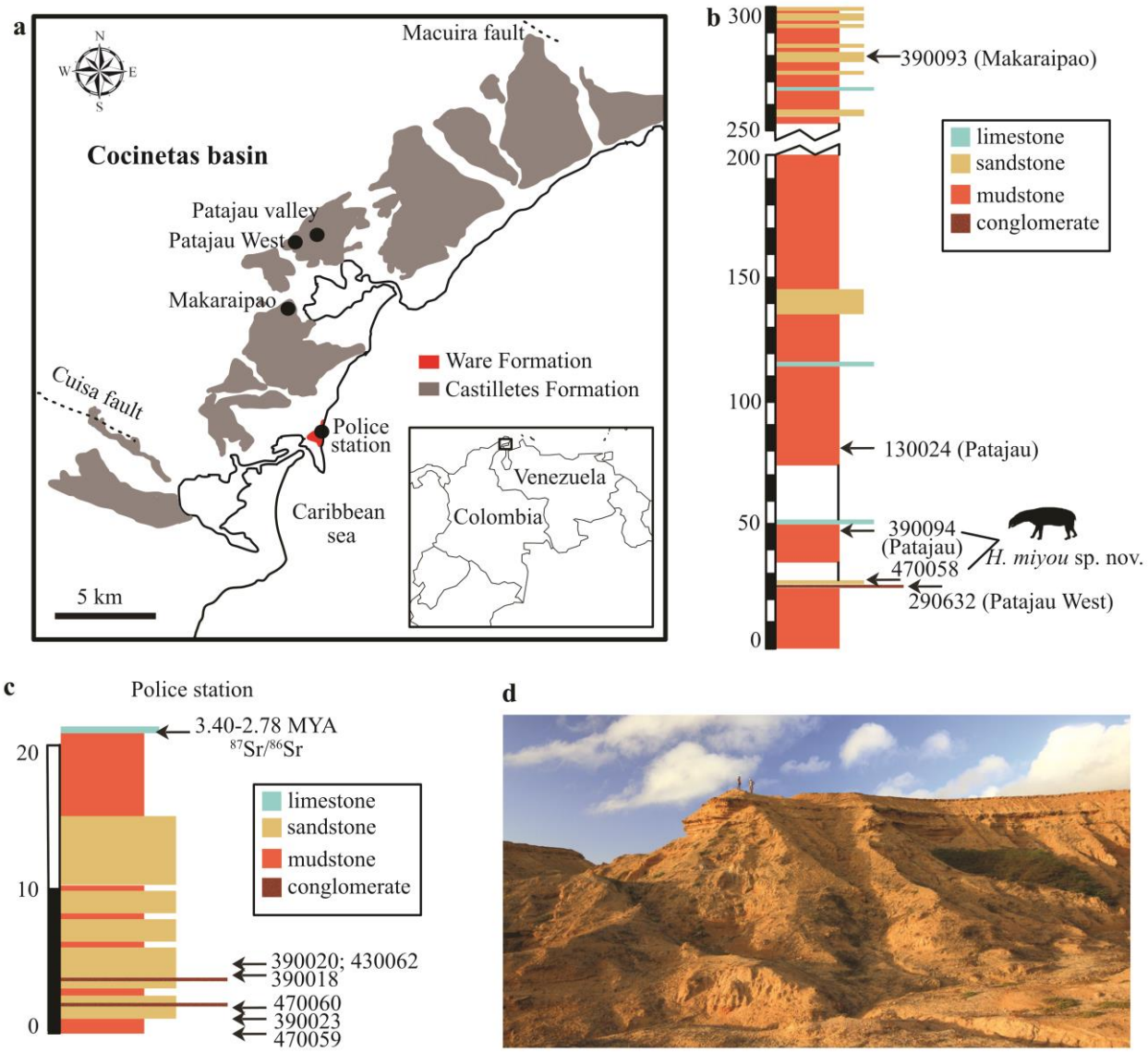

Figure 3. Geographic and stratigraphic occurrence of South American Native Ungulates (SANUs) in the Cocinetas basin: (a) location of fossiliferous localities with SANUs; (b) stratigraphic profile of the Castilletes Formation indicating the stratigraphic position of each locality; (c) stratigraphic profile of the Ware Formation indicating the stratigraphic position of each locality; both profiles are modified from Moreno et al. (2015); (d) landscape view at the Police Station locality, picture by Christian Ziegler.

Leontiniidae

The leontiniid molar comes from the Castilletes Formation (Figure 3); for its description, we considered recent systematic works on leontiniids (e.g., Villaroel and Colwell Danis, 1997; Shockey et al. 2012; Cerdeño and Vera, 2015). Dental terminology follows Ribeiro et al. (2010).

Toxodontidae

The toxodontid material described here comes from the Algodones Member of the Codore Formation and the Vergel Member of the San Gregorio Formation (Figure 4). Dental morphology and terminology follow Madden (1990, 1997). Craniodental material is described in comparison with other Toxodontinae *sensu* (Nasif et al. 2000; Forasiepi et al. 2015). Postcranial elements are described in comparison with toxodontids whose postcranial elements are best known, in particular *Nesodon imbricatus* and *Toxodon platensis*.

For the toxodontid foot bones, we measured the length and width of the calcaneus and tarsals. For the astragalus, we took nine measurements following Tsubamoto (2014), and we used these measurements in a Principal Component Analysis (PCA) to explore astragalar variation in toxodontids.

Proterotheriidae

The proterotheriid material described here comes from the Castilletes and Ware Formations in the Cocinetas basin, and the Algodones Member of the Codore Formation in the Falcón basin (Figures 3-4). Dental terminology follows Soria (2001) and Schmidt (2015). Dental and postcranial remains are described in comparison with recent systematic works on Proterotheriidae (Cifelli and Villaroel, 1997; Scherer et al. 2009; Schmidt, 2015). Postcranial measurements were taken following Schmidt (2013).

Camelidae

The camelid molar comes from the Ware Formation (Figure 3). Dental terminology follows Scherer et al. (2007) and Rincón et al. (2012). We follow Scherer (2013) for the taxonomy of South American camelids.

Phylogenetic Analyses

Astrapotheriidae

We conducted a phylogenetic analysis using maximum parsimony. The analysis included 17 taxa and 64 characters; 61 characters were ordered and three unordered. Studies on

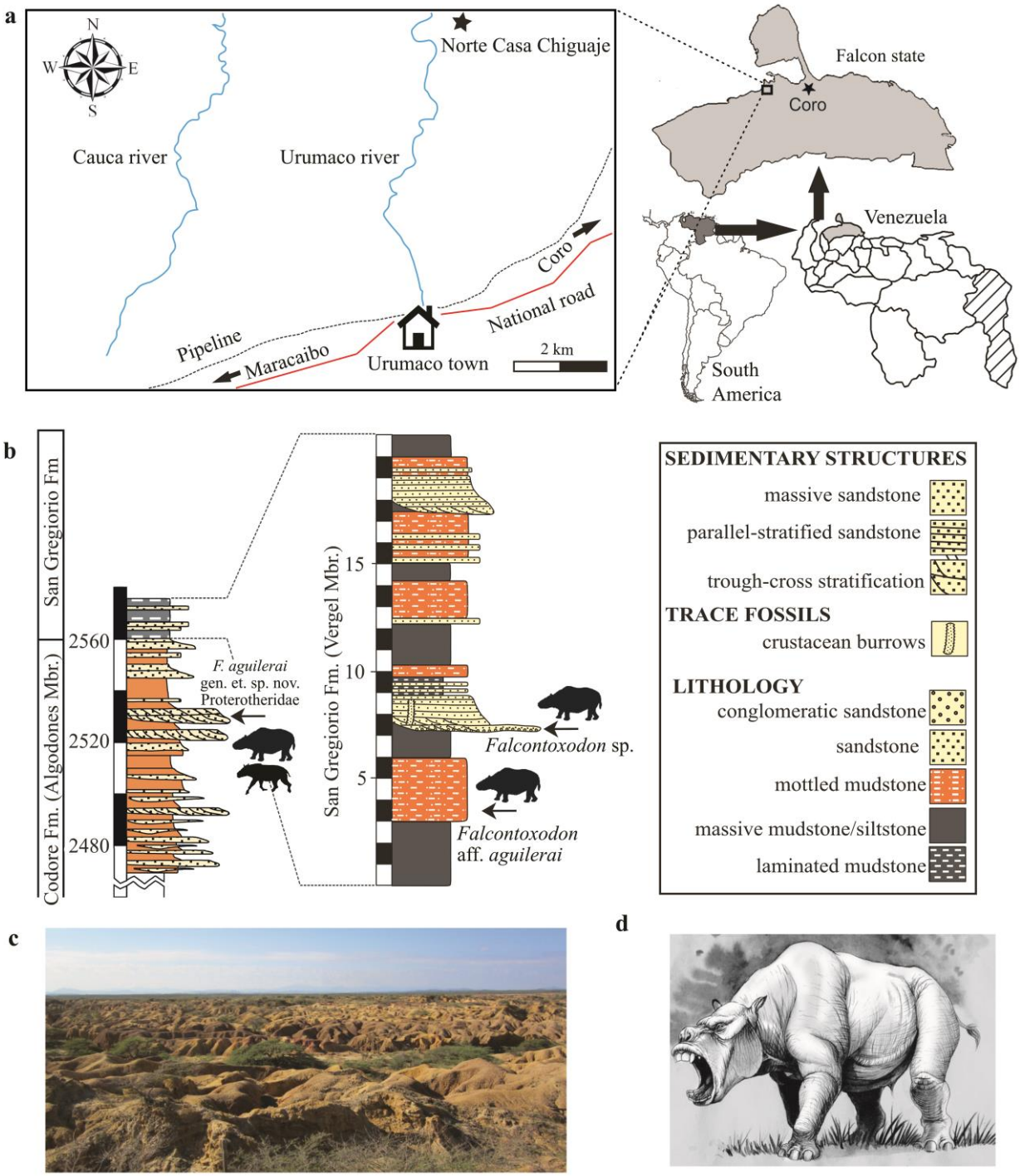

Figure 4. Geographic and stratigraphic occurrence of *Falcontoxodon* gen. nov. and Proterotheriidae: (a) location and (b) stratigraphic profile of the localities from the Codore and San Gregorio Formations where specimens of *Falcontoxodon* and Proterotheriidae were found; (c) landscape view in the Norte Casa Chiguaje locality, of the Vergel Member, San Gregorio Formation; (d) artistic reconstruction of a toxodontid by Jorge González (modified from Sánchez-Villagra et al. 2010).

simulated and empirical data showed that parsimony analyses with ordered states perform better when using characters that form morphoclines (Grand et al. 2013). Taxa included are *Eoastrapostylops* as the outgroup, and 16 astrapotheriids. We used the matrix presented by Vallejo-Pareja et al. (2015), and we added *Xenastrapotherium kraglievichi*, *Xenastrapotherium christi*, and the new Uruguaytheriinae from the Castilletes Formation. We excluded *Xenastrapotherium aequatorialis*, *Xenastrapotherium chaparralensis*, and *Xenastrapotherium amazonense*, because they are known only from fragmentary elements. We analyzed the character matrix with the program PAUP* 4.0 (Swofford, 2002). We used equally weighted characters, excluded uninformative characters, treated gaps as missing, and taxa with multiple states as polymorphic. We did a search using the branch-and-bound algorithm with a furthest addition sequence. A normal bootstrap resampling was performed, with 1000 replications.

Toxodontidae

We performed a maximum parsimony analysis on 27 notoungulate taxa and 59 morphological characters with PAUP* 4.0 (Swofford, 2002). We used the matrix presented by Forasiepi et al. (2015), and we added *Piauhytherium* as described by Guérin and Faure (2013), and the new toxodontine from Codore Formation. We excluded uninformative characters, treated gaps as missing, and taxa with multiple states as polymorphic. Forasiepi et al. (2015) performed a phylogenetic analysis using implied and equals weights. In order to be comparable, we also used equally weighted characters and implied weighting with a concavity constant (k) value of 3. The implied weighting weights characters against homoplasy and improves the resampling metrics associated with the quality of the results (Goloboff et al. 2008; Goloboff, 2014). We did a heuristic search with a starting tree obtained via stepwise addition using the closest addition sequences and tree bisection reconnection (TBR), saving ten trees per round. A normal bootstrap resampling was performed, with 1000 replications.

Body Mass Estimations

In order to estimate the body mass in toxodonts, we used the multivariate regression functions proposed by Mendoza et al. (2006), based on craniodental measurements of living ungulates. Multiple regression techniques provide better body mass estimates than single regression methods (e.g., Janis, 1990). For astrapotheres, we used the bivariate regression equation of the m2 length for non-selenodont ungulates from Damuth (1990: table 16.9), and the equation of the humerus length (H2) for all ungulates from Scott (1990: table 16.7).

Abbreviations

AMU-CURS Alcaldía del Municipio de Urumaco-Colección Urumaco Rodolfo Sánchez

MACN Museo Argentino de Ciencias Naturales, Buenos Aires

MLP Museo de La Plata, La Plata

MNHN Muséum national d'Histoire naturelle, Paris

MUN Mapuka Museum, Universidad del Norte, Barranquilla

NHMUK Natural History Museum, London

NMB Naturhistorisches Museum Basel, Basel

PIMUZ Paläontologisches Institut und Museum Universität Zürich, Zurich

SALMA South American Land Mammal Age

STRI Smithsonian Tropical Research Institute, Panama

YPM Yale Peabody Museum, New Haven

M-m Upper molar – lower molar

P-p Upper premolar – lower premolar

C-c Upper canine – lower canine

I-i Upper incisor – lower incisor

Chronostratigraphic framework

The Neogene sequence of the Falcón basin is one of the thickest and best exposed sedimentary sequences in the Neotropics,

with more than 7 kilometers of stratigraphic thickness outcropping. Most of the sequence is highly fossiliferous and we expect that the paleontological exploration of this large region will continue for many decades to come. To help this and future studies in the region, we established a chronology for the region based on an extensive literature review, as this region has had many biostratigraphic studies over the past few decades. Most of these studies, especially in the western region, have been correlated to Bolli's zonal schemes in Trinidad (Bolli et al. 1994), which is the base for the biostratigraphy of tropical latitudes in the Americas. Furthermore, we include in the Appendix 1 the lithological description of ten stratigraphic sections that encompass the entire Neogene sequence and could be used as a stratigraphic reference for future paleontological research.

RESULTS

Systematic Paleontology

Astrapotheria Lydekker, 1884

Astrapotheriidae Ameghino, 1887

Uruguaytheriinae Kraglievich, 1928 sensu Vallejo-Pareja et al. (2015)

Hilarcotherium Vallejo-Pareja et al. 2015

Type species *Hilarcotherium castanedaii* Vallejo-Pareja et al. 2015

Hilarcotherium miyou sp. nov.

(Figures 5 and 7)

Diagnosis *H. miyou* differs from *H. castanedaii* in having lower canines oval in cross section and implanted horizontally, the absence of lingual cingulid, the presence of a continuous lingual cingulum in P4, and the absence of lingual cingulum in M2. The molar dimensions are 30 to 40 % larger than in *H. castanedaii.*

Etymology The species is named after the word "miyo'u", which means big or large in Wayuunaiki (Captain and Captain, 2005), the language of the Wayuu community that inhabits in the Guajira Department.

Holotype IGMp 881327, partial mandible with left ramus bearing left m3, m2, canines, and alveoli for the incisors. Fragment of the left condylar process, right M2 and distal portion of femur.

Referred material MUN-STRI

16778, left and right upper tooth-rows highly fragmented bearing P4-M3. MUN-STRI 34216, fragmentary skull with portion of the occipitals, palatines, and left upper canine, associated P4 and M2, and fragmentary mandibular symphysis with the base of the lower canines and alveoli for left i3, i2, and i1 and right i1 and i2.

Type locality and horizon Patajau, Castilletes Formation. The holotype and MUN-STRI 34216 come from STRI locality 470058; 11.95062º N, 71.32370º W. MUN-STRI 16778 comes from STRI locality 390094; 11.9465ºN, 71.3255ºW (Figure 3).

Description The specimens are referred to Uruguaytheriinae based on the well-developed mesiolingual pocket in the upper molars, the absence of labial cingulum, and the absence of hypoflexid and pillars in the lower molars (Johnson and Madden, 1997; Kramarz and Bond, 2009, 2011; Vallejo-Pareja et al. 2015). The material is further referred to *Hilarcotherium* based on the unique dental formula, with three lower incisors and only one upper premolar (P4), and the presence of a mesiolingual pocket in P4 (Vallejo-Pareja et al. 2015).

The width of the mandible (measured as the mediolateral width between the labial margin of the canines) of *H. miyou* is comparable to that of *H. castanedaii* and *Granastrapotherium snorki,* and larger than that of *Xenastrapotherium christi* (Table 3; Vallejo-Pareja et al. 2015). The symphysis is wide (Figure 5b) as in *H. castanedaii* (Vallejo-Pareja et al. 2015: fig. 4b) and *X. christi* (Figure 6b), and unlike *G. snorki,* where the symphysis is very narrow due to the absence of lower incisors (Johnson and Madden, 1997: fig. 22.5). In IGMp 881327 the most anterior portion of the mandible is not well preserved, but it is possible to identify at least three alveoli for the incisors, which are interpreted as the right and left i1 and the left i2 (Figure 5c). It is not possible to assess with confidence the size of the alveoli and the presence of i3. However, MUN-STRI 34216 preserves the most anterior portion of the mandibular symphysis, which clearly shows five large incisors' alveoli and the base of the lower canines (Figure 7b-c). The incisors of uruguaytheriines are single rooted (Vallejo-Pareja et al. 2015: fig. 4 f-g), and therefore the alveoli of MUN-STRI 34216

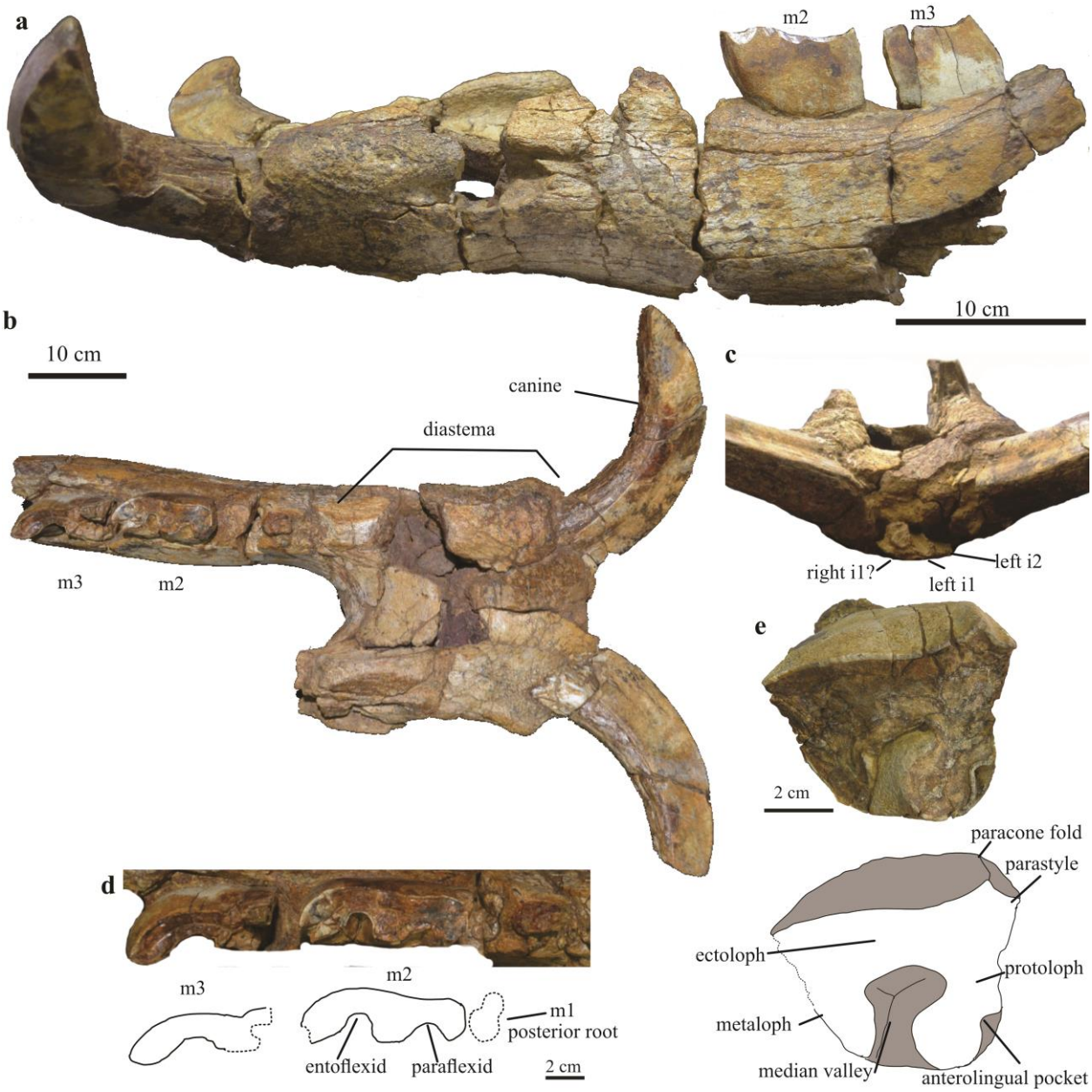

Figure 5. Mandible of *Hilarcotherium miyou* sp. nov. (Uruguaytheriinae, Astrapotheria) (holotype, IGMp 881327): (a) left lateral view; (b) occlusal view; (c) anterior view of the symphysis indicating the alveoli for the incisors; (d) detail of dentition in occlusal view; (e) photograph and drawing of M2 in occlusal view.

are interpreted as left i1, i2, i3 and right i1, i2. The alveolus of the right i3 is not observable due to diagenetic deformation after burial, as evident also from the more irregular shape of the alveoli of the right i1 and i2 (Figure 7c).

The incisors' alveoli of *H. miyou* are slightly larger (Table 3) than in *H. castanedaii* (Vallejo-Pareja et al. 2015).

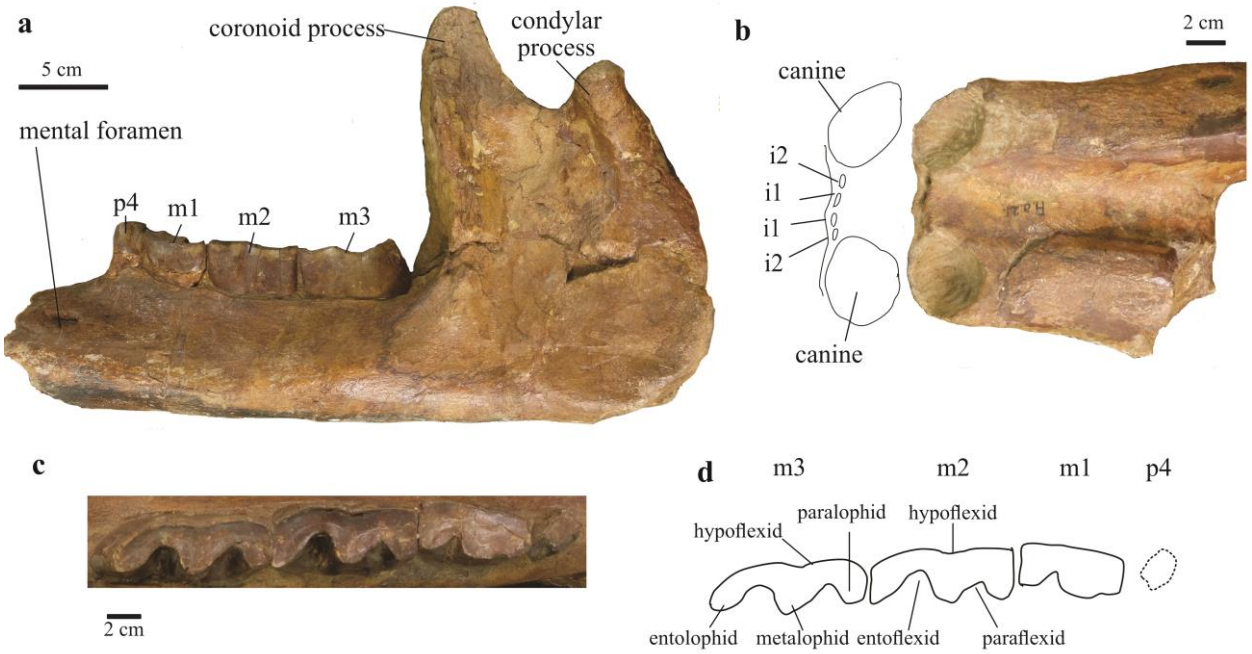

Figure 6. Mandible of *Xenastrapotherium christi* (Uruguaytheriinae, Astrapotheria) (NMB Aa21): (a) left lateral view; (b) dorsal view of the symphysis showing the alveoli of canines and incisors; (c) left dentition in occlusal view; (d) drawing and dental features of the dentition in occlusal view.

Xenastrapotherium has only two lower incisors. Johnson and Madden (1997) noted that in some specimens of *X. kraglievichi*, the lower incisors root alveoli were very small, "indicating that the lower incisor are either variably developed or may have worn out and been shed" (Johnson and Madden, 1997:360). There is intra-specific variation in the size of the incisors. This seems to be the case also in *H. miyou* (Figure 5c) and *X. christi* (Figure 6b), whose incisors have very small alveoli. *G. snorki* has no lower incisors (Johnson and Madden, 1997).

The lower canines of *H. miyou* are oval in cross section, whereas in *H. castanedaii* they are triangular. In *H. miyou* the canines are implanted horizontally and curved labially, unlike *H. castanedaii,* which has canines with a diagonal implantation. Based on size differences and morphology of the canines, Johnson and Madden (1997) inferred sexual dimorphism in *Granastrapotherium*, with the larger (male?) morphotype having longer and nearly straight lower canines, and the smaller (female?) morphotype having shorter and more curved lower canines

Table 3. Dental measurements (mm) of *Hilarcotherium miyou* sp. nov. from Castilletes Formation. *Tooth crown incomplete, **measured at the alveolus. Measurements follow Johnson and Madden (1997).

Specimen	Feature	Side	Measurement	Value
IGMp881327	c	Left	Maximum diameter	64.0
			Transverse diameter	45.8
	c	Right	Maximum diameter	65.7
			Transverse diameter	48.4
	p4**	Left	Length	28.8
			Width	22.2
	m1**	Left	Length	52.6
			Width	28.2
	m2	Left	Length	81.8
			Width	28.8
	m3*	Left	Length	79.9
			Width	27.9
	M2	Right	Length	71.7
			Width	59.8
	Mandible	Left	depth at m2	104.5
	Mandible	Left	thickness at m2	78.2
	Mandible		width between the labial margin of lower canines	125
MUN-STRI 34216	i1**	Left	Anteroposterior length	21.0
			Transverse length	11.0
	i2**	Left	Anteroposterior length	18.0
			Transverse length	8.4
	i3**	Left	Anteroposterior length	19.8
			Transverse length	14.5

MUN-STRI 16778	P4**	Left	Length	31.8
			Width	40.7
	M1*	Left	Length	59.2
			Width	65.4
	M2*	Left	Length	71.2
			Width	76.7
	M3*	Left	Length	73.6
			Width	60.1

(Johnson and Madden, 1997).

IGMp 881327 preserves the left m2 and m3, and the root of m1, which is biradiculated, as in all astrapotheres (Figure 5d). They lack a hypoflexid, as is the case in *H. castanedaii, U. beaulieui,* and *X. aequatorialis.* In *G. snorki* "the hypoflexid is indicated as a faint indentation opposite to the metalophid" (Johnson and Madden, 1997:371). In *X. christi* the hypoflexid is located opposite to the metalophid (Figure 6c-d), whereas in *X. kraglievichi* it is opposite to the paraflexid (Johnson and Madden, 1997). The m2 crown is undamaged in IGMp 881327 and is 40% larger than the m2 of *H. castanedaii* (Figure 8a; Vallejo-Pareja et al. 2015). The entoflexid is deeper linguo-labially in occlusal view than the paraflexid (Figure 5d), a feature related to wear and observed in other Uruguaytheriinae (Vallejo-Pareja et al. 2015). *H. miyou* has no lingual cingulid, unlike *H. castanedaii, X. christi* and *X. aequatorialis* (Johnson and Madden, 1997; Vallejo-Pareja et al. 2015).

MUN-STRI 16778 is a left upper tooth-row with P4-M3. It is very fractured, and not much can be discerned about crown morphology, although it is possible to clearly identify each tooth in situ. MUN-STRI 16778 has no P3, unlike *Xenastrapotherium* (Johnson and Madden, 1997). The dental dimensions of MUN-STRI 16778 are approximately 30% larger than *H. castanedaii* (Vallejo-Pareja et al. 2015). The isolated P4 of MUN-STRI 34216 has a well-defined parastylar fold

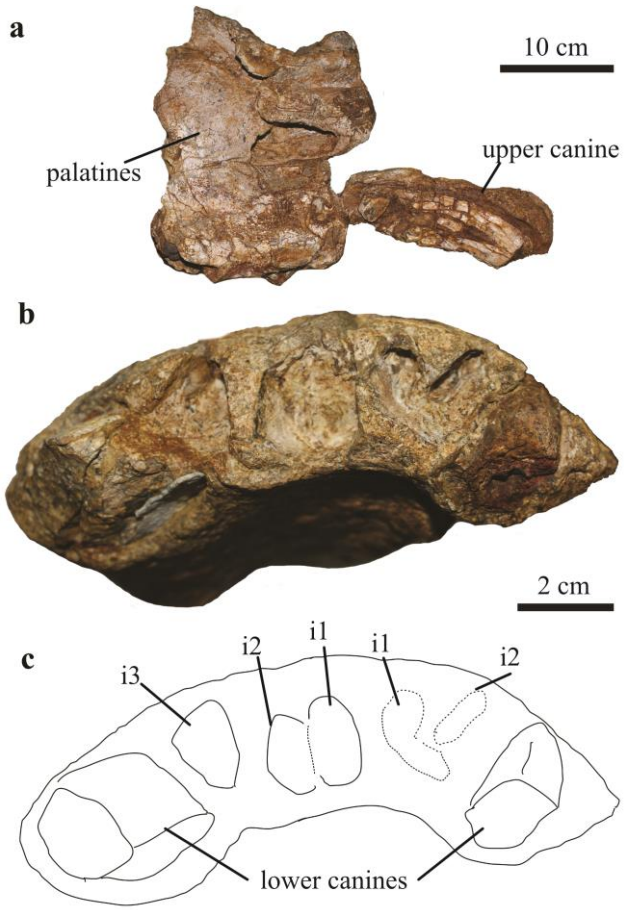

Figure 7. Partial skull and mandibular symphysis of *Hilarcotherium miyou* sp. nov. (referred specimen MUN-STRI 34216): (a) partial palate in ventral view; (b) mandibular symphysis in occlusal view; (c) drawing of the mandibular symphysis showing the canines and the alveoli of the incisors.

and a mesio-lingual pocket, unlike *G. snorki.* In addition to the mesio-lingual pocket, the P4 of *H. miyou* shares with that of *H. castanedaii* the absence of a hypocone and the presence of a lingual cingulum (Vallejo-Pareja et al. 2015); however, in *H. miyou* the cingulum is continuous.

Two M2 are referred to *H. miyou* (IGMp 881327 and MUN-STRI 34216), and these display a nearly quadrangular contour and the Y-shaped median valley, characteristic of the M2 in astrapotheriids (Figure 5e). They do not have a labial cingulum, which is present in *X. chaparralensis* (Johnson and Madden, 1997). *H. miyou* has a well-defined mesio-lingual pocket, parastyle, and paracone fold (Figure 5e). There is no evidence of a lingual cingulum, as in *G. snorki*, and unlike *H. castanedaii* and other Uruguaytheriinae (Vallejo-Pareja et al. 2015).

URUGUAYTHERIINAE INDET.

REFERRED MATERIAL MUN-STRI 16777, almost complete left humerus, left radius with unfused and missing distal epiphysis, vertebral centrum, distal tibia and associated bone fragments. MUN-STRI 16779, lower canine. MUN-STRI 16785, three fragmentary caudal vertebrae. MUN-STRI 34212, patella. MUN-STRI 34217, sacrum, fragment of

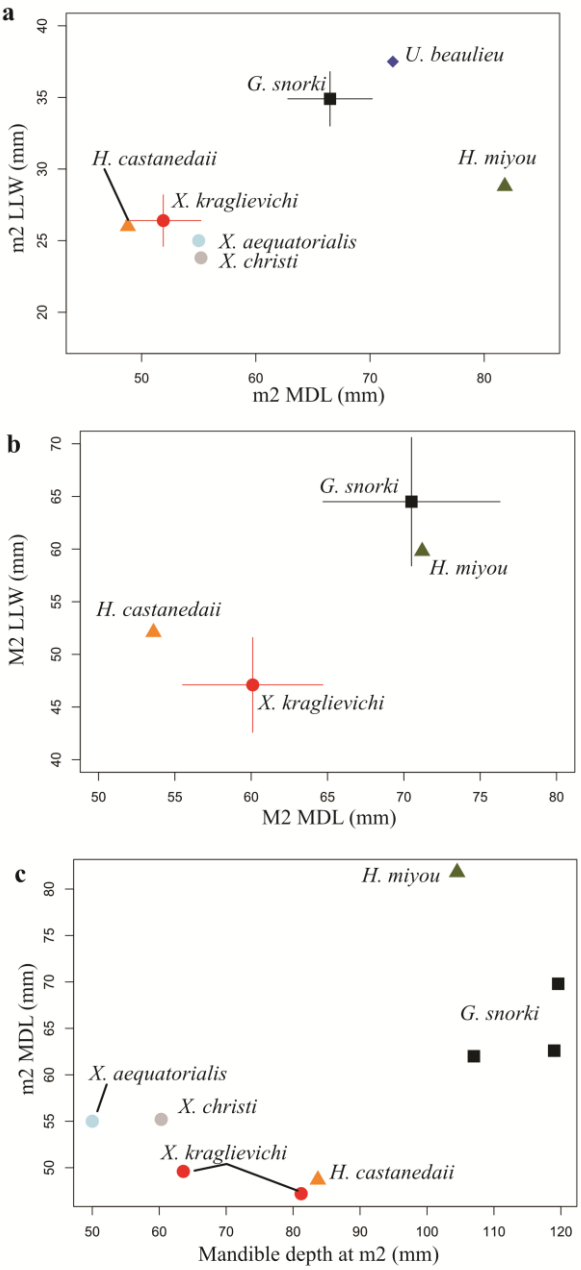

Figure 8. Bivariate plots with measurements of Uruguaytheriinae (Astrapotheria): (a) m2 mesiodistal length (MDL) vs. labiolingual width (LLW). In *G. snorki* and *X. kraglievichi,* the dot represents the mean and the bars the standard deviation provided by Johnson and Madden (1997); (b) M2 mesiodistal length (MDL) vs. labiolingual width (LLW). The values of *G. snorki* and *X. kraglievichi* are shown as explained earlier; (c) depth of the mandible at the level of m2 vs. m2 mesiodistal length (MDL).

acetabulum, and thoracic vertebra. MUN-STRI 34221, atlas, almost complete left radius, metapodial, molar fragment, rib fragments and a fragment of a neural arch. MUN-STRI 34222, proximal portion of left humerus. MUN-STRI 34223, almost complete left ulna, distal epiphysis of left humerus, distal portion of left scapula, ribs, and vertebrae fragments. MUN-STRI 34225, distal portion of scapula. MUN-STRI 34229, partial right femur, tibia, and fibula. MUN-STRI 34292, patella. MUN-STRI 34310, distal portion of femur. MUN-STRI 36644, posterior portion of basicranium (cast PIMUZ A/V 5292). MUN-STRI 37384, dorsal portion of left

scapula. MUN-STRI 37765, dorsal portion of scapula, partial radius and lunar. MUN-STRI 37390, distal tibia.

Locality and horizon

Castilletes Formation. MUN-STRI 16777, 16779, 16785, 34217, 34221, 34222, 34223, 34225, 34229, 34310, 36644, 37384, and 37390 come from Patajau, STRI locality 390094; 11.9465ºN, 71.3255ºW. MUN-STRI 37765 comes from STRI locality 130024; 11.9348ºN, 71.3344ºW. MUN-STRI 34212 comes from Patajau west, STRI locality 290632; 11.9458ºN, 71.3299ºW. MUN-STRI 34292 comes from Makaraipao, STRI locality 930093; 11.9089º N, 71.3401º W (Figure 3).

Description The isolated distal fragment of a canine (MUN-STRI 16779) has an oval wear facet that forms an acute chisel-like shape. The partial basicranium (MUN-STRI 36644) preserves the occipital condyles and part of the basioccipital and exoccipital (Figure 9a-b). The occipital condyles are large, measuring 85.5 mm in dorsoventral height and the maximum width between the condyles is 153.5 mm. The foramen magnum is larger than in *H. castanedaii* (Vallejo-Pareja et al. 2015). It is almost circular, as in *Astrapotherium* (Scott, 1928). The foramen magnum's mediolateral width measures 54.7 mm and its dorsoventral height is 52.4 mm. In contrast, the foramen magnum in *Astraponotus* is considerably more wide than high (Kramarz et al. 2011). The median notch at the dorsal margin of the foramen magnum is not as clearly differentiated as in *Astraponotus* (Kramarz et al. 2011). The exoccipital has a distinct process dorsal to the foramen magnum (Figure 9a-b).

The atlas (MUN-STRI 34221) preserves the cranial articular foveae, caudal articular surfaces, the neural and ventral arches, part of the transverse processes, and the transverse foramina (Figure 9c-d). It is comparable in size to that of *Parastrapotherium herculeum*? (Table 4; Figure 9e-f). The transverse process is wide as in *Astrapotherium* and *Parastrapotherium.* The cranial articular foveae for the occipital condyles are large, deeply concave, widely separated dorsally, and more proximate ventrally (Figure 9c), as in *Astrapotherium* (Scott, 1928, 1937) and *Parastrapotherium*

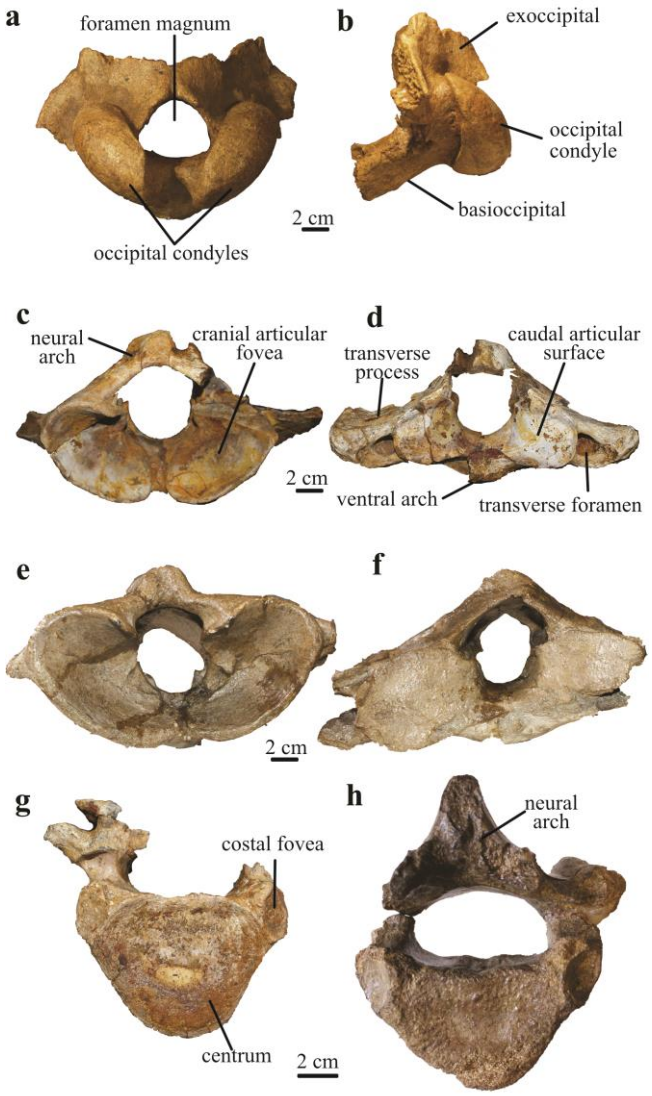

Figure 9. Basicranium and vertebrae of Uruguaytheriinae indet. from the Castilletes Formation, and selected astrapotheres for comparison. Uruguaytheriinae indet. basicranium (MUN-STRI 36644) in (a) caudal view, and (b) left lateral view. Uruguaytheriinae indet. atlas (MUN-STRI 34221) in (c) cranial view, and (d) caudal view. *Parastrapotherium herculeum*? (MNHN COL 6) atlas, from the Colhuehuapian of Argentina in (e) cranial view, and (f) caudal view. (g) Uruguaytheriinae indet. thoracic vertebra (MUN-STRI 34217) in caudal view; (h) *Parastrapotherium* sp. thoracic vertebra (MNHN DES 112) from the Deseadan of Argentina in caudal view.

(Figure 9e). The neural canal is circular in anterior and posterior view. The ventral side of the ventral arch is convex. The caudal articular surface is oval and nearly flat. The posterior opening of the large arterial foramen opens posteroventrally (Figure 9d), as in *Astrapotherium* (Scott, 1928). The thoracic vertebra (MUN-STRI 34217) preserves the centrum and a small fragment of the neural arch (Figure 9g). The centrum forms a triangle with rounded corners in anterior view, with the widest border on the dorsal side, as in *Parastrapotherium*. It has an oval articular surface for the rib on the dorsolateral edge of the centrum, also present in *Parastrapotherium* (Figure 9g-h).

The sacrum (MUN-STRI 34217) preserves three fused vertebrae of total

Table 4. Postcranial measurements (cm) of Astrapotheriidae. *=estimated. For the humerus in parenthesis is the acronym used in Scott (1990).

Atlas	Uruguaytheriinae	P. herculeum?
	MUN-STRI 34221	MNHN COL 6
Anteroposterior length	15.6*	16.5
Dorsoventral height	12.9*	14.8
Mediolateral width	26.2*	27.4
Caudal vertebra	Uruguaytheriinae	Parastrapoterium sp.
	MUN-STRI 34217	MNHN DES 112
Dorsoventral height of the centra	7.65	6.27
Anteroposterior length of the centra	5.95	5.19
Mediolateral width of centra	9.64	8.72
Scapula	Uruguaytheriinae	
	MUN-STRI 34384	MUN-STRI 37765
Dorso-ventral width at distal end	10.28	
Medio-lateral thickness at distal end		12.0*
Humerus	Uruguaytheriinae	P. herculeum?
	MUN-STRI 16777	MNHN COL 127
Length from head (H1)	65.0	
Length from external tuberosity (H2)	67.5	

Transverse diameter of the distal articulation surface (H4)	18.25	10.68				
Transverse epicondylar diameter (H5)	25.5*	19.0*				
Transverse diameter of the diaphysis below the deltoid process (H7)	9.1*					
Anteroposterior diameter of the diaphysis below the deltoid process (H8)	13.1*					
Ulna	Uruguaytheriinae	*P. hombergi*	Parastrapotherium sp.	P. herculeum?		
	MUN-STRI 34223	MNHN DES 985	MNHN DES 1013	MNHN COL 128		
Length		4.60	6.00	6.10		
Median width of diaphysis	5.06	6.55	8.79	8.10		
Olecranon height	6.34*	7.49	12.41	12.78		
Olecranon thickness		6.60	9.31	9.17		
Length of the trochlear notch	10.94	10.15	13.72	13.73*		
Width at distal epiphysis		8.46	6.92			
Thickness at distal epiphysis		6.92				
Radius	Uruguaytheriinae			*P. holmbergi*	Parastrapotherium sp.	
	MUN-STRI 16777	MUN-STRI 34221	MUN-STRI 37765	MNHN DES 989	MNHN DES 1013	MNHN COL 129
Length	40.0			33.5	43.5	
Width at proximal end	11.70	11.61		8.60	11.82	8.43
Thickness at proximal end	7.70	6.71	6.6*	5.27	6.95	5.28

Median width of diaphysis	5.72	4.34		5.18	8.71	
Width at distal epiphysis	11.77		12.0*	9.00	11.07	
Thickness at distal epiphysis	9.07		7.5*	5.57	8.14	
Femur	Uruguaytheriinae		*P. holmbergi*	Parastrapotherium sp.		
	MUN-STRI 34310	MUN-STRI 34229	MNHN DES 988	MNHN DES 1017		
Length from head		104.0*				
Length from greater trochanter		98.0*				
Median width of diaphysis	11.05	13.94*	9.52*			
Width at epicondyles	15.5*			17.2		

length 26.8 cm. It is likely that the sacrum was formed by more vertebrae, given that in *Astrapotherium* it consists of four and probably five vertebrae (Scott, 1937). In anterior view the vertebral centrum is oval, but in the most caudal vertebra the centrum is strongly compressed dorsoventrally. The neural arches of the vertebrae are fused, forming a continuous plate. The transverse processes are also fused, and one sacral foramen is observed.

Tree partial scapulae were recovered; they all represent the most dorsal portion of the scapula (Figure 10a-b). The scapula of astrapotheres has a distinctive club-like shape, not blade-like as in most mammals. In *Astrapotherium*, it narrows dorsally, but is wider anteroposteriorly than in the Uruguaytheriinae indet., forming a more quadrangular end (Figure 10a,c; Scott 1909, 1937). In the Uruguaytheriinae indet., the dorsal end seems more bulbous. The fragmentary Uruguaytheriinae scapulae show a spine that is wide and well developed laterally (Figure 10a-b), as in *Astrapotherium* and *Parastrapotherium* (Loomis, 1914).

One almost complete humerus (Figure 10e-h) reveals that the Uruguaytheriinae indet. from the Castilletes Formation was large and comparable in size only to *G. snorki* (Johnson and Madden, 1997: table 22.6). The associated radius with unfused distal epiphysis (see below) indicates that

Figure 10. Scapulae and humeri of Uruguaytheriinae indet. from the Castilletes Formation, and selected astrapotheres for comparison. Uruguaytheriinae indet. scapulae, (a) MUN-STRI 38384 in lateral view; (b) MUN-STRI 34223 in anterior or posterior view; left scapula of *Astrapotherium magnum* from the Santa Cruz Formation, Argentina (YPM PU 15255) in (c) lateral view and (d) posterior view. Uruguaytheriinae indet. left humerus (MUN-STRI 16777), (e) anterior view; (f) schematic drawing in anterior view; (g) medial view; (h) posterior view. Uruguaytheriinae indet. partial humeri, (i) proximal portion of left humerus (MUN-STRI 34222); Uruguaytheriinae indet. distal epiphysis of left humerus (MUN-STRI 34223), (j) anterior view and (k) posterior view. Left humerus of *Astrapotherium magnum* (YPM PU 15255) in (l) anterior and (m) posterior view.

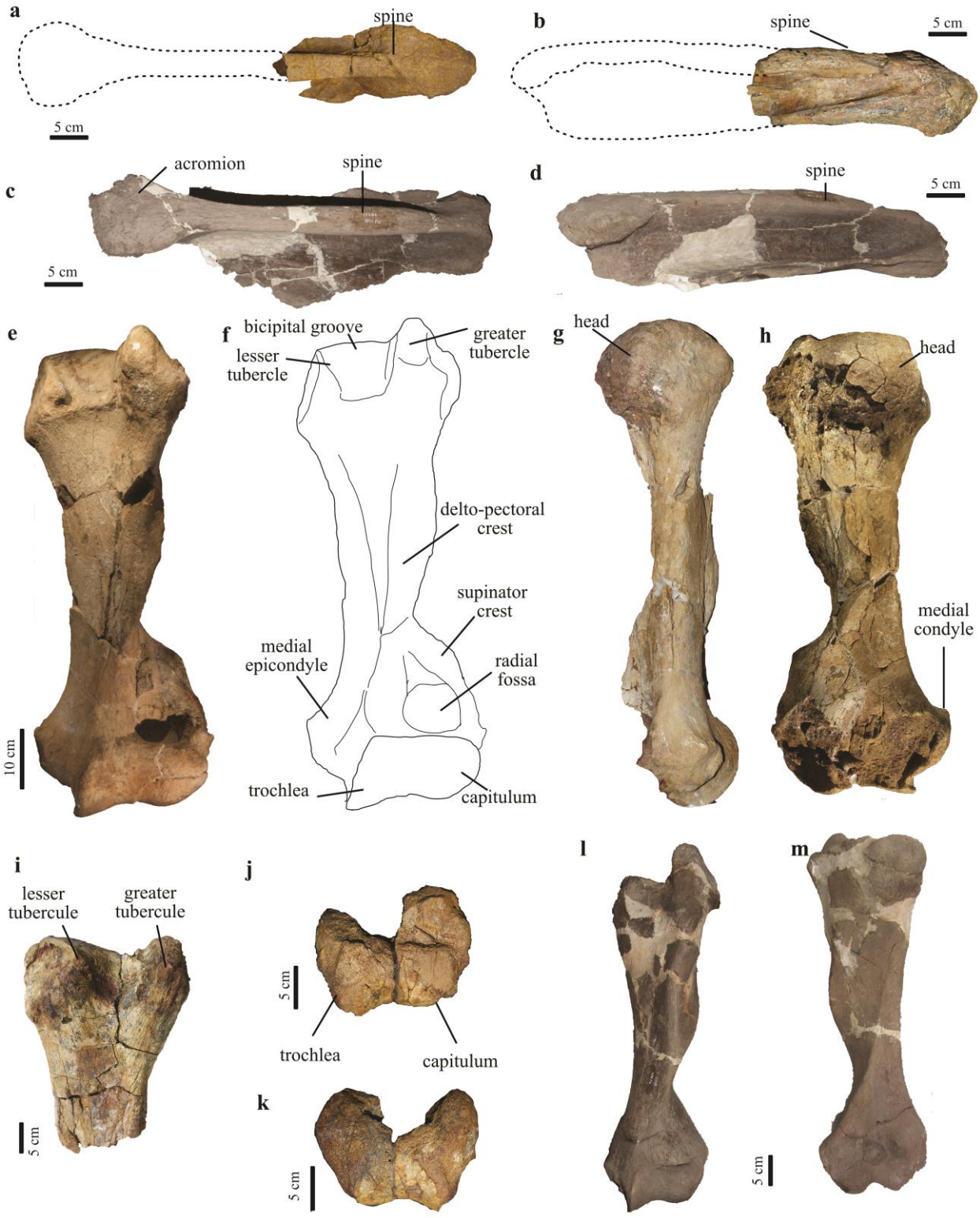

this individual was not skeletally mature. The humerus is larger and more robust than in *H. castanedaii, A. magnum*, and *P. herculeum*? (Figure 10e-m; Table 4). The head is large and projects posteriorly to the plane of the shaft (Figure 10g), as in *H. castanedaii* and *A. magnum* (Scott, 1928, 1937; Vallejo-Pareja et al.

2015). The greater tubercle extends more proximally than the lesser tubercle (Figure 10e,i), as in *H. castanedaii* and *A. magnum*. The bicipital groove is broad and shallow, more than in *H. castanedaii* and *A. magnum.* The shaft is proportionally slender, but it has an elongated and marked delto-pectoral crest, which extends up to about two-thirds of the humeral length, as in *Parastrapotherium* (Loomis, 1914). The supinator crest is small and narrow. The radial fossa is large and deep, with no foramen (Figure 10e-f), as in *H. castanedaii* and *A. magnum* (Scott, 1928, 1937; Vallejo-Pareja et al. 2015). The capitulum is rounded and extends less distally than the trochlea, as in *H. castanedaii* and *A. magnum* (Figure 10e,j). The medial epicondyle is well developed as in *H. castanedaii* and unlike in *A. magnum* (Vallejo-Pareja et al. 2015).

An almost complete ulna (MUN-STRI 34223) was recovered and lacks only its most distal portion (Figure 11a-d). The shaft is antero-posteriorly deeper than mediolaterally wide. The olecranon is short and robust, as in *Parastrapotherium* (Figure 11a-f; Loomis, 1914). In anterior view, the olecranon projects more medially than the plane of the shaft (Figure 11a), but in lateral view the olecranon and the shaft are on the same plane (Figure 11c), as in *Parastrapotherium* (Figure 11e-f) and *A. magnum* (Scott, 1937). The length of the trochlear notch is similar to that in *P. holmbergi*, but smaller than in *P. herculeum*? (Table 4). The trochlear notch forms a semicircle in lateral view (Figure 11c). The coronoid process is large and is almost perpendicular to the axis of the shaft (Figure 11c-d), whereas in *Parastrapotherium* it is more oblique (Figure 11f). Distal and lateral to the coronoid process is the radial notch (Figure 11b), as in *Parastrapotherium* (Figure 11e).

Remains of several Uruguaytheriinae radii were recovered from Castilletes. The most complete (MUN-STRI 16777; Figure 11g-h) is from a juvenile, as determined from the unfused and missing distal epiphysis. It is comparable in size to the large specimens of *Parastrapotherium* (Table 4). The proximal end is wider than the shaft (Figure 11g-j) as in

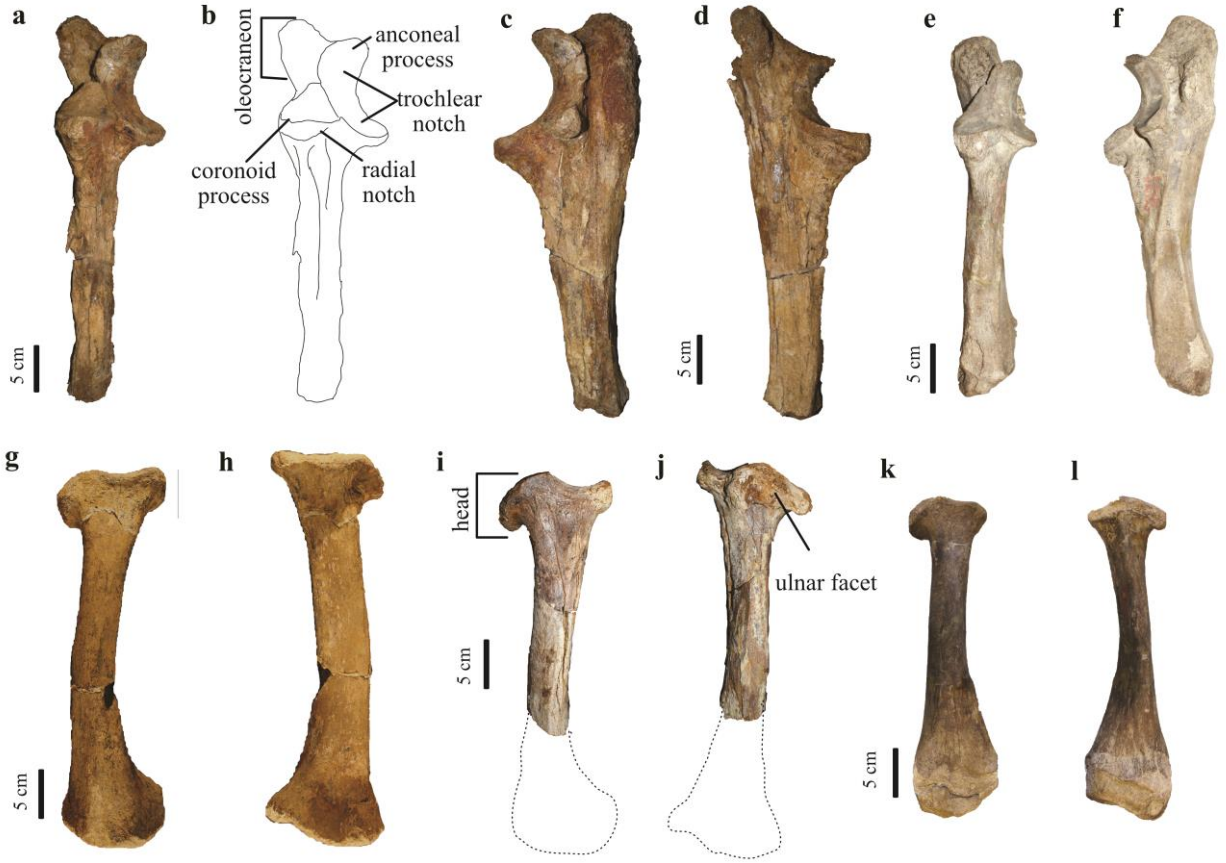

Figure 11. Antebrachial bones of Uruguaytheriinae indet. from the Castilletes Formation, and selected astrapotheres for comparison. Uruguaytheriinae indet. left ulna (MUN-STRI 34223), (a) anterior view; (b) schematic drawing in anterior view; (c) lateral view; (d) medial view. Left ulna of *Parastrapotherium holmbergi* (MNHN DES 985) from the Deseadan of Argentina in (e) anterior and (f) lateral view. Left radius of Uruguaytheriinae indet. (MUN-STRI 16777), (g) anterior, and (h) posterior view. MUN-STRI 34221, (i) anterior, and (j) posterior view. Left radius of *Parastrapotherium holmbergi* (MNHN DES 989) in (k) anterior and (l) posterior view.

Astrapotherium and *Parastrapotherium* (Figure 11k-l). The articular surface for the humerus is divided into two sections, the medial is concave and the lateral is saddle-shape, as in *A. magnum* (Scott, 1928, 1937). The anterior border of the proximal epiphysis is more proximal than the posterior one. The shaft is slightly curved (Figure 11g-h).

Two fragmentary femora were recovered from Castilletes. MUN-STRI 34229 is almost complete but badly preserved, and no details from the

epiphyses can be observed. MUN-STRI 34310 preserves part of the shaft and the distal epiphysis. The median and lateral epicondyles project distally to the same level, and the articulation surface for the patella seems narrower than in *A. magnum* (Scott, 1937). The patella (MUN-STRI 34212) is oval and elongated proximodistally, narrowing at its distal end, as in *A. magnum* (Scott, 1937). It measures 15 cm in length. It is curved in lateral view, with a convex anterior border. The articular facet is quadrangular and measures 8.5 cm proximodistally and 6.2 cm mediolaterally. MUN-STRI 16777 includes a partial distal left tibia. The shaft is trihedral in cross section. The medial malleolus is broad, very similar to the condition of the tibiae reported from the Castillo Formation (Weston et al. 2004). MUN-STRI 34229 also includes a fibula, which is slender and straight, as in *A. magnum* (Riggs, 1935; Scott, 1937).

Body mass estimation

The body mass estimate from the m2 length of the holotype of *H. miyou* is 6456.6 kg (Table 5). Previous studies used the m1-m3 length to estimate the body mass in astrapotheres (Johnson and Madden, 1997; Kramarz and Bond, 2011; Vallejo-Pareja et al. 2015). For other taxa, including the uruguaytheriines *H. castanedaii, G. snorki*, and *X. kraglievichi*, the body mass estimates from the m2 length are similar to the ones obtained from the m1-m3 length in the same specimen (Table 5), suggesting that if the lower molar row length could be measured in *H. miyou*, it would yield a similar estimate than the m2 length. The length of proximal limb bones is highly correlated with body mass in ungulates (Scott, 1990). The humerus length of the large Uruguaytheriinae indet. from Castilletes (MUN-STRI 16777) yields an estimate of 4985.0 kg (Table 5), 23% less than the value obtained from the m2 length in *H. miyou.*

Phylogenetic analysis of Astrapotheriidae

The cladistic analysis resulted in nine most parsimonious trees of 127 steps, with a consistency index of 0.685 and retention index of 0.763. Ten characters

Table 5. Body mass estimates of astrapotheres (in kg). BM= Body mass; %PE= Percent of error. The estimations from the m2 length and m1-m3 length uses the equations of non-selenodont ungulates (Damuth, 1990). For m2 length: log(BM)= 2.98*log(m2 length)+1.11; with a r^2=0.97 and %PE=30.61. For m1-m3 length: log(BM)= 3.03*log(m1-m3 length)-0.39; with a r^2=0.96 and %PE=37.19. The estimate from the humerus length follows the equation of all ungulates for H2 in Scott (1990). The equation is: log (BM)=3.4026*log(H2)-2.513; with a r^2=0.9196 and %PE=29. [a], reported by Vallejo-Pareja et al. (2015); [b], reported by Johnson and Madden (1997); [c], reported by Kramarz and Bond (2011).

Taxa	Specimen	BM estimate from m2 length			
		Value (mm)	BM	BM+PE	BM-PE
Hilarcotherium miyou	IGMp 881327	81.8	6456.6	8433.0	4480.2
Hilarcotherium castanedaii[a]	IGM p881231	48.8	1385.1	1809.1	961.1
Granastrapotherium snorki[b]	mean of 9 specimens	66.5	3483.4	4549.7	2417.2
Xenastrapotherium kraglievichi	MLP 12-96	49.3	1427.9	1864.9	990.8
Parastrapotherium martiale	MACN A 52604	66.9	3546.3	4631.8	2460.7
Astrapotherium giganteum	MACN-A 3274 -3278	64.6	3195.2	4173.2	2217.1
		BM estimate from m1-m3 length			
		Value (mm)	BM	BM+PE	BM-PE
Hilarcotherium castanedaii[a]	IGM p881231	140.2	1302.7	1787.1	818.2
Granastrapotherium snorki[b]	UCMP 40017	187.5	3141.9	4310.4	1973.4
Xenastrapotherium kraglievichi[c]	MLP 12-96	141	1324.7	1817.4	832.1
Parastrapotherium martiale[c]	MACN A 52604	194	3483.7	4779.3	2188.1
Astrapotherium giganteum[c]	MACN-A 3274 -3278	196	3593.7	4930.1	2257.2
		BM estimate from humerus length			
		Value (cm)	BM	BM+PE	BM-PE
Hilarcotherium castanedaii[a]	IGM p881231	45.5	1306.5	1685.4	817.7
Uruguaytheriinae indet.	MUN-STRI 16777	70	4985.0	6430.7	3120.1
Granastrapotherium snorki[b]	UCMP 40192	65.5	4501.1	5806.4	2817.3
Astrapotherium magnum[b]	FMNH 14251	52.3	2096.5	2704.4	1312.2

were parsimony uninformative. We present the strict consensus and the 50% majority rule consensus (Figure 12). The obtained consensus topologies differ from

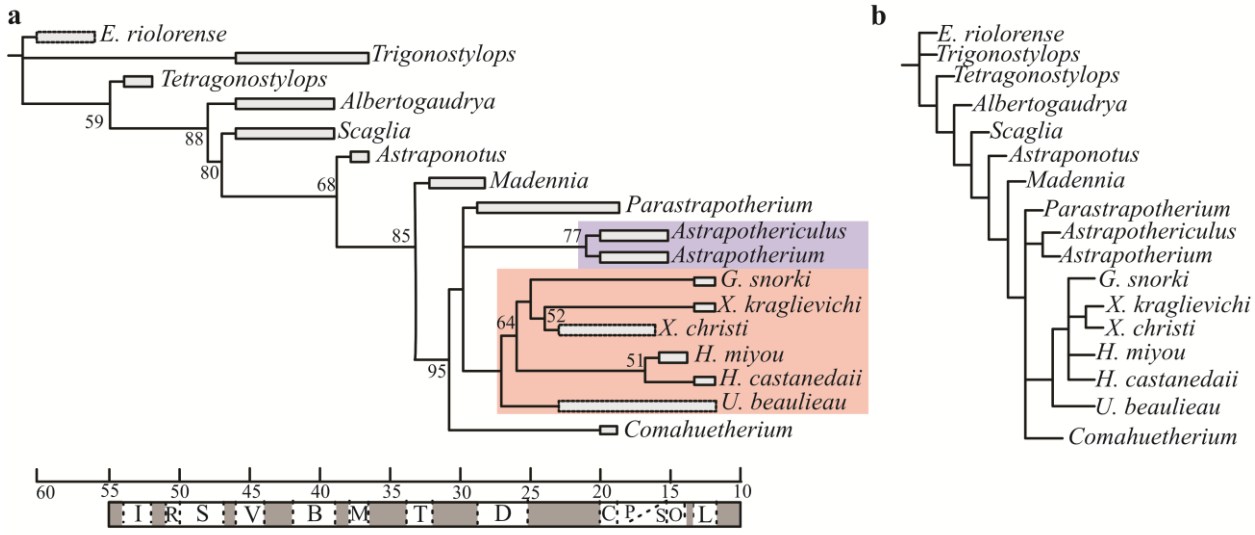

Figure 12. Hypothesis of phylogenetic relationships within Astrapotheriidae. (a) Time-calibrated topology of the 50% majority rule consensus resulting from the analysis with PAUP* 4.0. Bootstrap values are indicated for several nodes. Blue= Astrapotheriinae, red= Uruguaytheriinae. The letters below the time line denote the SALMAs; I=Itaboraian, R=Riochican, S=Sapoan, V=Vacan, B=Barrancan, M=Mustersan, T=Tinguirican, D=Deseadan, C=Colhuehuapian, P=Pinturan, S=Santacrucian, O=Colloncuran, L=Laventan. (b) Strict consensus resulting from the analysis of the same data matrix.

the one presented by Vallejo-Pareja et al. (2015; fig. 6) only in the relationships of northern Uruguaytheriinae. In the strict consensus, *Comahuetherium, Parastrapotherium*, and the clades Astrapotheriinae and Uruguaytheriinae form a polytomy (Figure 12b), whereas in the 50 percent majority rule consensus, *Comahuetherium* is the sister taxon of all the other taxa just mentioned, and *Parastrapotherium,* Astrapotheriinae, and Uruguaytheriinae for a polytomy (Figure 12a). The Astrapotheriinae (*Astrapotherium*, *Astrapothericulus*) clade has a bootstrap value of 77 and is supported by four unambiguous synapomorphies that concern the molars: deep hypoflexid (26[0]), the presence of a lingual cingulid (30[1]), a rounded hypocone (40[0]), and an ephemeral median fossette (44[1]). The Uruguaytheriinae clade has a bootstrap value of 64 and is supported by two unambiguous synapomorphies: the absence of molar hypoflexid (26[2]) and the absence of labial cingulum in the

molars (27[0]). The Uruguaytheriinae from northern South America (*Hilarcotherium, Granastrapotherium*, and *Xenastrapotherium*) form a clade supported by one unambiguous synapomorphy, the presence of a superficial paraflexid on the molars (28[1]).

In the 50 percent majority rule consensus (Figure 12a), the two species of *Hilarcotherium* appear as sister group of (*G. snorki, (X. kraglievichi, X. christi)*). In this topology, *H. castanedaii* and *H. miyou* form a clade that has a bootstrap value of 51 and is supported by having lophodont cheek teeth with high crowns, with the crown height being smaller than the mesiodistal length of the tooth (61[1]). The clade formed by *Granastrapotherium* and *Xenastrapotherium* is supported by the absence of i3 (3[1]) and the absence of a mesiolingual pocket in P4 (23[0]). Finally, *X. kraglievichi* and *X. christi* form a clade supported unambiguously by the presence of a superficial hypoflexid (26[1]).

NOTOUNGULATA ROTH, 1903

TOXODONTIA OWEN, 1853

LEONTINIIDAE AMEGHINO, 1895

cf. *Huilatherium* Villaroel and Guerrero, 1985

TYPE SPECIES *Huilatherium pluripicatum* Villaroel and Guerrero, 1985

REFERRED MATERIAL MUN-STRI 34312 right m3 (cast PIMUZ A/V 5290).

LOCALITY AND HORIZON MUN-STRI 34312 comes from Patajau, Castilletes Formation, STRI locality 340094; 11.9465ºN, 71.3255ºW (Figure 3).

DESCRIPTION The isolated tooth is interpreted as an m3 because of its elongate talonid that narrows distally (Figure 13a). It is protohypsodont (rooted teeth, crown height <50% of mesiodistal length [Pérez and Vucetich, 2012]), with a mesiodistal length of 40.4 mm and labiolingual width of 14.5 mm, approximately 30% smaller than the m3 of *H. pluripicatum* (Villaroel and Colwell Danis, 1997: table 19.4). The crown height measured at the labial side is 14.4 mm, yielding a hypsodonty index of 0.4, although this value may be an underestimation for this animal as

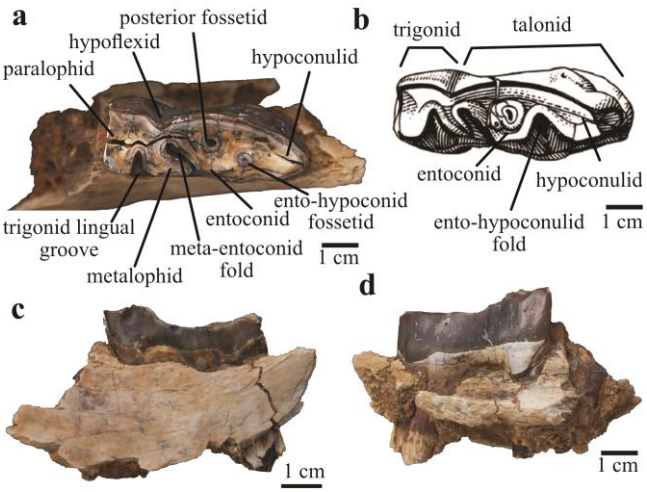

Figure 13. Leontiniidae (Notoungulata) right m3: (a) cf. *Huilatherium* (MUN-STRI 34312) in occlusal view; (b) *H. pluripicatum* (UCMP 40280), modified from Villaroel and Colwell Danis (1997); (c) MUN-STRI 34312 in lingual and (d) labial view.

the appearance of the ento-hypoconulid as a fossettid indicates high wear in the specimen (Figure 13 a-b; see below).

The paralophid is wide and perpendicular to the mesiodistal axis of the crown. The trigonid lingual groove is well developed and straight, projecting from the lingual to the labial side of the crown. The metalophid is wider than in *H. pluripicatum* and it is oblique. The meta-entoconid fold is well developed and projects linguomesially, as in *H. pluripicatum* (Figure 13a). It has a posterior fossettid, which is rounded and not U-shaped, as in *H. pluripicatum* (Figure 13a-b). Due to wear, the ento-hypoconid fold appears as a fossettid between the entoconid and the hypoconulid (Figure 13a). According to Villaroel and Colwell Danis (1997), in *H. pluripicatum* the ento-hypoconid fold (treated as "entoflexid" by these authors) appears as a "large rounded pit" with extensive wear. The hypoconulid is large and almost parallel to the mesiodistal axis of the tooth, as in *H. pluripicatum* (Villaroel and Colwell Danis, 1997). There are neither lingual nor labial cingulids (Figure 13c-d). In *H. pluripicatum* and *Colpodon distinctus,* the labial cingulid is absent, and the lingual cingulid is present but reduced (Villaroel and Colwell Danis, 1997; Ribeiro et al. 2010). In *Henricofilholia* the labial and lingual cingulids are variably developed (Ribeiro et al. 2010), and *Martinmiguelia*, *Scarritia, Elmerriggsia* and *Gualta* have both lingual and labial cingulids (Ubilla et al. 1994; Bond and López, 1995; Ribeiro et al. 2010; Shockey et al. 2012; Cerdeño and Vera, 2015).

Toxodontidae (Gervais, 1847)

Toxodontinae

Falcontoxodon gen. nov.

Type species *Falcontoxodon aguilerai* sp. nov.

Diagnosis As for the type and only species.

Falcontoxodon aguilerai sp. nov.

(Figures 14 and 16)

Etymology The genus name is for the Falcón state in Venezuela, where the holotype was found. The species name is after Orangel Aguilera, in recognition of his lifetime contribution to paleontology in Venezuela.

Holotype AMU-CURS 765, fairly complete skull with left I1 and P3-M3 and right P3-M1 in situ, and associated right I2, M2, and M3. Alveoli of the other teeth are preserved. Mandible with complete dentition excepting left i2 and right i1-i2.

Referred material AMU-CURS 70, left m3.

Type locality and horizon The holotype and AMU-CURS 70 were collected in the Algodones Member, Codore Formation, Urumaco, Falcón State, Venezuela. 11°17´39.8´´N 070°14´15.6´´W (Figure 4a-b).

Diagnosis The dental formula is i 2/3, c 1/0, p 4/4, m 3/3. Mandibular symphysis reaches the level of m1-m2. Comparable in size to *Pericotoxodon*, larger than *Nesodon* and *Xotodon*, and smaller than *Toxodon* and *Mixotoxodon*. Upper molars with simple enamel lingual fold. Well-defined protoloph lingual column present only in M3. It differs from *Gyrinodon* in the sigmoid shape of the zygomatic arch, the broad metaloph, and the absence of a ventral extension of the dentary. It differs from *Mixotoxodon* in having a short diastema posterior to i3, lingual enamel band of m1 restricted between the anterior fold and the hypoconulid, a less developed lower molar anterior fold, and less procumbent lower incisors. It differs from *Trigodonops* in the absence of a labial groove in p3 and p4. It differs from *Piauhytherium* in having a long nasal and the presence of an upper canine. It differs from *Pericotoxodon* in the position of the infraorbital foramen, widely separated from the zygomatic arch, the absence of I3, the upper molars with

a simple enamel fold, and the absence of a ventral extension of the horizontal ramus of the mandible. It differs from *Andinotoxodon* in the presence of p1, absence of lingual enamel in the lower premolars, and in having a labiolingually narrower entolophid. It differs from *Hoffstetterius* in the presence of the upper canine and P1, and the absence of a mandibular ventral extension. It differs from *Paratrigodon* and *Trigodon* in the presence of P1 and lingual enamel in P3-P4. It differs from *Calchaquitherium* in the rounded angle of the posteroventral border of the vertical ramus of the mandible, the incisors being at the same level as the cheek teeth, and the absence of a median symphyseal labial keel.

Description The skull is pyriform in ventral view (Figure 14b), and the nasal is long as in most toxodontids (Forasiepi et al. 2015). The premaxilla is not expanded laterally, as in most Toxodontinae except for *Toxodon* (Owen, 1840) and *Hoffstetterius* (Saint-André, 1993). The infraorbital foramen is distant from the zygomatic arch (Figure 14a), as in *Adinotherium, Nonotherium, Nesodon, Palyeidodon, Hoffstetterius, Gyrinodon*, and *Toxodon,* and unlike *Pericotoxodon, Posnanskytherium, Trigodon, Piauhytherium, Paratrigodon*, and *Xotodon* in which the infraorbital foramen is in close proximity to the zygomatic arch (Madden, 1997; Guérin and Faure, 2013; Forasiepi et al. 2015). The zygomatic arch is sigmoid (Figure 14a), unlike the condition in *Gyrinodon, Toxodon, Hoffstetterius, Palyeidodon*, and *Trigodon,* and the root of the zygomatic process of the squamosal is located dorsal to the M3 (Figure 14a-b), as in most toxodontids except for *Posnanskytherium*, in which it is positioned dorsal to the M2 (Madden 1997).

The palate is widest at the level of M3 and narrows towards P1. Anterior to P1 the palate is elongate and the lateral borders are parallel (Figure 14b). The I1 is approximately oval in cross section, similar to *Calchaquitherium* (Nasif et al. 2000). The I2 is developed as a tusk. It has enamel only on the labial side of the crown (Figure 14e), as in *Gyrinodon* (Figure 15c). The I3 is absent, unlike in *Pericotoxodon, Trigodon, Pisanodon, Palyeidodon,* and *Nesodon.* There is a diastema of 51 mm between I2 and C

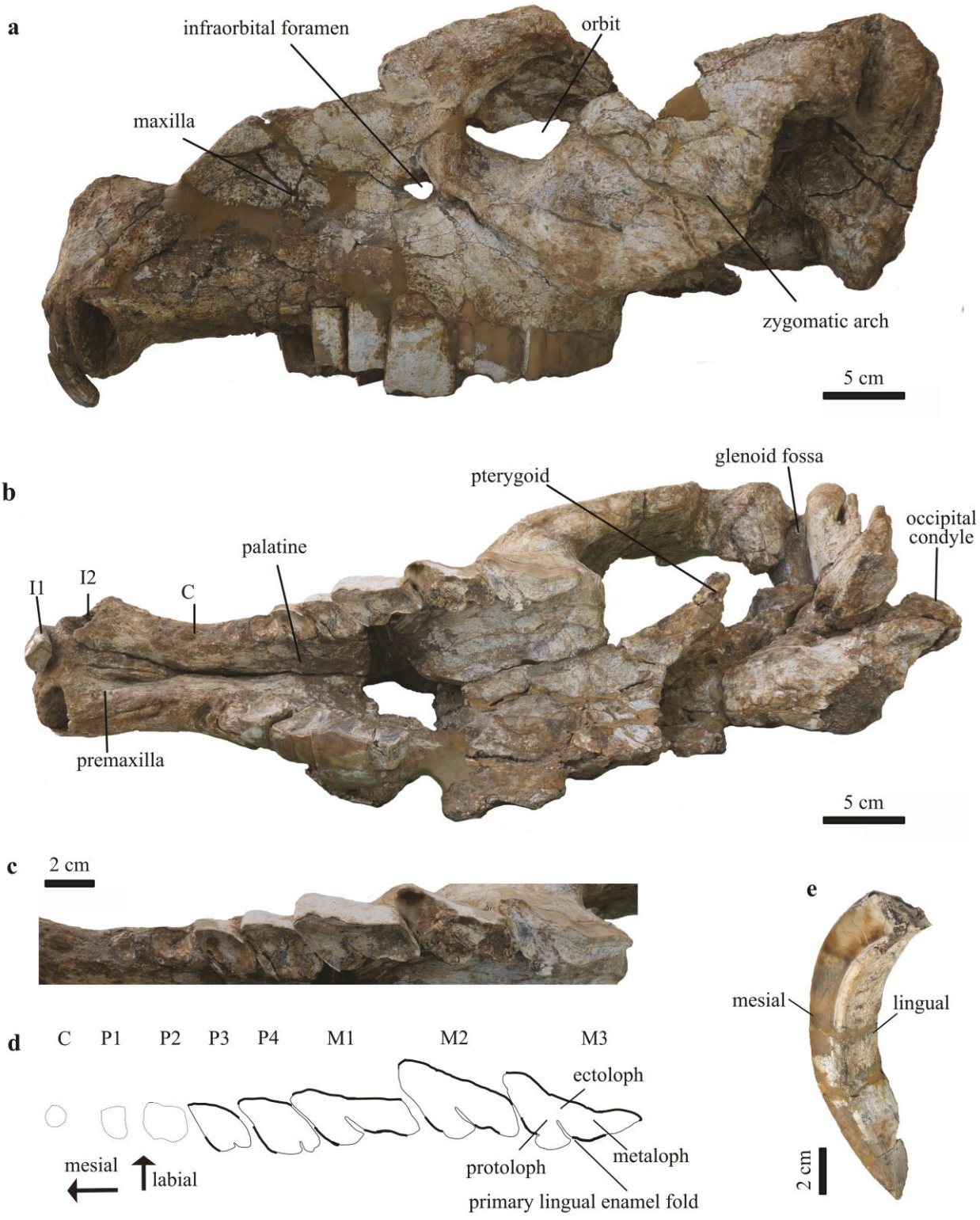

Figure 14. Skull of *Falcontoxodon aguilerai* gen. et sp. nov. (Toxodontidae, Notoungulata) (holotype, AMU-CURS 765): (a) left lateral view; (b) ventral view; (c), detail of the upper left dentition in occlusal view; (d) schematic drawing of the dentition, the distribution of enamel is shown by the thick lines; (e) right I2 in mesio-lingual view.

(Figure 14b), and a shorter diastema between C and P1 (Figure 14d), as in *Pericotoxodon* (Madden, 1997). The upper canine is greatly reduced, as shown by the size of the alveolus, with a diameter of approximately seven millimeters (Table 6).

The upper and lower cheek teeth are hypselenodont (rootless) as in most toxodontids (Forasiepi et al. 2015). Only the alveoli of P1 and P2 are preserved. The P3 does not have a lingual enamel fold, but one is present in P4 (Figure 14d), as in *Mixotoxodon* and *Piauhytherium* (Van Frank, 1957; Guérin and Faure, 2013). The P4, and in a lesser degree the P3, are elongate mesiolabially, resulting in tear-drop shape in cross section (Figure 14d), similar to *Pericotoxodon* and *Mixotoxodon* (Van Frank, 1957; Madden, 1997). In occlusal view, there is a broad labial enamel band that reaches the mesiolabial corner, and a second enamel band in the mesio-lingual portion of the P3-P4 (Figure 14d) as in *Pericotoxodon* and *Mixotoxodon*. Madden (1997) noted that this band is obliterated in advanced stages of wear in *Pericotoxodon.*

The upper molars have a simple, persistent primary lingual enamel fold, which separates the protoloph from the metaloph (Figure 14d; see also Madden 1990; 1997), as observed in individuals of *Pericotoxodon* with an advanced stage of dental wear (Madden 1997, fig. 21.5), as well as in *Andinotoxodon* (Madden, 1990), *Mixotoxodon* (Laurito, 1993), *Piauhytherium* (Guérin and Faure, 2013), and *Gyrinodon* (Figure 15d). The protoloph does not support a lingual column in M1 and M2, but one is present in M3 (Figure 14d). In contrast, the lingual column is present in all molars in *Pericotoxodon* (Madden, 1997), and it is absent in *Mixotoxodon* (Laurito, 1993) and *Andinotoxodon* (Madden, 1990). The metaloph is broad and does not taper distally, as in most specimens of *Pericotoxodon* (Madden, 1997).

The horizontal ramus of the mandible of *Falcontoxodon* does not have a ventral extension (Figure 16a), in contrast to the presence of this feature in *Pericotoxodon* (Madden, 1997) and *Gyrinodon* (Figure 15a). The vertical ramus is wide and

Table 6. Dental measurements of *Falcontoxodon* (in mm). *Tooth crown incomplete, **measured at the alveolus

Taxa	Specimen	Feature	Side	Measurement	Value
Falcontoxodon aguilerai	AMU-CURS 765	I1	Left	Maximum length	16
				Maximum width	25
		I2	Left	Maximum length	24
				Maximum width	35
		C	Left	Maximum length**	7
				Maximum width**	6
			Right	Maximum length**	7
				Maximum width**	6
		P1	Left	Maximum length**	13
				Maximum width**	16
		P2	Left	Maximum length	19
				Maximum width	19
			Right	Maximum length	19
				Maximum width	19
		P3	Left	Maximum length	22
				Maximum width	24
			Right	Maximum length	22
				Maximum width	25
		P4	Left	Maximum length	30
				Maximum width	29
			Right	Maximum length	29
				Maximum width	30
		M1	Left	Ectoloph length	45
				Maximum length	55
			Right	Ectoloph length	49
				Maximum length	36
		M2	Left	Ectoloph length	50
				Maximum width	44
			Right	Ectoloph length	51
				Maximum width	45

		M3	Left	Ectoloph length	63
				Maximum width	41
			Right	Ectoloph length	64
				Maximum width	41
		Diastema I2-C	Left	Length	51
			Right	Length	51
		Upper molar row	Left	Length	150
		i1	Left	Length	21
				Width	17
		i3	Left	Length	39
				Width	25
			Right	Length	40
				Width	24
		p1	Left	Length**	14
				Width**	9
		p2	Left	Length**	19
				Width**	22
		p3	Left	Length	22
				Width	16
			Right	Length	22
				Width	16
		m1	Left	Length	42
				Talonid width	17
			Right	Length	43
				Talonid width	21
		m2	Left	Length	42
				Trigonid width	18
				Talonid width	15
			Right	Length	41
				Trigonid width	18
				Talonid width	15
		m3	Left	Length	59
				Trigonid width	17
				Talonid width	11

			Right	Length	59
				Trigonid width	17
				Talonid width	12
		Lower molar row	Left	Length	14.6
			Right	Length	14.5
	AMU-CURS 70	m3	Left	Length	49.9
				Trigonid width	13.4
				Talonid width	9.2
Falcontoxodon aff. *aguilerai*	AMU-CURS 585	C	Right	Maximum length	21.6
				Maximum width	15.6
		P2	Left	Maximum length	14.9
				Maximum width	16.7
		P3	Left	Maximum length	16.3
				Maximum width	18.0
		P4	Left	Maximum length	26.0
				Maximum width	21.5
		M1	Left	Ectoloph length	44.4
				Maximum width	23.5
		M2	Left	Ectoloph length	47.2
				Maximum width	22.6
		M3	Left	Ectoloph length	54.6
				Maximum width	25.1
		Diastema	Right	Length	88.0
		Upper molar row	Left	Length	115.9
Falcontoxodon sp.	AMU-CURS 69	m1	Left	Length*	34.4
				Talonid width	12.0
		m2	Left	Length	36.1
				Trigonid width	13.3
				Talonid width	11.4
		m3	Left	Length	48.3
				Trigonid width	12.7
				Talonid width*	9.3
		Lower molar row	Left	Length	119.0

	AMU-CURS 270	m3	Left	Length	44.5
				Trigonid width	13.0
				Talonid width	8.7

has a rounded caudoventral border (no distinct angular process), in contrast with the right-angle border of *Pericotoxodon* and *Calchaquitherium* (Madden, 1997; Nasif et al. 2000). The coronoid process is at the same level as the condyle, as in *Mixotoxodon* (Van Frank, 1957). There is no median symphyseal labial keel, unlike in *Nesodon* and *Calchaquitherium* (Nasif et al. 2000; Forasiepi et al. 2015). The symphysis extends caudally up to the level of m1-m2 (Figure 16b), in contrast to *Trigodonops, Piauhytherium*, *Mixotoxodon*, and *Gyrinodon* where it extends until the p4-m1.

The i1 is triangular in cross section, with a broad labial enamel band and a narrow lingual band, as in *Mixotoxodon* (Van Frank, 1957; Laurito, 1993). Only the alveolus of i2 is preserved. The i3 is tusk-like, with broad labial and lingual enamel bands (Figure 16c). There is a short diastema between i3 and p1. The c is absent, as in *Mixotoxodon, Calchaquiterium, Paratrigodon, Trigodon*, and *Piauhytherium* (Guérin and Faure, 2013; Forasiepi et al. 2015). Only the alveoli of p1 and p2 are preserved. The p3 and p4 are approximately rectangular in cross section, without a labial groove in p3 but present in p4 (Figure 16d), similar to *Mixotoxodon* (Van Frank, 1957), and unlike *Trigodonops* and *Piauhytherium*, which have a marked labial groove in both p3 and p4 (Paula Couto, 1979; Guérin and Faure, 2013).

The lower molars are bicrescentic and ever growing, with a well-defined labial enamel fold (Figure 16c-d). The m1 has a lingual enamel band between the anterior fold and the hypoconulid (Figure 15d). In contrast, the lingual enamel of the m1 of *Mixotoxodon* is between the meta-entoconid fold and the hypoconulid (Van Frank, 1957; Rincón, 2011). The m1 and m2 have a shallow mesial fold at the same level as the labial fold, as in *Mixotoxodon* and *Gyrinodon* (Hopwood, 1928; Van

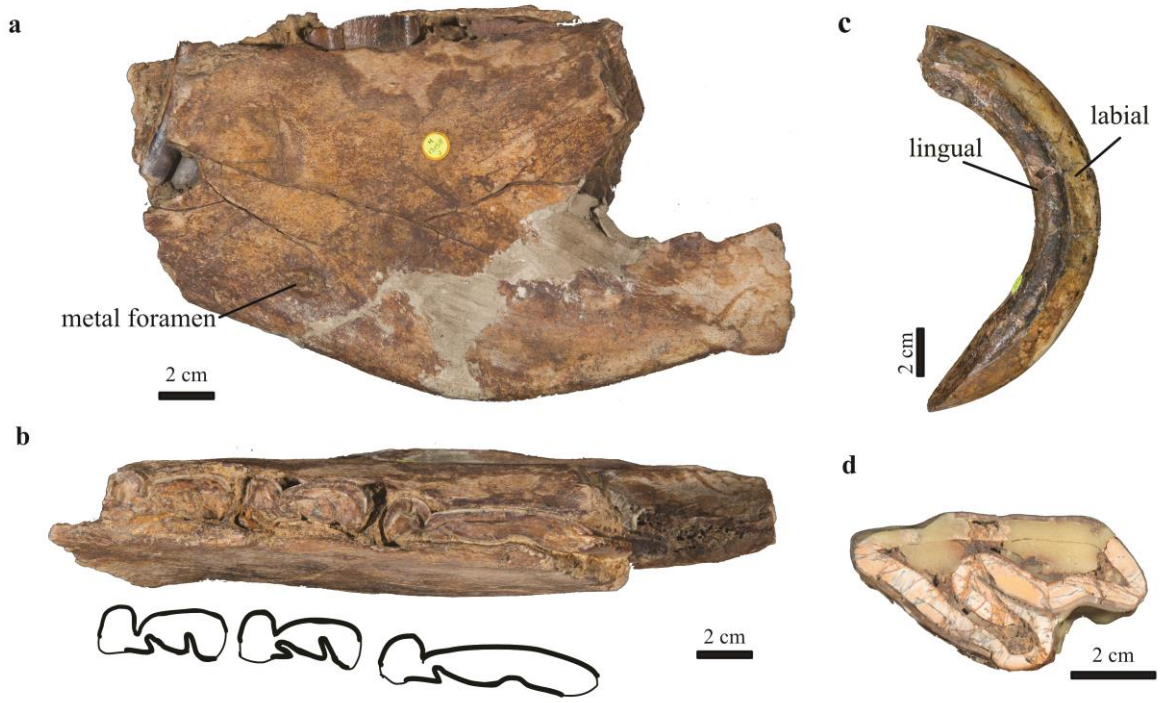

Figure 15. *Gyrinodon quassus* (Toxodontidae, Notoungulata) (holotype, NHMUK PV M 13158): (a) right partial mandible in lateral view; (b) top, right partial mandible in occlusal view; bottom, schematic drawing of m1-m3, the distribution of enamel is shown by the thick lines; (c) right I2 in labial view; (d) cross section of M1or M2. Pictures by Lucie Goodayle and courtesy of the Natural History Museum, London.

Frank, 1957). The meta-entoconid and ento-hypoconulid folds are well defined in m1, but in the m2 the meta-entoconid fold is shallow, as in *Mixotoxodon* (Van Frank, 1957). In contrast, in the m2 of *Gyrinodon* the ento-hypoconulid and meta-entoconid folds are well defined (Hopwood, 1928). The m2 and m3 have a lingual enamel band between the anterior fold and the hypoconulid, as in all Toxodontinae (Forasiepi et al. 2015). The m3 has meta-entoconid and ento-hypoconulid folds, both absent in *Calchaquitherium* (Nasif et al. 2000). The ento-hypoconulid fold is present, but open, similar to *Mixotoxodon* and *Gyrinodon.* An open ento-hypoconulid fold is correlated with increasing mesiodistal crown length, a feature that appears as the tooth grows and is worn away (Madden 1997).

Falcontoxodon aff. *aguilerai*

Referred material AMU-CURS

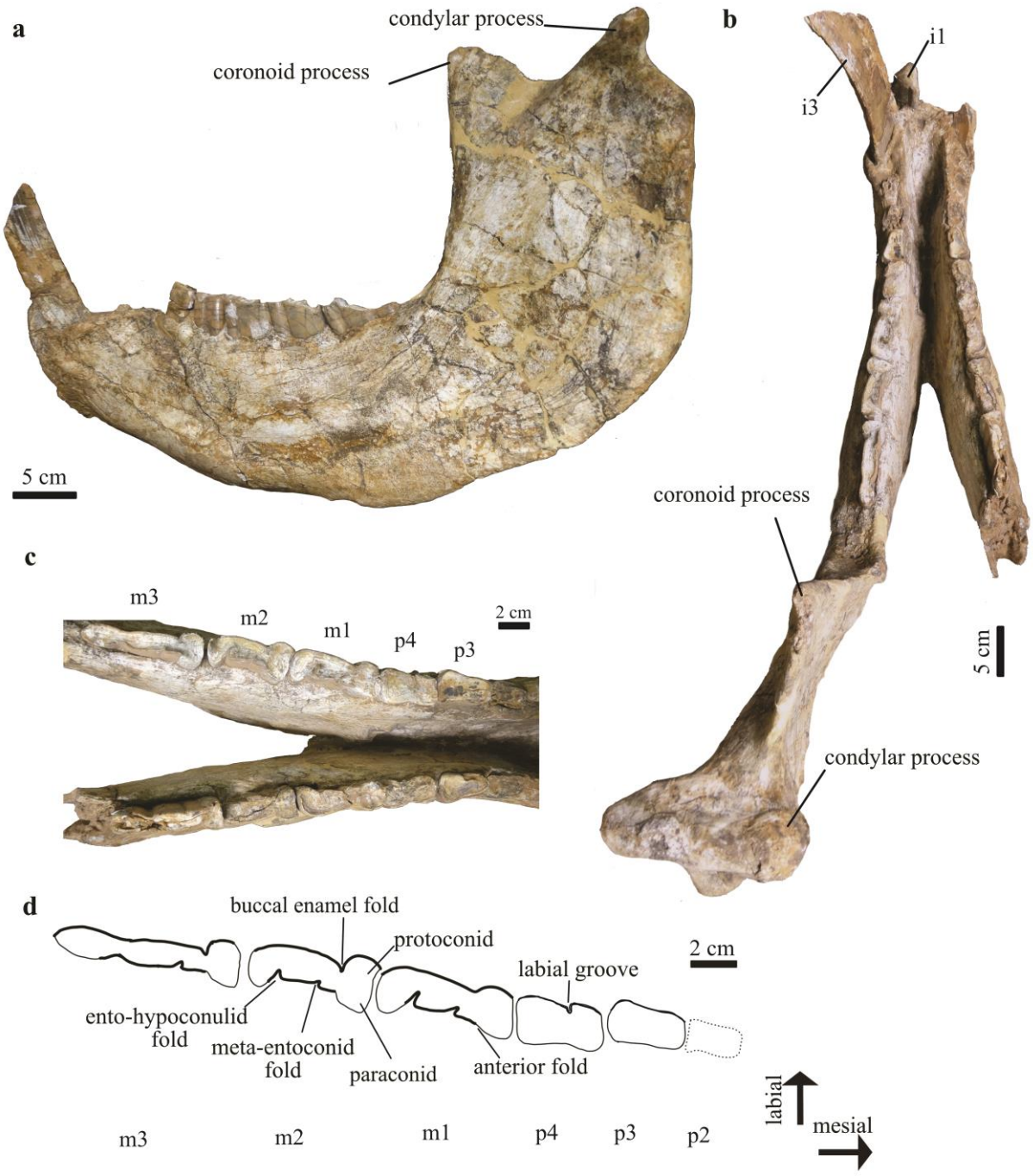

Figure 16. Mandible of *Falcontoxodon aguilerai* gen. et sp. nov. (holotype, AMU-CURS 765): (a) left lateral view; (b) dorsal view; (c) detail of dentition and symphysis in occlusal view; (d) schematic drawing of the left dentition, the distribution of enamel is shown by the thick lines.

585, maxilla with left M3-P2 and right I2.

LOCALITY AND HORIZON

Norte Casa Chiguaje, Vergel Member, San Gregorio Formation, Urumaco, Falcón State, Venezuela. 11°17′52.5′′N 070°14′11.1′′W (Figure 4a-b).

DESCRIPTION In AMU-CURS 585 the skull is pyriform in ventral view and

the infraorbital foramen is separated from the zygomatic arch (Figure 17a-b), as in *F. aguilerai*. Only the zygomatic process of the maxilla is preserved, which is dorsal to the M3. The I3 and C are absent, as in *Hoffstetterius, Posnanskytherium, Paratrigodon*, and some specimens of *Toxodon* (Forasiepi et al. 2015). In *F. aguilerai* the I3 is absent and the C is greatly reduced. The P1 is absent, unlike in *F. aguilerai*, and as in *Hoffstetterius, Trigodon* and *Paratrigodon* (Saint-André, 1993; Forasiepi et al. 2015). There is a large diastema between the I2 and P2 (Figure 17b). The P2 is nearly square in cross section, it does not have a lingual fold or fossette, and it shows enamel bands on the labial and mesiolingual sides (Figure 17c-d).

In AMU-CURS 585 the lingual enamel fold is absent in P3, but present in P4, and there are labial and mesiolingual enamel bands in P3 and P4. These features are also seen in the P3-P4 of *F. aguilerai.* In addition, the upper molars of AMU-CURS 585 have a simple lingual fold, and the protoloph supports a lingual column only in M3, as in *F. aguilerai.* However, AMU-CURS 585 differs from *F. aguilerai* in the absence of C and P1. These characters suggest that AMU-CURS 585 represents a closely related but different taxon from *F. aguilerai.* However, in the absence of more complete material, we prefer to refer AMU-CURS 585 to *Falcontoxodon* sp. nov. aff. *aguilerai*, following the recommendations for open nomenclature of Bengtson (1988).

Falcontoxodon sp.

Referred material AMU-CURS 69, partial left mandible with m1-m3. AMU-CURS 77, upper right I2, right P2, right P3 and unidentified left upper tooth. AMU-CURS 270, partial right mandible with m3 (cast PIMUZ A/V 4786). AMU-CURS 542, right astragalus, metatarsals III-IV, and two phalanges (cast PIMUZ A/V 5287). AMU-CURS 544, mandibular symphysis and four isolated lower teeth fragments. AMU-CURS 548, left M1/M2. AMU-CURS 562, left metatarsal IV and metatarsals II-III. AMU-CURS 563, distal portion of humerus. AMU-CURS 570, upper right I2 fragment, two unidentified upper premolars and seven teeth fragments. AMU-CURS 738, left calcaneus

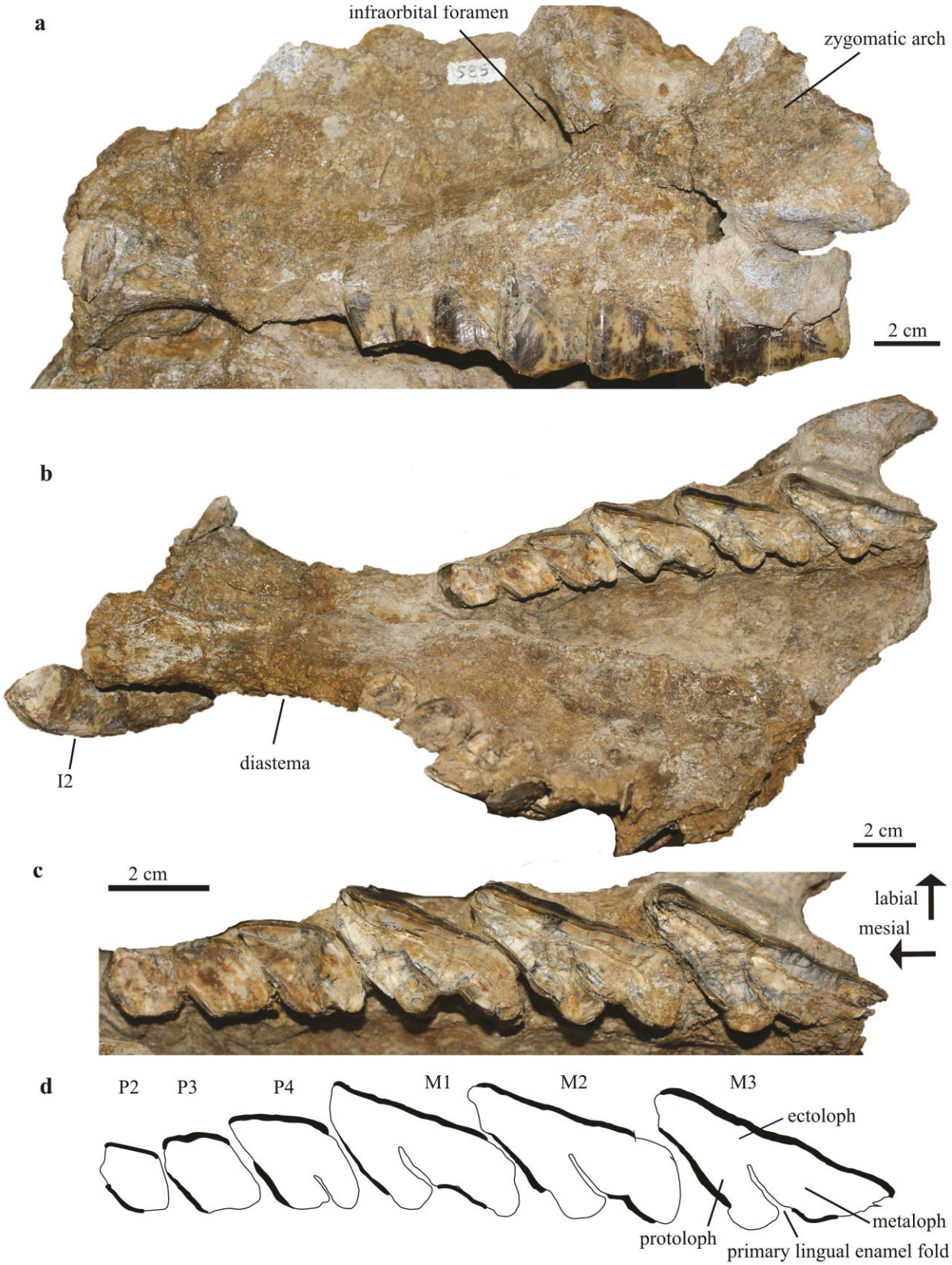

Figure 17. Partial skull of *Falcontoxodon* aff. *aguilerai* (AMU-CURS 585): (a) left lateral view; (b) ventral view; (c) detail of the upper left dentition in occlusal view; (d) schematic drawing of the dentition, the distribution of enamel is shown by the thick lines.

and three phalanges. AMU-CURS 739, partial m1/m2. AMU-CURS 741, right upper I2.

Locality and horizon

Norte Casa Chiguaje, Vergel Member, San Gregorio Formation, Urumaco, Falcón State, Venezuela. 11°17′52.5′′N 070°14′11.1′′W (Figure 4a-b).

Description In AMU-CURS 69 the m1 is not complete, but it shows lingual enamel extending mesially, reaching the meta-entoconid fold, as seen in *F. aguilerai* and in contrast to *Mixotoxodon,* where the lingual enamel does not extend mesially beyond the meta-entoconid fold. The lingual enamel of m2 does not extent distally to the hypoconulid, as in most Toxodontinae (Forasiepi et al. 2015). The m2 has a marked ento-hypoconulid fold and shallow meta-entoconid fold (Figure 18b), as in *Mixotoxodon* (Van Frank, 1957; Laurito, 1993; Rincón, 2011) and *F. aguilerai*. The m2 of AMU-CURS 69 differs from that of *F. aguilerai, Gyrinodon*, and *Mixotoxodon* in the presence of a mesial fossettid and distal fossettids (Figure 17b).

The m3 of AMU-CURS 69 and 270 have lingual enamel between the mesial fold and the hypoconulid. They show an open ento-hypoconulid fold, similar to the condition in *F. aguilerai, Gyrinodon* (Hopwood, 1928), and *Mixotoxodon* (Van Frank, 1957; Laurito, 1993; Rincón, 2011). The m3 of AMU-CURS 270 shows mesial, accessory, and distal fossettids (Figure 18g). Madden (1997) noted that during life the lower molar enamel folds can become isolated forming fossettids, and eventually obliterate in individuals with advanced wear. In *Pericotoxodon* the ento-hypoconulid fold first becomes isolated and eventually wears away completely, and in an even more advanced stage the meta-entoconid fold becomes isolated as a fossettid.

Several isolated foot bones were recovered in the San Gregorio Formation. Among toxodontids, foot anatomy is best known for the Santacrucian *Nesodon imbricatus* (Figure 19) and *Adinotherium ovinum* (Scott, 1912), and for the Pleistocene *Toxodon platensis* (Owen, 1840). The right astragalus (AMU-CURS 542) from San Gregorio is comparable in size to that of *Nesodon,* larger than in

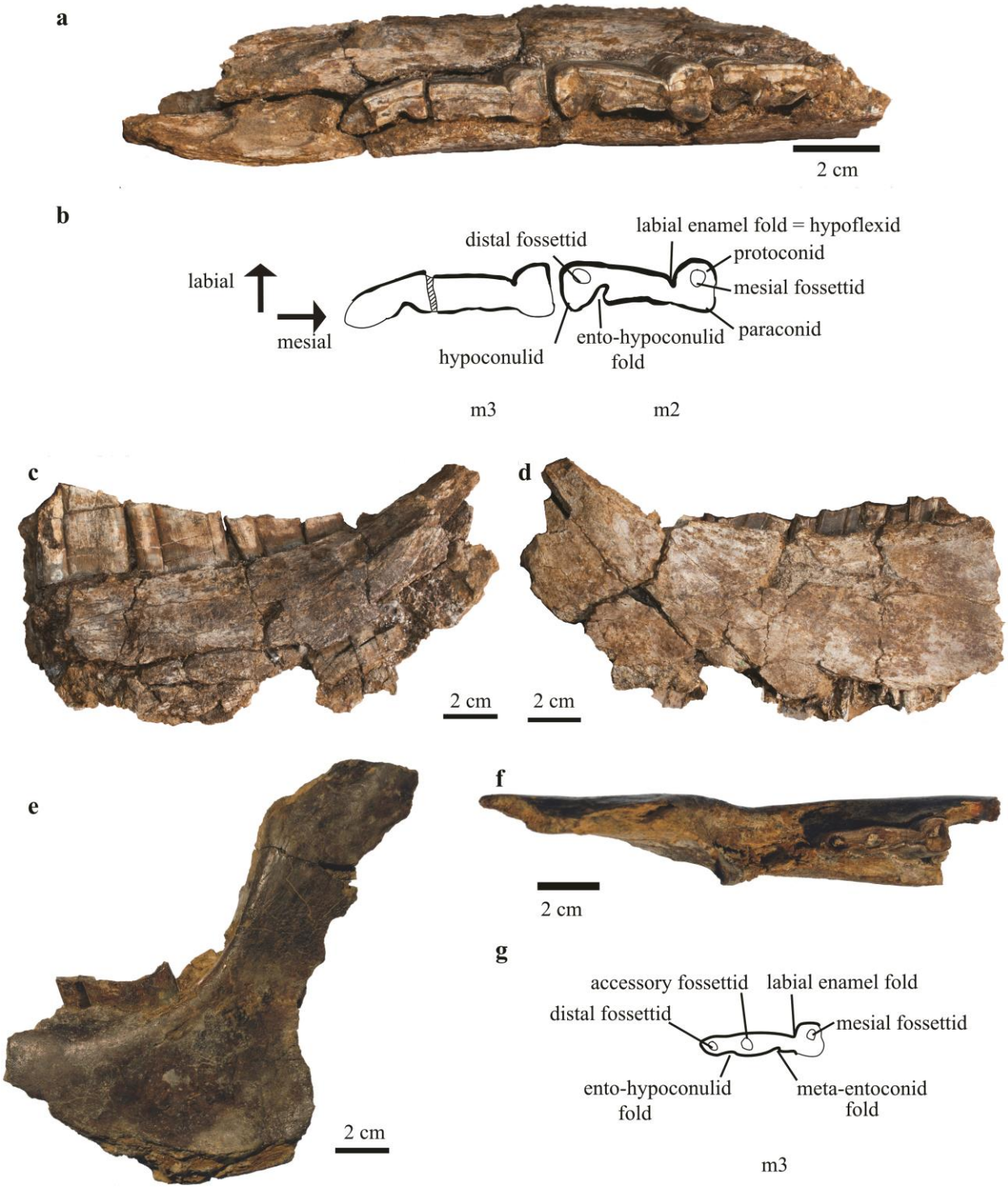

Figure 18. Partial mandibles of *Falcontoxodon* sp.: (a) left mandible (AMU-CURS 69), in occlusal view; (b) schematic drawing of the m2 and m3 of AMU-CURS 69, the distribution of enamel is shown by the thick lines; (c) AMU-CURS 69 in lateral view; (d) AMU-CURS 69 in medial view; (e) left partial mandible (AMU-CURS 270) in lateral view; (f) AMU-CURS 270 in occlusal view; (g) schematic drawing of the m3 of AMU-CURS 270, the distribution of enamel is shown by the thick lines.

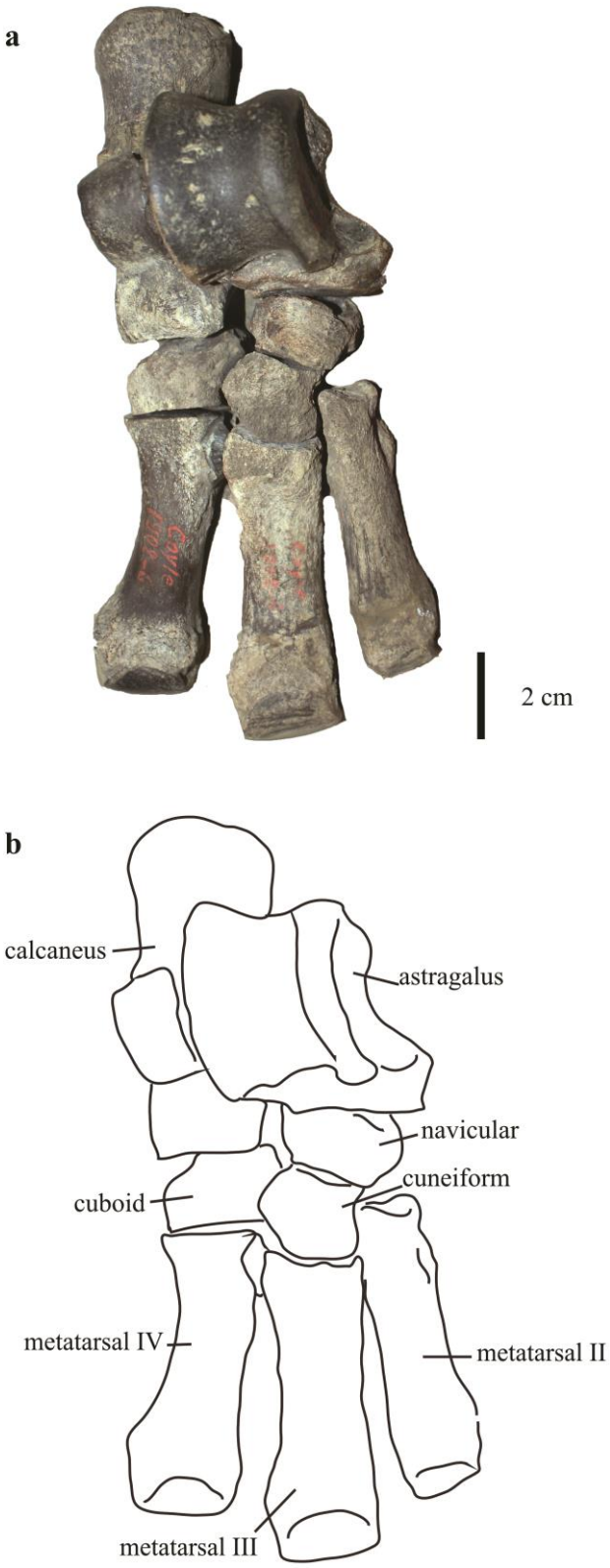

Figure 19. Right foot (without phalanges) of *Nesodon imbricatus* (Toxodontidae) (MNHN F SCZ 212) from the Santa Cruz Formation (Santacrucian SALMA) in Argentina: (a) articulated right foot in dorsal view; (d) schematic drawing of the foot.

Adinotherium, and smaller than in *Toxodon* (Table 7). AMU-CURS 542 has a shallow trochlear groove (Figure 20a), which is deeper in *Nesodon* (Figure 20c), and shallower in *Toxodon* (Figure 20e). The neck is very short (Figure 20a), similar to *Toxodon* (Figure 20e), and somehow less defined than in *Nesodon* (Figure 20c). The

Table 7. Astragalar measurements (mm) of toxodontids. Measurements followed those of Tsubamoto (2014: fig. 1). Li1=transverse width of the tibial trochlea; Li2 = proximodistal length of the lateral trochlear ridge of the tibial trochlea; Li3 = proximodistal length of the medial trochlear ridge of the tibial trochlea; Li4 = transverse width of the astragalus; Li5 = proximodistal length of the astragalus; Li6 = proximodistal length of the central part of the tibial trochlea; Li7 = transverse width between the medial and lateral trochlear ridges of the tibial trochlea; Li8 = dorsoventral thickness of the lateral part of the astragalus; Li9= dorsoventral thickness of the medial part of the astragalus. Measurements are shown in Figure 21b

Taxa	**Specimen**	**Li1**	**Li2**	**Li3**	**Li4**	**Li5**	**Li6**	**Li7**	**Li8**	**Li9**
Adinotherium sp.	MLP 67-XII-8-1	18.0	21.6	20.9	24.2	27.0	17.0	14.7	14.6	21.3
	MLP 67-XII-8-2	23.8	33.6	29.7	32.8	34.4	24.8	20.3	24.2	34.4
Nesodon imbricatus	MNHN SCZ 1902-6	34.08	45.1	43.81	54.13	56.79	35.27	27.69	33.5	43.08
	MNHN SCZ 30	35.62	42.31	43.25	47.1	48.25	32.07	26.19	30.08	35.17
	NHM UK M 96594	32	41.3	41.5	48.9	48.8	35.1	25	28.3	42.4
	NHM UK M5475	31.9	41.9	41.6	49.3	48.2	34.5	27.9	22.7	37.7
Toxodon platensis	MNHN PAM 284	58.33	67.22	60.72	83.68	66.55	48.3	53.01	36.44	59.03
	NHM UK M 5486	63	69.4	58.1	86.6	67.2	50.4	56	36	56.1
Falcontoxodon sp.	AMU-CURS 542	40.3	45.2	44.1	60.9	51.3	36.7	34	31.2	38.1

medial tibial facet is expanded medially, forming a tuberosity (Figure 20a), which is absent in *Nesodon* (Figure 20c) and less developed in *Toxodon* (Figure 20e). In plantar view, the sustentacular and navicular facets are connected (Figure 20b), whereas in *Nesodon* and *Toxodon* they are separate (Figure 20d, f). The navicular facet is larger than the sustentacular facet, as in other toxodontids. In *Nesodon,* the navicular facet reaches the distal plane and it can be observed in dorsal view (Figure 20c), whereas in AMU-CURS 542 and *Toxodon*, it

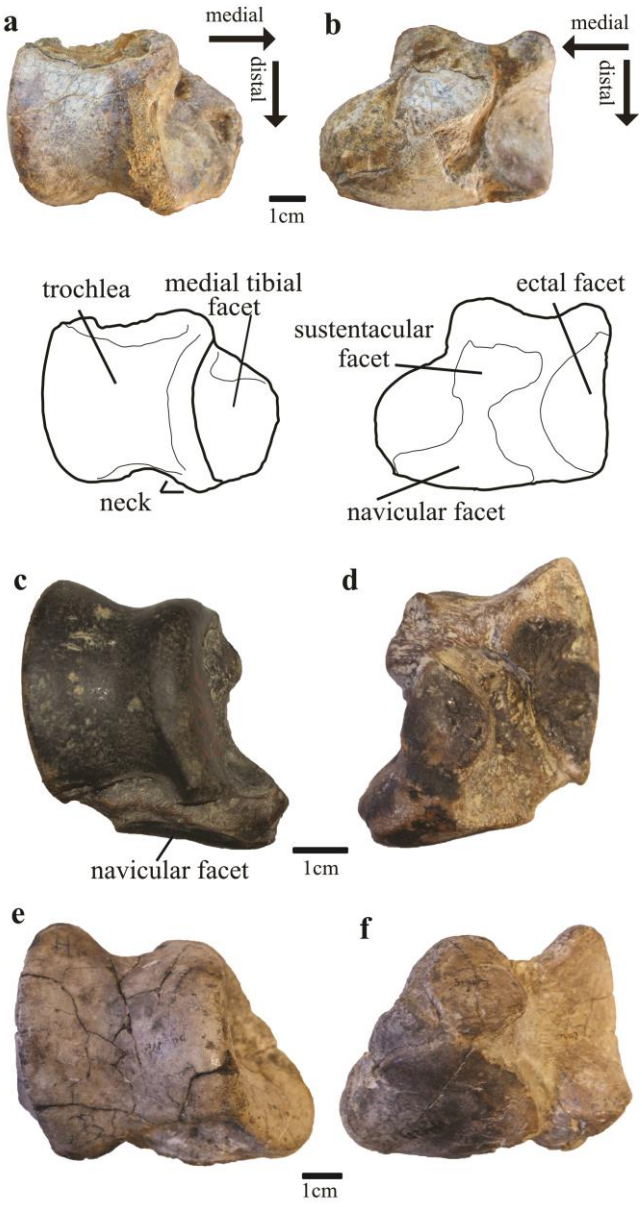

Figure 20. Toxodontid astragali: (a) *Falcontoxodon* sp. (gen. nov.), right astragalus (AMU-CURS 542) in dorsal view; (b) AMU-CURS 542 in plantar view; (c) schematic drawing of AMU-CURS 542 in dorsal view; (d) schematic drawing of AMU-CURS 542 in plantar view; (e) *Nesodon imbricatus,* right astragalus (MNHN F SCZ 212) in dorsal and (f) plantar view; (g) *Toxodon platensis,* right astragalus (MNHN PAM 284) in dorsal and (h) plantar view.

is restricted to the plantar plane. The ectal facet is concave and elongate. The PCA of toxodontid astragalar measurements (Table 7) roughly differentiates the four taxa, *Adinotherium, Nesodon, Toxodon*, and *Falcontoxodon* (Figure 21a). They are mainly separated along the PC1, which correlates with size, with the smaller *Adinotherium* towards the negative values, the larger *Toxodon* towards the positive values, and *Nesodon* and *Falcontoxodon* in between.

The left calcaneus of *Falcontoxodon* (AMU-CURS 738) is of comparable length but wider, and somehow more robust than the calcanei of *Nesodon.* It is smaller than the calcaneus of *Toxodon* (Table 8; Figure

Table 8. Measurements of the calcaneus and metatarsals of toxodontids. Metatarsal= Mt.

Taxa	Specimen	Element	Length	Distal width	Proximal width
Falcontoxodon sp.	AMU-CURS 542	Mt IV	93	39	39.5
		Mt III	70.6	29.7	27.6
	AMU-CURS 562	Mt IV	91.4	46.8	39.8
		Mt III	-	42.7	-
		Mt II	-	32	-
	AMU-CURS 738	Calcaneus	88.8	46.7	46.4
Nesodon imbricatus	MNHN SCZ 30	Mt IV	77.3	28.8	32
		Mt III	82.8	29.9	29.7
		Calcaneus	87.9	34.3	40
	MNHN SCZ 212	Mt IV	78.9	27	31.7
		Mt III	83.7	28.9	25
		Calcaneus	82.7	31	35.3
	NHM UK M96586	Calcaneus	88.2	33.6	38
	NHM UK M96585	Calcaneus	87.9	32.3	43.2
Toxodon platensis	NHM UK M 5487	Mt III	160	78.8	72.7
	NHM UK M 5486	Calcaneus	133	67.2	73.9

22a-h). In *Falcontoxodon* the cuboid facet is wider than in *Nesodon.* The ectal facet is approximately perpendicular to the fibular facet, and the sustentacular facet is inclined anteromedially (Figure 22a). AMU-CURS 542 and 562 includes tarsals consisting of a fragment of metatarsal II, and complete metatarsals III (Figure 22i-k) and metatarsal IV (Figure 22l-n). Overall, they are comparable in length and width to those of *Nesodon*, and much smaller than in *Toxodon* (Table 8).

TOXODONTINAE INDET.

REFERRED MATERIAL MUN-STRI 13103, lower molar fragment. MUN-STRI 13118, upper molar fragment. MUN-STRI 37507, lower molar fragment; MUN-STRI 37561, lower molar fragment.

LOCALITY AND HORIZON Ware Formation, Police Station. MUN-STRI 13103 and MUN-STRI 13118 come from STRI locality 390020; MUN-STRI 37507 comes from STRI locality 470062; MUN-

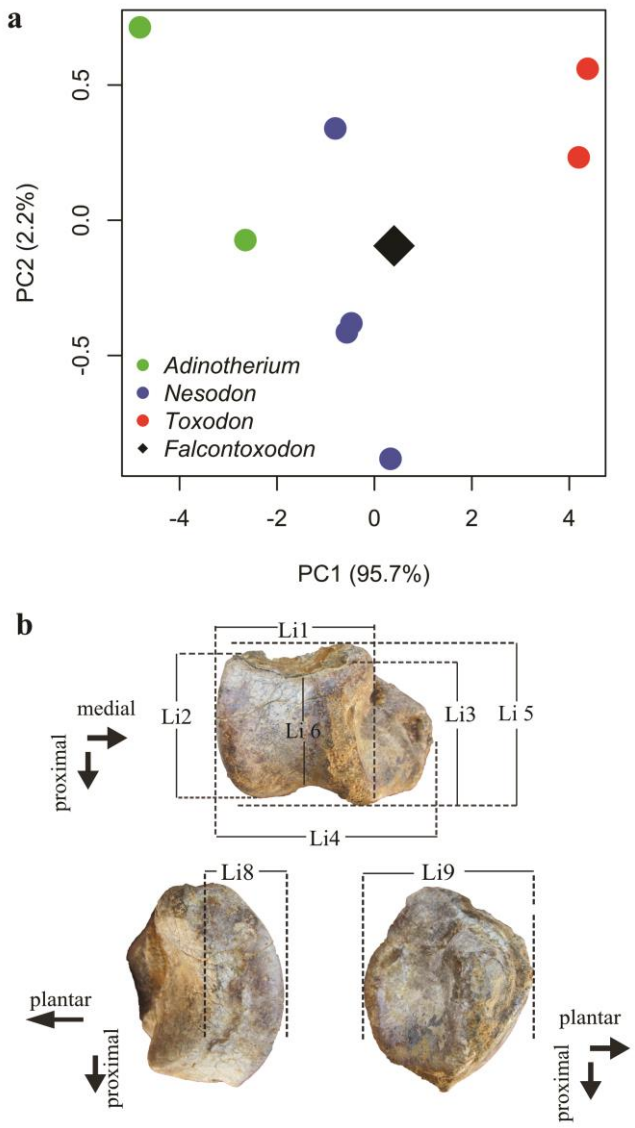

Figure 21. Astragalar morphospace in selected toxodontids: (a) bivariate plot of the first two principal components of the PCA; (b) linear measurements follow Tsubamoto (2014).

STRI 34561 comes from STRI locality 470059 (Figure 3).

DESCRIPTION The isolated teeth are upper molars (Figure 23). The enamel is not well preserved (Figure 23b). They have a simple primary lingual enamel fold, which separates the protoloph from the metaloph (Figure 23a), as in *Falcontoxodon,* some specimens of *Pericotoxodon* with an advanced stage of dental wear (Madden 1997), *Andinotoxodon* (Madden, 1990), *Mixotoxodon* (Laurito, 1993), *Piauhytherium* (Guérin and Faure, 2013), and *Gyrinodon* (Figure 15d). The protoloph does not support a lingual column (Figure 23a); the metaloph is broad and does not taper distally, as in *Falcontoxodon* and most specimens of *Pericotoxodon* (Madden, 1997).

Body mass estimation

The different craniodental measurements (Table 9) yielded body mass estimates for *F. aguilerai*'s holotype that range from 616 to 1075 kg (Table 10). The arithmetic mean is 796 kg. The mean minimum estimate taking into account the percentage of error is 735 kg, and the maximum is 946 kg.

Phylogenetic analysis of Toxodontidae

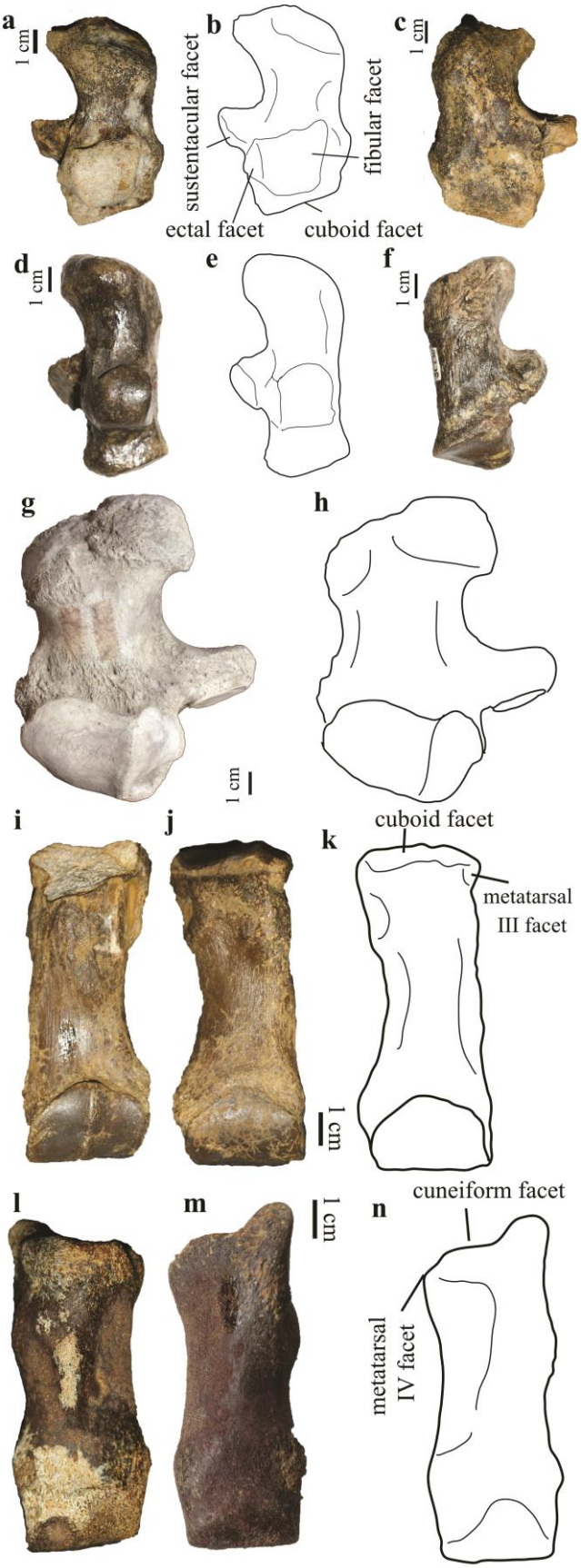

Figure 22. Toxodontid calcanei and metatarsals: left calcaneus of *Falcontoxodon* sp. (gen. nov.) (AMU-CURS 738); (a) photograph and (b) schematic drawing in dorsal view; (c) plantar view. Left calcaneus of *Nesodon imbricatus* (MNHN SCZ 30); (d) photograph and (e) schematic drawing in dorsal view; (f) plantar view. Right calcaneus of *Toxodon platensis* (MHMUK PV M 5486); (g) photograph and (h) schematic drawing in dorsal view. Metatarsals of *Falcontoxodon* sp. (gen. nov.) (AMU-CURS 542): left metatarsal III; (i) plantar view; (j) photograph and (k) schematic drawing in dorsal view. Left metatarsal IV; (l) plantar view; (m) photograph and (o) schematic drawing in dorsal view.

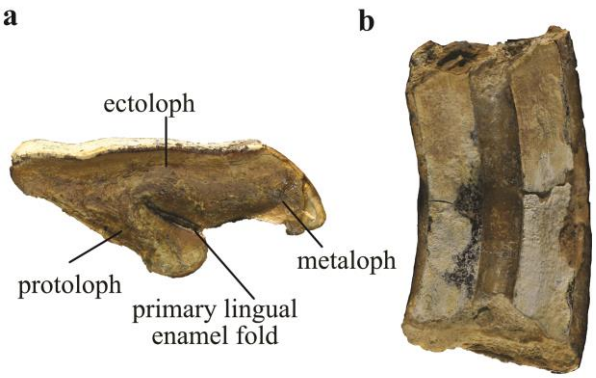

Figure 23. Toxodontinae indet. left M1 or M2 from Ware Formation. (a) Occlusal, and (b) lingual view.

The parsimony analysis with extended implied weighting resulted in one most parsimonious tree of 265 steps, with a consistency index of 0.52 and retention index of 0.68 (Figure 24a). The clade Toxodontidae has a bootstrap value of 55 and is supported by two unambiguous synapomorphies: i1 triangular in cross section (36[1]) and lingual enamel of i3 that is narrower than the labial one (40[3]). *Proadinotherium* is hypothesized as being the sister taxon of all the other toxodontids (Figure 24a). The Nesodontinae comprises *Adinotherium* and *Nesodon* (Figure 24a), and is supported by one unambiguous synapomorphy, the symphysis without a well-differentiated chin angle (16[0]). The clade Toxodontinae has a bootstrap value of 96 (Figure 24a) and is supported by ten unambiguous synapomorphies: short sagittal crest (4[1]), hypselodont cheek teeth (19[2]), molars without fossettes (29[1]), M1-M2 with distal groove/ fossette smooth or absent (31[1]), M3 with groove smooth or absent (32[1]), lingual enamel extending distally to the posterior groove (33[1]), the mesial fold of m1-m2 at the same level as the labial fold (49[1]), m1 with lingual enamel between the anterior fold and the hypoconulid (55[1]), lingual enamel of m2 restricted between the mesial fold and the hypoconulid (56[1]), and lingual enamel of m3 reaching the level of the hypoconulid (57[1]).

Palyeidodon is the first taxon to diverge within Toxodontinae, followed by *Hyperoxotodon* (Figure 24a). The remaining Toxodontinae are divided into two main clades (nodes 42 and 46). Node 42 is supported unambiguously by a P2 without groove or fossette (25[1]) and a marked and straight ento-hypoconid fold in m1-m2 (51[1]). It includes two clades (node 38 and 41; Figure 24a). Node 38 includes two groups; one

Table 9. Cranial and mandibular measurements (mm) of *Falcontoxodon aguilerai* sp. nov. (holotype, AMU-CURS 765).

Variable	Acronym	Definition	Value	Reference
Lower premolar row length	LPRL	Measured along the base of the teeth	96	Janis (1990)
Lower molar row length	LMRL	Measured along the base of the teeth	148	Janis 1990
Anterior jaw length	AJL	Measured from the boundary between p4 and m1 to the base of i1	164	Janis (1990)
Posterior jaw length	PJL	Measured as the horizontal distance from the back of the condyle to distal border of m3	150	Janis (1990)
Depth of mandibular angle	DMA	Measured from the top of the condyle to the deepest point of the mandibular angle	344	Janis (1990)
Maximum width of the mandibular angle	WMA	Measured from the junction of the distal part of m3 with the dentary to the most distant point on the mandibular angle	199	Janis (1990)
Length of the coronoid process	JD	Measured as the vertical distance from the base of the condyle to the tip of the coronoid process	35	Mendoza et al. (2006)
Length of the ridge for the masseteric attachment	MFL	Measured from the posterior portion of the glenoid to the most anterior extent of the scar for the origin of the masseter muscle	190	Janis (1990)
Posterior skull length	PSL	Measured from the occipital condyle to the distal edge of M3	240	Janis (1990)
Depth of the face under the orbit	SD	Measured from the boundary between premolar and molar tooth rows to the nearest point of the orbit	125	Mendoza et al. (2006)
Muzzle width	MZW	Measured between the most lateral points between the maxilla and premaxilla contact	100	Janis (1990)
Basicranial length	BCL	Measured from the ventral edge of the foramen magnum to the point of the basicranium where a change in angulation occurs between the basicranium and the palate	235	Janis (1990)
Total jaw length	TJL	TJL=PJL+LMRL+AJL	462	Janis (1990)
Total skull length	TSL	TSL=PSL+LMRL+AJL	552	Janis (1990)

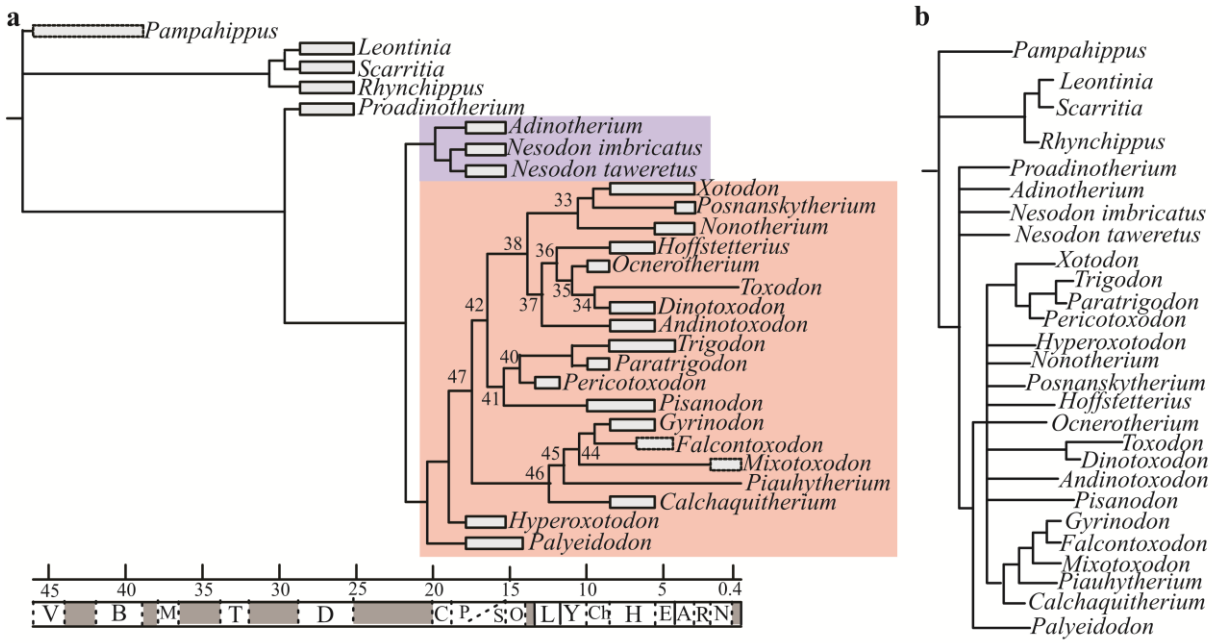

Figure 24. Hypothesis of phylogenetic relationships within Toxodontidae. (a) Time calibrated topology of the most parsimonious tree resulting from an analysis with PAUP using implied weighting (k=3). Node numbers are discussed in the text. Blue= Nesodontinae, red= Toxodontinae. The letters below the time line denote the SALMAs; V=Vacan, B=Barrancan, M=Mustersan, T=Tinguirican, D=Deseadan, C=Colhuehuapian, P=Pinturan, S=Santacrucian, O=Colloncuran, L=Laventan, Y=Mayoan, Ch=Chasicoan, H=Huayquerian, E=Montehermosan, A=Chapadmalalan, R=Marplatan, N=Ensenadan. (b) Strict consensus of the 12 most parsimonious trees resulting from the analysis of the same data matrix but without using character weighting.

(node 33) consists of (*Nonotherium* (*Posnanskytherium*, *Xotodon*)) and it is supported by a very concave ectoloph (34[1]). The second group (node 37) consists of (*Andinotoxodon* (*Hoffstetterius* (*Ocnerotherium* (*Toxodon*, *Dinotoxodon*)))), and is supported by a straight alveolar border of the symphysis (14[1]). Node 41 (Figure 24a) consists of (*Pisanodon* (*Pericotoxodon* (*Paratrigodon*, *Trigodon*))) and is supported by the absence of enamel in P1 (24[1]) and upper molars with median crista and an incipient median valley (30[1]).

Within Toxodontinae, node 46 (Figure 24a) groups the clade (*Calchaquitherium* (*Piauhytherium* (*Mixotoxodon* (*Falcontoxodon*, *Gyrinodon*)))), which is

Table 10. Body mass estimates (kg) for *Falcontoxodon aguilerai* sp. nov. (holotype, AMU-CURS 765) using the multivariate regression functions from Mendoza et al. (2006). BM=Body mass; RPE= Range of PE; PE= Percent of error. For the acronyms of the measurements used in the equations see Table 9.

Algorithm	Equation	Adj. R^2	%RPE	mid %PE	BM	BM + mid PE	BM – mid PE
2.1	ln BM= -1.602*ln(LMRL)+2,791*ln(SLML)+0.576*ln(JLB)+1.005*ln(JMA)+2.402	0.99	13.5-15	14.25	616	704	607
2.2	ln BM= -1.352*ln(LMRL)+2.434*ln(SLML)+0.587*ln(JLB)+0.866*ln(JMA)+0.263*ln(JMC)+1.890	0.99	13.5-15	14.25	674	770	578
2.3	ln BM= -1.366*ln(LMRL)+2.421*ln(SLML)+0.542*ln(JLB)+1.017*ln(JMA)+0.716*ln(JMC)-0.509*ln(JMB)+2.006	0.99	13.5-15	14.25	608	695	521
3.1	ln BM= 1.119*ln(LMRL)+0.210*ln(LPRL)+0.730*ln(JMA)+0.637*ln(JMC)+0.181*ln(JD)+0.619	0.98	21-25	23	1075	1322	1018
3.2	ln BM= 1.086*ln(LMRL)+0.176*ln(LPRL)+0.823*ln(JMA)+0.968*ln(JMC)+0.167*ln(JD)-0.331*ln(JMB)+0.573	0.98	21-25	23	1006	1237	952
Mean					796	946	735

supported by I1 with a median lingual groove (20[3]), absence of lower canines (41[1]), absence of lingual enamel in p2-p4 (44[2]) and a well-developed mesial fold in m1-m2 (48[0]). The Venezuelan toxodontids form a clade (node 44; Figure 24a) supported by the presence of a deep and narrow labial groove in the molars (54[2]). The clade that includes *Falcontoxodon* and *Gyrinodon* is supported by a smooth anterior fold in m1-m2 (48[1]).

The analysis using equal weights yielded 12 most parsimonious trees of 263 steps, with a consistency index of 0.52 and retention index of 0.68. The strict consensus (Figure 24b) recovered Toxodontinae, supported by the following unambiguous synapomorphies: short sagittal crest (4[1]), mandibular symphysis with smooth chin angle (16[1]), euhypsodont cheek teeth (18[2]), molars without fossettes (29[1]), upper molars without a groove, or if present being smooth (31[1]) and (32[1]), lingual enamel in M3 extending distally to the distal groove (33[2]), reduced lingual enamel in p2-p4 (44[1]), the mesial fold in m1-m2 at the same level as labial fold (49[1]), the lingual enamel of m1 (55[1]) and m2 (56[1]) between the mesial fold and the hypoconulid, and the lingual enamel of m3 reaching the level of the hypoconulid (57[1]).
In this analysis Nesodontinae was not recovered as monophyletic (Figure 24b). Within Toxodontinae, *Falcontoxodon* is the sister taxon of *Gyrinodon* (Figure 24b), and they are part of a clade that includes *Mixotoxodon*, *Piauhytherium*, and *Calchaquitherium*. This clade was also recovered during the analysis using implied weighting (Figure 24a).

LITOPTERNA (AMEGHINO, 1889)

PROTEROTHERIIDAE (AMEGHINO, 1887)

Neodolodus (Hoffstetter and Soria, 1986)

Neodolodus cf. *colombianus* (Hoffstetter and Soria, 1986)

REFERRED MATERIAL MUN-STRI 16716, a left dentary with the alveolus of p3, p4, m1, the alveolus of m2, and m3 (cast PIMUZ A/V 5291).

LOCALITY AND HORIZON

Makaraipao, Castilletes Formation. STRI locality 930093; 11.9089º N, 71.3401º W (Figure 3).

DESCRIPTION The partial mandible preserves part of the alveolus of p3, the p4, m1, the alveolus of m2, and a fragment of m3 (Figure 25a-d). The teeth are brachyodont, bicrescentic and very low crowned (Figure 25a), as in *N. colombianus* (Hoffstetter and Soria, 1986; Cifelli and Guerrero, 1989). The cheek teeth have four roots (Figure 25b,d). The lophs are not well defined (Figure 25b) due to the low crown height and wear, as in *N. colombianus* (Cifelli and Guerrero, 1989).

The p4 is molariform and narrows mesially in occlusal view (Figure 25d). It measures 12.4 mm in mesiodistal length and 8.5 mm in labiolingual width. The ectoflexid is shallow and the paraconid is reduced (Figure 25d). There is no evidence of labial or lingual cingula (Figure 25a,c), which are present in *N. colombianus* and poorly developed or absent in *Lambdaconus lacerum* (Cifelli and Guerrero, 1989; Soria, 2001; Kramarz and Bond, 2005). The p4 has a hypoconulid, unlike in *Megadolodus* where it is absent (Cifelli and Villaroel, 1997). The p4 and m1 have a well-developed hypoconid, and the metaflexid and entoflexid are present (Figure 25d).

The m1 measures 13.5 mm in mesiodistal length and 98.0 mm in labiolingual width. The protoconid and metaconid are well developed, as in *N. colombianus* (Hoffstetter and Soria, 1986). The paraconid is present, unlike in *Prolicaphrium* and *Megadolodus* (Cifelli and Guerrero, 1997; Cifelli and Villaroel, 1997). The ectoflexid is deep and the hypoconid is well developed, with a mark crescent shape, as in *N. colombianus* (Hoffstetter and Soria, 1986). The entoconid and hypoconulid are undifferentiated, due to wear (Figure 25d). The alveolus of the m2 accommodates four roots (Figure 25b,d). The crown of the m3 is broken, missing distal and mesio-lingual portions (Figure 25d). It measures 97 mm in labiolingual width, and it has a deep ectoflexid. MUN-STRI 16716 differs from *Megadolodus* (McKenna, 1956; Cifelli and Villaroel, 1997) in having less bunodont and more rectangular molars, having a

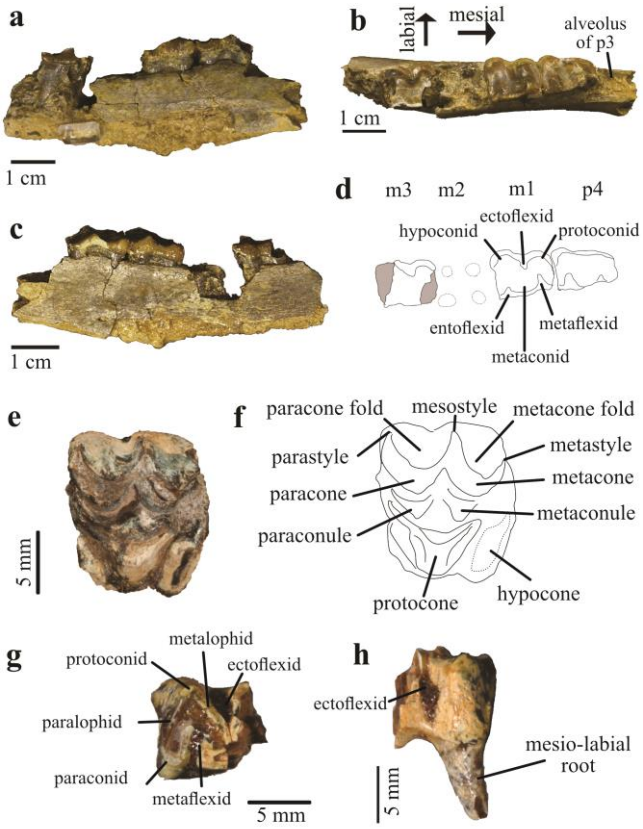

Figure 25. Proterotheriidae (Litopterna) from the Cocinetas basin. *Neodolodus* cf. *colombianus,* left dentary (MUN-STRI 16716) from the Castilletes Formation in: (a) lingual, (b) occlusal, and (c) labial view; (d) schematic drawing of the dentition in occlusal view. Proterotheriidae indet. from the Ware Formation: Left M1 or M2 (MUN-STRI 34170) in occlusal view: (e) photograph and (f) schematic drawing. Fragment of right lower molar (MUN-STRI 16289) in (g) occlusal and (h) labial view.

paraconid and lacking cingula.

PROTEROTHERIIDAE INDET.

REFERRED MATERIAL MUN-STRI 13119, diaphysis and distal epiphysis of left humerus. MUN-STRI 13120, right ulna. MUN-STRI 13121, left metacarpal III. MUN-STRI 16289, fragment of lower molar. MUN-STRI 19544, right calcaneus. MUN-STRI 34170, M1/M2. AMU-CURS 745, epiphysis of metacarpal III. AMU-CURS 746, left metacarpal III.

LOCALITY AND HORIZON Police station, Ware Formation; 11.8487ºN, 71.3243ºW. MUN-STRI 13119, 13120, 13121 come from STRI locality 390020. MUN-STRI 19544 comes from STRI locality 390018. MUN-STRI 16289 comes from STRI locality 430052. MUN-STRI 34170 comes from STRI locality 470060. AMU-CURS 745 and 746 come from the Algodones Member, Codore Formation, 11º17’39.8’’N, 70º14’15.6’’W.

DESCRIPTION The upper molar (MUN-STRI 34170) is brachyodont and quadrangular in occlusal view, suggesting that it represents an M1 or M2 (or a

molarized P4). The M3 in proterotheriids has a distinctive outline in occlusal view; for example, in *Brachytherium* it is trapezoidal (Schmidt, 2015), and in *Villarroelia* it is more triangular (Cifelli and Guerrero, 1997). It has a mesiodistal length of 10.4 mm and a labiolingual width of 10.6 mm (Figure 25e). MUN-STRI 34170 is referred to a Proterotheriidae indet. based on its size, the bunoselenodont (Janis, 2000; fig. 7.2) condition and the position of the hypocone posterior to the paracone (Schmidt, 2013).

MUN-STRI 34170 differs from the megadolodine *Bounodus enigmaticus (*Carlini et al. 2006a) in having a more developed protocone, and the paracone positioned less mesially. The mesiolingual border of the crown is broken, and the presence of the mesiolingual cingulum cannot be evaluated. The protocone is the largest cusp (Figure 25f), as in *Brachytherium* (Schmidt, 2015). The hypocone is broken, but it appear to have been separated from the protocone by a distolingual groove, as in *Brachytherium, Proterotherium*, and *Prothoatherium* (Cifelli and Guerrero, 1989; Schmidt, 2015). The paraconule is not connected with the protocone by a loph, as is in the Proterotheriinae (Schmidt, 2013). The metaconule is also an isolated cusp, as in *Prothoatherium* (Cifelli and Guerrero, 1989), and it is not reduced as in *Neolicaphrium* (Ubilla et al. 2011), or connected to the protocone, as in *Prolicaphrium* (Cifelli and Guerrero, 1997). The metaconule is located distal to the paraconule and mesiolingual to the hypocone (Figure 25f). MUN-STRI 34170 has three labial styles (Figure 25f), as in the Protherotheriinae (Schmidt, 2013). The mesostyle is well developed, as in *Villaroelia* (Cifelli and Guerrero, 1997), and as opposed to the reduced condition seen in *Neobrachytherium* (Schmidt, 2015). The paracone and metacone labial folds are well developed as in *Brachytherium* and *Proterotherium,* and unlike *Neobrachytherium* and *Thoatheriopsis* (Villafañe et al. 2012; Schmidt, 2015).

The lower molar fragment (MUN-STRI 16289) measures 8.2 mm in labiolingual width and 8.9 mm in crown height on the labial side. It preserves the mesial

portion of the crown, with well-defined paralophid and metalophid (Figure 25g). The protoconid and paraconid are well developed, and the metaflexid and ectoflexid are deep (Figure 25g-h). This lower molar fragment only preserves the mesio-labial root, which is long and narrow (Figure 25h).

The proterotheriid humerus (MUN-STRI 13119) preserves most of the diaphysis and the distal epiphysis (Figure 26a-c). The capitulum is rounded and projects less distally than the trochlea (Figure 26a). The medial and lateral epicondyles are weakly developed. The radial fossa is deep and located proximally to the capitulum. The olecranon fossa is not a fenestra (Figure 26c), as in *Prothoatherium* and *Proterotherium* (Cifelli and Guerrero, 1989). The diaphysis is mediolaterally compressed, as in other proterotheriids (Cifelli and Guerrero, 1989). The proximal portion of the diaphysis (at the level of the deltoid tuberosity) has the greatest antero-posterior depth, which decreases distally (Figure 26b) (Table 11).

The ulna (MUN-STRI 13120) is fairly complete, missing only a portion of the olecranon and a distal portion (Figure 26d-f; Table 11). The diaphysis is narrow and nearly straight. The anconeal process is not well developed, but projects laterally (Figure 26d). The coronoid process is small and projects disto-medially (Figure 26d). The preserved portion of the olecranon is in the same plane as the shaft (Figure 26d,f).

The calcaneus (MUN-STRI 19544) has an elongate shape, with the distal portion broader than the body (Figure 26g-h). The body is not lateromedially compressed, as in *Neolicaphrium* (Scherer et al. 2009). The ectal facet is oval and located in the midline of the body (Figure 26g), as in *Neolicaphrium*. The sustentacular facet is also oval and elongated posteroventrally (Figure 26g), as in *Neolicaphrium* (Scherer et al. 2009). The metatarsals III from the Ware (MUN-STRI 13121; Figure 26i-j) and Codore (AMU-CURS 746; Figure 26k-l) Formations are very similar. The diaphysis is straight and long (Table 11). The distal epiphysis has a well-defined median keel.

Table 11. Postcranial measurements (mm) of the Proterotheriidae indet. of the Ware Formation. *=estimated. Width = mediolateral; thickness = anteroposterior.

Humerus	Diaphysis width	Diaphysis thickness	Distal epiphysis width	Trochlea distal width	Lateral epicondyle thickness	Medial epicondyle thickness
MUN-STRI 13119	12.6	18.3	29.0	20.6	16.7	18.2
Ulna	Sigmoid cavity height	Olecranon thickness	Olecranon width	Diaphysis width	Diaphysis thickness	
MUN-STRI 13120	18.2	14.0	8.7	10.1	12.0	
Calcaneus	Total length	Maximum width	Maximum thickness			
MUN-STRI 19544	53.9	19.2	14.8			
Metacarpal III	Total length	Proximal width	Proximal thickness	Distal width	Diaphysis width	
MUN-STRI 13121	70.1	12.6	11.1	11.8	9.8	
AMU-CURS 746	89.3	19.9	-	21.2	15.9	

ARTIODACTYLA (OWEN, 1848)

CAMELIDAE (GRAY, 1821)

CAMELIDAE INDET.

REFERRED MATERIAL MUN-STRI 34380, right m1 or m2.

LOCALITY AND HORIZON Police Station, Ware Formation. STRI locality 470060. 11.8487º N, 71.3243ºW (Figure 3).

DESCRIPTION The tooth measures 15.2 mm in mesiodistal length and 8.9 mm in labiolingual width. The crown height at the labial side is 10.4 mm, yielding a hypsodonty index of 0.7. The molar is bicrescentic and the talonid is approximately the same size as the trigonid (Figure 27a). The trigonid and talonid fossae are deep, semilunar, and elongated mesiodistally (Figure 27b), as in *Hemiauchenia* (Scherer et al. 2007). The protoconid and hypoconid are well developed, the labial lophids are V-shaped, but the labial border is not as defined as in *Palaeolama* (Scherer et al. 2007).

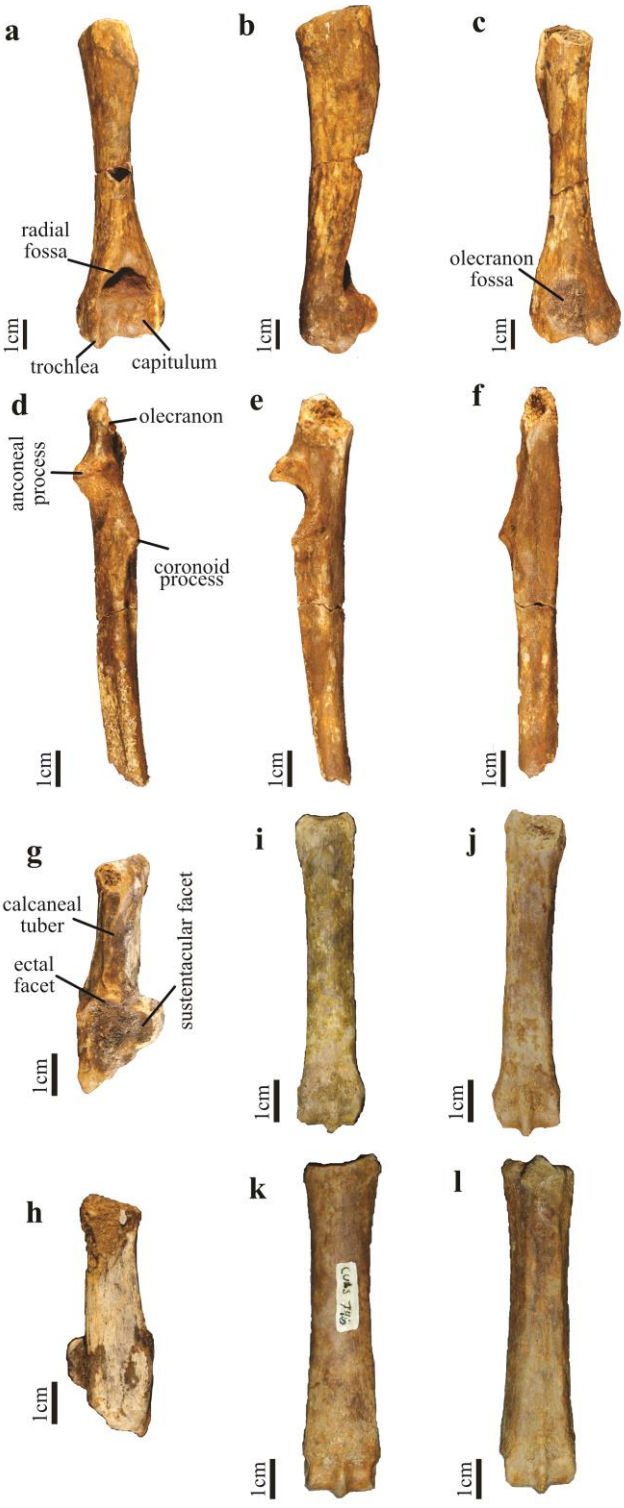

Figure 26. Proterotheriidae (Litopterna) postcrania from Ware and Codore Formations. Left humerus (MUN-STRI 13119) in: (a) anterior, (b) medial, and (c) posterior view. Right ulna (MUN-STRI 13120) in: (d) anterior, (e) medial, and (f) posterior view. Right calcaneus (MUN-STRI 19544) in (g) dorsal, and (h) plantar view. Left metacarpal III (MUN-STRI 13121) in: (i) anterior and (j) posterior view. Left metacarpal III (AMU-CURS 746) in: (k) anterior and (l) posterior view.

The most mesial portion of the crown is broken and the presence of the proto- and parastylid ("llama buttress") cannot be evaluated (Figure 27a). South America camelids belong to the clade Lamini (Scherer, 2013), and the presence of a "llama buttress" has been proposed as a synapomorphy of the clade (Harrison,

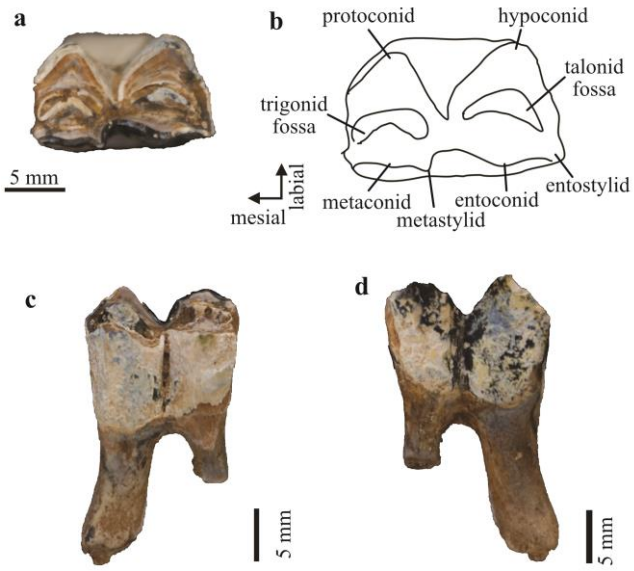

Figure 27. Camelidae indet. (Artiodactyla) from the Ware Formation. Right m1 or m2 (MUN-STRI 34380). (a) Photograph and (b) schematic drawing in occlusal view; (c) labial and (d) lingual views.

1985; Webb and Meachen, 2004). However, Scherer (2013) noticed that the development of proto- and parastylid is highly variable in camelids.

Chronostratigraphy of the Falcón Basin

The Falcón basin is divided between a western and an eastern sector. For each of the sectors, one of us (L. Quiroz) did an extensive stratigraphic study and described several stratigraphic sequences to produce a composite sequence of both regions (Quiroz and Jaramillo, 2010) (Figures 28-29). Seven sections were measured and described in western Urumaco, producing a composite sequence that is 8.75 km thick (Figure 28), while in eastern Urumaco three sections were measured and described producing a composite sequence that is 2.25 km thick (Figure 29). We provide a detailed description of each section, including its geographic position, in Appendix 1. The biostratigraphic record of foraminifera in the Urumaco region (both western and eastern) has been extensively studied by a numerous workers and correlated to Bolli's biostratigraphic schemes from Trinidad (Renz, 1948; Bermudez and Bolli, 1969; Blow, 1969; Díaz de Gamero 1977a,1 977b,1985a,1985b,1989,1996; Díaz de Gamero et al. 1988; Díaz de Gamero and Linares, 1989; Wozniak and Wozniak, 1987; Guerra and Mederos, 1988; Rey, 1990; Hambalek, 1993; Bolli et al. 1994; Pérez et al. 2016) (see Appendix 2 for a detailed description of the key studies). Nannoplankton also supports the age of the Querales Formation (Pérez et al. 2016). Vertebrates of the Urumaco Formation also support foraminiferal ages (Linares, 2004;

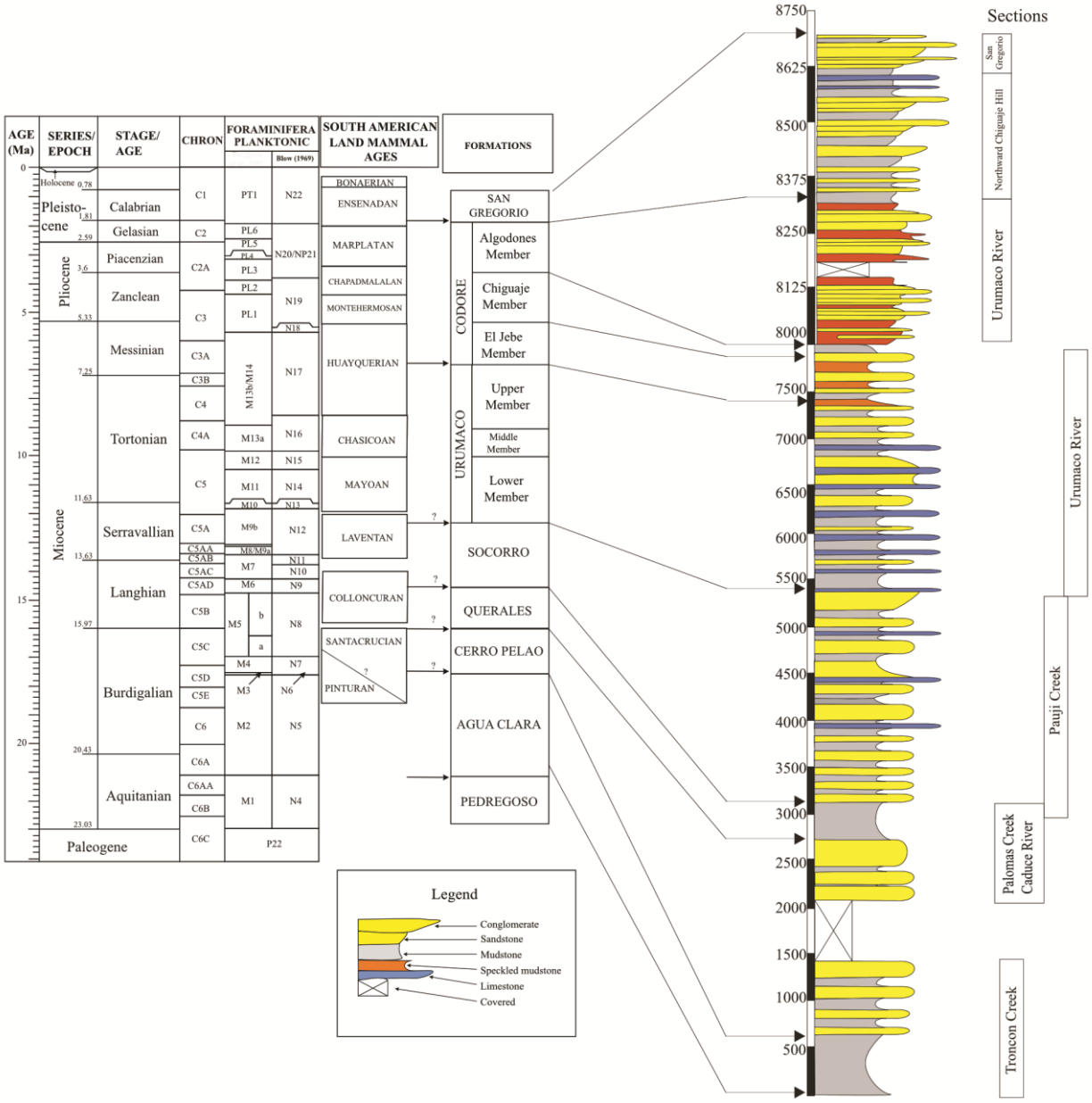

Figure 28. Urumaco western sequence chronostratigraphy. Composite section corresponds to several outcrop sections measured in western Urumaco and described in Quiroz and Jaramillo (2010). A detailed description of each individual section and its geographic position is given in Appendix 2. The ages are derived from multiples foraminiferal, nannoplankton, and magnetic stratigraphic studies (Renz, 1948; Bermudez and Bolli, 1969; Blow, 1969; Díaz de Gamero 1977a,1977b,1985a,1985b,1989,1996; Díaz de Gamero et al. 1988; Díaz de Gamero and Linares, 1989; Wozniak and Wozniak, 1987; Guerra and Mederos, 1988; Rey, 1990; Hambalek, 1993; Bolli et al. 1994; Pérez et al. 2016).

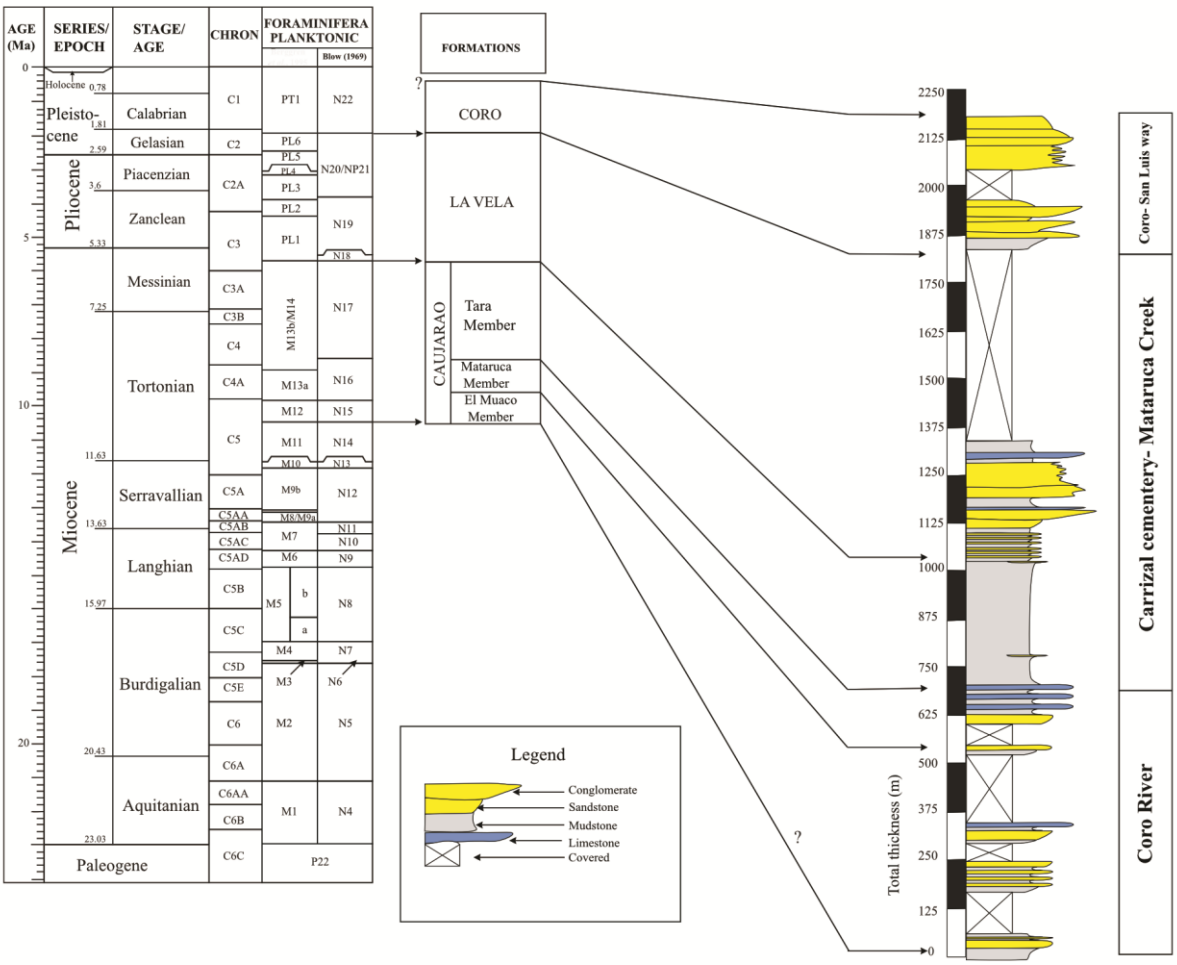

Figure 29. Chronostratigraphy of Falcón State east of Urumaco town. Composite section corresponds to several outcrop sections measured in eastern Urumaco. Formation ages are derived from multiples foraminiferal, nannoplankton, and magnetic stratigraphic studies (see text and Figure 28 for references).

Sánchez-Villagra, 2006; Sánchez-Villagra and Aguilera, 2006). A sample from the lower member of the Urumaco Formation (Urumaco West section, Figure 28) was analyzed for nannoplankton, and yielded a flora that includes *Coccolithus pelagicus, Discoaster deflandrei, Sphenolithus abies*, and *Sphenolithus moriformis.* This association corresponds to Nannoplankton Zone NN7, which is equivalent to Planktonic Zone N14, early Tortonian (Figure 28). Herrera (2008) studied the magnetic stratigraphy of the Urumaco Formation at the same locality of our Urumaco West section. Herrera identified the top of Chron C4 Ar2r within the Urumaco Formation at meter 6693 of our section (Figure 28). Overall, the top boundaries of the formations in the Urumaco

Table 12. Chronostratigraphic datums for composite Urumaco East and West sections. Numerical ages follow Gradstein et al. (2012).

datum (event top)	composite section (m)	age (MYA)
Codore Algodones	8285	1.81
Codore Chiguaje	7935	3.6
Codore Jebe	7886	5.33
Urumaco	7403	6.8
Top C4 Ar2r	6693.6	8.1
Socorro	5338	12.4
Querales	3130	14.5
Cerro Pelado	2704	16
Agua Clara	631	17.5
Coro	2185	0.4
La Vela	1838	1.81
Caujarao Tara	1025	5.6
Caujarao Mataruca	710	8.6
Caujarao Muaco	538	9.6

region, both East and West, are well dated and summarized in Table 12 and Figures 28-29.

In order to estimate the age of the stratigraphic horizons where the fossil mammals are recorded in the Falcón and Cocinetas basins, we used the age model presented by Hendy et al. (2015) for the Jimol and Castilletes Formations in the Cocinetas basin. We followed the chronostratigraphic framework described above for the Codore and San Gregorio Formations in the Falcón basin. The stratigraphic occurrence and age of each specimen are summarized in Table 13.

Table 13. Biochronology of the Cocinetas and Falcón basins. For Cocinetas, the age model of Hendy et al. (2015) used a linear regression of the stratigraphic position and the $^{87}Sr/^{86}Sr$ isotopes ages for the upper part of the Jimol and the Castilletes Formations. The regression function is: y = -0.0058 x + 16.722, where y is the age in MYA and x is the stratigraphic meter. The original equation cannot be applied for the Ware Formation, as there is an unconformity between the Castilletes and Ware Formations (Moreno et al. 2015). For the Ware Formation a mean age of 3.2 MYA was estimated for the shell bed at the top of the Formation (Hendy et al. 2015; Moreno et al. 2015). This shell bed is 17 to 20 meters above the stratigraphic horizons where the vertebrates were recovered. Assuming the same sedimentation rate for the Jimol, Castilletes, and Ware Formations, we used the regression equation presented by Hendy et al. (2015) to estimate the age of the horizons of fossil vertebrates from the Ware Formation. Using the data of the age of 3.2 MYA obtained for the horizon at the stratigraphic meter 22, we have that 3.2 = -0.0058* 22 + intercept, and we obtained regression function for the Ware formation, y = -0.0058x + 3.0724. SM= Stratigraphic meter

Basin	Clade		Taxa	Specimen ID	Formation	Locality	Section ID	Latitude	Longitude	SM	SM composite section	Age MYA
Falcón	Notoungulata	Toxodontidae	*Falcontoxodon aguilerai*	AMU-CURS 765	Codore	Codore Algodones	NA	11.29	-70.24	2530	8257	1.96
Falcón	Notoungulata	Toxodontidae	*Falcontoxodon aguilerai*	AMU-CURS 70	Codore	Codore Algodones	NA	11.29	-70.24	2530	8257	1.96
Falcón	Litopterna	Proterotheriidae	Proterotheriidae indet.	AMU-CURS 745	Codore	Codore Algodones	NA	11.29	-70.24	2530	8257	1.96
Falcón	Litopterna	Proterotheriidae	Proterotheriidae indet.	AMU-CURS 746	Codore	Codore Algodones	NA	11.29	-70.24	2530	8257	1.96
Falcón	Xenarthra	Glyptodontidae	*Boreostemma pliocena*	AMU-CRUS 158	Codore	Road to Tio Gregorio	NA	11.26	-70.29	2530	8257	1.96

Falcón	Notoungulata	Toxodontidae	*Falcontoxodon aff. aguilerai*	AMU-CURS 585	San Gregorio	Norte Casa Chiguaje	NA	11.3	-70.24	4	8291	1.78
Falcón	Notoungulata	Toxodontidae	*Falcotoxodon sp.*	AMU-CURS 69	San Gregorio	Norte Casa Chiguaje	NA	11.3	-70.24	7	8294	1.79
Falcón	Notoungulata	Toxodontidae	*Falcotoxodon sp.*	AMU-CURS 77	San Gregorio	Norte Casa Chiguaje	NA	11.3	-70.24	7	8294	1.79
Falcón	Notoungulata	Toxodontidae	*Falcotoxodon sp.*	AMU-CURS 270	San Gregorio	Norte Casa Chiguaje	NA	11.3	-70.24	7	8294	1.79
Falcón	Notoungulata	Toxodontidae	*Falcotoxodon sp.*	AMU-CURS 542	San Gregorio	Norte Casa Chiguaje	NA	11.3	-70.24	7	8294	1.79
Falcón	Notoungulata	Toxodontidae	*Falcotoxodon sp.*	AMU-CURS 544	San Gregorio	Norte Casa Chiguaje	NA	11.3	-70.24	7	8294	1.79
Falcón	Notoungulata	Toxodontidae	*Falcotoxodon sp.*	AMU-CURS 548	San Gregorio	Norte Casa Chiguaje	NA	11.3	-70.24	7	8294	1.79
Falcón	Notoungulata	Toxodontidae	*Falcotoxodon sp.*	AMU-CURS 562	San Gregorio	Norte Casa Chiguaje	NA	11.3	-70.24	7	8294	1.79
Falcón	Notoungulata	Toxodontidae	*Falcotoxodon sp.*	AMU-CURS 563	San Gregorio	Norte Casa Chiguaje	NA	11.3	-70.24	7	8294	1.79
Falcón	Notoungulata	Toxodontidae	*Falcotoxodon sp.*	AMU-CURS 570	San Gregorio	Norte Casa Chiguaje	NA	11.3	-70.24	7	8294	1.79

Falcón	Notoungulata	Toxodontidae	*Falcotoxodon sp.*	AMU-CURS 738	San Gregorio	Norte Casa Chiguaje	NA	11.3	-70.24	7	8294	1.79
Falcón	Notoungulata	Toxodontidae	*Falcotoxodon sp.*	AMU-CURS 739	San Gregorio	Norte Casa Chiguaje	NA	11.3	-70.24	7	8294	1.79
Falcón	Notoungulata	Toxodontidae	*Falcotoxodon sp.*	AMU-CURS 741	San Gregorio	Norte Casa Chiguaje	NA	11.3	-70.24	7	8294	1.79
Falcón	Carnivora	Procyonidae	*Cyonasua sp*	AMU-CURS 224	San Gregorio	Norte Casa Chiguaje	NA	11.3	-70.23	5	8292	1.78
Falcón	Rodentia	Caviomorpha	cf. Caviodon	UNEFM-VF-53	San Gregorio	Norte Casa Chiguaje	NA	11.3	-70.235750	5	8292	1.78
Falcón	Rodentia	Caviomorpha	*Hydrochoeropsis? wayuu*	UNEFM-VF-50	San Gregorio	Norte Casa Chiguaje	NA	11.3	-70.235750	5	8292	1.78
Falcón	Rodentia	Caviomorpha	*Hydrochoeropsis? wayuu*	UNEFM-VF-51	San Gregorio	Norte Casa Chiguaje	NA	11.3	-70.235750	5	8292	1.78
Falcón	Rodentia	Caviomorpha	*Hydrochoeropsis? wayuu*	UNEFM-VF-52	San Gregorio	Norte Casa Chiguaje	NA	11.3	-70.235750	5	8292	1.78
Falcón	Rodentia	Caviomorpha	*Marisela gregoriana*	UNEFM-VF-55	San Gregorio	Norte Casa Chiguaje	NA	11.3	-70.235750	5	8292	1.78
Falcón	Rodentia	Caviomorpha	*Neoepiblema sp.*	UNEFM-VF-54	San Gregorio	Norte Casa Chiguaje	NA	11.3	-70.235750	5	8292	1.78

Falcón	Xenarthra	Dasypodidae	*Pliodasypus vergelianus*	AMU-CURS 192	San Gregorio	Norte Casa Chiguaje	NA	11.3	-70.24	5	8292	1.78
Falcón	Xenarthra	Glyptodontidae	*Lycopsis padillai*	MUN-STRI 34113	Castilletes	STRI 390093	170514	11.91	-71.34	128	280	15.1
Cocinetas	Sparassodonta	Borhyaenoidea	*Hyperleptus?*	MUN-STRI 37413	Castilletes	STRI 130024	430103	11.93	-71.33	80	80	16.3
Cocinetas	Xenarthra	Megatheroidea	*Hilarcotherium miyou*	IGMp 881327	Castilletes	STRI 470058	430103	11.95	-71.32	28	28	16.6
Cocinetas	Astrapotheria	Uruguaytheriinae	*Hilarcotherium miyou*	MUN-STRI 34216	Castilletes	STRI 470058	430103	11.95	-71.32	28	28	16.6
Cocinetas	Astrapotheria	Uruguaytheriinae	*Hilarcotherium miyou*	MUN-STRI 16778	Castilletes	STRI 390094	430103	11.95	-71.33	46	46	16.5
Cocinetas	Astrapotheria	Uruguaytheriinae	Uruguaytheriinae indet.	MUN-STRI 34229	Castilletes	STRI 390094	430103	11.95	-71.33	46	46	16.5
Cocinetas	Astrapotheria	Uruguaytheriinae	Uruguaytheriinae indet.	MUN-STRI 34223	Castilletes	STRI 390094	430103	11.95	-71.33	46	46	16.5
Cocinetas	Astrapotheria	Uruguaytheriinae	Uruguaytheriinae indet.	MUN-STRI 34222	Castilletes	STRI 390094	430103	11.95	-71.33	46	46	16.5
Cocinetas	Astrapotheria	Uruguaytheriinae	Uruguaytheriinae indet.	MUN-STRI 34221	Castilletes	STRI 390094	430103	11.95	-71.33	46	46	16.5
Cocinetas	Astrapotheria	Uruguaytheriinae	Uruguaytheriinae indet.	MUN-STRI 34217	Castilletes	STRI 390094	430103	11.95	-71.33	46	46	16.5
Cocinetas	Astrapotheria	Uruguaytheriinae	Uruguaytheriinae indet.	MUN-STRI 16777	Castilletes	STRI 390094	430103	11.95	-71.33	46	46	16.5
Cocinetas	Astrapotheria	Uruguaytheriinae	Uruguaytheriinae indet.	MUN-STRI 34212	Castilletes	STRI 290632	430103	11.95	-71.33	28	28	16.6

Cocinetas	Astrapotheria	Uruguaytheriinae	Uruguaytheriinae indet.	MUN-STRI 37384	Castilletes	STRI 390094	430103	11.95	-71.33	46	46	16.5
Cocinetas	Astrapotheria	Uruguaytheriinae	Uruguaytheriinae indet.	MUN-STRI 37765	Castilletes	STRI 130024	430103	11.93	-71.33	80	80	16.3
Cocinetas	Astrapotheria	Uruguaytheriinae	Uruguaytheriinae indet.	MUN-STRI 34225	Castilletes	STRI 390094	430103	11.95	-71.33	46	46	16.5
Cocinetas	Astrapotheria	Uruguaytheriinae	Uruguaytheriinae indet.	MUN-STRI 34310	Castilletes	STRI 390094	430103	11.95	-71.33	46	46	16.5
Cocinetas	Astrapotheria	Uruguaytheriinae	Uruguaytheriinae indet.	MUN-STRI 36644	Castilletes	STRI 390094	430103	11.95	-71.33	46	46	16.5
Cocinetas	Astrapotheria	Uruguaytheriinae	Uruguaytheriinae indet.	MUN-STRI 37390	Castilletes	STRI 390094	430103	11.95	-71.33	46	46	16.5
Cocinetas	Astrapotheria	Uruguaytheriinae	Uruguaytheriinae indet.	MUN-STRI 34292	Castilletes	STRI 390093	170514	11.91	-71.34	128	280	15.1
Cocinetas	Astrapotheria	Uruguaytheriinae	Uruguaytheriinae indet.	MUN-STRI 16779	Castilletes	STRI 390094	430103	11.95	-71.33	46	46	16.5
Cocinetas	Astrapotheria	Uruguaytheriinae	Uruguaytheriinae indet.	MUN-STRI 16785	Castilletes	STRI 390094	430103	11.95	-71.33	46	46	16.5
Cocinetas	Astrapotheria	Uruguaytheriinae	cf. Huilatherium	MUN-STRI 34312	Castilletes	STRI 390094	430103	11.95	-71.33	46	46	16.5
Cocinetas	Notoungulata	Leontinidae	*Neodolodus cf. colombianus*	MUN-STRI 16716	Castilletes	STRI 390093	170514	11.91	-71.34	128	280	15.1
Cocinetas	Litopterna	Proterotheriidae	Lestodontini gen. et. sp. Nov.	MUN-STRI 36643	Ware	STRI 470060	430052	11.85	-71.32	4	NA	3.05
Cocinetas	Xenarthra	Lestodontini	Lestodontini gen. et. sp. Nov.	MUN-STRI 20424	Ware	STRI 390023	430052	11.85	-71.32	3.5	NA	3.05
Cocinetas	Xenarthra	Lestodontini	Lestodontini gen. et. sp. Nov.	MUN-STRI 34353	Ware	STRI 470060	430052	11.85	-71.32	4	NA	3.05

Cocinetas	Xenarthra	Lestodontini	Scelidotheriinae gen. et. sp. indet.	MUN-STRI 16535	Ware	STRI 390025	430052	11.85	-71.32	4.5	NA	3.05
Cocinetas	Xenarthra	Scelidotheriinae	Megalonychidae gen. et. sp. nov.	MUN-STRI 16601	Ware	STRI 390077	430052	11.85	-71.32	1.7	NA	3.06
Cocinetas	Xenarthra	Megalonychidae	Megalonychidae gen. et. sp. nov.	MUN-STRI 34226	Ware	STRI 470060	430052	11.85	-71.32	4	NA	3.05
Cocinetas	Xenarthra	Megalonychidae	*Pliomegatherium lelongi*	MUN-STRI 36685	Ware	STRI 390024	430052	11.85	-71.32	4.5	NA	3.05
Cocinetas	Xenarthra	Megatheriinae	*Pliomegatherium lelongi*	MUN-STRI 19747	Ware	STRI 390017	430052	11.85	-71.33	5	NA	3.04
Cocinetas	Xenarthra	Megatheriinae	*Pliomegatherium lelongi*	MUN-STRI 20446	Ware	STRI 390026	430052	11.85	-71.33	5	NA	3.04
Cocinetas	Xenarthra	Megatheriinae	cf. Nothrotherium	MUN-STRI 12924	Ware	STRI 390024	430052	11.85	-71.32	4.5	NA	3.05
Cocinetas	Xenarthra	Nothrotheriinae	*?Hydrochoeropsis wayuu*	MUN-STRI 12846	Ware	STRI 390017	430052	11.85	-71.33	5	NA	3.04
Cocinetas	Rodentia	Caviomorpha	*?Hydrochoeropsis wayuu*	MUN-STRI 37602	Ware	STRI 470062	430052	11.85	-71.32	5	NA	3.04
Cocinetas	Rodentia	Caviomorpha	*?Hydrochoeropsis wayuu*	MUN-STRI 16233	Ware	STRI 430052	430052	11.85	-71.32	5	NA	3.04
Cocinetas	Rodentia	Caviomorpha	*?Hydrochoeropsis wayuu*	MUN-STRI 16438	Ware	STRI 430052	430052	11.85	-71.32	5	NA	3.04
Cocinetas	Rodentia	Caviomorpha	*?Hydrochoeropsis wayuu*	MUN-STRI 34315	Ware	STRI 470062	430052	11.85	-71.32	5	NA	3.04
Cocinetas	Rodentia	Caviomorpha	Toxodontidae indet.	MUN-STRI 37507	Ware	STRI 470062	430052	11.85	-71.32	5	NA	3.04
Cocinetas	Notoungulata	Toxodontidae	Toxodontidae indet.	MUN-STRI 37561	Ware	STRI 470059	430052	11.85	-71.32	2	NA	3.06

Cocinetas	Notoungulata	Toxodontidae	Camelidae indet.	MUN-STRI 34380	Ware	STRI 470060	430052	11.85	-71.32	4	NA	3.05
Cocinetas	Artiodactyla	Camelidae	*Chapalmalania sp.*	MUN-STRI 34114	Ware	STRI 470061	430052	11.85	-71.32	4.3	NA	3.05
Cocinetas	Carnivora	Procyonidae	Proterotheriidae indet.	MUN-STRI 34170	Ware	STRI 470060	430052	11.85	-71.32	4	NA	3.05
Cocinetas	Litopterna	Proterotheriidae	Proterotheriidae indet.	MUN-STRI 13378	Ware	STRI 390023	430052	11.85	-71.32	3.5	NA	3.05
Cocinetas	Litopterna	Proterotheriidae	Proterotheriidae indet.	MUN-STRI 13121	Ware	STRI 390020	430052	11.85	-71.32	5	NA	3.04
Cocinetas	Litopterna	Proterotheriidae	Proterotheriidae indet.	MUN-STRI 19544	Ware	STRI 390018	430052	11.85	-71.32	4.5	NA	3.05
Cocinetas	Litopterna	Proterotheriidae	Proterotheriidae indet.	MUN-STRI 13119	Ware	STRI 390020	430052	11.85	-71.32	5	NA	3.04
Cocinetas	Litopterna	Proterotheriidae	Proterotheriidae indet.	MUN-STRI 13120	Ware	STRI 390020	430052	11.85	-71.32	5	NA	3.04
Cocinetas	Litopterna	Proterotheriidae	Proterotheriidae indet.	MUN-STRI 16289	Ware	STRI 430052	430052	11.85	-71.32	5	NA	3.04

DISCUSSION

Astrapotheria

The clade Uruguaytheriinae is registered in low and mid-latitudes (< 23ºS; Goillot et al. 2011; Vallejo-Pareja et al. 2015; Croft et al. 2016), with the exception of *Uruguaytherium*, the most basal Uruguaytheriinae, but its precise provenance and age are unknown. The oldest record of Uruguaytheriinae comes from the bank of Río Beu, near the Santa Rosa locality in Peru, and it is interpreted to be late Oligocene in age (Antoine et al. 2016). The time-calibrated tree (Figure 12a) is also consistent with the origin of Uruguaytheriinae in the late Oligocene. Given the current evidence it is unclear whether the clade's origin is tropical or extratropical, and more complete material from the late Oligocene deposits should help to clarify this issue. In any event, the middle Miocene (Laventan) uruguaytheriine taxa are the last occurring astrapotheres (Johnson and Madden, 1997; Goillot et al. 2011) (Figure 12a).

Within the northern Uruguaytheriinae, *Granastrapotherium* and *Xenastrapotherium* are sister groups (Figure 12a). *Hilarcotherium* is known only from Colombia, and its biochron extends from the upper Burdigalian-Langhian (Santacrucian/ Colloncuran;16.7-14.2 mya; Moreno et al. 2015) to the Servallian (?Laventan; Vallejo-Pareja et al. 2015). *Granastrapotherium* is a monospecific genus and *Xenastrapotherium* includes five species; some of them were described from fragmentary remains without associated upper and lower dentition, and more complete specimens are needed to evaluate their validity.

Postcranial elements of Uruguaytheriinae are rare, and their intra- and interspecific variation has not been studied. Isolated postcranial elements are common in the Castilletes fauna. They are not associated with dental remains and cannot be confidently assigned to *H. miyou* or to any other species. All the postcranial elements are large, and given the size of *H. miyou,* it is possible that the postcranial

elements from Castilletes belong to this taxon. The material described here will serve as a basis to compare the postcranial morphology of uruguaytheriine and non-uruguaytheriine astrapotheres in order to assess possible paleobiological differences or phylogenetically informative characters.

The dental measurements and associated body mass estimates of *H. miyou* (Figure 8; Tables 3,5) indicate that it is one of the largest astrapotheres, comparable in size to *G. snorki, Parastrapotherium martiale* (Deseadan-Colhuehuapian SALMAs), and *Parastrapotherium herculeum?* (Colhuehuapian; Kramarz and Bond, 2008, 2010, 2011). Few studies have addressed the estimation of body mass in astrapotheres, and the congruence between estimates from dental and postcranial measurements has not been studied. Previously reported body mass estimations in astrapotheres used only dental and cranio-mandibular measurements. The m2 length yields an estimate of 6456.6 kg for *H. miyou*, notably larger than *H. castanedaii* (~1303 kg; Vallejo-Pareja et al. 2015) and *X. kraglievichi* (~1238.7-1324.7 kg; Johnson and Madden, 1997; Kramarz and Bond, 2011). It is possible that the dental measurements overestimate the body mass of astrapotheres (Kramarz and Bond, 2011). The best known astrapotheriid is *Astrapotherium magnum* from the Santa Cruz Formation (Santacrucian SALMA) in Patagonia, which is known by almost complete skeletons with skulls and associated postcranial remains (Scott, 1928, 1937). The mean body mass estimate for *A. magnum* using bivariate and multivariate regression equations from cranio-mandibular measurements is 921.3 kg (Cassini et al. 2012), much smaller than the mean estimate of 1824.5 kg using the m1-m3 length (Kramarz and Bond, 2011). Similarly, the mean estimate for *G. snorki* using cranio-mandibular measurements reported by Johnson and Madden (1997; table 22.8) is 1126.1 kg, whereas the estimate using the m1-m3 length is 3141.9 kg.

Proximal limb bones are considered better estimators of body mass because they are weight-bearing elements and subject to greater biomechanical

constraints (Scott, 1990). Body mass estimates using the humeral length (Table 5) yield similar values to the estimates from dental measurements in *H. castanedaii* (1306.5 kg; Vallejo-Pareja et al. 2015), but this was not the case in *G. snorki* (4501.1 kg) and *A. magnum* (2096.5 kg), where the humeral estimates were larger than estimates from cranio-dental measurements. The estimate for the uruguaytheriine humerus from Castilletes (MUN-STRI 16777) is 4985.0 kg, 23% smaller than the estimate for *H. miyou* using the m2 length (Table 5). It is worth mentioning that the humerus of the former is associated with a radius, which indicates that the individual was a juvenile. These results emphasize the need for a comparative study on the relative proportions and scaling of teeth and limb bones in astrapotheres in order to choose an adequate living analog to estimate the body mass in this group.

Toxodontidae

The monophyly of Toxodontinae is strongly supported by our analysis with a high bootstrap value. However, within Toxodontinae, only (*Trigodon*, *Paratrigodon*) and (*Toxodon*, *Dinotoxodon*) have a bootstrap value higher than 50. The obtained topology differs from the one presented by Forasiepi et al. (2014: fig. 11) in the position of several taxa within Toxodontinae. The clades (*Paratrigodon*, *Trigodon*) and (*Toxodon*, *Dinotoxodon*) are recovered in both topologies but their positions are different in the cladograms. The main difference in our result is that the toxodontids recorded in Venezuela (*Mixotoxodon, Gyrinodon*, and *Falcontoxodon*) form a monophyletic group (node 44) and belong to a clade that also includes *Piauhytherium* and *Calchaquitherium* (node 46; Figure 24a).

Bond et al. (2006) described a specimen of Toxodontinae (UNEFM-CIAAP 616) from the middle member of the Urumaco Formation consisting of a partial mandibular ramus with m1-m3. UNEFM-CIAAP 616 shows unique characters not seen in combination in other toxodontids. Some of these characters are also seen in *Falcontoxodon*: a broad trigonid with a lingual enamel-less contour, a weakly developed meta-entoconid fold in m2, and

an open labial enamel fold. UNEFM-CIAAP 616 differs from *Falcontoxodon* in having a weakly developed meta-entoconid fold in m1, and a better developed ento-hypoconulid fold in m2 than in m1. The fragmentary nature of UNEFM-CIAAP 616 impedes the precise assessment of its phylogenetic affinities (Bond et al. 2006). More complete toxodontid material from the Urumaco Formation may confirm or refute if the clade that includes *Gyrinodon, Falcontoxodon* and *Mixotoxodon* was present in the region since the late Miocene.

The type of *Gyrinodon quassus* (NHMUK PV M13158) was collected in La Puerta Formation (middle to late Miocene) (Gonzalez de Juana et al. 1980), western Buchivacova, Falcón, Venezuela. Additional material from Acre, Brazil, has been referred to this taxon (Bond et al. 2006; Sánchez-Villagra et al. 2010). *Mixotoxodon larensis* is recorded in late Pleistocene sediments of tropical localities of South and Central America (between 15ºS and 18ºN) (Rincón, 2011). *Mixotoxodon* is the only toxodontid that migrated to Central America during the GABI (Webb and Perrigo, 1984; Laurito, 1993; Lucas et al. 1997; Cisneros, 2005; Lucas, 2008, 2014).

The estimated body mass of ~796 kg for *F. aguilerai* is comparable to that of *Pericotoxodon platignathus* (~798 kg; Madden, 1997), larger than estimates for *Nesodon taweretus* (~550 kg; Forasiepi et al. 2015), *Nesodon imbricatus* (~637 kg; Cassini et al. 2012), and *Xotodon* sp. (mean=626 kg, standard deviation= 59 kg; Elissamburu, 2012), and smaller than *Toxodon platensis* (mean=1642 kg, geometric mean= 1187 kg; Fariña et al. 1998), *Trigodon* (mean=1809 kg, standard deviation= 508 kg) and *Mixotoxodon larensis* (mean= 3797 kg, standard deviation=1296 kg; Elissamburu, 2012). With a sample size of six taxa, Elissamburu (2012) estimated a body mass range for toxodontids of 104 kg-3797 kg. *Falcontoxodon* shows an intermediate body mass among Toxodontinae, and did not reach the large sizes of the Pleistocene taxa.

Miocene fauna

Of the seven mammalian taxa currently recognized for the assemblage of the Castilletes Formation in the Cocinetas basin (Table 1), three are SANUs. The taxa previously described for this assemblage are the sparassodont *Lycopsis padillai* (Suarez et al. 2016) and the megatherioid sloth *Hyperleptus*? (Amson et al. 2016). These two taxa belong to genera that show a wide latitudinal range and are also recorded at higher latitudes in the Santacrucian fauna (Kay et al. 2012). In contrast, the SANUs from Castilletes represent tropical groups (*Neodolodus*, *Hilarcotherium*, and *Huilatherium*), which are also recorded in the Laventan fauna of the Magdalena valley in Colombia (Cifelli and Guerrero, 1989; Villaroel and Colwell Danis, 1997; Vallejo-Pareja et al. 2015). The records of these taxa in Castilletes expand their temporal and geographical distribution.

Neodolodus and *Megadolodus* are two small proterotheriids recorded in La Venta and originally referred to Didolodontidae (McKenna, 1956; Hoffstetter and Soria, 1986). However, additional material was used to hypothesize assignation to Proterotheriidae (Cifelli and Guerrero, 1989; Cifelli and Villaroel, 1997). The distinctiveness of *Megadolodus* warranted the recognition of a distinct clade within Proterotheriidae, the Megadolodinae (Cifelli and Villaroel, 1997). This clade also includes *Bounodus enigmaticus* from the Urumaco Formation (Carlini et al. 2006a). *Neodolodus colombianus* was transferred to *Prothoatherium* by Cifelli and Guerrero (1989). *Prothoatherium* was named by Ameghino (1902), who recognized two species and later on added a third one (Ameghino, 1904). Soria (2001) did not recognize *Prothoatherium* as valid, and transferred one species to *Lambdaconus* (*L. lacerum*) and established the other two as synonyms of *Paramacrauchenia scammata* (=*Prothoatherium scammatum* [partim] and *Prothoatherium plicatum*) and *Paramacrauchenia inexpectata* (=*Prothoatherium scammatum* [partim]). Soria died in 1989, and his dissertation (published posthumously in 2001) made no mention of *N. colombianus*, which he probably considered a didolodontid (Hoffstetter and Soria, 1986). We consider *Neodolodus* to be a valid name and acknowledge that it belongs to Proterotheriidae, as shown by Cifelli and

Guerrero (1989). Therefore, *Neodolodus* represents a genus of small tropical proterotheriids, but their relationships with Megadolodinae remain unresolved. Based on the body mass and skeletal adaptations of *N. colombianus,* Cifelli and Guerrero (1989) inferred cursorial and forest-dwelling habits for this species.

The deposition of the Castilletes Formation represents a shallow marine to fluvio-deltaic environment with transgressive sequences (Hendy et al. 2015; Moreno et al. 2015). The localities where the mammal remains were collected show a strong fluvial influence (Moreno et al. 2015), as indicated by the diverse assemblage of crocodiles (Moreno-Bernal et al. 2016) and turtles (Cadena and Jaramillo, 2015a). The mammal record is in agreement with this paleoenvironmental reconstruction (Figures 30-31). The astrapothere remains from the Castilletes Formation were collected from muddy sediments and often associated with freshwater "invertebrates" (Moreno et al. 2015). Astrapotheres are commonly reported to occur in sediments representing stream channels (Riggs, 1935; Scott, 1937; Marshall et al. 1990), and in association with aquatic fauna (Sánchez-Villagra et al. 2004). The bone microstructure (studied in *Parastrapotherium*) is similar to that of graviportal taxa, and it is possible that astrapotheres were specialized for graviportality and semi-aquatic habits (Houssaye et al. 2016).

Pliocene/Pleistocene faunas

The toxodontid and proterotheriid material from the Codore Formation comes from the upper part of the Algodones Member (Figure 4b), 30 stratigraphic meters below the contact with the San Gregorio Formation. At the moment, the mammal fauna of the Codore Formation includes four taxa (Table 2). The glyptodont *Boreostemma pliocena* is recorded in the lower member (El Jebe) of the Codore Formation (Carlini et al. 2008b). When compared with the better known underlying Urumaco Formation (Sánchez-Villagra and Aguilera, 2006) and even the San Gregorio Formation (Table 2), the mammal diversity of Codore is modest. This is due to undersampling and further efforts will increase the diversity

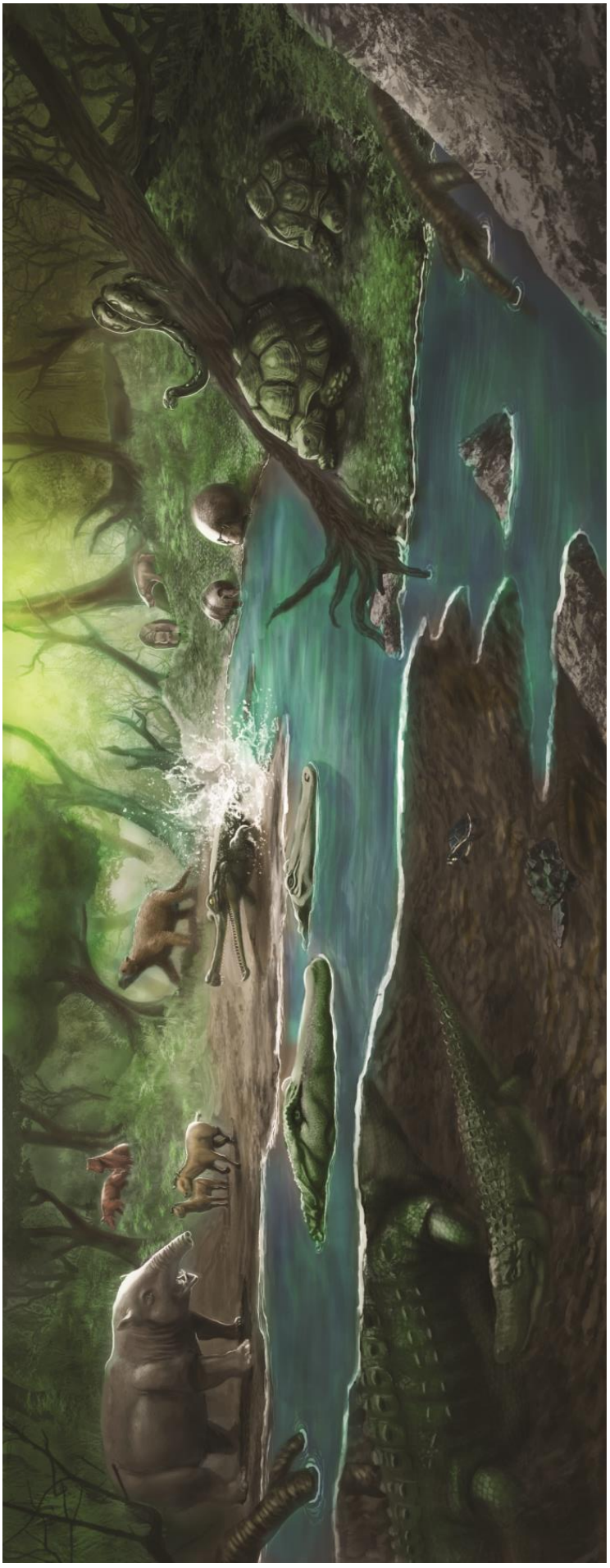

Figure 30. Life reconstruction of the Castilletes Formation faunal assemblage, Cocinetas basin, Colombia. Artist: Stjepan Lukac.

Figure 31. Key of the reconstruction shown in Figure 30. 1, *Hilarcotherium miyou* n. sp. (Astrapotheriidae). 2, *Lycopsis padillai* (Borhyaenoidea). 3, *Hyperleptus*? (Megatherioidea). 4, cf. *Huilatherium* (Leontiniidae). 5, Boidae indet. (Squamata). 6, *Neodolodus* cf. *colombianus* (Proterotheriidae). 7, Gavialoidea indet. (Crocodilia). 8, Pampatheriidae indet. 9, Glyptodontidae indet. 10, *Mourasuchus* sp. (Crocodilia). 11, *Chelonoidis* sp. (Testudines). 12, *Purussaurus* sp. (Crocodilia). 13, Podocnemidae (Testudines). 14, *Chelus colombiana* (Testudines).

of this unit (Carlini 2010).

The San Gregorio fauna includes macro and micro mammals (e.g., rodents) (Table 2). Small vertebrates have not been recovered in the Urumaco Formation, the fauna of which is mostly characterized by large crocodiles, turtles and xenarthrans. However, in San Gregorio the lithology favors the preservation of small vertebrates, and it promises for the late Pliocene/early Pleistocene to offer a more complete picture of the faunal assemblage in the Falcon basin (Figures 32-33). The age of San Gregorio overlaps with two GABI migration pulses (GABI 2 and 3; Figure 1) (Woodburne, 2010). Paleontological and molecular evidence shows that GABI significantly increased during the early Pleistocene (Woodburne, 2010; Bacon et al. 2015; Carrillo et al. 2015). However, in San Gregorio so far only one of the ten described mammalian taxa is a migrant from North America, the procyonid *Cyonasua* (Forasiepi et al. 2014). The age of San Gregorio corresponds to the Ensenadan SALMA (Figure 28), of which the type locality

Figure 32. Life reconstruction of the San Gregorio Formation faunal assemblage, Falcón basin, Venezuela. Artist: Stjepan Lukac.

Figure 33. Key of the reconstruction shown in Figure 32. 1, *Cyonasua* (Procyonidae). 2, *Tupinambis* sp. (Squamata). 3, *Boreostemma*? sp. (Glyptodontidae). 4, *Neoepiblema* (Neoepiblemidae). 5, *Hydrochoeropsis*? *wayuu* (Caviidae). 6, *Pliodasypus vergelianus* (Dasypodidae). 7, Pampatheriidae. 8, aff. *Proeremotherium* (Megatheriinae). 9, *Marisela gregoriana* (Octodontoidea). 10, *Falcontoxodon* sp. (Toxodontidae). 11, cf. *Caviodon* (Caviidae). 12, Characiformes indet. 13, Loricariidae indet. (Siluriformes). 14, *Crocodylus falconensis* (Crocodilia). 15, Potamotrygonidae indet. (Myliobatiformes). 16, Doradidae indet. (Siluriformes). 17, Podocnemidae indet. (Testudines).

is located in La Plata county (~34° S) in Argentina (Cione et al. 2015). In southern South America this time interval is characterized by the presence of several clades of Holarctic origin (e.g., Cervidae, Ursidae, Tapiridae, Felidae, and Gomphotheriidae) (Cione et al. 2015, which contrasts with the pattern observed in the Falcón basin.

A similar pattern is observed in the mammalian fauna of the Ware Formation, in the Cocinetas basin, which is slightly older than San Gregorio and close to the first GABI migration pulse (GABI 1; Figure 1) (Woodburne, 2010; Moreno et al. 2015). Despite its close proximity to the Isthmus of Panama, of the 13 taxa recorded for the Ware fauna (Table 1), only two are migrants from North

America, the procyonid *Chapalmalania* (Forasiepi et al. 2014) and a camelid. The latter is arguably the oldest well-dated record of Camelidae in South America. Hendy et al. (2015) reported a mean age of 3.2 MYA (range from 3.40 to 2.78 MYA) calculated from $^{87}Sr/^{86}Sr$ ratios for the shell bed at the top of the formation (Figure 3), which is 16 stratigraphic meters above where the camelid was collected. Macroinvertebrate biostratigraphy also yielded a Piacenzian age for the Ware Formation (Hendy et al. 2015; Moreno et al. 2015).

The oldest record of Camelidae in South America has been a problematic point in the understanding of the paleobiogeography of this group during GABI (Scherer, 2013). The most recent evidence suggests that the putative oldest camelid record in the continent is Barrancalobean (ca. 3 MYA), a subage of the Marplatan SALMA (Scherer, 2013; Cione et al. 2015). Barrancalobean records come from the Pampean region in Argentina, more than 5,000 km away from the Isthmus of Panama. The camelid record from Ware supports a minimum age of ca. 3.2 MYA for the arrival of camelids in South America, as would be expected given its proximity to the Isthmus. Unfortunately, the material available does not permit us to evaluate if it belongs to the Lamini, like the other South American camelids (Scherer, 2013), or to the group of camelids that inhabited the Central American tropics beginning in the early Miocene (Rincon et al. 2012).

The mammalian fauna of the Ware Formation is characterized by a high diversity of herbivores (Figure 34-35), which includes at least five different taxa of sloths (Amson et al. 2016), as well as cingulates, caviomorph rodents (Moreno et al. 2015; Pérez et al. 2016), a toxodont, a proterotheriid, and a camelid (Table 1). The diversity and wide body mass range of herbivores from the Ware Formation suggest that they occupied different ecological niches, and that there was enough vegetation cover to sustain a complex herbivorous community. Other vertebrates from the assemblage such as crocodiles, turtles, and freshwater fishes (Aguilera et al. 2013; Moreno et al. 2015; Moreno-Bernal et al. 2016), are

Figure 34. Life reconstruction of the Ware Formation faunal assemblage, Cocinetas basin, Colombia. Artist: Stjepan Lukac.

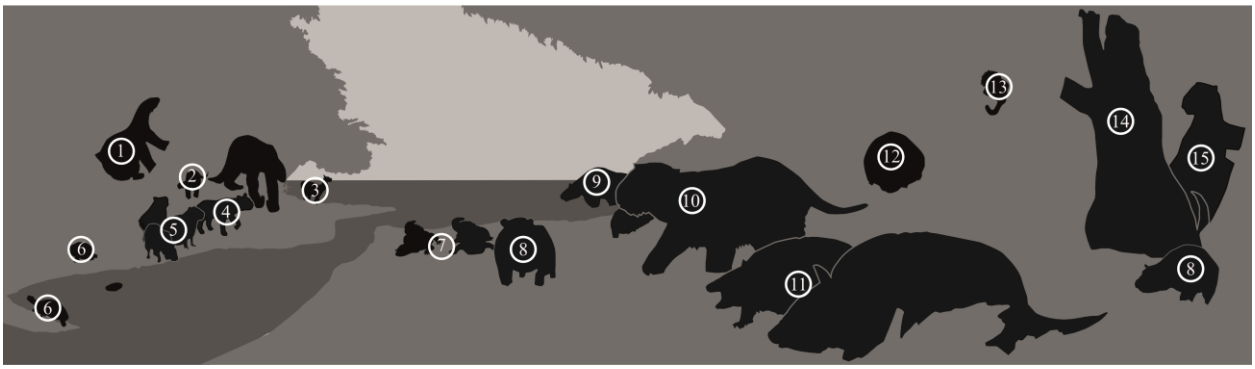

Figure 35. Key of the reconstruction shown in Figure 34. 1, *Pliomegatherium lelongi* (Megatheriinae). 2, cf. *Nothrotherium* (Nothrotheriinae). 3, Camelidae indet. 4, Proterotheriidae indet. 5, *Hydrochoeropsis*? *wayuu* (Caviidae). 6, Podocnemidae indet. (Testudines). 7, *Crocodylus* (Crocodylidae). 8, *Chapalmalania* sp. (Procyonidae). 9, Toxodontinae indet. 10, Lestodontini gen. et sp. nov. 11, Pampatheriidae indet. 12, Glyptodontidae indet. 13, Erethizontidae indet. 14, Megalonychidae gen. et sp. nov. 15, Scelidotheriinae gen. et sp. indet.

indicative of the fluvial influence in the region during the late Pliocene. Today, the Guajira peninsula is dominated by a dry landscape with low rainfall (less than 500 mm of mean annual precipitation), high seasonality, xerophytic vegetation and lack of large rivers (Pabón-Caicedo et al. 2001).

The Pliocene climate prior to the increase of the Northern Hemisphere glaciations was characterized by warmer mean annual temperatures than the preindustrial conditions, higher levels of CO_2 (>400 ppm), and reduced meridional and vertical ocean temperature gradients than today (Pagani et al. 2010). We hypothesize that the change in the landscape in the Cocinetas and Falcón basins relates to the increase of the Northern Hemisphere glaciations in the Pliocene (ca. 2.7 MYA), which was mainly controlled by a decrease of the atmospheric CO_2 (Lunt et al. 2008). During the early Pliocene (ca. 4-5 MYA) the CO_2 concentration ranges from ~390 to 280 ppm, and CO_2 atmospheric levels progressively decreased from 5 to 0.5 MYA (Pagani et al. 2010). Global rainfall is higher at the Intertropical Convergence Zone (ITCZ), a tropical belt of clouds. The ITCZ migrates seasonally between the boreal and austral summers towards the

warmest hemisphere, and its position is linked to the atmospheric energy transport (Schneider et al. 2014). The increase of the ice cover in the Northern Hemisphere during the Pliocene could have affected the migration of the ITCZ towards a more southern position. For example, Holocene sediments from the Cariaco basin (coast of north central Venezuela) indicate a southward ITCZ migration during time intervals when the high northern latitudes cooled (Schneider et al. 2014; fig. 6). A southward migration of the ITCZ would have reduced the amount of rainfall in northwestern South America, producing the landscape change observed in the Cocinetas and Falcón basins.

CONCLUSION

We describe new material of SANUs from the Neogene deposits of the Cocinetas and Falcón basins, in northern South America, a region underrepresented in the fossil record in comparison with the southern portion of the continent. The middle Miocene deposits of the Castilletes Formation, in the Cocinetas basin, is characterized by the presence of a large uruguaytheriine astrapothere (*Hilarcotherium miyou* sp. nov.), the leontiniid cf. *Huilatherium*, and the proterotheriid *Neodolodus* cf. *colombianus*. They all belong to tropical groups, which are otherwise recorded in the Laventan fauna of the Magdalena valley, Colombia. This biogeographic pattern contrasts with that represented by other members of the mammal fauna (the sparassodont *Lycopsis padillai* and the sloth *Hyperleptus*?), which belong to taxa with a wide latitudinal distribution across the continent. *H. miyou* is one of the largest astrapotheres, with an estimated body mass of ~6456.6 kg, although estimations based on dental measurements in astrapotheres should be taken with caution. Astrapothere postcranial elements are common in the Castilletes Formation and found in association with freshwater "invertebrates".

We describe a new species of Toxodontinae (*Falcontoxodon aguilerai* gen. et sp. nov.), the holotype of which was found in the Codore

Formation, and we refer some dental and postcranial remains from the San Gregorio Formation to the same genus. *F. aguilerai* shows an intermediate body mass among Toxodontinae, with an estimate of ~796 kg. The new material allows us to recognize a tropical clade within Toxodontinae that includes the Venezuelan toxodonts recorded from the Miocene (*Gyrinodon*) to the Pleistocene (*Mixotoxodon*). The latter is the only toxodont that migrated to Central America as part of the GABI. The Pliocene/Pleistocene faunas of Codore and San Gregorio Formations in the Falcón basin and Ware Formation in the Cocinetas basin are characterized by a predominance of South American native taxa in spite of their age and proximity to the Isthmus of Panama. This suggests that biotic interactions and biogeography influenced the timing and distribution of migrations in northern South America during the interchange.

The North American immigrants include procyonids and the putative oldest record of Camelidae in South America, which was recovered in the Ware Formation and has a minimum age of ca. 3.2 MYA, based on $^{87}Sr/^{86}Sr$ ratios and "macroinvertebrate" biostratigraphy.

ACKNOWLEDGEMENTS

Our gratitude goes to all the other members of the different field efforts in the Cocinetas and Falcón basins. In particular, J. D. Carrillo-Briceño, T. M. Scheyer, A. Wegmann, G. Aguirre-Fernández (PIMUZ), A. A. Carlini (MLP), A. Hendy (NHMLA), A. Reyes, D. Gutierrez, and the students from the University of Zürich for the 2013 field projects in Falcón. The Gonzalez family kindly provided access to collect in their land. We thank the authorities at the Instituto del Patrimonio Cultural of the República Bolivariana de Venezuela and the Alcaldía Municipio de Urumaco for their generous support. For fieldwork in Cocinetas, we are grateful to J. W. Moreno-Bernal, M.C Vallejo (STRI), F. Moreno (Rochester), A. Hendy (NHMLA), J. D. Carrillo-Briceño (PIMUZ), C. Suarez, K. Jimenez (MLP), E. Cadena (Yachay), C. Montes (UniAndes). The constant help of L. Londono (STRI) is also acknowledged. Thanks to Carlos Rosero for managing all the logistics in the field

in Colombia. Thanks to the communities of Warpana, Patajau, Aulechit, Nazareth, Wososopo, Sillamana, Paraguachon, La Flor de la Guajira, and Ipapura. Thanks to the Colombian National Police (Castilletes base) and the Colombian Army. We express special thanks to our drivers, Grillo, Lalo, and Medardo. We thank M. L. Parra and the Centro de Investigaciones Paleontológicas in Villa de Leyva, for the preparation of the specimens from the Cocinetas basin. We thank J. E. Arenas, M. Pardo (Servicio Geologico Colombiano), J. Escobar (Uninorte), C. Montes (UniAndes), L. Costeur (NMB), G. Billet (MNHN), P. Brewer (NHMUK), A. Kramarz, S. Alvarez (MACN), M. Reguero, A. Scarano (MLP), G. Ojeda (CIAAP-UNEFM), and H. Moreno (MCNC) for allowing access to the collections under their care. We are grateful to J. D. Carrillo-Briceño, T. M. Scheyer, C. Pimiento (PIMUZ), A. A. Carlini (MLP), A. Forasiepi (Conicet), R. Salas-Grismondi (STRI), D. Croft (CWRU), G. Billet (MNHN), R. J. Asher (U. Cambridge), M. Pardo (SGC) and the Evolutionary Morphology and Palaeobiology of Vertebrates group in Zurich for valuable advice. S. Lukac made the graphic reconstructions of the faunas. L. Goodayle took the pictures shown in Figure 15, which were kindly provided by the NHMUK. G. Billet (MNHN) kindly provided pictures from the YPM collections, and L. Costeur (NMB) kindly provided pictures from *X. christi*. J. D. Carrillo was supported by Swiss National Fund P1ZHP3_165068, and by SNF 31003A-149605 and 31003A-169395 to M. R. Sánchez-Villagra. E. Amson was granted a short-term postdoctoral fellowship of the STRI, and was subsequently funded by the Alexander von Humboldt Foundation. The Swiss National Science Foundation, the Smithsonian Institution, the National Geographic Society, the Anders Foundation, Gregory D. and Jennifer Walston Johnson, Universidad del Norte, the National Science Foundation (Grant EAR 0957679) also helped to support this work.

REFERENCES

Aguilera, O. A., H. Moraes-Santos, S. Costa, F. Ohe, C. Jaramillo, and A. Nogueira. 2013a. Ariid Sea Catfishes from the Coeval Pirabas (Northeastern Brazil), Cantaure, Castillo (Northwestern Venezuela) and Castilletes (North

Colombia) Formations (Early Miocene), with Description of Three New Species. *Swiss Journal of Palaeontology*, 132(1):45-68. doi:10.1007/s13358-013-0052-4

Aguilera, O. A., J. Lundberg, J. Birindelli, M. Sabaj Pérez, C. Jaramillo, and M. R. Sánchez-Villagra. 2013b. Palaeontological Evidence for the Last Temporal Occurrence of the Ancient Western Amazonian River Outflow into the Caribbean. *PLoS ONE*, 8(9):e76202. doi:0.1371/journal.pone.0076202

Aguirre-Fernández, G., J. D. Carrillo-Briceño, R. Sánchez, E. Amson, and M. R. Sánchez-Villagra. 2017a. Fossil Cetaceans (Mammalia, Cetacea) from the Neogene of Colombia and Venezuela. *Journal of Mammalian Evolution,* 24(1):71-90. doi:10.1007/s10914-016-9353-x

Aguirre-Fernández, G., B. Mennecart, M. R. Sánchez-Villagra, R. Sánchez, and L. Costeur. 2017b. A Dolphin Fossil Ear Bone from the Northern Neotropics - Insights into Habitat Transitions in Iniid Evolution. *Journal of Vertebrate Paleontology*, e1315817. doi: 10.1080/02724634.2017.1315817

Ameghino, F. 1887. Enumeración sistemática de las especies de mamíferos fósiles coleccionados por Carlos Ameghino en los terrenos eocenos de la Patagonia austral y depositados en el Museo La Plata. *Boletín del Museo de La Plata,* 1:1-26.

Ameghino, F. 1889. Contribución al conocimiento de los mamíferos fósiles de la República Argentina. *Actas Academia Nacional Ciencias Córdoba*, 6:1-1027.

Ameghino, F. 1895. Première contribution à la connaissance de la faune mammalogique des couches à *Pyrotherium*. *Boletín Del Instituto Geográfico Argentino,* 15:603-660.

Ameghino, F. 1902. Première contribution à la connaissance de la faune mammalogique des couches a *Colpodon*. *Boletín de La Academia Nacional de Ciencias de Córdoba,* 17:71-138.

Ameghino, F. 1904. Rechérches de morphologie phylogénétique sur les molaires supérieures des ongulés. *Anales Del Museo Nacional de Buenos*

Aires, III:1689-1699.

Amson, E., J. D. Carrillo, and C. Jaramillo. 2016. Neogene Sloth Assemblages (Mammalia, Pilosa) of the Cocinetas Basin (La Guajira, Colombia): Implications for the Great American Biotic Interchange. *Palaeontology,* 59(4): 563-582. doi:10.1111/pala.12244

Antoine, P.-O., L. Marivaux, D. A. Croft, G. Billet, M. Ganerød, C. Jaramillo, T. Martin, M. J. Orliac, J. Tejada, A. J. Altamirano, F. Duranthon, G. Fanjat, S. Rousse, and R. Salas-Gismondi. 2012. Middle Eocene Rodents from Peruvian Amazonia Reveal the Pattern and Timing of Caviomorph Origins and Biogeography. *Proceedings of the Royal Society B: Biological Sciences,* 279:1319-1326. doi:10.1098/rspb.2011.1732

Antoine, P.-O., R. Salas-Gismondi, F. Pujos, M. Ganerød, and L. Marivaux. 2016. Western Amazonia as a Hotspot of Mammalian Biodiversity Throughout the Cenozoic. *Journal of Mammalian Evolution,* 24(1):5-17. doi: 10.1007/s10914-016-9333-1

Bacon, C. D., D. Silvestro, C. Jaramillo, B. T. Smith, P. Chakrabarty, and A. Antonelli. 2015. Biological Evidence Supports an Early and Complex Emergence of the Isthmus of Panama. *Proceedings of the National Academy of Sciences of the United States of America,* 112(19):6110-6115. doi: 10.1073/pnas.1423853112

Bacon, C. D., P. Molnar, A. Antonelli, A. J. Crawford, C. Montes, and M. C. Vallejo-Pareja. 2016. Quaternary Glaciation and the Great American Biotic Interchange. *Geology,* 44:375-378. doi:10.1130/g37624.1

Barnosky, A. D., and E. L. Lindsey. 2010. Timing of Quaternary Megafaunal Extinction in South America in Relation to Human Arrival and Climate Change. *Quaternary International,* 217(1-2):10-29. doi:dx.doi.org/10.1016/j.quaint.2009.11.017

Bengtson, P. 1988. Open Nomenclature. *Palaeontology,* 31(1):223-227.

Bermudez, P. J., and H. M. Bolli. 1969. Consideraciones sobre los sedimentos del Mioceno medio al reciente de las costas central y oriental de Venezuela. Tercera parte: Los

foraminíferos planctónicos. *Boletín de Geología, Ministerio de Minas e Hidrocarburos*, 10/20:137-223.

Billet, G. 2010. New Observations on the Skull of *Pyrotherium* (Pyrotheria, Mammalia) and New Phylogenetic Hypotheses on South American Ungulates. *Journal of Mammalian Evolution,* 17(1):21-59. doi:10.1007/s10914-009-9123-0

Billet, G. 2011. Phylogeny of the Notoungulata (Mammalia) Based on Cranial and Dental Characters. *Journal of Systematic Palaeontology,* 9(4):481-497. doi:10.1080/14772019.2010.528456

Billet, G., and T. Martin. 2011. No Evidence for an Afrotherian-like Delayed Dental Eruption in South American Notoungulates. *Naturwissenschaften,* 98(6):509-517. doi:10.1007/s00114-011-0795-y

Blow, W. H. 1969. Late middle Eocene to Recent Planktonic Foraminiferal Biostratigraphy. *Proceedings International Conference on Planktonic Microfossils 1st, Geneva, 1967*, 1: 199-421.

Bolli, H. M., J. P. Beckmann, and J. B. Saunders. 1994. *Benthic Foraminiferal Biostratigraphy of the South Caribbean Region*. London: Cambridge University Press.

Bond, M. 2016. "Ungulados nativos de Sudamérica. Una corta síntesis." In *Historia evolutiva y paleobiogeográfica de los vertebrados de América del Sur,* ed. F. L. Agnolin, G. L. Lio, F. Brissón Egli, N. R. Chimento, and F. E. Novas, pp. 293-301. Buenos Aires: Contribuciones del MACN.

Bond, M., and G. López. 1995. Los mamíferos de la Formación Casa Grande (Eoceno) de la Provincia de Jujuy, Argentina. *Ameghiniana,* 32:310-309.

Bond, M., and J. N. Gelfo. 2010. "The South American Native Ungulates of the Urumaco Formation." In *Urumaco and Venezuelan Paleontology. The Fossil Record of the Northern Neotropics,* ed. M. R. Sánchez-Villagra, O. A. Aguilera, and A. A. Carlini, pp. 256-268. Bloomington and Indianapolis: Indiana University Press.

Bond, M., R. H. Madden, and A. A. Carlini. 2006. A New Specimen

of Toxodontidae (Notoungulata) from the Urumaco Formation (Upper Miocene) of Venezuela. *Journal of Systematic Palaeontology,* 4(3):285-291. doi:10.1017/S1477201906001854

Bond, M., D. Perea, M. Ubilla, and A. Tauber. 2001. *Neolicaphrium recens* Frenguelli, 1921, the Only Surviving Proterotheriidae (Litopterna, Mammalia) into the South American Pleistocene. *Palaeovertebrata,* 30(1-2):37-50.

Bond, M., M. F. Tejedor, K. E. Campbell, L. Chornogubsky, N. Novo, and F. Goin. 2015. Eocene Primates of South America and the African Origins of New World monkeys. *Nature,* 520:538-541. doi:10.1038/nature14120

Buckley, M. 2015. Ancient Collagen Reveals Evolutionary History of the Endemic South American "Ungulates". *Proceedings of the Royal Society B: Biological Sciences,* 282(1806):20142671. doi:10.1098/rspb.2014.2671

Cabrera, A. 1929. Un astrapoterido de Colombia. *Comunicaciones de La Sociedad Argentina de Ciencias Naturales,* 9:436-443.

Cadena, E., and C. Jaramillo. 2015a. Early to Middle Miocene Turtles from the Northernmost tip of South America: Giant Testudinids, Chelids, and Podocnemidids from the Castilletes Formation, Colombia. *Ameghiniana,* 52:188-203. doi:dx.doi.org/10.5710/AMGH.10.11.2014.2835

Cadena, E. A., and C. A. Jaramillo. 2015b. The First Fossil skull of *Chelus* (Pleurodira: Chelidae, Matamata turtle) from the Early Miocene of Colombia. *Paleontologia Electronica,* 18.2.32A:1-10.

Captain, D. M., and L. B. Captain. 2005. *Diccionario Basico Ilustrado: Wayuunaiki-Espanol, Espanol-Wayuunaiki*. Bogotá: Editorial Buena Semilla.

Carlini, A. A. 2010. Fossil Xenarthran Mammals from Venezuela – Taxonomy, Patterns of Evolution and Associated Faunas. Ph.D. Diss., University of Zurich, Switzerland.

Carlini, A. A., J. N. Gelfo, and R. Sánchez. 2006a. A new Megadolodinae

(Mammalia, Litopterna, Protherotheriidae) from the Urumaco Formation (Late Miocene) of Venezuela. *Journal of Systematic Palaeontology,* 4(3):279-284. doi:10.1017/S1477201906001830

Carlini, A. A., G. J. Scillato-Yané, and R. Sánchez. 2006b. New Mylodontoidea (Xenarthra, Phyllophaga) from the Middle Miocene–Pliocene of Venezuela. *Journal of Systematic Palaeontology,* 4(3):255-267. doi:10.1017/s147720190600191x

Carlini, A. A., D. Brandoni, and R. Sánchez. 2006c. First Megatheriines (Xenarthra, Phyllophaga, Megatheriidae) from the Urumaco (Late Miocene) and Codore (Pliocene) Formations, Estado Falcón, Venezuela. *Journal of Systematic Palaeontology,* 4(3):269-278. doi:10.1017/S1477201906001878

Carlini, A. A., D. Brandoni, and R. Sánchez. 2008a. Additions to the Knowledge of *Urumaquia robusta* (Xenarthra, Phyllophaga, Megatheriidae) from the Urumaco Formation (Late Miocene), Estado Falcón, Venezuela. *Paläontologische Zeitschrift,* 82(2):153-162. doi:10.1007/BF02988406

Carlini, A. A., A. E. Zurita, G. J. Scillato-Yané, R. Sánchez, and O. A. Aguilera. 2008b. New Glyptodont from the Codore Formation (Pliocene), Falcón State, Venezuela, its Relationship with the *Asterostemma* problem, and the Paleobiogeography of the Glyptodontinae. *Paläontologische Zeitschrift,* 82(2):139-152. doi:10.1007/BF02988405

Carrillo, J. D., and M. R. Sánchez-Villagra. 2015. Giant Rodents from the Neotropics: Diversity and Dental Variation of Late Miocene Neoepiblemid Remains from Urumaco, Venezuela. *Paläontologische Zeitschrift,* 89(4):1057-1071. doi:10.1007/s12542-015-0267-3

Carrillo, J. D., A. Forasiepi, C. Jaramillo, and M. R. Sánchez-Villagra. 2015. Neotropical Mammal Diversity and the Great American Biotic Interchange: Spatial and Temporal Variation in South America's Fossil Record. *Frontiers in Genetics* 5:451. doi:10.3389/fgene.2014.00451

Carrillo, J. D., and R. J. Asher. 2017.

An Exceptionally Well-Preserved Skeleton of *Thomashuxleya externa* (Mammalia, Notoungulata), from the Eocene of Patagonia, Argentina. *Paleontologia Electronica* 20.2.35A:1-33.

Cassini, G. H., E. Cerdeño, A. L. Villafañe, and N. A. Muñoz. 2012. "Paleobiology of Santacrucian Native Ungulates (Meridungulata: Astrapotheria, Litopterna and Notoungulata)". In *Early Miocene Paleobiology in Patagonia: High Latitude Paleocommunities of the Santa Cruz Formation,* ed. S. F. Vizcaíno, R. F. Kay, and M. S. Bargo, pp. 243-286. Cambridge: Cambridge University Press.

Castro, M. C., A. A. Carlini, R. Sánchez, and M. R. Sánchez-Villagra. 2014. A new Dasypodini Armadillo (Xenarthra: Cingulata) from San Gregorio Formation, Pliocene of Venezuela: Affinities and Biogeographic Interpretations. *Naturwissenschaften,* 101(2):77-86. doi:10.1007/s00114-013-1131-5

Cerdeño, E., and B. Vera. 2015. A new Leontiniidae (Notoungulata) from the Late Oligocene beds of Mendoza Province, Argentina. *Journal of Systematic Palaeontology,* 13(11):943-962. doi:10.1080/14772019.2014.982727

Cifelli, R. L. 1983. The Origin and Affinities of the South American Condylarthra and Early Tertiary Litopterna (Mammalia). American Museum Novitates 49.

Cifelli, R. L. 1993. "The Phylogeny of the Native South American Ungulates". In *Mammal Phylogeny, Placentals,* ed. F. S. Szalay, M. J. Novacek, and M. C. McKenna, pp.195-214. New York: Springer-Verlag.

Cifelli, R. L., and J. Guerrero. 1989. New Remains of *Prothoatherium colombianus* (Litopterna, Mammalia) from the Miocene of Colombia. *Journal of Vertebrate Paleontology,* 9(2):222-231.

Cifelli, R. L., and C. Villaroel. 1997. "Paleobiology and affinities of *Megadolodus*". In *Vertebrate Paleontology in the Neotropics. The Miocene Fauna of La Venta, Colombia,* ed. R. F. Kay, R. H. Madden, R. L. Cifelli, and J. J. Flynn, pp.265-288.

Washington and London: Smithsonian Institution Press.

Cifelli, R. L., and J. Guerrero. 1997. "Litopterns". In *Vertebrate Paleontology in the Neotropics. The Miocene Fauna of La Venta, Colombia,* ed. R. F. Kay, R. H. Madden, R. L. Cifelli, and J. J. Flynn, pp.289-302. Washington and London: Smithsonian Institution Press.

Cione, A. L., and E. P. Tonni. 1999. Biostratigraphy and Chronological Scale of Upper Most Cenozoic in Pampean Area. *Quaternary of South America and Antarctic Peninsula*, 3:23-51.

Cione, A. L., and E. P. Tonni. 2001. Correlation of Pliocene to Holocene Southern South American and European Vertebrate-Bearing Units. *Bollettino della Società Paleontologica Italiana*, 40:167-173.

Cione, A. L., E. P. Tonni, and E. Soibelzon. 2003. The Broken Zig-Zag: Late Cenozoic Large Mammal and Tortoise Extinction in South America. *Revista Del Museo Argentino de Ciencias Naturales,* 51:1-19.

Cione, A. L., G. M. Gasparini, E. Soibelzon, L. H. Soibelzon, and E. P. Tonni. 2015. "The GABI in Southern South America". In *The Great American Biotic Interchange: A South American Perspective,* pp.71-96. Dordrecht: Springer Netherlands.

Cisneros, J. C. 2005. New Pleistocene Vertebrate Fauna from El Salvador. *Revista Brasileira de Paleontologia,* 8:239-255.

Cody, S., J. E. Richardson, V. Rull, C. Ellis, and R. T. Pennington. 2010. The Great American Biotic Interchange revisited. *Ecography,* 33(2):326-332. doi:10.1111/j.1600-0587.2010.06327.x

Croft, D. A. 1999. "Placentals: Endemic South American Ungulates". In *Encyclopedia of Paleontology vol. 2,* ed. R. Singer, pp.890-906. Chicago and London: Fitzroy Dearborn Publishers,

Croft, D. A. 2012. "Punctuated isolation. The Making and Mixing of South America's Mammals". In *Bones, Clones and Biomes. The History and Geography of Recent Neotropical Mammals,* ed. B. D. Patterson and L. P. Costa, pp.9-19. Chicago and London:

University of Chicago Press.

Croft, D. A. 2016. *Horned Armadillos and Rafting Monkeys. The Fascinating Fossil Mammals of South America*. Bloomington: Indiana University Press.

Croft, D. A., and D. Weinstein. 2008. The First Application of the Mesowear Method to Endemic South American Ungulates (Notoungulata). *Palaeogeography, Palaeoclimatology, Palaeoecology,* 269(1-2):103-114. doi: dx.doi.org/10.1016/j.palaeo.2008.08.007

Croft, D. A., A. A. Carlini, M. R. Ciancio, D. Brandoni, N. E. Drew, R. K. Engelman, and F. Anaya. 2016. New Mammal Faunal Data from Cerdas, Bolivia, a Middle-Latitude Neotropical Site that Chronicles the End of the Middle Miocene Climatic Optimum in South America. *Journal of Vertebrate Paleontology,* e1163574. doi: 10.1080/02724634.2016.1163574

Damuth, J. 1990. "Problems in Estimating Body Masses of Archaic Ungulates Using Dental Measurements". In *Body size in Mammalian Paleobiology. Estimation and Biological Implications,* ed. J. Damuth and B. J. MacFadden, pp.229-253. Cambridge: Cambridge University Press.

Díaz de Gamero, M. L. 1977a. Estratigrafía y micropaleontología del Oligoceno y Mioceno inferior del centro de la cuenca de Falcón, Venezuela. *GEOS*, 22:2-50.

Díaz de Gamero, M. L. 1977b. "Revisión de las unidades litoestratigráficas en Falcón central en base a su contenido de foraminíferos planctónicos" In *Memorias V Congreso Geológico de Venezuela*, Volume 1, pp. 81-86. Caracas.

Díaz de Gamero, M. L. 1985a. "Estratigrafía de Falcón Nororiental" In *Memorias VI Congreso Geológico de Venezuela*. Volume 1, pp. 454-502. Caracas.

Díaz de Gamero, M. L. 1985b. "Micropaleontología de la Formación Agua Salada, Falcón Nororiental" In *Memorias VI Congreso Geológico de Venezuela*. Volume 1, pp. 384-453. Caracas.

Díaz de Gamero, M. L. 1989. El Mioceno Temprano y Medio de Falcón septentrional. *GEOS*, 29:25-35.

Díaz de Gamero, M. L. 1996. The Changing Course of the Orinoco River during the Neogene: a review. *Palaeogeography, Palaeoclimatology, Palaeoecology*, 123:385-402.

Díaz de Gamero, M. L., and O. J. Linares. 1989. "Estratigrafía y paleontología de la Formación Urumaco, del Mioceno tardío de Falcón noroccidental" In *Memorias VII Congreso Geológico de Venezuela* Volume 1, pp. 419-439. Caracas.

Díaz de Gamero, M. L., V. Mitacchione, and M. Ruiz. 1988. La Formación Querales en su área tipo, Falcón noroccidental, Venezuela. *Boletín Sociedad Venezolana de Geología*, 34:34-46.

Eizirik, E. 2012. "A Molecular View on the Evolutionary History and Biogeography of Neotropical Carnivores (Mammalia, Carnivora)" In *Bones, Clones and Biomes. The History and Geography of Recent Neotropical Mammals,* ed. B. D. Patterson and L. P. Costa, pp.123-142.Chicago and London: University of Chicago Press.

Elissamburu, A. 2012. Estimación de la masa corporal en géneros del Orden Notoungulata. *Estudios Geológicos,* 68:91-111.

Fariña, R. A., S. F. Vizcaíno, and M. S. Bargo. 1998. Body Mass Estimations in Lujanian (Late Pleistocene-Early Holocene of South America) Mammal Megafauna. *Matozoología Neotropical,* 5:87-108.

Flynn, J. J., and C. C. Swisher. 1995. Cenozoic South American Land Mammal Ages: *Correlation to Global Geochronology. Geochronology Time Scales and Global Stratigraphic Correlation, SEPM Special Publication*, 54:317-333.

Forasiepi, A. M., L. H. Soibelzon, C. Suarez-Gomez, R. Sánchez, L. I. Quiroz, C. Jaramillo, and M. R. Sánchez-Villagra. 2014. Carnivorans at the Great American Biotic Interchange: new Discoveries from the Northern Neotropics. *Naturwissenschaften,* 101(11):965-974. doi:10.1007/s00114-014-1237-4

Forasiepi, A. M., E. Cerdeño, M. Bond, G. I. Schmidt, M. Naipauer, F. R. Straehl, A. G. Martinelli, A. C. Garrido, M. D. Schmitz, and J. L. Crowley. 2015. New toxodontid (Notoungulata) from the Early Miocene of Mendoza, Argentina.

Paläontologische Zeitschrift, 89(3):611-634. doi:10.1007/s12542-014-0233-5

Forasiepi, A.M., R. D. E. MacPhee, S. Hernández del Pino, G. I. Schmidt, E. Amson, and C. Grohe. 2016. Exceptional Skull of *Huaqueriana* (Mammalia, Litopterna, Macraucheniidae) from the Late Miocene of Argentina: Anatomy, Systematics, and Paleobiological Implications. *Bulletin of the American Museum of Natural History*, 404:1-76. doi: 10.5531/sd.sp.23

Geiger, M., Wilson, L.A.B., Costeur, L., Sánchez, R., Sánchez-Villagra, M.R. 2013. Diversity and Growth in Giant Caviomorphs from the Northern Neotropics - A Study of Femoral Variation in *Phoberomys* (Rodentia). *Journal Vertebrate Paleontology,* 33(6):1449-1456. doi:10.1080/02724634.2013.780952

Gelfo, J. N., F. J. Goin, M. O. Woodburne, and C. de Muizon. 2009. Biochronological Relationships of the Earliest South American Paleogene Mammalian Faunas. *Palaeontology,* 52(1):251-269. doi:10.1111/j.1475-4983.2008.00835.x

Gervais, H. 1847. Observations sur les mammifères fossiles du midi de la France. *Annales de Sciences Naturelles, Zoologie,* 3:203-224.

Giannini, N., and D. García-López. 2014. Ecomorphology of Mammalian Fossil Lineages: Identifying Morphotypes in a Case Study of Endemic South American Ungulates. *Journal of Mammalian Evolution,* 21(2):195-212. doi:10.1007/s10914-013-9233-6

Goillot, C., P.-O. Antoine, J. Tejada, F. Pujos, and R. Salas-Gismondi. 2011. Middle Miocene Uruguaytheriinae (Mammalia, Astrapotheria) from Peruvian Amazonia and a Review of the Astrapotheriid Fossil Record in Northern South America. *Geodiversitas,* 33(2):331-345. doi:10.5252/g2011n2a8

Goloboff, P. A. 2014. Extended Implied Weighting. *Cladistics,* 30(3):260-272. doi:10.1111/cla.12047

Goloboff, P. A., J. M. Carpenter, J. S. Arias, and D. R. M. Esquivel. 2008. Weighting Against Homoplasy Improves Phylogenetic Analysis of

Morphological Datasets. *Cladistics,* 24:758-773. doi:10.1111/j.1096-0031.2008.00209.x

Gomes-Rodrigues, H., A. Herrel, and G. Billet. 2017. Ontogenetic and Life History Trait Changes Associated with Convergent Ecological Specializations in Extinct Ungulate Mammals. *Proceedings of the National Academy of Sciences,*114(5):1069-1074. doi:10.1073/pnas.1614029114

Gonzalez de Juana, C., J. M. Iturralde de Arozena, and X. Picard Cadillat. 1980. *Geologia de Venezuela y sus cuencas petroliferas*. Caracas: FONINVES

Grand, A., A. Corvez, L. M. Duque-Velez, and M. Laurin. 2013. Phylogenetic Inference Using Discrete Characters: Performance of Ordered and Unordered Parsimony and of Three-Item Statements. *Biological Journal of the Linnean Society,* 110(4):914-930. doi:10.1111/bij.12159

Gradstein, F. M., J. G. Ogg, M. D. Schmitz, and G. M. Ogg. 2012. *The Geological Time Scale 2012 Volume 2*. Amsterdam: Elsevier.

Gray, J. E. 1821. On the natural arrangement of vertebrate animals. *London Medical Repository,* 15:296-310.

Guérin, C., and M. Faure. 2013. Un nouveau Toxodontidae (Mammalia, Notoungulata) du Pléistocène supérieur du Nordeste du Brésil. *Geodiversitas,* 35(1):155-205. doi:10.5252/g2013n1a7

Guerra, A., and S. Mederos. 1988. Estudio sedimentológico y bioestratigráfico de una zona ubicada entre las poblaciones de Urumaco y Sabaneta, estado Falcón. Undergraduate diss., Universidad Central de Venezuela. Venezuela.

Hambalek, N. 1993. Palinoestratigrafia del Mioceno-Plioceno de la región de Urumaco, Falcón Noroccidental. Undergraduate diss., Universidad Central de Venezuela.

Harrison, J. a. 1985. Giant Camels from the Cenozoic of North America. *Smithsonian Contributions to Paleobiology,* 57:1-29.

Hendy, A. J. W., D. S. Jones, F. Moreno, V. Zapata, and C. Jaramillo. 2015. Neogene Molluscs, Shallow

Marine Paleoenvironments, and Chronostratigraphy of the Guajira Peninsula, Colombia. *Swiss Journal of Palaeontology,* 134(1):45-75. doi:10.1007/s13358-015-0074-1

Herrera, C. 2008. Estratigrafía de la Formación Urumaco y geología estructural entre el Domo de Agua Blanca y Hato Viejo (Edo. Falcón). Msc. Diss., Universidad Simón Bolivar. Venezuela.

Hoffstetter, R., and M. F. Soria. 1986. *Neodolodus colombianus* gen. et sp. nov., un nouveau Condylarthre (Mammalia) dans le Miocène de Colombie. *Comptes Rendus de l'Académie Des Sciences. Paris II,* 303(17):1619-1622.

Hopwood, A. T. 1928. *Gyrinodon quassus*, A new Genus and Species of Toxodont from Western Buchivacoa (Venezuela). *Quarterly Journal of the Geological Society of London,* 84:573-583.

Horovitz, I. 2004. Eutherian Mammal Systematics and the Origins of South American Ungulates as Based on Postcranial Osteology. *Bulletin of Carnegie Museum of Natural History,* 36:63-79. doi:10.2992/0145-9058(2004)36[63:EMSATO]2.0.CO;2

Horovitz, I., M. R. Sánchez-Villagra, T. Martin, and O. a. Aguilera. 2006. The Fossil Record of *Phoberomys pattersoni* Mones 1980 (Mammalia, Rodentia) from Urumaco (Late Miocene, Venezuela), with an Analysis of its Phylogenetic Relationships. *Journal of Systematic Palaeontology,* 4(3):293-306. doi:10.1017/S1477201906001908

Horovitz, I., M. R. Sánchez-Villagra, M. G. Vucetich, O. A. Aguilera, and J. O. Farlow. 2010. "Fossil Rodents from the Late Miocene Urumaco and Middle Miocene Cumaca Formations, Venezuela". In *Urumaco and Venezuelan Paleontology. The Fossil Record of the Northern Neotropics,* ed. M. R. Sánchez-Villagra, O. A. Aguilera, and A. A. Carlini. pp.214-232. Bloomington: Indiana University Press.

Houssaye, A., V. Fernandez, and G. Billet. 2016. Hyperspecialization in Some South American Endemic Ungulates Revealed by Long Bone Microstructure. J*ournal of Mammalian*

Evolution, 23(3):221-235. doi:10.1007/s10914-015-9312-y

Janis, C. M. 1990. "Correlation of Cranial and Dental Variables with Body Size in Ungulates and Macropodoids". In *Body Size in Mammalian Palaeobiology: Estimation and Biological Implications,* ed. J. Damuth and B. J. MacFadden, pp. 255-299. Cambridge: Cambridge University Press.

Janis, C. M. 2000. "Patterns in the Evolution of Herbivory in Large Terrestrial Mammals: the Paleogene of North America". In *Evolution of Herbivory in Terrestrial Vertebrates. Perspectives from the Fossil Record*, ed. H-D. Sues, pp. 168-222. Cambridge: Cambridge University Press.

Jaramillo, C., F. Moreno, A. J. W. Hendy, M. R. Sánchez-Villagra, and D. Marty. 2015. Preface: La Guajira, Colombia: a New Window into the Cenozoic Neotropical Biodiversity and the Great American Biotic Interchange. *Swiss Journal of Palaeontology*, 134(1):1-4. doi: 10.1007/s13358-015-0075-0

Johnson, S. C. 1984. Astrapotheres from the Miocene of Colombia, South America. Ph.D. diss., University of California, Berkeley, California.

Johnson, S. C., and R. H. Madden. 1997. "Uruguaytheriine Astrapotheres of Tropical South America". In *Vertebrate Paleontology in the Neotropics. The Miocene Fauna of La Venta,* ed. R. F. Kay, R. H. Madden, R. L. Cifelli, and J. J. Flynn. pp.355-381. Washington and London: Smithsonian Institution Press.

Kay, R. F., S. F. Vizcaíno, and M. S. Bargo. 2012. "A Review of the Paleoenvironment and Paleoecology of the Miocene Santa Cruz Formation". In *Early Miocene Paleobiology in Patagonia: High Latitude Paleocommunities of the Santa Cruz Formation,* ed. S. F. Vizcaíno, R. F. Kay, and S. Bargo. pp.331-365. Cambridge: Cambridge University Press.

Koepfli, K. P., M. E. Gompper, E. Eizirik, C. C. Ho, L. Linden, J. E. Maldonado, and R. K. Wayne. 2007. Phylogeny of the Procyonidae (Mammalia: Carnivora): Molecules, morphology and the Great American Interchange. *Molecular Phylogenetics and Evolution,*

43:1076-1095. doi:10.1016/j.ympev.2006.10.003

Kraglievich, L. 1928. *Sobre el supuesto Astrapotherium christi Stehlin descubierto en Venezuela (Xenastrapotherium n. gen) y sus relaciones con Astrapotherium magnum y Uruguaytherium beaulieui.* Buenos Aires: La Editorial Franco

Kramarz, A. G., and M. Bond. 2005. Los Litopterna (Mammalia) de la Formación Pinturas, Mioceno temprano-medio de Patagonia. *Ameghiniana,* 42:611-625.

Kramarz, A. G., and M. Bond. 2008. Revision of *Parastrapotherium* (Mammalia, Astrapotheria) and Other Deseadan Astrapotheres of Patagonia. *Ameghiniana,* 45:537-551.

Kramarz, A. G., and M. Bond. 2009. A new Oligocene Astrapothere (Mammalia, Meridiungulata) from Patagonia and a new Appraisal of Astrapothere Phylogeny. *Journal of Systematic Palaeontology,* 7(1):117-128. doi:10.1017/S147720190800268X

Kramarz, A. G., and M. Bond. 2010. "Colhuehuapian Astrapotheriidae (Mammalia) from Gran Barranca south of Lake Colhue-Huapi". In *The Paleontology of Gran Barranca. Evolution and Environmental Change through the middle Cenozoic of Patagonia,* ed. R. H. Madden, A. A. Carlini, M. G. Vucetich, R. F. Kay, pp.182-192. Cambridge: Cambridge University Press.

Kramarz, A. G., M. G. Vucetich, A. A. Carlini, M. R. Ciancio, M. A. Abello, C. M. Deschamps, and J. N. Gelfo. 2010. "A new Mammal Fauna at the Top of the Gran Barranca Sequence and its Biochronological Significance". In *The Paleontology of Gran Barranca. Evolution and Environmental Change through the middle Cenozoic of Patagonia,* ed. R. H. Madden, A. A. Carlini, M. G. Vucetich, R. F. Kay, pp.264-277. Cambridge: Cambridge University Press.

Kramarz, A., and M. Bond. 2011. A new Early Miocene Astrapotheriid (Mammalia, Astrapotheria) from Northern Patagonia, Argentina. *Neues Jahrbuch für Geologie und Paläontologie – Abhandlungen,* 260(3):277-287. doi:10.1127/0077-

7749/2011/0132

Kramarz, A. G., M. Bond, and A. M. Forasiepi. 2011. New Remains of *Astraponotus* (Mammalia, Astrapotheria) and Considerations on Astrapothere Cranial Evolution. *Paläontologische Zeitschrift,* 85:185-200. doi:10.1007/s12542-010-0087-4

Kramarz, A., and M. Bond. 2013. On the Status of *Isolophodon* Roth, 1903 (Mammalia, Astrapotheria) and Other Little-Known Paleogene Astrapotheres from Central Patagonia. *Geobios,* 46(3):203-211. doi:10.1016/j.geobios.2012.10.015

Kramarz, A., and M. Bond. 2014. Critical Revision of the Alleged Delayed Dental Eruption in South American "Ungulates." *Mammalian Biology,* 79(3):170-175. doi:dx.doi.org/10.1016/j.mambio.2013.11.001

Laurito, C. A. 1993. Análisis topológico y sistemático del toxodonte de bajo de los Barrantes, Provincia de Alajuela, Costa Rica. *Revista Geológica de America Central,* 16:61-68.

Leigh, E. G., A. O'Dea, and G. J. Vermeij. 2014. Historical Biogeography of the Isthmus of Panama. *Biological Reviews,* 89(1):148-172. doi:10.1111/brv.12048

Leite, R. N., S. O. Kolokotronis, F. C. Almeida, F. P. Werneck, D. S. Rogers, and M. Weksler. 2014. In the Wake of Invasion: Tracing the Historical Biogeography of the South American Cricetid Radiation (Rodentia, Sigmodontinae). *PLoS ONE,* 9(6):e100687. doi:10.1371/journal.pone.0100687

Linares, O. J. 2004. Bioestratigrafía de la fauna de mamíferos de las Formaciones Socorro, Urumaco y Codore (Mioceno Medio-Plioceno Temprano) de la región de Urumaco, Falcón, Venezuela. *Paleobiología Neotropical,* 1:1-26.

Loomis, F. B. 1914. *The Deseado Formation of Patagonia: Eighth Amherst Expedition.* Concord, N. H: Rumford Press.

Lucas, S. G. 2008. Pleistocene Mammals from Yeroconte, Honduras. *New Mexico Museum of Natural History and Science Bulletin,* 44:403-408.

Lucas, S. G. 2014. Late Pleistocene mammals from El Hatillo, Panama. *Revista Geológica de América Central,* 50:139-151.

Lucas, S. G., G. E. Alvarado, and E. Vega. 1997. The Pleistocene Mammals of Costa Rica. *Journal of Vertebrate Paleontology,* 17:413-427.

Lundelius, E. L., V. M. Bryant, R. Mandel, K. J. Thies, and A. Thoms. 2013. The First Occurrence of a Toxodont (Mammalia, Notoungulata) in the United States. *Journal of Vertebrate Paleontology,* 33:1:229-232. doi:10.1080/02724634.2012.711405

Lunt, D., G. L. Foster, A. M. Haywood, and E. J. Stone. 2008. Late Pliocene Greenland Glaciation Controlled by a Decline in Atmospheric CO_2 Levels. Nature, 454(7208):1102-1105. doi:10.1038/nature07223

Lydekker, R. 1884. Contribution to the Knowledge of the Fossil Vertebrates of Argentina: A Study of Extinct Argentine Ungulates. *Anales Del Museo de La Plata,* 2:1-32.

MacFadden, B. J. 2005. Diet and Habitat of Toxodont Megaherbivores (Mammalia, Notoungulata) from the Late Quaternary of South and Central America. *Quaternary Research,* 64:113-124. doi:dx.doi.org/10.1016/j.yqres.2005.05.003

Madden, R. H. 1990. Miocene Toxodontidae (Notoungulata, Mammalia) from Colombia, Ecuador and Chile. Ph.D. diss., Duke University, North Carolina.

Madden, R. H. 1997. "A new Toxodontid Notoungulate". In *Vertebrate Paleontology in the Neotropics. The Miocene Fauna of La Venta,* ed. R. F. Kay, R. H. Madden, R. L. Cifelli, and J. J. Flynn. pp.335-354. Washington and London: Smithsonian Institution Press.

Madden, R. H., J. Guerrero, R. F. Kay, J. J. Flynn, C. C. Swisher III, and A. Watson. 1997. "The Laventan Stage and Age". In *Vertebrate Paleontology in the Neotropics. The Miocene Fauna of La Venta,* ed. R. F. Kay, R. H. Madden, R. L. Cifelli, and J. J. Flynn. pp.499-519. Washington and London: Smithsonian Institution Press.

Madden, R. H. 2015. "Hypsodonty in the South American Fossil Record". In

Hypsodonty in Mammals: Evolution, Geomorphology and the Role of Earth Surface Processes. pp.12-59. Cambridge: Cambridge University Press.

Marshall, L. G., P. Salinas, and M. Suarez. 1990. *Astrapotherium* sp. (Mammalia, Astrapotheriidae) from Miocene Strata Along the Quepuca River, Central Chile. *Revista Geologica de Chile* 17:215-223.

Marshall, L. G., S. D. Webb, J. J. Sepkoski Jr., and D. M. Raup. 1982. Mammalian Evolution and the Great American Interchange. *Science,* 215:1351-1357. doi:10.1126/science.215.4538.1351

McKenna, M. C. 1956. Survival of Primitive Notoungulates and Condylarths into the Miocene of Colombia. *American Journal of Science,* 254:736-743.

McKenna, M. C. 1975. "Towards a Phylogenetic Classification of the Mammalia". In *Phylogeny of Primates. A multidisciplinary Approach,* ed. W. P. Luckett and F. S. Szalay, pp.21-46. New York and London: Plenum Press.

McKenna, M. C., and S. K. Bell. 1997. *Classification of Mammals above the Species Level*. New York: Columbia University Press.

Mendoza, M., C. M. Janis, and P. Palmqvist. 2006. Estimating the Body Mass of Extinct Ungulates: A Study on the Use of Multiple Regression. *Journal of Zoology,* 270:90-101. doi:10.1111/j.1469-7998.2006.00094.x

Mones, A. 1982. An Equivocal Nomenclature: What Means Hypsodonty? *Paläontologische Zeitschrift*, 56(1-2):107-111. doi: 10.1007/BF02988789

Moreno-Bernal, J. W., J. Head, and C. A. Jaramillo. 2016. Fossil crocodilians from the High Guajira Peninsula of Colombia: Neogene faunal change in northernmost South America. *Journal of Vertebrate Paleontology,* 36(3):e1110586. doi:10.1080/02724634.2016.1110586

Moreno, F., A. J. W. Hendy, L. Quiroz, N. Hoyos, D. S. Jones, V. Zapata, S. Zapata, G. A. Ballen, E. Cadena, A. L. Cárdenas, J. D. Carrillo-Briceño, J. D. Carrillo, D. Delgado-Sierra, J. Escobar, J. I. Martínez, C. Martínez, C. Montes, J. Moreno, N. Pérez, R. Sánchez, C. Suárez, M. C. Vallejo-Pareja, and C.

Jaramillo. 2015. Revised Stratigraphy of Neogene Strata in the Cocinetas Basin, La Guajira, Colombia. *Swiss Journal of Palaeontology,* 134(1):5-43. doi:10.1007/s13358-015-0071-4

Muizon, C. de, and R. L. Cifelli. 2000. The "Condylarths" (Archaic Ungulata, Mammalia) from the Early Palaeocene of Tiupampa (Bolivia): Implications on the Origin of the South American ungulates. *Geodiversitas* 22(1):47-150.

Nasif, N. L., S. Musalem, and E. Cerdeño. 2000. A New Toxodont from the Late Miocene of Catamarca, Argentina, and a Phylogenetic Analysis of the Toxodontidae. *Journal of Vertebrate Paleontology,* 20(3):591-600. doi:10.1671/0272-4634(2000)020[0591:ANTFTL]2.0.CO;2

O'Dea, A., H. A. Lessios, A. G. Coates, R. I. Eytan, S. A. Restrepo-Moreno, A. L. Cione, L. S. Collins, A. de Queiroz, D. W. Farris, R. D. Norris, R. F. Stallard, M. O. Woodburne, O. Aguilera, M.-P. Aubry, W. A. Berggren, A. F. Budd, M. A. Cozzuol, S. E. Coppard, H. Duque-Caro, S. Finnegan, G. M. Gasparini, E. L. Grossman, K. G. Johnson, L. D. Keigwin, N. Knowlton, E. G. Leigh, J. S. Leonard-Pingel, P. B. Marko, N. D. Pyenson, P. G. Rachello-Dolmen, E. Soibelzon, L. Soibelzon, J. A. Todd, G. J. Vermeij, and J. B. C. Jackson. 2016. Formation of the Isthmus of Panama. *Science Advances,* 2(8):e1600883. doi:10.1126/sciadv.160088

O'Leary, M. A., J. I. Bloch, J. J. Flynn, T. J. Gaudin, A. Giallombardo, N. P. Giannini, S. L. Goldberg, B. P. Kraatz, Z. Luo, J. Meng, X. Ni, M. J. Novacek, F. A. Perini, Z. S. Randall, G. W. Rougier, E. J. Sargis, M. T. Silcox, N. B. Simmons, M. Spaulding, P. M. Velazco, M. Weksler, J. R. Wible, and A. L. Cirranello. 2013. The Placental Mammal Ancestor and the Post-K-Pg Radiation of Placentals. *Science,* 339(6120):662-667. doi:10.1126/science.1229237

Owen, P. 1853. Description of Some Species of the Extinct Genus *Nesodon*, with Remarks on the Primary Group (Toxodontia) of Hoofed Quadrupeds, to Which that Genus is Referable. *Philosophical Transactions of the Royal Society of London,* 143:291-310.

Owen, R. 1840. "Fossil Mammalia". In *The*

Zoology of the H.M.S. Beagle, under the Command of Captain Fitzroy, R.N., during the years 1832-1836, ed. C. Darwin. London: Smith Elder and Co.

Owen, R. 1848. Description of Teeth and Portions of Two Extinct Anthracothroid quadrupeds (*Hyopotamus vectianus* and *H. bovinus*) Discovered by Marchioness of Hastings in the Eocene Deposits of the N.W. Coast of the Isle of Wight, with an Attempt to Develop Cuvier's idea. *Quarterly Journal of the Geological Society of London,* 4:104-141.

Pabón-Caicedo, J. D., J. A. Eslava-Ramirez, R. E. Gómez-Torres. 2001. Generalidades de la distribución espacial y temporal de la temperatura del aire y de la precipitación en Colombia. *Metereología Colombiana*, 4:47-59.

Pagani, M., Z. Liu, J. LaRiviere, and A. C. Ravelo. 2010. High Earth-System Climate Sensitivity Determined from Pliocene Carbon Dioxide Concentrations. *Nature Geoscience*, 3(1):27-30. doi:10.1038/ngeo724

Paula Couto, C. 1979. *Tratado de Paleonastozoologia*. Rio de Janeiro: Academia Brasileira de Ciencias.

Pérez, L. M., J. P. Pérez-Panera, O. A. Aguilera, D. I. Ronchi, R. Sánchez, M. O. Manceñido, and M. R. Sánchez-Villagra. 2016. Palaeontology, Sedimentology, and Biostratigraphy of a Fossiliferous Outcrop of the Early Miocene Querales Formation, Falcón Basin, Venezuela. *Swiss Journal of Palaeontology*, 135:187-203. doi: 10.1007/s13358-015-0105-y

Pérez, M. E., and Vucetich, M.G. 2012. A Revision of the Fossil Genus *Phanomys* Ameghino, 1887 (Rodentia, Hystricognathi, Cavioidea) from the Early Miocene of Patagonia (Argentina) and the Acquisition of Euhypsodonty in Cavioidea sensu stricto. *Paläontologische Zeitschrift*, 86(2):187-204. doi:10.1007/s10914-011-9154-1

Pérez, M. E., M. C. Vallejo-Pareja, J. D. Carrillo, and C. A. Jaramillo. 2017. A new Pliocene Capybara (Rodentia, Caviidae) from Northern South America (Guajira, Colombia), and its Implications for the Great American Biotic Interchange. *Journal of*

*Mammalian Evolution,*24(1):111-125. doi:10.1007/s10914-016-9356-7

Quiroz, L. I., and C. A. Jaramillo. 2010. "Stratigraphy and Sedimentary Environments of Miocene Shallow to Marginal Marine Deposits in the Urumaco Trough, Falcón basin, Western Venezuela". In *Urumaco and Venezuelan Paleontology. The fossil record of the Northern Neotropics,* ed. M. R. Sánchez-Villagra, O. A. Aguilera, and A. A. Carlini, pp.153-172. Bloomington and Indianapolis: Indiana University Press.

Ré, G. H., S. E. Geuna, and J. F. Vilas. 2010. "Paleomagnetism and Magnetostratigraphy of Sarmiento Formation (Eocene-Miocene) at Gran Barranca, Chubut, Argentina" In *The Paleontology of Gran Barranca. Evolution and Environmental Change through the middle Cenozoic of Patagonia.* ed. R. H. Madden, A. A. Carlini, M. G. Vucetich, and R. F. Kay, pp.32-58. Cambridge: Cambridge University Press.

Renz, H. H. 1948. *Stratigraphy and Fauna of the Agua Salada Group, State of Falcón, Venezuela*. Boulder, Colorado: Geologic Society of America Memoir.

Rey, O. 1990. Análisis comparativo y correlación de las formaciones Codore y La Vela, estado Falcón. M. Sc., diss. Universidad Central de Venezuela. Venezuela.

Ribeiro, A. M., G. López, and M. Bond. 2010. "The Leontiniidae (Mammalia, Notoungulata) from the Sarmiento Formation at Gran Barranca, Chubut Province, Argentina" In *The Paleontology of Gran Barranca. Evolution and Environmental Change through the middle Cenozoic of Patagonia.* ed. R. H. Madden, A. A. Carlini, M. G. Vucetich, and R. F. Kay, pp.170-181. Cambridge: Cambridge University Press.

Riggs, E. S. 1935. A skeleton of *Astrapotherium*. *Geological Series of Field Museum of Natural History,* 6:167-177.

Rincón, A. D. 2011. New Remains of *Mixotoxodon larensis* Van Frank 1957 (Mammalia: Notoungulata) from Mene de Inciarte tar pit, North-Western Venezuela. *Interciencia,* 36:894-899.

Rincón, A. D., H. G. McDonald, A. Solórzano, M. N. Flores, and D. Ruiz-Ramoni. 2015. A new Enigmatic Late Miocene Mylodontoid Sloth from Northern South America. *Royal Society Open Science,* 2:140256. doi:10.1098/rsos.140256

Rincón, A. F., J. I. Bloch, C. Suarez, B. J. MacFadden, and C. A. Jaramillo. 2012. New Floridatragulines (Mammalia, Camelidae) from the Early Miocene Las Cascadas Formation, Panama. *Journal of Vertebrate Paleontology,* 32:456-475. doi:10.1080/02724634.2012.635736

Roth, S. 1903. Los ungulados sudamericanos. *Anales Del Museo de La Plata,* 5:1-36.

Saint-André, P.-A. 1993. *Hoffstetterius imperator* n.g., n.sp. du Miocène supérieur de l'Altiplano bolivien et le statut des Dinotoxodontinés (Mammalia, Notoungulata). *Comptes Rendus de l'Académie Des Sciences*. *Série 2, Mécanique, Physique, Chimie, Sciences de L'univers, Sciences de La Terre,* 316:539-545.

Sánchez-Villagra, M. R. 2006. Vertebrate Fossils from the Neogene of Falcón State, Venezuela: Contributions on Neotropical Palaeontology. *Journal of Systematic Palaeontology*,4(3):211. doi:10.1017/S1477201906001842

Sánchez-Villagra, M. R. 2010. "A Short History of the Study of Venezuelan Vertebrate Fossils. In *Urumaco and Venezuelan Paleontology. The fossil record of the Northern Neotropics,* ed. M. R. Sánchez-Villagra, O. A. Aguilera, and A. A. Carlini, pp.9-18. Bloomington and Indianapolis: Indiana University Press.

Sánchez-Villagra, M. R., and O. A. Aguilera. 2006. Neogene Vertebrates from Urumaco, Falcón State, Venezuela: Diversity and Significance. *Journal of Systematic Palaeontology,* 4(3):213-220. doi:10.1017/S1477201906001829

Sánchez-Villagra, M. R., O. A. Aguilera, and I. Horovitz. 2003. The Anatomy of the World's Largest Extinct Rodent. *Science,* 301(5640):1708-1710. doi:10.1126/science.1089332

Sánchez-Villagra, M. R., R. J. Asher, A. D. Rincón, A. A. Carlini, P. Meylan, and R. W. Purdy. 2004. New Faunal Reports from the Cerro La Cruz

Locality (Lower Miocene), North-Western Venezuela. *Special Papers in Palaeontology,* 71:105-112.

Sánchez-Villagra, M. R., O. A. Aguilera, R. Sánchez, and A. A. Carlini. 2010. "The Fossil Vertebrate Record of Venezuela of the Last 65 Million Years". In *Urumaco and Venezuelan Paleontology. The fossil record of the Northern Neotropics,* ed. M. R. Sánchez-Villagra, O. A. Aguilera, and A. A. Carlini, pp.19-51. Bloomington and Indianapolis: Indiana University Press.

Scherer, C., J. Ferigolo, A. M. Ribeiro, and C. Cartelle. 2007. Contribution to the Knowledge of *Hemiauchenia paradoxa* (Artiodactyla, Camelidae) from the Pleistocene of Southern Brazil. *Revista Brasileira de Paleontologia,* 10:35-52.

Scherer, C., V. Pitana, and A. M. Ribeiro. 2009. Proterotheriidae and Macraucheniidae (Litopterna, Mammalia) from the Pleistocene of Rio Grande do Sul State, Brazil. *Revista Brasileira de Paleontologia,* 12:231-246.

Scherer, C. S. 2013. The Camelidae (Mammalia, Artiodactyla) from the Quaternary of South America: Cladistic and Biogeographic Hypotheses. *Journal of Mammalian Evolution,* 20(1):45-56. doi:10.1007/s10914-012-9203-4

Schmidt, G. I. 2011. Los Proterotheriidae (Litopterna) de Entre Ríos (Argentina): consideraciones nomenclaturales e implicancias sistemáticas. *Ameghiniana,* 48(3):605-620. doi:10.5710/AMGH.v48i2(291)

Schmidt, G. I. 2013. Litopterna y Notoungulata (Mammalia) de la Formación Ituzaingó (Mioceno tardío-Plioceno) de la Provincia de Entre Ríos: sistemática, bioestratigrafía y paleobiogeografía. Tomo I. Ph.D. diss., Universidad Nacional de La Plata. Argentina

Schmidt, G. I. 2015. Actualización sistemática y filogenia de los Proterotheriidae (Mammalia, Litopterna) del "Mesopotamiense" (Mioceno tardío) de Entre Ríos, Argentina. *Revista Brasileira de Paleontologia,* 18:521-546.

Schneider, T., T. Bischoff, and G. H. Haug.

2014. Migrations and Dynamics of the Intertropical Convergence Zone. *Nature*, 513(7516):45-53. doi: 10.1038/nature13636

Scott, K. M. 1990. "Postcranial Dimensions of Ungulates as Predictors of Body Mass". In *Body Size in Mammalian Paleobiology. Estimation and Biological Implications,* ed. J. Damuth and B. J. MacFadden, pp.301-335. Cambridge: Cambridge University Press.

Scott, W. B. 1912. "Mammalia of the Santa Cruz Beds. Paleontology III. Part II. Toxodonta". In *Reports of the Princeton University Expeditions to Patagonia, 1896–1899,* ed. W. B. Scott, pp.111-300. Princeton and Stuttgart: Princeton University, E. Schweizerbart'sche Verlagshandlung (E. Nägele), Stuttgart.

Scott, W. B. 1928. "Mammalia of the Santa Cruz beds. Paleontology III. Part IV Astrapotheria". In *Reports of the Princeton University Expeditions to Patagonia (1896-1899),* ed. W. B. Scott. pp. 301-351. Princeton and Stuttgart: Princeton University, E. Schweizerbart'sche Verlagshandlung (E. Nägele), Stuttgart.

Scott, W. B. 1937. The Astrapotheria. *Proceedings of the American Philosophical Society,* 77:309-393.

Shockey, B. J., J. J. Flynn, D. A. Croft, P. Gans, and A. R. Wyss. 2012. New Leontiniid Notoungulata (Mammalia) from Chile and Argentina: Comparative Anatomy, Character Analysis, and Phylogenetic Hypotheses. *American Museum Novitates,* 3737:1-64.

Simpson, G. G. 1980. *Splendid Isolation. The Curious History of South American Mammals*. New Haven and London: Yale University Press.

Smith, J. B., and P. Dodson. 2003. A proposal for a standard terminology of anatomical notation and orientation in fossil vertebrate dentitions. *Journal of Vertebrate Paleontology,* 23:1-12. doi:10.1671/0272-4634(2003)23[1:APFAST]2.0.CO;2

Soria, M. F. 1987. Estudios sobre los Astrapotheria (Mammalia) del Paleoceno y Eoceno. *Ameghiniana,* 24:21-34.

Soria, M. F. 2001. Los Proterotheriidae

(Litopterna, Mammalia), sistemática, origen y filogenia. *Monografías Del Museo Argentino de Ciencias Naturales,* 1:1-167.

Soria, M. F., and J. E. Powell. 1981. Un primitivo Astrapotheria (Mammalia) y la edad de la Formación Río Loro, Provincia de Tucumán, República Argentina. *Ameghiniana,* 18:155-168.

Stange, M. M. R. Sánchez-Villagra, W. Salzburger, and M. Matschiner. 2017. Bayesian Divergence-Time Estimation with Genome-Wide SNP Data of Sea Catfishes (Ariidae= Supports Miocene Closure of the Panamanian Isthmus. *BioRxiv*. doi: doi.org/10.1101/102129ß

Stehlin, H. G. 1928. Ein *Astrapotherium* fund aus Venezuela. *Eclogae Geologicae Helvetiae,* 21:227-232.

Suarez, C., A. M. Forasiepi, F. J. Goin, and C. Jaramillo. 2016. Insights into the Neotropics Prior to the Great American Biotic Interchange: new Evidence of Mammalian Predators from the Miocene of Northern Colombia. *Journal of Vertebrate Paleontology,* 36(1):e1029581. doi:10 .1080/02724634.2015.1029581

Swofford, D. L. 2002. *Phylogenetic Analysis Using Parsimony (*and Other Methods). Version 4*. Sunderland: Sinauer Associates.

Tomassini, R. L., C. I. Montalvo, C. M. Deschamps, and T. Manera. 2013. Biostratigraphy and Biochronology of the Monte Hermoso Formation (early Pliocene) at its Type Locality, Buenos Aires Province, Argentina. *Journal of South American Earth Sciences,* 48:31-42. doi:dx.doi.org/10.1016/j. jsames.2013.08.002

Tonni, E. P. 2009. "Los mamíferos del Cuaternario de la región Pampeana de Buenos Aires, Argentina". In *Quaternário do Rio Grande do Soul: integrando conhecimentos.* ed. A. M. Ribeiro, S. G. Bauermann, and C. S. Scherer, pp.193-205. Porto Alegre: Monografias da Sociedade Brasilera de Paleontologia.

Townsend, K. E. B., and D. A. Croft. 2008. Diets of Notoungulates from the Santa Cruz Formation, Argentina: new Evidence from Enamel Microwear. *Journal of Vertebrate Paleontology,* 28:217-230. doi:10.1671/0272-4634(2008)28

Tsubamoto, T. 2014. Estimating Body Mass from the Astragalus in Mammals. *Acta Palaeontologica Polonica,* 59:259-265. doi:10.4202/app.2011.0067

Ubilla, M., D. Perea, and M. Bond. 1994. The Deseadan Land Mammal Age in Uruguay and the Report of *Scarrittia robusta* nov. sp. (Leontiniidae, Notoungulata) in the Fray Bentos Formation (Oligocene-?Lower Miocene). *Geobios,* 27:95-102. doi:10.1016/S0016-6995(06)80217-2

Ubilla, M., D. Perea, M. Bond, and A. Rinderknecht. 2011. The First Cranial Remains of the Pleistocene Proterotheriid *Neolicaphrium* Frenguelli, 1921 (Mammalia, Litopterna): A Comparative Approach. *Journal of Vertebrate Paleontology,* 31:193-201. doi:10.1080/02724634.2011.539647

Vallejo-Pareja, M. C., J. D. Carrillo, J. W. Moreno-Bernal, M. Pardo-Jaramillo, D. F. Rodriguez-Gonzalez, and J. Muñoz-Durán. 2015. *Hilarcotherium castanedaii*, gen. et sp. nov., a new Miocene Astrapothere (Mammalia, Astrapotheriidae) from the Upper Magdalena Valley, Colombia. *Journal of Vertebrate Paleontology,* 35:e903960. doi:10.1080/02724634.2014.903960

Van Frank, R. 1957. A Fossil Collection from Northern Venezuela 1. Toxodontidae (Mammalia, Notoungulata). *American Museum Novitates,* 1-38.

Villafañe, A. L., E. Ortiz-Jaureguizar, and M. Bond. 2006. Cambios en la riqueza taxonómica y en las tasas de primera y última aparición de los Proterotheriidae (Mammalia, Litopterna) durante el Cenozoico. *Estudios Geológicos,* 62:155-166.

Villafañe, A. L., G. I. Schmidt, and E. Cerdeño. 2012. Consideraciones sistemáticas y bioestratigráficas acerca de *Thoatheriopsis mendocensis* Soria, 2001 (Litopterna, Proterotheriidae). *Ameghiniana,* 49:365–374.

Villaroel, C., and J. Guerrero. 1985. Un nuevo y singular representante de la familia Leontiniidae? (Notoungulata, Mammalia) en el Mioceno de La Venta, Colombia. *Geologia Norandina,* 9:35-40.

Villaroel, C., and J. Colwell Danis. 1997. "A new Leontiniid Notoungulate". In *Vertebrate Paleontology in the Neotropics. The Miocene Fauna of La Venta,* ed. R. F. Kay, R. H. Madden, R. L. Cifelli, and J. J. Flynn, pp.303-318. Washington and London: Smithsonian Institution Press.

Vizcaíno, S. F., G. H. Cassini, N. Toledo, and M. S. Bargo. 2012. "On the Evolution of Large Size in Mammalian Herbivores of Cenozoic Faunas of Southern South America". In *Bones, Clones and Biomes. The History and Geography of Recent Neotropical Mammals.* ed. B. D. Patterson and L. P. Costa, pp.76-101. Chicago and London: The University of Chicago Press.

Vucetich, M. G., A. A. Carlini, O. Aguilera, and M. R. Sánchez-Villagra. 2010. The Tropics as Reservoir of Otherwise Extinct Mammals: The Case of Rodents from a New Pliocene Faunal Assemblage from Northern Venezuela. *Journal of Mammalian Evolution,* 17:265-273. doi:10.1007/s10914-010-9142-x

Webb, S. D. 1985. "Late Cenozoic mammal dispersal between the Americas". In *The Great American Biotic Interchange,* ed. F. G. Stehli and S. D. Webb, pp.357-386. New York and London. Plenum Press.

Webb, S. D. 1991. Ecogeography and the Great American Interchange. *Paleobiology,* 17:266-280.

Webb, S. D. 2006. The Great American Biotic Interchange: Patterns and Processes. *Annals of the Missouri Botanical Garden,* 93:245-257. doi:10.3417/0026-6493(2006)93

Webb, S. D., and S. C. Perrigo. 1984. Late Cenozoic Vertebrates from Honduras and El Salvador. *Journal of Vertebrate Paleontology,* 4:237-254.

Webb, S. D., and J. Meachen. 2004. On the Origin of Lamine Camelidae Including a New Genus from the Late Miocene of the High Plains. *Bulletin of Carnegie Museum of Natural History,* 36:349-362. doi:10.2992/0145-9058(2004)36[349:OTOOLC]2.0.CO;2

Weir, J. T., E. Bermingham, and D. Schluter. 2009. The Great American Biotic Interchange in Birds. *Proceedings of the National Academy of Sciences,*

106(51):21737-21742. doi:10.1073/pnas.0903811106

Welker, F., M. J. Collins, J. A. Thomas, M. Wadsley, S. Brace, E. Cappellini, S. T. Turvey, M. Reguero, J. N. Gelfo, A. Kramarz, J. Burger, J. Thomas-Oates, D. A. Ashford, P. D. Ashton, K. Rowsell, D. M. Porter, B. Kessler, R. Fischer, C. Baessmann, S. Kaspar, J. V Olsen, P. Kiley, J. A. Elliott, C. D. Kelstrup, V. Mullin, M. Hofreiter, E. Willerslev, J.-J. Hublin, L. Orlando, I. Barnes, and R. D. E. MacPhee. 2015. Ancient Proteins Resolve the Evolutionary History of Darwin's South American Ungulates. *Nature,* 522:81-84. doi:10.1038/nature14249

Westbury, M., S. Baleka, A. Barlow, S. Hartmann, J. L. A. Paijmans, A. Kramarz, A. Forasiepi, M. Bond, J. N. Gelfo, M. A. Reguero, P. López-Mendoza, M. Taglioretti, F. Scaglia, A. Rinderknecht, W. Jones, F. Mena, G. Billet, C. Muizon de, J. L. Aguilar, R. D.E. MacPhee, M. Hofreiter. 2017. A Mitogenomic Timetree for Darwin's Enigmatic South American mammal *Macrauchenia patachonica*. *Nature communications*, 8:15951. doi:0.1038/ncomms15951

Weston, E. M., R. H. Madden, and M. R. Sánchez-Villagra. 2004. Early Miocene Astrapotheres (Mammalia) from Northern South America. *Special Papers in Palaeontology,* 71:81-97.

Wilf, P., N. R. Cúneo, I. H. Escapa, D. Pol, and M. O. Woodburne. 2013. Splendid and Seldom Isolated: The Paleobiogeography of Patagonia. *Annual Review of Earth and Planetary Sciences,* 41:561-603. doi:10.1146/annurev-earth-050212-124217

Woodburne, M. 2010. The Great American Biotic Interchange: Dispersals, Tectonics, Climate, Sea Level and Holding Pens. *Journal of Mammalian Evolution,* 17:245-264. doi:10.1007/s10914-010-9144-8

Woodburne, M. O., F. J. Goin, M. Bond, A. A. Carlini, J. N. Gelfo, G. M. López, A. Iglesias, and A. N. Zimicz. 2014a. Paleogene Land Mammal Faunas of South America; a Response to Global Climatic Changes and Indigenous Floral Diversity. *Journal of Mammalian Evolution,* 21:1-73. doi:10.1007/s10914-012-9222-1

Woodburne. M. O., F. J. Goin, M. S. Raigemborn, M. Heizler, J. N. Gelfo, and E. V. Oliveira. 2014b. Revised Timing of the South American Early Paleogene Land Mammal Ages. *Journal of South American Earth Sciences*, 54:109-119. doi:10.1016/j.jsames.2014.05.003

Wozniak, J., and M. H. Wozniak. 1987. Bioestratigrafía de la región nor-central de la Serranía de Falcón, Venezuela nor-occidental. *Boletín de Geología Venezuela*, 16:101-139.

Zurita, A. E., A. A. Carlini, D. Gillette, and R. Sánchez. 2011. Late Pliocene Glyptodontinae (Xenarthra, Cingulata, Glyptodontidae) of South and North America: Morphology and Paleobiogeographical Implications in the GABI. *Journal of South American Earth Sciences,* 31:178-185. doi:10.1016/j.jsames.2011.02.001

Appendix 1. Stratigraphic description of ten sections and their geographical location.

POLIGONAL SECCIÓN ESTRÁTIGRAFICA CEMENTERIO CARRIZAL - QUEBRADA EL MUACO
Formación Caujarao Miembro Taratara y Formación La Vela

Coordenadas UTM, Datum La Canoa.

Escala 1:10.000

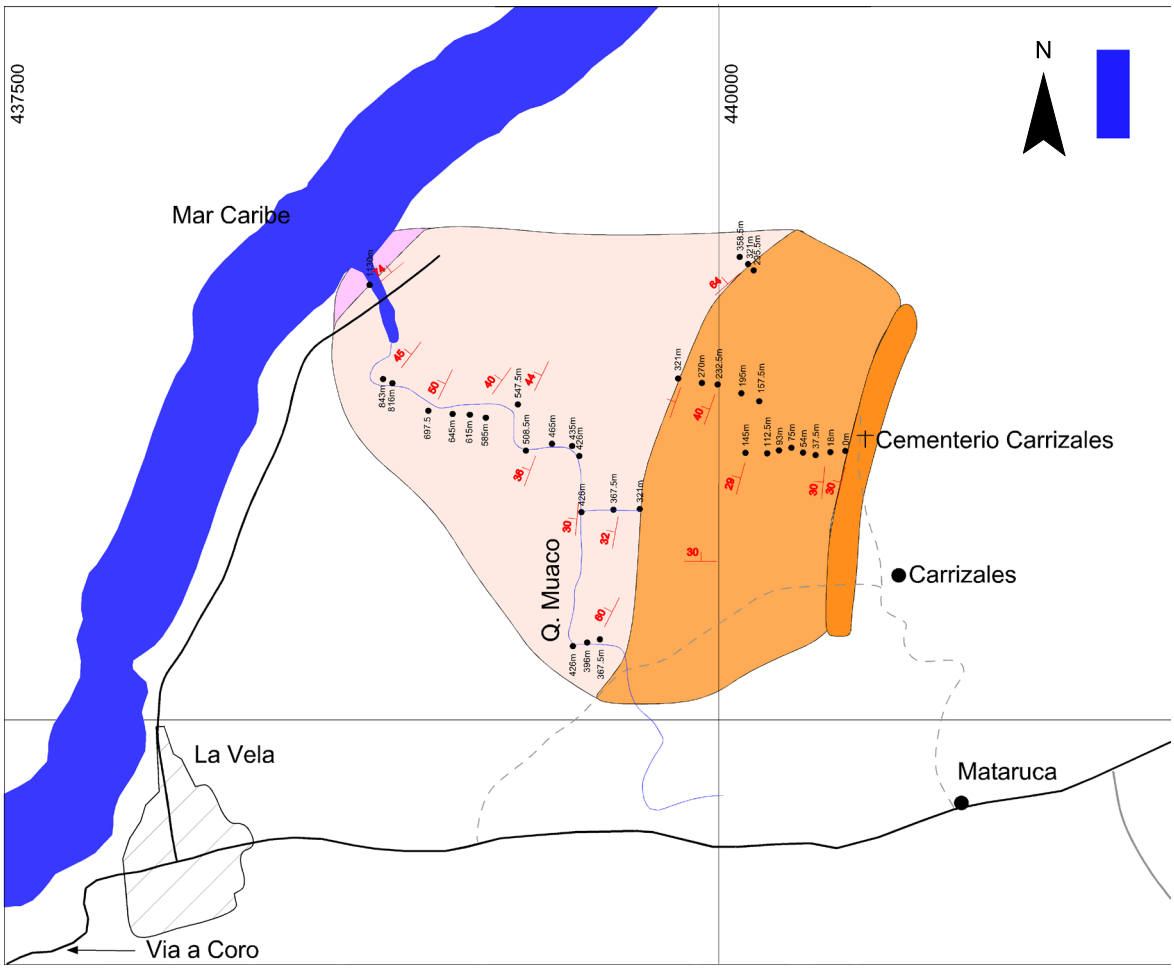

CONVENCIONES

- Formación Coro
- Formación La Vela
- Formación Caujarao Miembro Tara Tara
- Formación Caujarao Miembro Mataruca
- Metro Estratigráfico
- 40 Rumbo y Buzamiento
- Vía

0 500 1000 m

POLIGONAL SECCIÓN ESTRÁTIGRAFICA RIO CORO - VIA CORO SAN LUIS
Formación Caujarao Miembros Muaco y Mataruca, Formación Coro

Coordenadas UTM, Datum La Canoa.

Escala 1:10.000

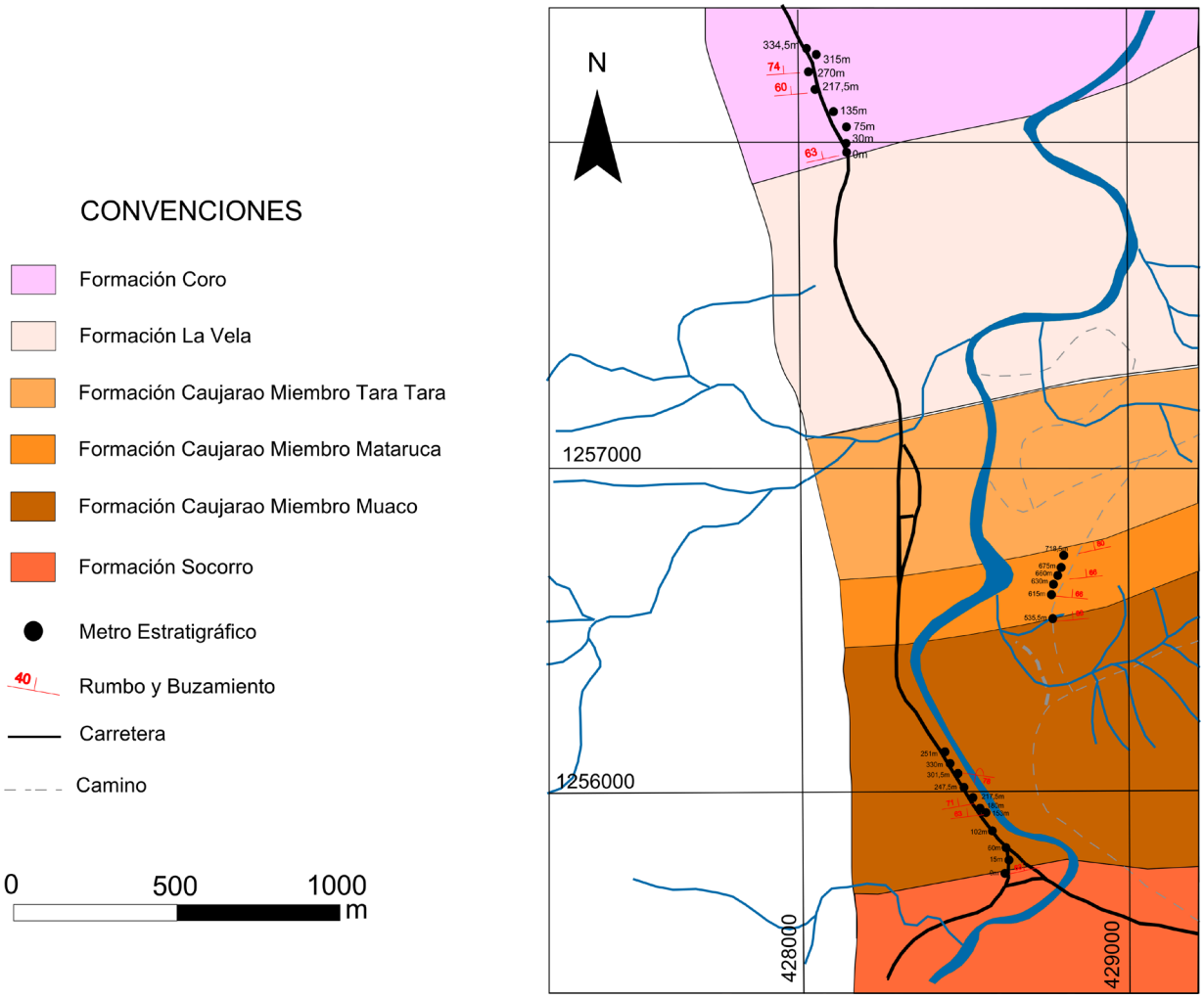

POLIGONAL SECCIÓN ESTRÁTIGRAFICA NORTE CHIGUAJE
Formación San Gregorio, Miembros Vergel y Cocuiza

Coordenadas UTM, Datum La Canoa.

Escala 1:10.000

CONVENCIONES

- Formación San Gregorio Miembro Río Seco
- Formación San Gregorio Miembro Cocuiza
- Formación San Gregorio Miembro Vergel
- Formación Codore Miembro Algodones
- Metro Estratigráfico
- 40 Rumbo y Buzamiento
- Oleoducto
- Camino

0 500 1000 m

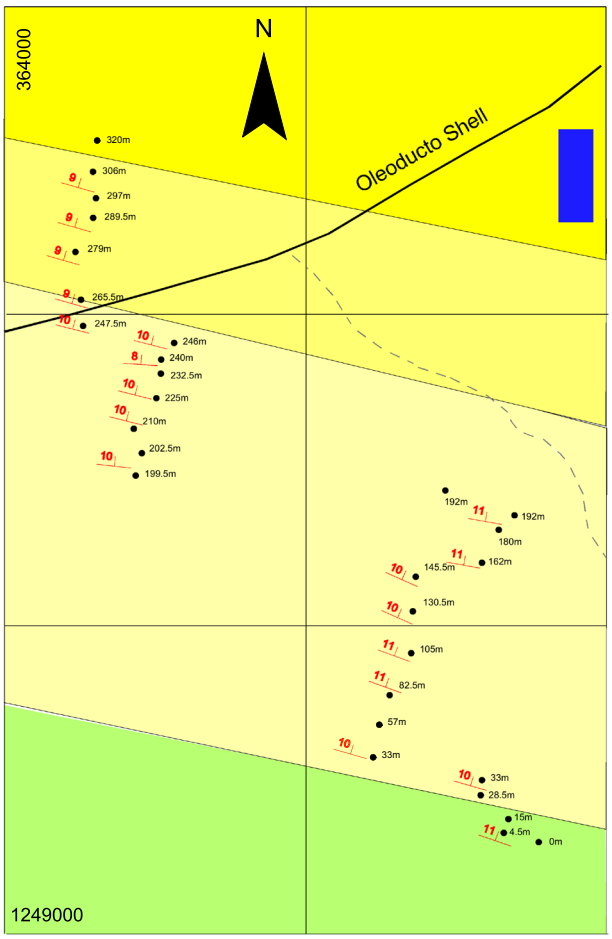

POLIGONAL SECCION ESTRATIGRAFICA QUEBRADA LA PALOMA Y RIO CADUCE
Formaciones Cerro Pelado, Querales.

Modificado de Hambaleck, 1993.
Coordenadas UTM, datum La Canoa.

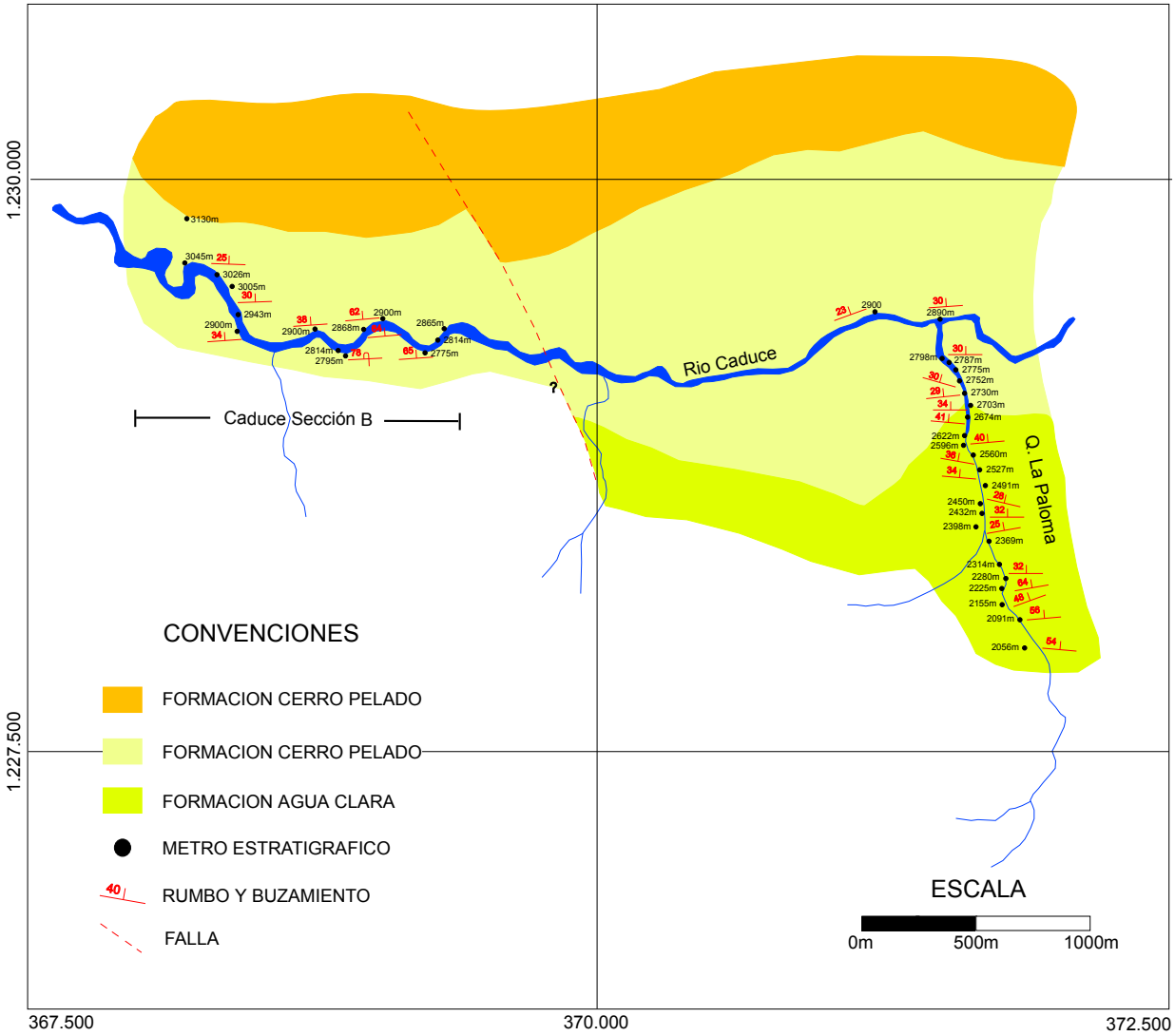

POLIGONAL SECCIÓN ESTRÁTIGRAFICA SAN GREGORIO
Formación San Gregorio Miembro Río Seco

Coordenadas UTM, Datum La Canoa.

Escala 1:10.000

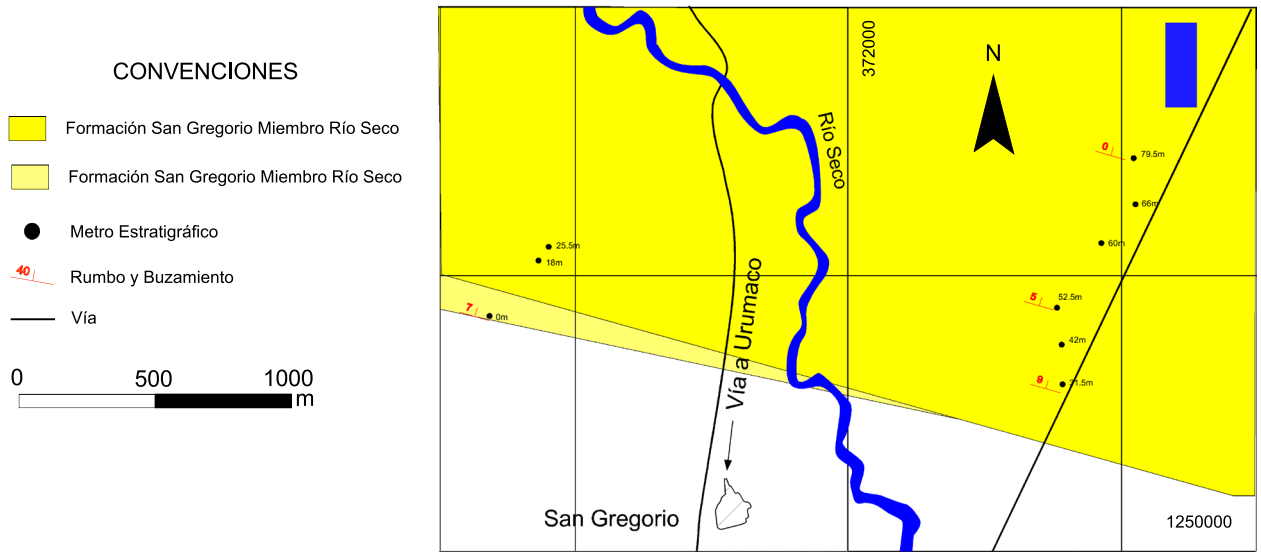

NORTHWARD CHIGUAJE HILL

SAN GREGORIO FM (VERGEL AND COCUIZA)

ESCALA 1:500

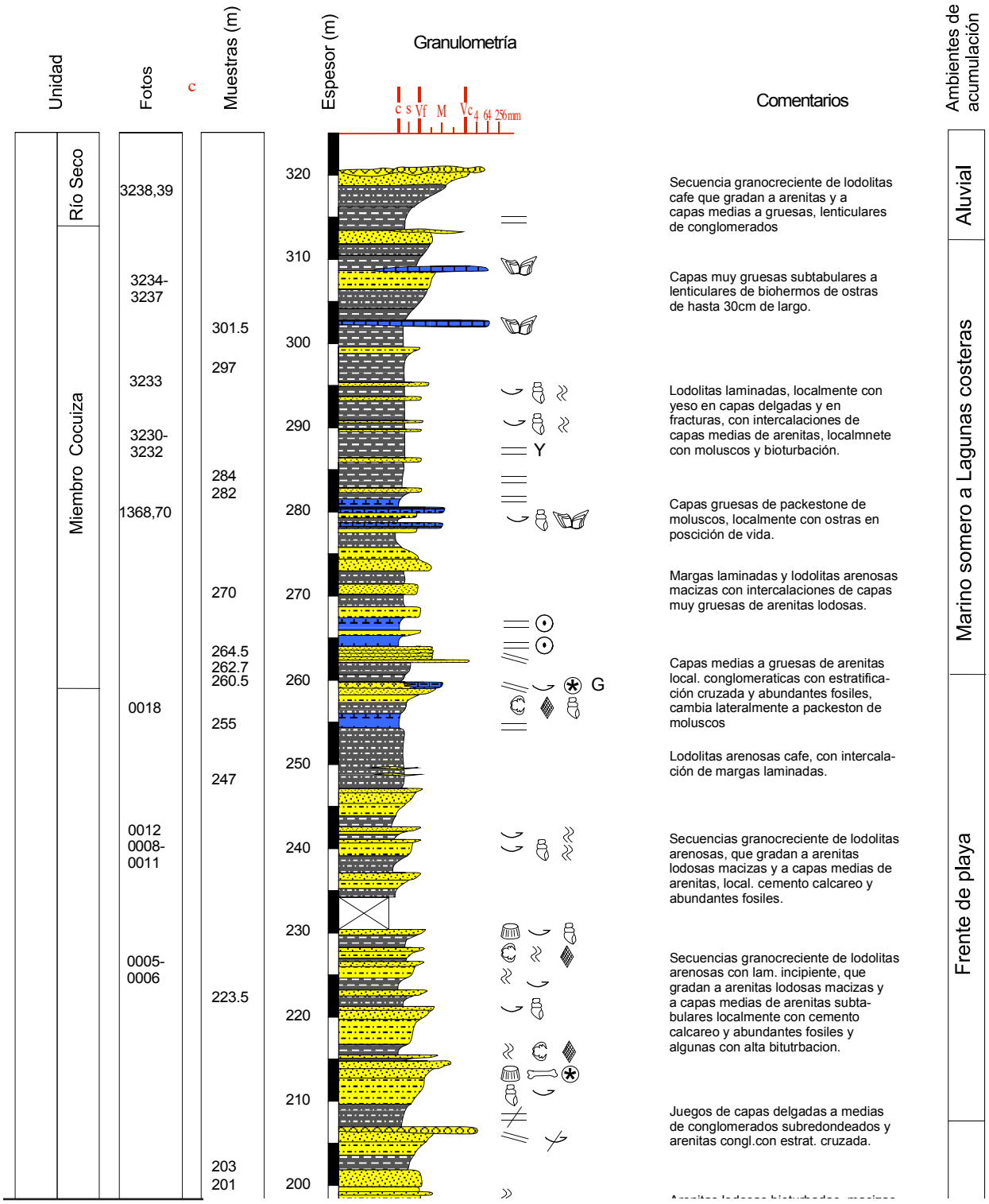

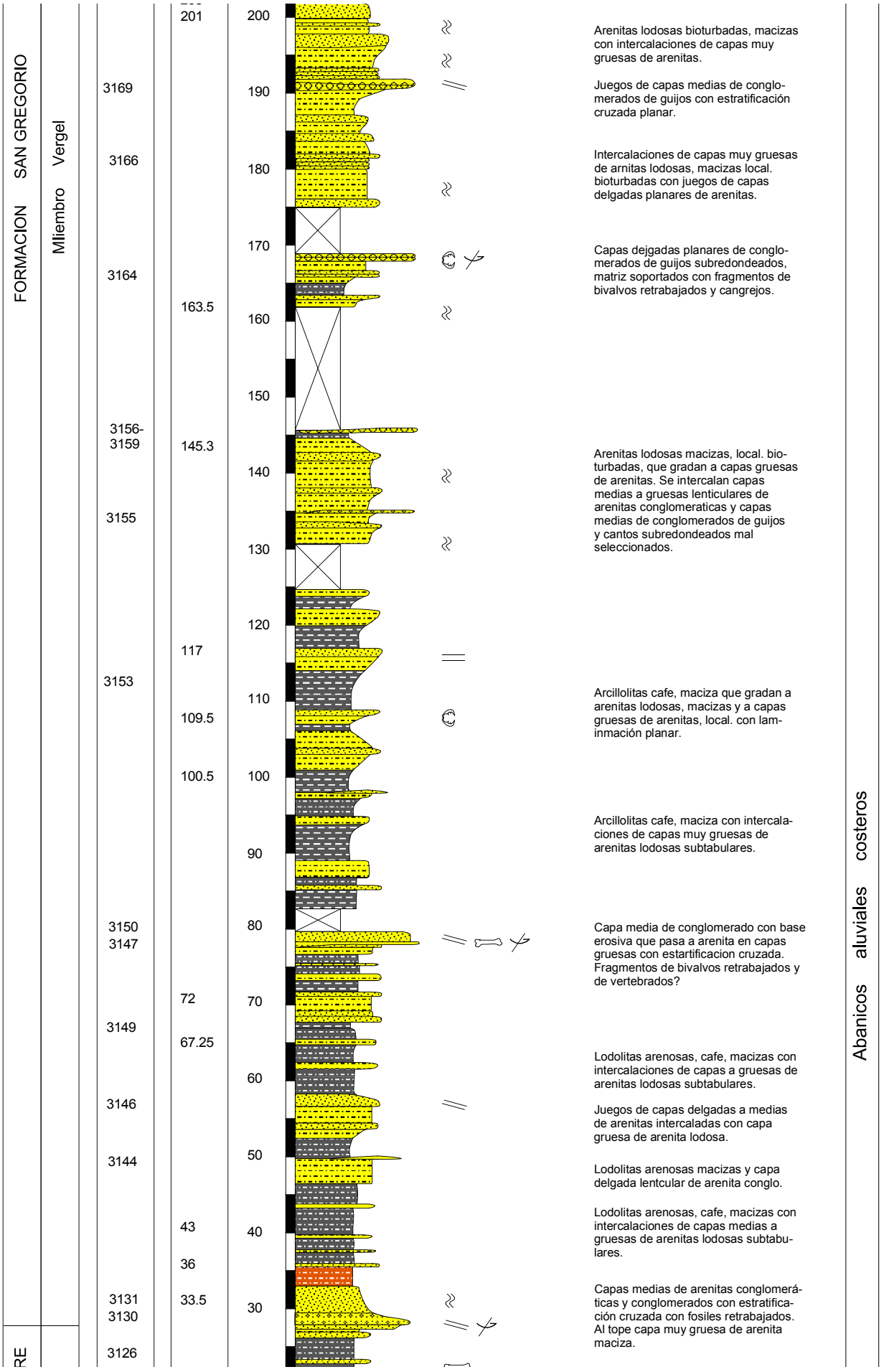
FORMACION SAN GREGORIO
Miembro Vergel
RE
Abanicos aluviales costeros
3169
3166
3164
3156-
3159
3155
3153
3150
3147
3149
3146
3144
3131
3130
3126
201
163.5
145.3
117
109.5
100.5
72
67.25
43
36
33.5
200
190
180
170
160
150
140
130
120
110
100
90
80
70
60
50
40
30
Arenitas lodosas bioturbadas, macizas con intercalaciones de capas muy gruesas de arenitas.
Juegos de capas medias de conglomerados de guijos con estratificación cruzada planar.
Intercalaciones de capas muy gruesas de arnitas lodosas, macizas local. bioturbadas con juegos de capas delgadas planares de arenitas.
Capas dejgadas planares de conglomerados de guijos subredondeados, matriz soportados con fragmentos de bivalvos retrabajados y cangrejos.
Arenitas lodosas macizas, local. bioturbadas, que gradan a capas gruesas de arenitas. Se intercalan capas medias a gruesas lenticulares de arenitas conglomeraticas y capas medias de conglomerados de guijos y cantos subredondeados mal seleccionados.
Arcillolitas cafe, maciza que gradan a arenitas lodosas, macizas y a capas gruesas de arenitas, local. con laminación planar.
Arcillolitas cafe, maciza con intercalaciones de capas muy gruesas de arenitas lodosas subtabulares.
Capa media de conglomerado con base erosiva que pasa a arenita en capas gruesas con estartificacion cruzada. Fragmentos de bivalvos retrabajados y de vertebrados?
Lodolitas arenosas, cafe, macizas con intercalaciones de capas a gruesas de arenitas lodosas subtabulares.
Juegos de capas delgadas a medias de arenitas intercaladas con capa gruesa de arenita lodosa.
Lodolitas arenosas macizas y capa delgada lentcular de arenita conglo.
Lodolitas arenosas, cafe, macizas con intercalaciones de capas medias a gruesas de arenitas lodosas subtabulares.
Capas medias de arenitas conglomeráticas y conglomerados con estratificación cruzada con fosiles retrabajados. Al tope capa muy gruesa de arenita maciza.

Appendix 2. Detailed description of each of the studies used to define the chronostratigraphy of the Urumaco region.

Author	Year	Title	Information
Cushman, J.A.	1918	Some Pliocene and Miocene foraminifera of the Coastal plain of the United States.	Description of species and distribution (some localities are menctioned).
Cushman, J.A.	1922	The foraminifera of the Atlantic ocean	Description of foraminifera species.
Cushman J. A. and McCulloch, I.	1940	Some Nonionidae in the collections of the Allan Hancock foundation	Description of foraminifera species from Pacific and Caribbean region.
Robertson, B.E.	1947	Systematics and Paleoecology of the Benthic Foraminiferida from the Buff bay section, Miocene of Jamaica. Journal of Paleonotology, 21 (4): 346- 350.	Description of species an some localities are showed.
Stainforth, R.M.	1948	Description, correlation and paleoecology of Tertiary Cipero Marl Formation, Trinidad, B.W.I., Bulletin. Am. Assoc. Petrol. Geol., 32., 1230-1292.	General description of the formations. Three samples were localized.
Cushman, J.A.	1951	Paleocene Foraminifera of the Gulf coastal region of the United States and adjacent areas. Geological survey professional paper 232.	Description of species. Some localities of Trinidad are menctioned but not the stratigraphic meter is specified.
Bartenstein, H., Bettenstaedt, F., and Bolli, H.M.	1957	Die foraminiferen der unterkreide von Trinidad, B.W.I. Eclogae Geol Herv. 50, 1	Description of species and occurrence in formations.
Bolli, H.M.	1957	Planktonic foraminifera from the Eocene Navet and San Fernando Formations of Trinidad, B.W.I.	Descriptions of species and zonations.
Bolli, H.M.	1959	Planktonic foraminifera from the Cretaceous of Trinidad, B.W.I. Bulletins of American Paleontology, 39 (179): 257- 277.	Descriptions of species but not neogene.
Bolli, H.M.	1959	Planktonic foraminifera from the Oligocene-Miocene Cipero and Lengua formations of Trinidad. B.W.I.	Descriptions of species and zonations.
Jenkins, D.G.	1965	Planktonic foraminifera and tertiary intercontinental correlations. Micropaleontology. 11 (3): 265- 277.	General information.
Bolli, H.S.	1967	The subspecies of *Globorotalia fohsi* Cushman and Ellisor and the zones based on them	Discuss the zonations of foraminifera based on this species.
Closs, D.	1967	Miocene planktonic foraminifera from Southern Brazil	Description of species.
Blow, W.H.	1969	Late Middle Eocene to recent planktonic foraminiferal bostratigraphy in: Proceedings of the first International conference on planktonic microfossils.	Description of species and zonations.
Bermudez, P.J. and Bolli, H.M.	1969	Consideraciones sobre los sedimentos del Mioceno medio al Reciente de las costas central y oriental de venezuela. Tercera parte: Los foraminiferos planctonicos. Boletin de Geologia, Minist. De Min. e Hidrocarb., 10/20, 137-223.	Interesting comments about correlation of studies of Blow and Bolli. Correlation among Trinidad and Venezuela. Stratigraphic meters are not indicated.
Premoli Silva, I. and Bolli, H.M.	1973	Late cretaceous to Eocene planktonic foraminifera and stratigraphy of Leg 15 sites in the Caribbean sea.	Occurrence of species and stratigraphic meter but not to neogene.

Appendix 3. Character-taxon matrix used in the phylogenetic analysis of Astrapotheriidae

Eoastrapostylops sp.	?????0?0000000000010000000-00000000-00-000-000?0?????00????0000
Trigonostylops sp.	0000010000000000000001010000{0 1}-00100000-00-10{0 1}-01000000000100000001
Tetragonostylops sp.	000?000000000000000001010000{0 1}010000000-1101{0 1}1-01?10????????????0000
Albertogaudrya sp.	???0??0000001 0?0?01?0101001010101000-110001-?1??????????????1000
Scaglia sp.	??????????????????????????????????00001??11011-??1?011????0????100?
Astraponotus sp.	0001?2000001101010??01110{0 1}101{0 1}{1 2}01001-111011-01??????????????110{0 2}
Maddenia lapidaria	?????10101000110101100121110001000 11-1110110{0 1}1??????????????1110
Parastrapotherium sp.	0001121101001111-00110101110100120110011011010?1112???1?11012110
Astrapotherium sp.	00011211011-1011-00110101010110220110010011110211121111211012110
Granastrapotherium snorki	111-1001111-1111-1-0100012011000211100100101 10?1?1?2?212??122110
Astrapothericulus sp.	0001111{0 1}011-1111-000101010101101101100100111101?1?????????????2110
Xenastrapotherium kraglievichi	00111011011-1111-00110001101100021211011011110??????????????2110
Xenastrapotherium christi	001?????11-?????????????1?110002???????????10???????????????2???
Uruguaytherium beaulieau	??????????????????????????20010?02????????????????????????????2???
Comahuetherium coccaorum	??????111?????1111-110100?1?????101110110110??????????????????21??
Hilarcotherium castandeaii	000111???11-??11-1-?10101201110021211111011110?????2?2??????111?
Hilarcotherium miyou	000??0???11-??11-1-11010120110002 1?1??1?01?1??????????????????111?

Appendix 4. Character-taxon matrix used in the phylogenetic analysis of Toxodontidae.

Pampahippus arenalesi	0?000??000?1000?0?0?0000000002000000000000000000000100000000
Leontinia gaudri	00100100010100010201100000000000000000000000000000100100000
Scarritia canquelensis	00100100010100010200000000000000000000000000000000000000000
Rhynchippus sp.	000001000???000100010000000000010000000000{0 1}000000000101200
Proadinotherium leptognathum	????????0??????????01?0??0{0 1}000100?001???30????00??0?00000?0?
Adinotherium sp.	1{0 2}00011100?10000101310000000010000017?10{1 3}0{0 1}0000010000010000{0 1}1
Nesodon imbricatus	1{0 2}00011100?000101012100000000100000101030000000{0 1}100000100000
Xotodon sp.	11{0 1}0001100010012{0 1}22211001010121101011 1{1 2}20000111000{0 1}0{0 1}111100
Hyperoxotodon speciosus	????????0??100?1?2211?000000121120011100010001111 0{0 1}00111100
Nonotherium henningi	10010111??????????2411001010121121 0??????????????????????
Posnanskytherium desaguadero	10010000011100011024011010{0 1}012112001123012 1{0 1}11100201011100
Trigodon gaudri	1202000100?10001202110021111121110121123111111112101011111 1
Paratrigodon euguii	120?0011??????????24?112111110111011111211 11{1 2}011??111011?1??
Palyeidodon obtusum	120101000?000010021100000001111100101010001 00{0 1}230000111101
Hoffstetterius imperator	12001101110101002022111210101011200111210122111110111121101
Ocnerotherium intermedium	??0??????????????24???010101011200????????2011110 0??1?1?0?
Toxodon platensis	10011100 00?01100112411{0 1}0100010112011112{1 2 3}012{0 2}{0 1}110100001{0 1}{0 1}{0 1}00
Andinotoxodon bolivariensis	??0?????00?001?1002?1???????12???00111{1 2}?0?210{0 1}1110100111100
Pisanodon nazari	1???0???0???0?????2??0?1??0?1011200??????????110{0 1}0{0 1}0011110?
Gyrinodon quassus	1002?1011???????1?2?1???000{0 1}1211201????????2011110{0 1}0121110?
Pericotoxodon platignathus	11010011 11?100??0021100111101111{1 2}01111110121 0{0 1}1100100111100
Dinotoxodon paranensis	????????{0 1}???????1?2???????0010012 01????????2011010000111 10?
Mixotoxodon larensis	??0?????00??0000102???????001211?001111310120 1101{0 1}00122110?
Calchaquitherium mixtum	??0?????0111001112 23??????????2?120011111101211101001111 1101
Nesodon taweretus	00010111 0??0001010 1??00?????01?0?00??????????00230000100 00?
Falcotoxodon aguilerai	1?0?011?00?000002023110{0 1}??{0 1}0121120{0 1}1?11{1 2 3}11{0 1}2{0 1}1111{0 1}00121110?
Piauhytherium capivarae	10110011 0??00?001?2?111000{0 1}012??{1 2}00111?{1 2 3}11{0 1}2011010000111 10?

Conclusions and future perspectives

The contributions of this dissertation can be grouped in two main subjects: (1), the phylogenetic relationships of Notoungulata; and (2), the Neogene mammalian evolution in northern South America. Regarding the first subject, prior to this work, they were two main conflicting hypotheses of relationships of Notoungulata within placentals. O'Leary et al. (2013) hypothesis placed Notoungulata as a sister group of Tethytheria (Proboscidea and Sirenia), within Afrotheria. O'Leary et al. (2013) studied the anatomy of *Thomashuxleya* (Isotenmidae) as representative of Notoungulata in their dataset, which consisted in 4551 morphological characters and 27 nuclear genes for 40 extinct and 46 extant terminal taxa. The second hypothesis was proposed independently by Welker et al. (2015) and Buckley (2015). To date, the data of Welker et al. (2015) are publicly available, whereas the data of Buckley (2015) are not; and therefore, only the results from Welker et al. (2015) are discussed here. Welker et al. (2015) used an alignment of 76 (six extinct and 70 extant) mammalian type I collagen sequences to study the relationships of Notoungulata (represented by *Toxodon*) and Litopterna (represented by *Macrauchenia*). Their hypothesis placed Notoungulata and Litopterna as the sister group of Perissodactyla, within Laurasiatheria.

As summarized above, there are conflicting phylogenetic hypotheses for Notoungulata as informed by analyses of either morphological or molecular data. It has been noticed that in some cases the combination of morphological and molecular data in extant and extinct taxa can provide more precise and robust hypotheses for several extinct clades of mammals (e.g., Pattinson et al., 2015); it was thus desirable to perform a phylogenetic analysis combining the different datasets. The contribution in chapter one presents such analysis; the character matrix analyzed included 3660 morphological characters presented by O'Leary et al. (2013), enhanced with the information derived from the study of new and exceptionally complete material of *Thomashuxleya externa*. The morphological dataset was concatenated with the amino acid alignment presented by Meredith et al. (2011), and the collagen alignment of Welker et al. (2015). The final dataset consisted of 16698 characters (13038 amino acids, and 3360 morphological characters) for 182 taxa. Frustratingly, the variety of optimal criteria applied did not unambiguously confirmed the hypothesis of Welker et al. (2015), nor did the analysis ruled out the alternative hypothesis of O'Leary et al. (2013). There are three (not exclusive) possible causes behind this lack of confident resolution: (1) there is still some part of the anatomy not sampled, which contains key phylogenetic information, (2) the early radiation of Notoungulata occurred in geographic regions not yet well sampled, and (3) the potential synapomorphies of Notoungulata with extant clades have been overwritten by homoplasy.

In order to dissipate phylogenetic uncertainty, the first two possible causes require the inclusion of additional morphological characters and the discovery

of more complete notoungulate fossils predating the Eocene. The third cause can be studied with the available data with artificial extinction experiments, which provide an empirical baseline to assess the confidence of the paleontological phylogenetic reconstructions. (e.g., Asher and Hofreiter, 2006; Pattinson et al., 2015). Artificial extinction analyses simulated the extinction of living species by deleting the taxon's molecular data and keeping only the morphological characters present in the fossils (Asher and Hofreiter, 2006). It then measures the congruence between a well-corroborated phylogeny and the ones including artificial fossils in order to test if artificial extinction of a living species leads to bias in the phylogenetic reconstruction (Pattinson et al., 2015).

In another section of chapter one, we estimated a body size of approximately 235 kg for *Thomashuxleya externa.* This result together with other existing data document a large range of body sizes of notoungulates by the middle Eocene. The notoungulate radiation encapsulates different morphotypes (Giannini and García-López, 2014), degrees of hypsodonty, and body sizes (Gomes-Rodrigues et al., 2017). The evolution of body size is a fundamental topic in evolutionary biology because it correlates with life history and ecological traits (Damuth and MacFadden, 1990). Because body size can be estimated for fossils and it can be directly compared among different clades, it has become a common feature to study the tempo and mode of phenotypic evolution (e.g., Harmon et al., 2010; Slater, 2013; Cuff et al., 2015). Given the wide range of body size exhibited by notoungulates already in the middle Eocene, future efforts should apply phylogenetic comparative methods to study body size evolution in this group.

Concerning the second subject of this dissertation, Neogene mammal evolution in northern South America, in chapter two we presented a review of the Neogene mammal fossil record in South America which revealed a sampling bias towards higher latitudes and more younger localities. Chapters three and four represent contributions towards filling the temporal and geographic gap in the fossil record of Neotropical mammals. In chapter three we presented evidence of higher diversity of neoepiblemid rodents in the Urumaco Formation (late Miocene, Venezuela), and in chapter four we described the Neogene ungulate-grade mammals from the Cocinetas and Falcón basins in northern South America. In the Cocinetas basin, the middle Miocene fauna of the Castilletes Formation includes *Hilarcotherium* sp. nov. (Astrapotheriidae), cf. *Huilatherium* (Leontiniidae), and *Neodolodus* cf. *colombianus* (Proterotheriidae). The late Pliocene fauna of the Ware Formation includes Toxodontinae indet. and the oldest record of Camelidae indet. (Artiodactyla) in South America. In the Falcón basin, the Pliocene faunas of the Codore and San Gregorio Formations include Toxodontidae gen. et sp. nov. and Protherotheriidae indet.

Figure 1. Contrast of landscape in the Falcón basin between the late Pliocene and the present. **a,** Artistic reconstruction of the fauna and landscape of the San Gregorio Formation by Stjepan Lukac. **b,** View of the San Gregorio Formation today.

Moreno et al. (2015) and Hendy et al. (2015) presented age estimates for the Castilletes and Ware formations in the Cocinetas basin using $^{87}Sr/^{86}Sr$ ratios and macroinvertebrate biostratigraphy. The systematic revision of the native ungulates from the Falcón and Cocinetas basins adds data to previous contributions on other mammalian clades (e.g., Carlini et al., 2006, 2008a, 2008b; Vucetich et al., 2010; Castro et al., 2014; Forasiepi et al., 2014; Amson et al., 2016; Suarez et al., 2016; Pérez et al., 2017). Expansion of this work should make possible to perform better mammalian biostratigraphic correlations across Neogene faunas in the continent.

The Pliocene faunal assemblages from the Ware and San Gregorio Formations in the Cocinetas and Falcón basins, respectively, show evidence that an important landscape change in the region took place sometime between the late Pliocene and the present (Figure 1). Future fieldwork efforts and systematic works will likely increase the diversity of these assemblages, and the new information could be incorporated in a cenogram analysis comparing fossil and living mammal assemblages in order to provide additional evidence to this landscape change (e.g., Croft, 2001). Cenogram analyses together with studies on the oxygen and carbon isotopes ratios could provide empirical estimates of past climate parameters such as the mean annual temperature (Fricke and Scott, 2004) for the Pliocene assemblages of the Ware and San Gregorio Formations. More precise mammalian biochronological correlations of the Neogene faunas of northern South America together with a more precise paleoecological and paleoenvironmental characterizations of these localities will facilitate the incorporation of ecological and environmental variables in the analyses of diversity changes and biogeography during the Great American Biotic Interchange.

References

Amson, E., J. D. Carrillo, and C. Jaramillo. 2016. Neogene sloth assemblages (Mammalia, Pilosa) of the Cocinetas Basin (La Guajira, Colombia): implications for the Great American Biotic Interchange. *Palaeontology* 59:563–582.

Asher, R. J., and M. Hofreiter. 2006. Tenrec phylogeny and the noninvasive extraction of nuclear DNA. *Systematic Biology* 55:181–194.

Buckley, M. 2015. Ancient collagen reveals evolutionary history of the endemic South American "ungulates." *Proceedings of Royal Society of Biology* 282:20142671.

Carlini, A. A., G. J. Scillato-Yané, and R. Sánchez. 2006. New Mylodontoidea (Xenarthra, Phyllophaga) from the Middle Miocene-Pliocene of Venezuela. *Journal of Systematic Palaeontology* 4:255–267.

Carlini, A. A., D. Brandoni, and R. Sánchez. 2008a. Additions to the knowledge of *Urumaquia robusta* (Xenarthra, Phyllophaga, Megatheriidae) from the Urumaco Formation (Late Miocene), Estado Falcón, Venezuela. *Paläontologische Zeitschrift* 82:153–162.

Carlini, A. A., A. E. Zurita, G. J. Scillato-Yané, R. Sánchez, and O. A. Aguilera. 2008b. New glyptodont from the Codore Formation (Pliocene), Falcón State, Venezuela, its relationship with the *Asterostemma* problem, and the paleobiogeography of the Glyptodontinae. *Paläontologische Zeitschrift* 82:139–152.

Castro, M. C., A. A. Carlini, R. Sánchez, and M. R. Sánchez-Villagra. 2014. A new Dasypodini armadillo (Xenarthra: Cingulata) from San Gregorio Formation, Pliocene of Venezuela: affinities and biogeographic interpretations. *Naturwissenschaften* 101:77–86.

Croft, D. 2001. Cenozoic environmental change in South America as indicated by mammalian body size distributions (cenograms). *Diversity and Distributions* 7:271–287.

Cuff, A. R., M. Randau, J. Head, J. R. Hutchinson, S. E. Pierce, and A. Goswami. 2015. Big cat, small cat: Reconstructing body size evolution in living and extinct Felidae. *Journal of Evolutionary Biology* 28:1516–1525.

Damuth, J., and B. J. MacFadden. 1990. *Body Size in Mammalian Paleobiology. Estimations and Biological Implications*. Cambridge University Press, Cambridge.

Forasiepi, A., L. Soibelzon, C. Gomez, R. Sánchez, L. Quiroz, C. Jaramillo, and M. R. Sánchez-Villagra. 2014. Carnivorans at the Great American Biotic Interchange: new discoveries from the northern Neotropics. *Naturwissenschaften* 101:965–974.

Fricke, H. C., and L. W. Scott. 2004. Oxygen isotope and paleobotanical estimates of temperature and $\delta^{18}O$-latitude gradients over

North America during the Early Eocene. *American Journal of Science* 304:612–635.

Giannini, N., and D. García-López. 2014. Ecomorphology of mammalian fossil lineages: Identifying morphotypes in a case study of endemic South American ungulates. *Journal of Mammalian Evolution* 21:195–212.

Gomes-Rodrigues, H., A. Herrel, and G. Billet. 2017. Ontogenetic and life history trait changes associated with convergent ecological specializations in extinct ungulate mammals. *Proceedings of the National Academy of Sciences* 114(5):1069-1074

Harmon, L. J., J. B. Losos, T. J. Davies, R. G. Gillespie, J. L. Gittleman, W. B. Jennings, K. H. Kozak, M. A. McPeek, F. Moreno-Roark, T. J. Near, A. Purvis, R. E. Ricklefs, D. Schluter, J. A. Schulte, O. Seehausen, B. L. Sidlauskas, O. Torres-Carvajal, J. T. Weir, and A. T. Mooers. 2010. Early bursts of body size and shape evolution are rare in comparative data. *Evolution* 64:2385–2396.

Hendy, A. J. W., D. S. Jones, F. Moreno, V. Zapata, and C. Jaramillo. 2015. Neogene molluscs, shallow marine paleoenvironments, and chronostratigraphy of the Guajira Peninsula, Colombia. *Swiss Journal of Palaeontology* 134:45–75.

Meredith, R. W., J. E. Janečka, J. Gatesy, O. A. Ryder, C. A. Fisher, E. C. Teeling, A. Goodbla, E. Eizirik, T. L. L. Simão, T. Stadler, D. L. Rabosky, R. L. Honeycutt, J. J. Flynn, C. M. Ingram, C. Steiner, T. L. Williams, T. J. Robinson, A. Burk-Herrick, M. Westerman, N. A. Ayoub, M. S. Springer, and W. J. Murphy. 2011. Impacts of the Cretaceous terrestrial revolution and KPg extinction on mammal diversification. *Science* 334:521–4.

Moreno, F., A. J. W. Hendy, L. Quiroz, N. Hoyos, D. S. Jones, V. Zapata, S. Zapata, G. A. Ballen, E. Cadena, A. L. Cárdenas, J. D. Carrillo-Briceño, J. D. Carrillo, D. Delgado-Sierra, J. Escobar, J. I. Martínez, C. Martínez, C. Montes, J. Moreno, N. Pérez, R. Sánchez, C. Suárez, M. C. Vallejo-Pareja, and C. Jaramillo. 2015. Revised stratigraphy of Neogene strata in the Cocinetas Basin, La Guajira, Colombia. *Swiss Journal of Palaeontology* 134:5–43.

O'Leary, M. A., J. I. Bloch, J. J. Flynn, T. J. Gaudin, A. Giallombardo, N. P. Giannini, S. L. Goldberg, B. P. Kraatz, Z. Luo, J. Meng, X. Ni, M. J. Novacek, F. A. Perini, Z. S. Randall, G. W. Rougier, E. J. Sargis, M. T. Silcox, N. B. Simmons, M. Spaulding, P. M. Velazco, M. Weksler, J. R. Wible, and A. L. Cirranello. 2013. The placental mammal ancestor and the post-K-Pg radiaton of placentals. *Science* 339:662–667.

Pattinson, D. J., R. S. Thompson, A. K. Piotrowski, and R. J. Asher. 2015. Phylogeny, paleontology, and primates: do incomplete fossils bias the tree of life? *Systematic Biology* 64:169–86.

Pérez, M. E., M. C. Vallejo-Pareja, J. D. Carrillo, and C. Jaramillo. 2017. A new Pliocene capybara (Rodentia, Caviidae) from Northern South America (Guajira, Colombia), and its implications for the Great American Biotic Interchange. *Journal of Mammalian Evolution* 24:111–125.

Slater, G. J. 2013. Phylogenetic evidence for a shift in the mode of mammalian body size evolution at the Cretaceous-Palaeogene boundary. *Methods in Ecology and Evolution* 4:734–744.

Suarez, C., A. M. Forasiepi, F. J. Goin, and C. Jaramillo. 2016. Insights into the Neotropics prior to the Great American Biotic Interchange: new evidence of mammalian predators from the Miocene of Northern Colombia. Journal of Vertebrate Paleontology 36: e1029581.

Vucetich, M. G., A. A. Carlini, O. Aguilera, and M. R. Sánchez-Villagra. 2010. The tropics as reservoir of otherwise extinct mammals: The case of rodents from a new Pliocene faunal assemblage from northern Venezuela. *Journal of Mammalian Evolution* 17:265–273.

Welker, F., M. J. Collins, J. A. Thomas, M. Wadsley, S. Brace, E. Cappellini, S. T. Turvey, M. Reguero, J. N. Gelfo, A. Kramarz, J. Burger, J. Thomas-Oates, D. A. Ashford, P. D. Ashton, K. Rowsell, D. M. Porter, B. Kessler, R. Fischer, C. Baessmann, S. Kaspar, J. V Olsen, P. Kiley, J. A. Elliott, C. D. Kelstrup, V. Mullin, M. Hofreiter, E. Willerslev, J.-J. Hublin, L. Orlando, I. Barnes, and R. D. E. MacPhee. 2015. Ancient proteins resolve the evolutionary history of Darwin's South American ungulates. *Nature* 522:81–84

APPENDIX

Collaborations with other publications

(Abstracts only)

Revised stratigraphy of Neogene strata in the Cocinetas Basin, La Guajira, Colombia

F. Moreno, A.J.W. Hendy, L. Quiroz, N. Hoyos, D.S. Jones, V. Zapata, S. Zapata, G.A. Ballén, E. Cadena, A.L. Cárdenas, J.D. Carrillo-Briceño, **J.D. Carrillo**, D. Delgado-Sierra, J. Escobar, J.I. Martínez, C. Montes, J. Moreno, N. Pérez, R. Sánchez, C. Suárez, M.C. Vallejo-Pareja, C. Jaramillo. 2015. *Swiss Journal of Palaeontology* 134(1):5-43. doi:10.1007/s13358-015-0071-4

The Cocinetas Basin of Colombia provides a valuable window into the geological and paleontological history of northern South America during the Neogene. Two major findings provide new insights into the Neogene history of this Cocinetas Basin: (1) a formal re-description of the Jimol and Castilletes formations, including a revised contact; and (2) the description of a new lithostratigraphic unit, the Ware Formation (Late Pliocene). We conducted extensive fieldwork to develop a basin-scale stratigraphy, made exhaustive paleontological collections, and performed $^{87}Sr/^{86}Sr$ geochronology to document the transition from the fully marine environment of the Jimol Formation (ca. 17.9–16.7 Ma) to the fluvio-deltaic environment of the Castilletes (ca. 16.7–14.2 Ma) and Ware (ca. 3.5–2.8 Ma) formations. We also describe evidence for short-term periodic changes in depositional environments in the Jimol and Castilletes formations. The marine invertebrate fauna of the Jimol and Castilletes formations are among the richest yet recorded from Colombia during the Neogene. The Castilletes and Ware formations have also yielded diverse and biogeographically significant fossil vertebrate assemblages. The revised lithostratigraphy and chronostratigraphy presented here provides the necessary background information to explore the complete evolutionary and biogeographic significance of the excellent fossil record of the Cocinetas Basin.

Hilarcotherium castanedaii, gen. et sp. nov., a new Miocene astrapothere (Mammalia, Astrapotheriidae) from the upper Magdalena valley, Colombia

M.C Vallejo-Pareja, **J.D. Carrillo**, J.W. Moreno-Bernal, M. Pardo-Jaramillo, D.F. Rodriguez-Gonzalez, and J. Muñoz-Durán. 2015. *Journal of Vertebrate Paleontology* 35(2):e903960. doi:10.1080/02724634.2014.903960

Astrapotheria is an order of extinct South American herbivores recorded throughout the continent, from the late Paleocene to middle Miocene. Here we describe *Hilarcotherium castanedaii*, gen. et sp. nov., an Uruguaytheriinae astrapothere from sediments of La Victoria Formation (middle Miocene) in the Tolima Department, upper Magdalena valley, Colombia.

H. castanedaii, represented by a partial skull, mandible, and some postcranial remains, is characterized by (1) unique dental formula, with 0/3i, 1/1c, 1/1p, and 3/3 m; and (2) lower canines with subtriangular transverse section at the base. *Hilarcotherium* differs from the equatorial Uruguaytheriinae genera *Xenastrapotherium* and *Granastrapotherium* in (1) having three lower incisors; (2) the diagonal implantation of the lower canines; (3) lower molars with lingual cingulid; (4) the presence of the hypocone in the third upper molar; and (5) the presence of an anterolingual pocket in the fourth upper premolar. Our phylogenetic analysis supports the monophyly of the subfamilies Astrapotheriinae and Uruguaytheriinae. Within the latter, we confirm the monophyly of the neotropical clade (*Hilarcotherium*, *Xenastrapotherium*, and *Granastrapotherium*). *H. castanedaii* shows some plesiomorphic features such as the aforementioned presence of the i3 and the developed hypocone in the last upper molar. Its estimated body mass (1303 kg) is intermediate among Astrapotheriidae.

Neogene sloth assemblages (Mammalia, Pilosa) of the Cocinetas basin (La Guajira, Colombia): implications for the Great American Biotic Interchange

E. Amson, **J.D. Carrillo**, and C. Jaramillo. 2016. *Palaeontology* 59(4):562-582. doi:10.1111/pala.12244

We describe sloth assemblages from the Cocinetas Basin (La Guajira peninsula, Colombia), found in the Neogene Castilletes and Ware formations, located in northernmost South America, documenting otherwise poorly known biotas. The tentative referral of a specimen to a small megatherioid sloth, *Hyperleptus*?, from the early–middle Miocene Castilletes Formation, suggests affinities of this fauna with the distant Santa Cruz Formation and documents a large latitudinal distribution for this taxon. The late Pliocene Ware Formation is much more diverse, with five distinct taxa representing every family of 'ground sloths'. This diversity is also remarkable at the ecological level, with sloths spanning over two orders of magnitude of body mass and probably having different feeding strategies. Being only a few hundred kilometres away from the Isthmus of Panama, and a few hundred thousand years older than the classically recognized first main pulse of the Great American Biotic interchange (GABI 1), the Ware Formation furthermore documents an important fauna for the understanding of this major event in Neogene palaeobiogeography. The sloths for which unambiguous affinities were recovered are not closely related to the early immigrants found in North America before GABI 1.

On the growth of the largest living rodent: Postnatal skull and dental shape changes in capybara species (*Hydrochoerus* spp.)

M. Aeschbach, **J.D. Carrillo**, and M.R. Sánchez-Villagra. 2016. Mammalian Biology 81(6):558-570. doi:10.1016/j.mambio.2016.02.010

We report on intraspecific and interspecific morphological variation in the cranium, mandible and teeth along the ontogenetic trajectories of the two species of the largest living rodent, the capybara. A three dimensional geometric morphometrics approach was used to compare 171 *Hydrochoerus hydrochaeris* and 44 *Hydrochoerus isthmius* specimens ranging from newborn to adult. The specimens were assigned to seven different age classes according to cranial suture closure. The species can be differentiated in the morphospace occupation. They differ in the angle between the braincase and rostrum—*H. hydrochaeris* displays a straight transition whereas the snout of *H. isthmius* is inclined ventrally. The males in both species are bigger than the females, but no shape differences were detected. The youngest two age classes (up to 0.5 months and 0.5–10 months; before reaching sexual maturity) can be morphologically differentiated from the older age classes. Shape changes during growth are similar in both species: with increasing age, the round neurocranium flattens and the proportionally short snout elongates. Moreover, both species follow similar ontogenetic trajectories. *H. hydrochaeris* and *H. isthmius* can be differentiated by size and shape; the shape differences may indicate differences in diet and habitat. This study illustrates the relevance of an ontogenetic perspective to characterize species and examine the bases of disparity in adults. Furthermore, variation recorded in dental features serves to evaluate taxonomic and evolutionary aspects in fossil capybaras.

A new Pliocene capybara (Rodentia, Caviidae) from northern South America (Guajira, Colombia), and its implications for the Great American Biotic Interchange

M.E. Pérez, M.C. Vallejo-Pareja, **J.D. Carrillo**, C. Jaramillo. 2017. *Journal of Mammalian Evolution* 24(1):111-125. doi:10.1007/s10914-016-9356-7

One of the most striking components of the modern assemblage of South American mammals is the semiaquatic capybara (Caviidae, Hydrochoerinae), the biggest rodent in the world. The large hydrochoerines are recorded from the middle Miocene to the present, mainly in high latitudes of South America. Although less known, they are also recorded in low latitudes of South America, and in Central and North America. We report the first record of capybaras from the late Pliocene of Colombia, found in deposits of the Ware Formation, Guajira

Peninsula in northeastern Colombia. We analyze the phylogenetic position within Caviidae, the possible environmental changes in the Guajira Peninsula, and the implications of this finding for the understanding of the Great American Biotic Interchange. The morphological and phylogenetic analyses indicate that the hydrochoerine of the Guajira Peninsula is a new species, *?Hydrochoeropsis wayuu*, and this genus is most closely related to *Phugatherium*. According to the latest phylogenetic results, this clade is the sister group of the lineage of the recent capybaras (*Neochoerus* and *Hydrochoerus*). *?Hydrochoeropsis wayuu* is the northernmost South American Pliocene hydrochoerine record and the nearest to the Panamanian bridge. The presence of this hydrochoerine, together with the fluvio-deltaic environment of the Ware Formation, suggests that during the late Pliocene, the environment that dominated the Guajira Peninsula was more humid and with permanent water bodies, in contrast with its modern desert habitats.

Acknowledgments

A sincere thanks and appreciation to my advisor Prof. Dr. Marcelo Sánchez-Villagra, whose enthusiasm and advice were essential for the success of this work. I am very grateful for the opportunity he granted me to conduct my PhD in Zurich, and for the scientific and personal guidance and friendship that helped me to improve as a researcher.

I am greatly thankful to Dr. Robert Asher for hosting me in his lab in Cambridge and served as external advisor providing invaluable advice and mentorship. I also thank Dr. Carlos Jaramillo, who introduced me to the study of Neotropical palaeontology and has provided continuous academic support ever since. I thank Dr. Guillaume Billet, and PD. Dr. Torsten Scheyer for agreeing to be part of my dissertation committee.

I am indebted to many friends and colleagues (and ex-colleagues) in Zurich: PD. Dr. Torsten Scheyer, Dr. Jorge Carrillo-Briceño, Dr. Eli Amson, Dr. Madeleine Geiger, Dr. Gabriel Aguirre-Fernandez, Dr. Christian Kolb, Dr. James Neenan, Dr. Catalina Pimiento, Madlen Stange, Laura Heck, Kristof Veitschegger, Thodoris Argyriou, Ashley Latimer, Alexandra Wegmann, Morgane Brosse, Marc Leu, Heinrich Walter, Beat Scheffold, Markus Hebeisen among others. Special thanks to Heike Götzmann for her diligence and assistance.

For valuable comments and inspiring discussions, I thank Dr. Analía Forasiepi, Dr. Alfredo Carlini, Dr. Javier Gelfo, Dr. Malena Lorente, Dr. Guiomar Vucetich, Dr. Alejandro Kramarz, Mariano Bond, Dr. Leonardo Kerber, Prof. Pierre-Oliver Antoine, and Dr. Rodolfo Salas. For their camaraderie in the field and friendship I thank my former colleagues at the Smithsonian, and very especially I thank Rodolfo Sánchez and family in Urumaco. I thank Tanja Enseroth and Laura Heck for translating the abstract to german.

I would like to thank to my family, my brother Jorge Luis, my sister María Fernanda, and my parents Jairo and María del Carmen, for their love and unconditional support throughout my studies and sharing every achievement as their own. Finally, I thank my girlfriend Tanja, for her continuous support, love, advice and understanding.

CURRICULUM VITAE

CARRILLO SÁNCHEZ Juan David

Date of birth: 06.04.1987
Place of birth: Bogotá (Colombia)
Nationality: Colombian

Education

2014-2017 PhD student, Paleontological Institute and Museum, University of Zurich, Switzerland.
Dissertation: Systematics of the South American native ungulates and the Neogene evolution of mammals from northern South America.
Supervisor: Prof. Dr. M. Sánchez-Villagra (University of Zurich, Switzerland).

2014 MSc Biology-Paleontology. University of Zurich. Zurich, Switzerland.
Supervisor: Prof. Dr. M. Sánchez-Villagra (University of Zurich, Switzerland).

2011 B. Sc. Biology, Universidad Nacional de Colombia, Colombia.

Scholarship during the doctoral studies

2016-2017 SNF doc mobility (host University of Cambridge): Morphology, phylogeny and body size evolution of the South American native ungulates – P1ZHP3_165068 (51 800 CHF).